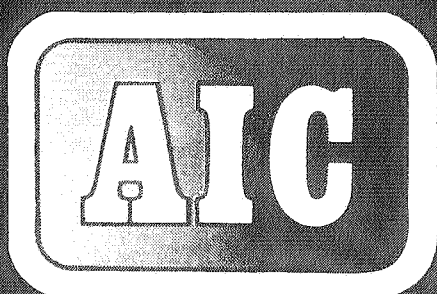


INTERNATIONAL ENERGY AGENCY
energy conservation in buildings and
community systems programme

1st AIC Conference

Air Infiltration Instrumentation and Measuring Techniques

Proceedings



Air Infiltration Centre

Old Bracknell Lane, Bracknell,
Berkshire, Great Britain, RG12 4AH

This report is part of the work of the IEA Energy Conservation in Buildings & Community Systems Programme

Annex 5 Air Infiltration Centre

Document AIC-PROC-1-80

Distribution: Unrestricted

Participants in this task:

Additional copies of this report may be obtained from:

Canada, Denmark, Italy, Netherlands, Sweden, Switzerland, United Kingdom and United States of America.

The Air Infiltration Centre, Old Bracknell Lane, Bracknell, Berkshire, RG12 4AH, England.

Price: £35 sterling (US \$90)

1st AIC Conference

Air Infiltration Instrumentation and Measuring Techniques

(held at Cumberland Lodge,
Windsor Great Park, Berkshire, UK.
6- 8 October 1980)

Proceedings

©Copyright Oscar Faber Partnership 1981.

All property rights, including copyright are vested in the operating agents (The Oscar Faber Partnership) on behalf of the International Energy Agency.

In particular, no part of this publication may be reproduced, stored in a retrieval system or transmitted in any form or by any means, electronic, mechanical, photocopying, recording or otherwise, without the prior written permission of the operating agent.

CONTENTS

Preface	(iii)
List of participants	(vii)
Conference photograph	(ix)
Keynote Paper	(xi)
1. "Instrumentation and measuring techniques" James Dick	1
Session 1: Alternative Measurement Procedures <i>Chairman – Peter Jackman, Head of Air Infiltration Centre</i>	
2. "Air infiltration measurement techniques" M. H. Sherman, D. T. Grimsrud, P. E. Condon and B. V. Smith <i>presented by Max Sherman, USA</i>	9
3. "Experimental techniques for ventilation research" D. K. Alexander, D. W. Etheridge and R. Gale <i>presented by David Etheridge, UK</i>	45
Session 2: Automatic Monitoring Using Tracer Gas Techniques <i>Chairman – Peter Warren, Building Research Establishment, Garston, UK</i>	
4. "An automated air infiltration measuring system using SF ₆ tracer gas in constant concentration and decay methods" R. Kumar, A. D. Ireson and H. W. Orr <i>(reproduced by kind permission of ASHRAE)</i> <i>presented by Robert Dumont, Canada</i>	73
5. "Automatic measurements of air change rates (decay method) in a small residential building without any forced-air-heating system" P. Hartmann and H. Mühlebach <i>presented by Peter Hartmann, Switzerland</i>	87

6. "Automated air infiltration measurements in large buildings" 103
R. A. Grot, C. M. Hunt and D. T. Harrie
presented by Richard Grot, USA

Session 3: Pressurization Test Methods

Chairman – Martin Liddament, Air Infiltration Centre, UK

7. "Problems and consequences of the pressurization test for the air leakage of houses" 129
W. F. de Gids
presented by Willem de Gids, Netherlands
8. "The application of reciprocity in tightness testing" 143
P. O. Nylund
presented by Per-Olof Nylund, Sweden
9. "Tightness and its testing in single and terraced houses" 157
P. O. Nylund
presented by Per-Olof Nylund, Sweden
10. "Air leakage measurements of the exterior walls of tall buildings" 171
C. Y. Shaw, D. M. Sander and G. T. Tamura
presented by John (Chia) Shaw, Canada
11. "Studies on the exterior wall air tightness and air infiltration of tall buildings" 183
G. T. Tamura and C. Y. Shaw
presented by John (Chia) Shaw, Canada
12. "Air tightness and air infiltration of school buildings" 199
C. Y. Shaw and L. Jones
presented by John (Chia) Shaw, Canada
13. "Methods for conducting small-scale pressurization tests and air leakage data of multi-storey apartment buildings" 213
C. Y. Shaw
presented by John (Chia) Shaw, Canada

(papers 10 to 13 reproduced by kind permission of ASHRAE)

Session 4: Correlation of Tracer Gas and Pressurization Measurements

Chairman – David Etheridge, British Gas, Watson House, UK

- | | | |
|-----|---------------------------------------------------------------------------------------------------------------------------------------------------------|-----|
| 14. | “Correlating pressurization and infiltration rate data – tests of an heuristic model”
J. Kronvall
<i>presented by Johnny Kronvall, Sweden</i> | 225 |
| 15. | “The relationship between tracer gas and pressurization techniques in dwellings”
P. R. Warren and B. C. Webb
<i>presented by Peter Warren, UK</i> | 245 |
| 16. | “Measurement of infiltration using fan pressurization and weather data”
M. H. Sherman and D. T. Grimsrud
<i>presented by Max Sherman, USA</i> | 277 |

Session 5: Other Measurements

Chairman – Peter Jackman, Head of Air Infiltration Centre

- | | | |
|-----|--------------------------------------------------------------------------------------------------------------------------------------------------------------------|-----|
| 17. | “The measurement of rapidly fluctuating air flows”
P. Robertson and J. P. Cockroft
<i>presented by Peter Robertson, UK</i> | 323 |
| 18. | “Development of a dynamic pressure anemometer for measuring the axial velocity component”
J. C. Phaff
<i>presented by Hans Phaff, Netherlands</i> | 331 |
| 19. | “Evaluation of the indoor air quality as a criterion for minimum ventilation rates”
G. Huber and H. V. Wanner
<i>presented by Gabriel Huber, Switzerland</i> | 341 |

Discussion	355
-------------------	------------

International Energy Agency

In order to strengthen cooperation in the vital area of energy policy, an Agreement on an International Energy Program was formulated among a number of industrialised countries in November 1974. The International Energy Agency (IEA) was established as an autonomous body within the Organisation for Economic Cooperation and Development (OECD) to administer that agreement. Twenty-one countries are currently members of the IEA, with the Commission of the European Communities participating under a special arrangement.

As one element of the International Energy Program, the Participants undertake cooperative activities in energy research, development, and demonstration. A number of new and improved energy technologies which have the potential of making significant contributions to our energy needs were identified for collaborative efforts. The IEA Committee on Energy Research and Development (CRD), assisted by a small Secretariat staff, coordinates the energy research, development, and demonstration programme.

Energy Conservation in Buildings and Community Systems

The International Energy Agency sponsors research and development in a number of areas related to energy. In one of these areas, energy conservation in buildings, the IEA is sponsoring various exercises to predict more accurately the energy use of buildings, including comparison of existing computer programmes, building monitoring, comparison of calculation methods, etc. The difference and similarities among these comparisons have told us much about the state of the art in building analysis and have led to further IEA sponsored research.

Annex V Air Infiltration Centre

The IEA Executive Committee (Buildings and Community Systems) has highlighted areas where the level of knowledge is unsatisfactory and there was unanimous agreement that infiltration was the area about which least was known. An infiltration group was formed drawing experts from most progressive countries, their long term aim to encourage joint international research and to increase the world pool of knowledge on infiltration and ventilation. Much valuable but sporadic and uncoordinated research was already taking place and after some initial ground-work the experts group recommended to their executive the formation of an Air Infiltration Centre. This recommendation was accepted and proposals for its establishment were invited internationally.

The aims of the Centre are the standardisation of techniques, the validation of models, the catalogue and transfer of information, and the encouragement of research. It is intended to be a review body for current world research, to ensure full dissemination of this research and based on a knowledge of work already done to give direction and a firm basis for future research, in the Participating Countries.

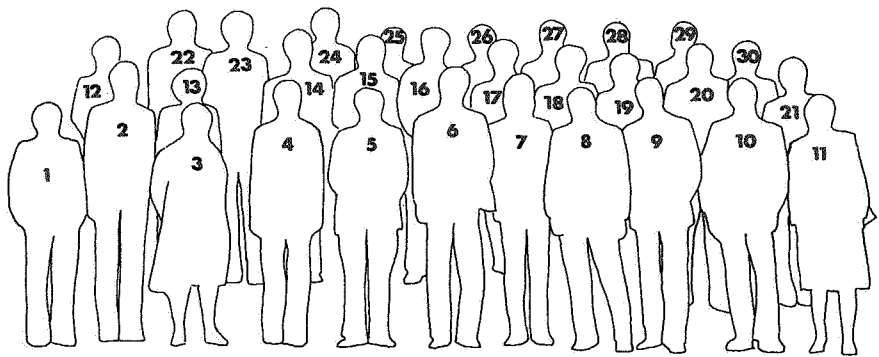
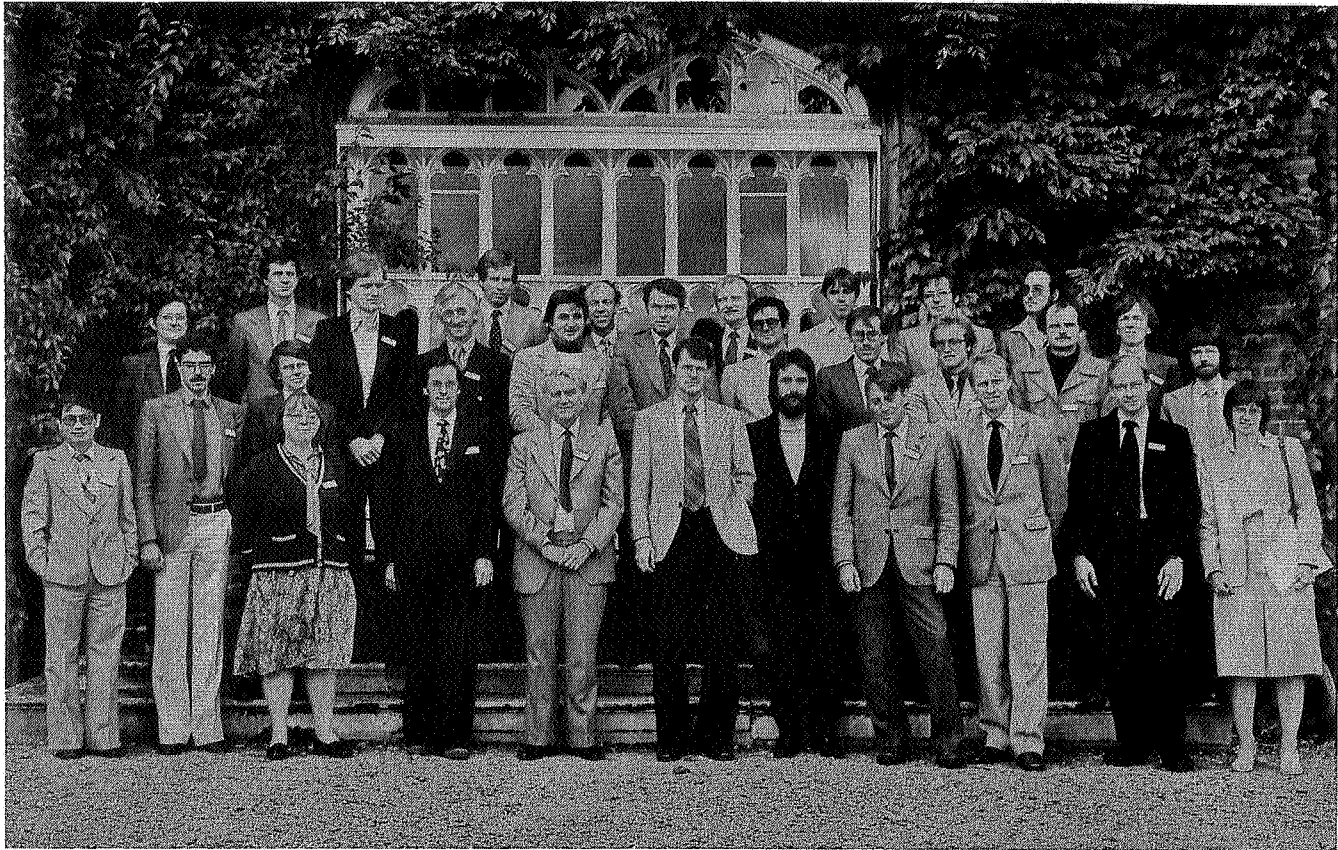
The Participants in this task are Canada, Denmark, Italy, Netherlands, Sweden, Switzerland, United Kingdom and the United States.

1

LIST OF PARTICIPANTS

Name	Organisation
C. Allen	Air Infiltration Centre, U.K.
T. Baumgartner	E.M.P.A. Switzerland
M. Cali	Tech. Politec Turin, Italy
P. Coles	Director, Building Services Research and Information Association, Bracknell, U.K.
P. Collett	Tech. Inst. Denmark
J. Dick	Former Director of the Building Research Establishment, Garston, U.K.
R. Dumont	National Research Council, Canada
A. Elmroth	Royal Inst. Tech., Sweden
D. Etheridge	British Gas, U.K.
R. Gale	SEGAS, U.K.
W. De Gids	IMG-TNO, Netherlands
R. Grot	National Eng. Lab. U.S.A.
D. Harrje	Princeton University, U.S.A.
P. Hartmann	EMPA, Switzerland
G. Huber	ETH Zurich, Switzerland
S. Irving	Oscar Faber, U.K.
P. Jackman	Air Infiltration Centre, U.K.
G. Kennedy	ETSU, U.K.
J. Kronvall	Lund Inst. of Tech., Sweden
P. Levin	Royal Inst. of Technology, Sweden
M. Liddament	Air Infiltration Centre, U.K.
S. Manning	Air Infiltration Centre, U.K.
P. O. Nylund	Tyrens, Sweden
J. Phaff	IMG-TNO, Netherlands
P. Robertson	Glasgow University, U.K.
R. Scott	Birmingham Polytechnic, U.K.
C. Y. Shaw	National Research Council, Canada
M. Sherman	Lawrence Berkeley Lab., U.S.A.
I. Ward	Sheffield University, U.K.
B. Warren	Newcastle University, U.K.
P. Warren	Building Research Establishment, U.K.
B. Webb	Building Research Establishment, U.K.

Participants at 1st AIC Conference



- | | | |
|---------------------|------------------------|----------------------|
| 1. Chia Shaw | 11. Sheila Manning | 21. Martin Liddament |
| 2. Gabriel Huber | 12. Peter Warren | 22. Willem de Gids |
| 3. Carolyn Allen | 13. Peter Robertson | 23. Hans Phaff |
| 4. Peter Jackman | 14. Brian Warren | 24. Steve Irving |
| 5. James Dick | 15. Dick Grot | 25. Peter Hartmann |
| 6. Peter Collet | 16. David Harrje | 26. Gordon Kennedy |
| 7. Rod Gale | 17. Michele Cali | 27. Robert Scott |
| 8. Per Olof Nylund | 18. Thomas Baumgartner | 28. Brian Webb |
| 9. Arne Elmroth | 19. Per Levin | 29. Max Sherman |
| 10. Johnny Kronvall | 20. Rob Dumont | 30. David Etheridge |

PAPER 1 – KEYNOTE ADDRESS

**INSTRUMENTATION AND
MEASURING TECHNIQUES**

J. B. DICK

1. Introduction

I was very interested earlier this year to learn from Mr Jackman, Head of the Air Infiltration Centre, of the proposal to hold a conference on the subject of instrumentation and measuring techniques to assess air infiltration rates. My reaction to his invitation to present a key-note address was rather more mixed ! It is many years since I was engaged in detailed research on ventilation and, although I have retained an interest over the intervening years, it is only recently, as part of some consultancy work on energy conservation, that I have once again become involved in the subject. The question facing me was whether, from my earlier experience in the fifties as a member of the Building Research Station team researching on the ventilation of buildings, I could abstract any information which might be helpful to those working in this field now.

Reflecting on the early work, it was clear that, although perhaps not all the results of the research had been published, most of the major results had found their way into the literature; on the other hand, although we had included in our publications brief descriptions of the instrumentation and measuring techniques used in specific studies, no connected account of our overall approach to the development of our studies had been published. It seemed to me that some discussion of the approach adopted (rather than the results obtained) could still have relevance and might be helpful in setting the scene for your discussions at this conference. It was with this background in mind that I felt able to accept the invitation to prepare a key-note address. The notes which follow briefly outline our approach - an account which, perhaps, can be expanded somewhat in the actual address.

Before describing the development of our approach to the measurement of ventilation rates, I need to describe the context in which our early studies of ventilation were undertaken. During the Second World War a wide range of desk studies relevant to post-war housing were made in the U.K. Problems of heating and ventilation received due attention and the need for research to fill in certain gaps in knowledge was identified. For this purpose, a series of some thirty experimental houses was subsequently constructed; these incorporated a range of different heating systems using different fuels and had various provisions for ventilation and also for insulation of the fabric. The primary task of the ventilation team was to assess the ventilation rates in practice, firstly in the unoccupied houses and subsequently when occupied. The main interest was in two aspects: assessment of actual ventilation rates in rooms from the point of view of standards of ventilation in relation to air purity; and then assessment of rates of heat loss associated with ventilation. The latter results were then to be combined with those obtained by the research team concerned with heating who were measuring fuel consumptions and the temperatures attained throughout the dwellings; in this way an assessment could be made of the overall performance of the systems in their settings. Although priority had to be given to ensuring adequate results from measurements in practice, it was clear that long term progress was dependent on developing a better understanding of the various processes involved which affected the performance both as regards heating and ventilation, and therefore every opportunity was taken to develop related, more specialised studies which

could contribute to this understanding. On the ventilation side, this led to more detailed studies of air movement in rooms, and also of the acting pressures and the effective resistances to air flow in practice. In such ways we tried to develop an integrated approach, supplementing our field studies of what happened in practice by studies of specific factors.

2. Outline of approach to measurement in unoccupied houses

Our starting point for measurement of ventilation was the earlier work undertaken by Marley at the Building Research Station. He had used hydrogen as a tracer gas, measuring its concentration with a katharometer (essentially a thermal conductivity meter) and had shown in a controlled experiment with a known rate of air flow through a room, that this method provided, on the basis of the decay rate of the concentration, a good estimate of the air flow rate. Clearly the extent of the agreement and the accuracy of the method was dependent on the degree of mixing of the incoming air with the air in the room. The question which arose in our minds was whether, in the circumstances with which we were concerned, mixing would be adequate.

We therefore undertook a series of controlled experiments in which we mixed the hydrogen with the air in the room using a fan and then measured the rates of decay in various parts of the room after the mixing fan had been switched off. Clearly, near an inlet, e.g. under a door, one could get much higher rates indicated than in the main body of the room but elsewhere in the rooms we found that the variation in air change rates measured was small; a controlled series of experiments suggested a coefficient of variation between three simultaneous measurements of the order of 8 or 9%. These results were obtained in normal rectangular rooms; we found considerably more variation in the hall and landing space of our two-storey experimental houses, a variation which was mainly due to a ventilator near an outside door which acted as an inlet. Based on these studies, the technique we adopted in the unoccupied houses (which had their internal doors closed) was to use a fan only for initial mixing of the tracer gas and to measure the decay in rooms using a single katharometer placed centrally, but to have at least two katharometers when measuring in hall and landing. We also complemented the measurements in individual rooms by simultaneous measurements of the leakage of tracer gas to adjacent rooms, on these occasions using a slow running fan to help mixing in the adjacent room and thus ensuring that the leakage was detected. From such measurements we could estimate the ventilation loss to outside from the main room being examined.

I should add a few detailed points which were checked regarding the characteristics of the tracer gas and the katharometer measurements:

- (1) Provision was made to absorb water vapour and carbon dioxide which could affect katharometer readings, essentially a diffusion chamber containing Carbosorb.
- (2) The time constant of the katharometer and its diffusion chamber was small compared with the decay constants.
- (3) The effect of the higher diffusion rate of hydrogen as compared with air over the typical path length to outside from a room was small - it was equivalent to a very low air speed.

- (4) There was no sign of absorption or adsorption of the tracer gas on surfaces - processes which can limit the usefulness of some vapour and gases as possible tracers.

3. Approach to measurement in occupied houses

During the first year of the studies, as the programme of measurements of ventilation rates was undertaken in the unoccupied houses, we also started investigating methods by which we might continue our measurements when the houses were occupied. We decided that we should, if at all possible, make these measurements from outside the houses thus avoiding any interference with the living patterns of the occupants. The basic idea was that we should instal a system by which we could pump a tracer into individual rooms and measure its decay by extracting a continuous sample from each room.

Our earlier experience was that, with closed individual rooms, the normal circulation of convection currents down walls and windows, the distributed inlets around windows and doors, and the typical convection from heat sources with their increased eddy diffusion, combined to provide a general mixing process. We recognised that this might not apply universally with all possible systems such as are based on warm air inlets at high level where stratification and temperature gradients would inhibit the mixing process to some extent. I think that there could also be reservations about the mixing that might be achieved in large enclosed spaces where walls in particular would have a smaller contribution to make to mixing. With this background, we now extended our exploration of measuring techniques, recognising that we now had to accommodate cases where windows and internal doors might be open and also that any sampling tubes had to be installed round the perimeter of the room and could not terminate centrally in the room itself.

We started by examining the effects of open windows. We did a series of controlled experiments in which we mixed our tracer gas using a fan in the rooms with windows closed and then measured the rates of decay at three points on the room after the windows were opened. The differences in the rates observed were much larger than in the closed rooms, and it was clear that representative sampling would only be achieved if we sampled from a considerable number of points. This, as related later, did not present undue difficulty.

To introduce and obtain adequate mixing of a tracer gas without the use of a fan was rather more complicated and required a more detailed series of investigations. These were done on the assumption that we could instal 6mm copper tubes running from an external terminal to each room where they could be fitted to the baseboards and would be unobtrusive. The development of this work can be summarised as below:

- (1) Tracer gas introduced at a point, direct from a hydrogen cylinder over a period of 1 minute to give the required concentration of 0.15%; this produced a difference in the maximum concentrations measured near ceiling and floor of 6:1 with a time lag between the peaks of 25 minutes.
- (2) We then tried introducing the gas through copper tubes which were drilled with holes of equal size and ran along two sides of the room; this only gave a slightly better distribution and time lag between peaks.

- (3) The next stage was to improve the uniformity of the input by installing miniature carburettor jets at intervals along the copper tube which could be sized to provide equal flow rates; and also to reduce the buoyancy of the input by using a mixture of about 5 or 6% hydrogen in air (just below the explosive limit !) which was pumped in for a period of about 10 minutes. These modifications produced a radical improvement in the distribution of tracer gas.
- (4) On this basis, the system was further developed in the houses themselves. We had a range of jets with sizes from 0.4mm up to 3mm and these could be screwed into fittings mounted on copper tubing which ran round the baseboards. The number of jets used was between 25 and 40 per room and the sizes used could be selected not only to equalise flow rates but also to tailor the installation to allow for the presence of furniture and to take advantage of convection currents such as those induced by radiators; smaller jets were also used in corners to avoid undue accumulations of tracer gas. Practical trials showed that acceptable distributions were generally being achieved.
- (5) For sampling, a second series of copper tubes was installed also fitted with mountings to accept jets of different sizes as required; some 6 to 8 jets were used to extract equal samples of the air in the room with perhaps half or more of the jets at mid-level up the walls and the remainder along the baseboard; mountings behind furniture which might restrict circulation were sealed.
- (6) One reservation about the system we had developed was that it involved using a mixture of hydrogen and air which was rather close to the explosive limit. It was with some relief that we managed to obtain a supply of helium to use in the occupied houses, a gas suitable for measurement by katharometer and with the further advantage of a rather lower buoyancy in air.

4. Programme of measurements

The techniques described above were applied to measure ventilation rates in the experimental houses in a programme lasting over three years. The main results were published at the time and I do not propose to discuss these in any detail here; rather I shall deal with the experience we gained of the various types of measurements made in practice and with their interpretation.

When the houses were unoccupied, the main emphasis was on measuring ventilation rates in individual rooms together with leakages to adjacent rooms. The results were correlated with temperature difference, wind speed and direction, and estimates were then made of seasonal air change rates and consequent heat loss rates. These measurements were supplemented by direct measurements of house air change rates during which internal doors were open and slow-running fans were used to encourage internal mixing. Some measurements were also made with small windows open and the effects on rates in individual rooms and in houses were assessed.

In the occupied houses, we started by measuring individual rooms but it was soon clear that we were getting two sets of results according to whether the internal doors were open or not; consequently when rooms were obviously linked, we injected tracer gas into both rooms and measured the joint rate of decay. The variability in the position of internal doors and the degree of window opening adopted by the occupants clearly made the task of developing, on the basis of individual room measurements, overall estimates of air change rates for the houses much more difficult

than in the unoccupied closed houses. Consequently, we began placing much more emphasis on measuring the overall air change rate by pumping in tracer gas to achieve the same concentration in each room and then measuring the rate of decay. This approach was later extended to set the initial concentration in each room at a level proportional to the temperature difference above that outside - for the subsequent rate of decay, the heat loss rate by ventilation could be assessed.

5. Complementary studies

I mentioned in the introduction that, although our initial programme had to give priority to measuring ventilation rates in the experimental houses, we also started a complementary set of longer term studies. These studies were concerned with three main topics: the examination of other possible tracers; air circulation processes within rooms; the magnitude of the acting pressures and the resistances in the air flow paths. I shall deal very briefly with each of these in turn.

Carbon dioxide was considered as a possible tracer gas but, apart from a few trials, was not used on any scale because of the need to swamp background variations arising from occupants or appliances such as flueless gas heaters. We also explored the use of radioactive tracers: our first essay was with radioactive ethylene dibromide which was readily available but we encountered difficulties due to absorption of the tracer, particularly on walls. We moved on to explore the use of radioactive argon which we found satisfactory as a tracer although it had some limitations because of its rather short half-life of 2 hours - at the time, a suitable alternative appeared to be radioactive krypton with a half-life of 9 years, but health hazards would have to be checked.

The studies of air movement within rooms were directed at a better understanding of the factors contributing to the air circulation pattern - a pattern which could have implications for the choice of measurement techniques and their interpretation, and is also important as regards the effectiveness of ventilation to occupants of the space. The main studies were concerned with the air flow induced down cold walls and windows, and above heated sources either adjacent to walls or in the centre of the room. The air flow, for example above radiators, was measured by photographing the paths of particles of meta-fuel and also by hot-wire anemometry. This work clearly demonstrated the vigorous mixing which could occur as air was entrained in the various jets and these expanded and circulated in the space. Some work on model studies was also undertaken using point and live heat sources in a small tank containing paraffin oil; it was not possible to simulate simultaneously the laminar and turbulent components of flow in practice, but the results proved useful in a qualitative sense. I would stress the importance of appreciating possible circulation and mixing patterns not only in housing but particularly in larger spaces, such as foundries, where ventilation systems can be designed to take advantage of local airstreams rather than simply providing a general level of ventilation.

The third group of complementary studies was concerned with the pressures promoting air flow and the resistance of the various air passages. A series of measurements was made of the wind pressures acting across the walls of the experimental houses and the results were correlated with wind speed and direction, and compared with the results of model studies in wind tunnels. In the laboratory, systematic measurements were made of the air flow through gaps for a range of different types of windows as pressures and sizes of gaps were varied; we found that the results

could best be expressed in the form $P = AV + BV^2$ where P was the pressure difference, V the volume rate of air flow, and A and B were parameters which could be interpreted as representing the laminar and turbulent aspects of flow respectively. We also studied the air flows induced by flued heating appliances, relating these to their efficiencies and the resistances presented by the flues and the air inlets. We also tried to measure the overall characteristics of individual houses by pressurising them but without success, due mainly to the inadequacy of the fans we had available at the time and also the low sensitivity of our manometers; I was very interested to read in the conference papers of the progress since achieved on this aspect.

6. Conclusions

In my address, I have presented a review based on the early experience of the Building Research Station team engaged on ventilation research in the fifties. Since then there is no doubt that considerable progress has been possible so far as instrumentation is concerned: new tracers; much higher sensitivity in measuring concentrations; modern data processors and recorders; much more effective automatic control systems. On the other hand, it appears to me that the basic problems, so far as techniques of measurement and the subsequent interpretation of results are concerned, have not changed so radically and I hope that my contribution on this aspect will still provide food for thought. In conclusion, I would emphasise once again the need for an understanding of the air circulation and mixing patterns which occur in practice and for a predictive model reflecting the acting pressures promoting ventilation and the various resistances to air flow which are involved. I hope that my reflections will provide a background against which your discussions of the various problems involved will develop profitably at this conference.

PAPER 2

**AIR INFILTRATION MEASUREMENT
TECHNIQUES**

**M. SHERMAN, D. T. GRIMSRUD,
P. E. CONDON AND B. V. SMITH**

**Lawrence Berkeley Laboratory
University of California
USA**

Air Infiltration Measurement Techniques

M.H.Sherman, D.T.Grimsrud, P.E.Condon and B.V.Smith

Energy Efficient Buildings Program

Lawrence Berkeley Laboratory

Berkeley, California 94720

This paper presents a survey of tracer-gas techniques for measuring air infiltration and includes a theoretical derivation of the equations, a description of each method, and a short description of the experimental procedure. A qualitative error analysis which concentrates on mixing problems is derived and used to compare the strengths and weaknesses of each method.

The theory of multi-chamber infiltration measurement is derived for use in situations involving many interconnected spaces (network type models). A set of measurement techniques analogous to the single chamber techniques is discussed along with qualitative error analysis.

The question of effective volume and mixing is addressed for both the single and multi-chamber cases. Also discussed is the general topic of non-tracer techniques for measuring infiltration.

Keywords: infiltration, instrumentation, measurement techniques, tracer gas, decay, continuous flow, long term average.

This paper is to be presented at the first Symposium of the Air Infiltration Centre, entitled "Instrumentation and Measuring Techniques" Windsor, England, October 1980.

ABSTRACT

This paper presents a survey of tracer-gas techniques for measuring air infiltration and includes a theoretical derivation of the equations, a description of each method, and a short description of the experimental procedure. A qualitative error analysis which concentrates on mixing problems is derived and used to compare the strengths and weaknesses of each method.

The theory of multi-chamber infiltration measurement is derived for use in situations involving many interconnected spaces (network type models). A set of measurement techniques analogous to the single chamber techniques is discussed along with qualitative error analysis.

The question of effective volume and mixing is addressed for both the single and multi-chamber cases. Also discussed is the general topic of non-tracer techniques for measuring infiltration.

INTRODUCTION

The measurement of air infiltration has become increasingly important in recent years. In typical United States houses air infiltration accounts for 1/3 of the total heating and cooling loads. As the average insulation value of houses is increased, this fraction will rise. Accordingly, efforts should be made to reduce the infiltration loads in line with the other load reductions. As houses are made tighter to reduce infiltration, air quality can deteriorate and minimum ventilation rates must be established. If we are to balance these competing demands of energy conservation and adequate air quality, it is essential that we be able to accurately measure infiltration.

The work described in this report was funded by the Office of Buildings and Community Systems, Assistant Secretary for Conservation and Solar Applications of the U.S. Department of Energy under Contract No. W-7405-ENG-48.

Current research in infiltration has its origin in the set of three papers published by Dick et al. in the late forties.¹⁻³ Many of the problems we struggle with today were identified in these papers, which remain a starting point for any serious study of research problems in infiltration.

THEORY

One major change which has occurred since the Dick papers has been in instrumentation technology. Virtually all direct measurement schemes use the dilution of a tracer gas to estimate the infiltration; therefore, it is worthwhile to review the equations which govern tracer dilution techniques.

Continuity Equation

If a tracer-gas is released into a space the rate of change of the amount of that gas will be governed by the amount of gas injected and the amount of gas lost.

$$\frac{dV_g}{dt} = F - \frac{dV_e}{dt} \quad (1)$$

where

- t is the time [hr],
- V_g is the volume of tracer in the space [m^3],
- F is the injected flow of tracer from the source [m^3/hr] and
- V_e is the net volume of tracer lost to exfiltration [m^3].

[Note that we have used the word "exfiltration" above. Since there is no net build-up of air within the space, the infiltration and exfiltration will must be equal. Therefore, in general, we will use the word infiltration to mean either air flowing out (exfiltration) or air flowing in (infiltration).]

We can define the average concentration of tracer-gas as being the ratio of the volume of tracer-gas in the space to the volume of the space itself.

$$C = \frac{V_g}{V} \quad (2)$$

where

C is the average concentration of tracer-gas and
V is the volume of the space [m³].

If the concentration of tracer-gas outside the test space is negligible, the rate of volume of tracer-gas lost will be the product of the infiltration and the concentration inside the test space.

$$\frac{dV_e}{dt} = Q C \quad (3)$$

where

Q is the infiltration [m³/hr].

Combining all of these equations together and rearranging terms gives the continuity equation in its standard form:

$$V \frac{dC}{dt} + Q C = F \quad (4)$$

A quantity often used to characterize infiltration is the ratio of the infiltration to the volume of the space, the infiltration rate.

$$A = \frac{Q}{V} \quad (5)$$

where

A is the infiltration rate [hr⁻¹].

The infiltration rate is the number of volumes of room air displaced in a specified period of time (i.e. air changes per hour).

For a gas to be used as a tracer, it must fulfill certain requirements including ease of detectability, low ambient concentration, non-toxicity etc. A survey of commonly used tracer-gases and an experimental intercomparison, which includes a definition of a tracer gas, has been done by Grimsrud et al.⁴

Mixing and Effective Volume

The continuity equation presented was derived using the average concentration and instantaneous flow as the measured quantities. While the injected flow of tracer-gas is usually quite easy to measure, the average concentration is not. Conventional practice has been to measure the concentration in a small number of locations and to assume that this concentration is representative of the average concentration in the test space; however, there are many instances when this assumption may not be adequate.

Most of the inadequacies that arise can be broadly categorized as mixing problems. Mixing problems can be broken down into three types: mixing of fresh air into the space; mixing of tracer-gas into the space; and circulation of air within the space. Each of these mixing problems can have a different effect on the measured concentration.

When fresh air enters the space it may not be dispersed evenly, and this can cause the concentration of tracer-gas to vary from point to point. In a residence, this behavior can cause the average concentration to vary from room to room; the leakier room will have lower concentrations than the tighter rooms, and interior rooms will have higher concentrations than exterior rooms. This effect is not limited to rooms; any area may be affected (e.g. the concentration near walls may well be lower than the interior). If these variations are significant, it may be necessary to use a multi-chamber analysis to properly interpret the measurements.

The second effect that may occur is that air will infiltrate into the space and then exfiltrate out again without mixing. This air infiltration will not affect the concentration and hence will not be reflected in the calculated infiltration. However, in most cases, this type of air exchange is not of interest. If the air enters and leaves without any mixing then it can not affect the heat load nor the indoor air quality.

Another mixing problem arises because the injected tracer-gas does not instantaneously mix within the space. In general, injection and sampling are spatially separated, and there is a delay between the time a volume of tracer is injected into the space and the time the additional volume of tracer is reflected in the concentration. Because of this delay, the infiltration to appear to rise until the gas is well mixed; conversely, if the tracer-gas injection is decreased, incomplete mixing will show up as an apparent increase in the infiltration rate.

The two quantities, delay time and mixing time, can be used to define an effective flow. The effective flow is the flow rate that would account for the observed concentration if the flow were instantaneously mixed; it is related to the actual injected flow by the mixing function.

$$F_{\text{eff}}(t) = \int_0^{\infty} g(t' ; t_m, t_d) F(t - t') dt' \quad (6)$$

where

F_{eff} is the effective flow [m^3/hr],
 g is the mixing function,
 t_m is the mixing time [hr] and
 t_d is the delay time [hr]

The mixing function is normalized to unity.

$$\int_0^{\infty} g(t' ; t_m, t_d) dt' = 1 \quad (7)$$

Figure 1 shows a typical response of the concentration to a step function in flow. If there were perfect mixing, the increase in concentration would follow the flow (i.e. it would be a step function); however, when the mixing is not perfect the rise in concentration is slower and lags behind the flow. The rise-time of the concentration is another characteristic mixing time, and may be called the circulation time. Figure 1 also shows the approximate (normalized) mixing function for the measured site.

The third type of mixing difficulty arises because the physical volume of the space may not be the volume participating in the air exchange. In the derivation of the continuity equation we replaced the volume of tracer-gas by the concentration times the volume of the space. Since this is incorrect if the full volume of the space is not participating, the volume that appears in the continuity equation is not the physical volume of the space but, rather, the effective volume of the space.

The effective volume of the space may be smaller than the physical volume if there are parts of the space that don't communicate well with the rest — closets or cupboards, for example. It is relatively easy to recognize and compensate for these volumes; however, there can be other areas not participating in the air exchange that are quite difficult to identify: stratification may isolate large volumes near the ceiling; corners and alcoves may not communicate well with the interior etc.

Under some circumstances the effective volume may be larger than the physical volume. If there are attached spaces that can communicate with the rest of the living space, the attached volume may contribute to the effective volume. For example, if the air-distribution system goes through an unconditioned attic, basement, or crawlspace there may be significant air leakage, causing the attached space to participate in the air exchange and increasing the effective volume.

Furthermore, the effective volume may be a function of the type of experiment being done. If a particular sub-volume communicates with the rest of the interior, but does so very slowly, then it will be included as part of the effective volume only when the concentration is slowly

varying.

Consequently, we must consider the volume that appears in the continuity equation to be an unknown parameter, much as the infiltration is an unknown parameter. We can, however, begin with the plausible assumption that the effective volume should be roughly the same size as the physical volume.

MEASUREMENT TECHNIQUES

When care is taken to include these consideration regarding mixing and effective volume problems, the continuity equation can be used to compute the infiltration from measured concentration data. There are, however, specific advantages and disadvantages to every technique: some techniques work better for short-term measurements while others work better for longer term measurements; some techniques are less sensitive to mixing problems than others and some techniques use simpler and are less expensive than others. Below is a short description of each of the most popular techniques including a discussion regarding relative advantages and disadvantages.

Decay Technique

The tracer decay technique is by far the most widely used method for measuring air infiltration. It makes use of the solution of the continuity equation for no injected flow assuming that the infiltration rate remains constant.

$$C(t) = C_o e^{-At} \quad (8)$$

where

C_o is the concentration at $t=0$ and
 A is the infiltration rate [hr^{-1}].

Procedure: The tracer detector is connected to a single channel chart recorder (or data may be taken by hand).

A volume of tracer sufficient to bring the concentration of tracer to near the full scale of the analyzer is released. Additional mixing may be used at this point to assure even distribution of the tracer.

The system is allowed to stabilize and data is recorded until the concentration drops well below its starting value (1/2 hr to 2 hrs).

The data is analyzed by fitting the concentration data to a simple exponential. The time constant (coefficient of the time variable) yields the infiltration rate.

If longer term measurements are required, the procedure is repeated.

This system is simple, uses the minimum amount of equipment and is well suited for making short term measurements or spot checks at many sites. The analysis calculates the infiltration rate - the ratio of the infiltration (in m^3/hr) to the effective volume, which is used, in turn, to calculate the infiltration by multiplying it by the physical volume of the space. Therefore, the calculated infiltration will be in error by the ratio of the effective volume to the physical volume, a ratio which can be as large as 50%.

Because a given decay rarely lasts longer than a few hours, to get long-term information it is necessary to repeat the entire procedure frequently; a significant time period must be spent waiting for the mixing to be complete after each injection, making the system inappropriate to use for long term measurements.

Constant Concentration / Constant Flow

The best way to eliminate the problem of finding the effective volume is by finding a way to eliminate it from the continuity equation used to calculate infiltration. Since the coefficient of the effective volume is the time rate of change of the concentration it would be possible to remove any uncertainties due to the effective volume by maintaining a constant concentration. Thus, if there is automated injection with a feedback system to keep the concentration at a desired level the infiltration is simply,

$$Q = \frac{F}{C} \quad (9)$$

where F and Q may be time varying but C is a constant.

In practice, however, this technique is impossible because of the mixing function. The mixing function causes a delay in the response of the concentration to a change in the flow. When sensing no appreciable concentration change, the system continues to change the flow even further, causing an overshoot in the "constant" concentration level. Thus, if the automated system attempts to keep the concentration constant the delay will cause an (unstable) oscillation in the concentration and a breakdown in the experimental design.

The only way to prevent the unstable feedback system is to make the update time of the system long compared to any mixing time. If the update time is long enough (i.e. the loop gain of the system is small enough) the instabilities can be avoided. If this is done, the concentration can only be considered constant on time scales that are long compared to the update time which in turn must be long compared to the mixing times, and therefore, the assumption of constant concentration will be violated for all but the most highly mixed conditions. A modification to the constant concentration technique that might avoid this instability is to make the flow constant.

The constant flow technique minimizes mixing problems because after the initial warm-up period (a time long compared to any mixing time) the mixing function has no effect and the effective flow is equal to the

actual flow (See the mixing function in Fig. 1). However, since the concentration is not constant the volume term will be present; specifically,

$$Q = \frac{F}{C} - \frac{V}{C} \frac{dC}{dt} \quad (10)$$

where

V is the effective volume [m^3].

Care must be taken in interpreting the volume used in any of these infiltration equations. In most cases, the volume referred to by the symbol, "V" is the effective volume and not the physical one.

If the system is near equilibrium, the concentration will be slowly varying and the time rate of change of concentration will be quite small. In this case the last term in the above equation is a small correction term and the error introduced by replacing the effective volume with the physical volume should be negligible.

Procedure: The tracer detector and a mass flow controller (or other flow metering device) are connected to a two pen chart recorder and started.

Enough tracer-gas is released to bring the concentration up to mid-scale on the analyzer.

An estimate of the infiltration is made and used to set the flow so that at equilibrium the concentration should be mid-range on the gas analyzer.

The system is allowed to run continuously and data is considered to be valid once the time rate of change of the concentration is small.

The data is analyzed by using the equation above.

This system has the advantage of being relatively insensitive to the mixing function and minimizes the effect of the (unknown) effective volume. It will run for several days and give continuous infiltration measurements. It does have some disadvantages, however; if the infiltration deviates significantly from the estimate, the gas analyzer will go off scale and data will be lost. If the infiltration changes rapidly, there will be a rapid change in the concentration that will emphasize any effects due to effective volume. The system requires some warm-up time (approximately 1 hr) before the data can be considered valid.

Long Term Average Technique

One of the tasks that needs to be done in order to characterize any nation's housing stock is to make a survey of infiltration rates averaged over long periods of time (i.e. a month). In principle we could use one of the systems above for a month and average the results; however, it would be much more desirable to have a simpler, low-cost system available for such a purpose.

To measure long term average infiltration rates, we average the continuity equation divided by the infiltration.

$$\left[\frac{V}{Q} \frac{dC}{dt} \right] + [C] = \left[\frac{F}{Q} \right] \quad (11)$$

where

$[\dots]$ indicates a time average

If the flow is kept constant,

$$\left[\frac{F}{Q} \right] \rightarrow F \left[\frac{1}{Q} \right] \quad (12)$$

If the averaging interval is long enough (i.e. long compared to the inverse infiltration rate),

$$\left[\frac{V}{Q} \frac{dC}{dt} \right] \rightarrow 0 \quad (13)$$

Combining terms gives an expression for the average of the reciprocal infiltration.

$$\left[\frac{1}{Q} \right] = \frac{\left[C \right]}{F} \quad (14)$$

If the infiltration were constant, then the inverse of the average infiltration would be equal to the average of the inverse infiltration; however, over the long term the infiltration will not be constant. We must, then, define a correction factor, k , that allows us to convert the average of the inverse infiltration to the average infiltration:

$$\left[\frac{1}{Q} \right] = \frac{k}{\left[Q \right]} \quad (15)$$

where

$$k = \sqrt{1 + 2\sigma^2} \quad (16)$$

and σ is the fractional standard deviation of either the infiltration or the inverse infiltration.

Since the inverse average weights the small infiltration values more than the large ones (and more than they would be weighted if a simple average were taken), the correction factor will always be greater than unity.

Procedure: A two channel sampling pump and accessories are brought to the site of interest.

The pump is set so that one channel is used to inflate an initially empty bag with room air; and the other channel is used to evacuate a bag of tracer-gas.

The pump speed and tracer-gas concentration in the

initially full bag are set so that the concentration of gas in the initially empty bag will be within the range of the analyzer.

A volume of tracer-gas sufficient to bring the analyzer up to half scale is released and the pump started.

The equipment is left unattended on site for the duration of the experiment and then picked up and brought back to the laboratory for analysis.

The total amount of gas dispensed is measured by comparing the volume of the initially full bag to its volume after the experiment; the concentration in the initially empty bag is measured and the results used to calculate the average inverse infiltration.

We are currently using this system in the field. Because its concentration can be measured in the range of 1 part in 10^{12} to 1 part in 10^9 , the tracer we have chosen for this use is SF_6 , giving us both high sensitivity and large dynamic range, which are useful for long term average measurements. The analyzer costs about \$7000 but the total equipment cost for each site in the field is about \$500, which makes it inexpensive to do several long term average infiltration measurements simultaneously.

The trade off for the low cost comes is that a correction term is required to convert the average inverse infiltration into the average infiltration. We have used a large set of data⁵ to find values for parameters from the previous equation:

Site	$\left[\frac{1}{Q} \right]$	$[Q]$	σ	k
HTSG	1.22	.85	.21	1.05
HSLG	2.79	.38	.24	1.06

From this set of data we may conclude that the corrected factor is near unity for typical infiltration values, indicating that a independent measurement of the standard deviation of the infiltration will not be necessary.

Continuous Flow

It has been our desire to have a highly accurate continuous infiltration monitoring system that is capable of running unattended for significant periods of time (e.g. a week). In order to accomplish this, we have developed a microprocessor-based continuous-flow infiltration system.

Continuous flow is quite similar to the constant flow technique save that the effective volume is treated as an unknown parameter rather than being approximated by the physical volume. Furthermore, non-linear search routines are used to find the best fit of the unknown parameter over a cycle period to help eliminate random error.

During a cycle the flow is held constant; if we treat the infiltration and effective volume as constants during one cycle period (typically half an hour), the continuity equation can be solved for the concentration as a function of time.

$$C(t) = \frac{F}{Q} + \left[C_o - \frac{F}{Q} \right] e^{-\frac{Q}{V}t} \quad (17)$$

This expression contains three unknown parameters V , Q , C_o . C_o , the best fit to the initial concentration, is a parameter that is of no physical interest, but must be found simultaneously with the other two parameters.

Procedure: The flow rate for a cycle is set equal to a target concentration times the calculated infiltration from the previous cycle. This choice of flow assures that the concentration will always be near the target (usually chosen to be about 2/3 of full scale). If this is the

very first cycle the previous infiltration is assumed to be one physical volume per hour. This assumption is not critical since it is used only to decide what the flow rate for the first cycle should be.

For the first few minutes after the flow has been changed the analyzer is rezeroed using outside air. Aside from checking the zero drift of the analyzer, this time allows for the delay due to the mixing function. Since, in general, the flow will not change very much from cycle to cycle, the wait time necessary to overcome the mixing delays is quite small.

The flow rate is held constant by the use of a mass flow controller for the remainder of the cycle period and concentration data is collected at regular intervals from the tracer-gas analyzer.

At the end of the cycle period the concentration data is used in a simplex^{*} search routine to find the three parameters. The simplex algorithm contains constraints that do not allow the effective volume to vary much from cycle to cycle. The slow updating of the volume has the effect of "homing in" on the effective volume over a period of several cycles. If the effective volume changes slowly over time, this method can accurately follow these changes.

The calculated values are stored on a floppy disk for later use.

The computer monitors both the analyzer and mass flow controller, as well as, setting the mass flow controller and activating the solenoid

* The simplex algorithm is a standard type of nonlinear search routine that finds the set of parameters that have the maximum likelihood of fitting a set of data.

valves which are used to control the flow of sample or zeroing gas to the analyzer. While the infiltration system is in use, the computer can still be used to perform other functions, such as further data reduction or display. Figure 2 presents a block diagram of the continuous flow system.

The operating system for the microprocessor is a single-user time-sharing system called TORX (Task Oriented Real-time Executive), developed at the Lawrence Berkeley Laboratory for use on Z-80 based microprocessor systems.

This system solves the problems of effective volume, mixing and continuous operation; however, it costs about \$20,000 to build and therefore is unsuitable for widespread or short-term measurements.

Non-tracer Techniques

So far, the discussion of measurement techniques has been limited to those involving tracer-gas measurements. Recently much effort has been put into using indirect methods for estimating infiltration. The direct tracer-gas methods all require gas analyzers and on-site equipment for data acquisition. The indirect, non-tracer, methods attempt to correlate infiltration with the weather and structural parameters of the building.

Weather data can be obtained from nearby weather stations (e.g. airports) and requires no on-site equipment. The structural parameters (i.e. envelope leakage, geometry, shielding, and terrain factors) do not change significantly with time and, hence, need be measured only once.

Many researchers ⁶⁻⁸ including the authors ⁹⁻¹¹ have worked on developing models to solve the problem of infiltration prediction. We will present one such model very briefly.

Weather driven infiltration is broken up into two parts: stack driven and wind driven. Equations calculating the stack effect ignore

the wind effect and vice versa.

$$Q_{\text{stack}} = f_s^* A_o \sqrt{\Delta T} \quad (18.1)$$

$$Q_{\text{wind}} = f_w^* A_o v \quad (18.2)$$

where

Q_{stack} is the stack driven infiltration [m^3/hr],
 Q_{wind} is the wind driven infiltration [m^3/hr],
 f_s^* is the reduced stack parameter [$\text{m/s/K}^{1/2}$],
 f_w^* is the reduced wind parameter,
 A_o is the total leakage area [m^2],
 ΔT is the inside-outside temperature difference [K] and
 v is the measured wind speed [m/s].

The model assumes that the leakage of the structure can be characterized by a leakage area (which can be measured using fan pressurization). The reduced stack parameter depends on the leakage distribution, the height of the structure and the absolute internal temperature. To combine the wind and stack effect into one equation, we use the assumption that the infiltration is dominated by turbulent flow.

$$Q = \sqrt{Q_{\text{stack}}^2 + Q_{\text{wind}}^2} \quad (19)$$

where

Q is the total weather driven infiltration [m^3/hr].

These models are very useful because of their experimental simplicity and their great potential for widespread medium accuracy predictions(approx. 20%). However, the models will never be able to substitute for the highly accurate direct measurement techniques. For a complete description and derivation see Ref. 11.

MULTI-CHAMBER INFILTRATION

Whenever the communication between different parts of the interior space is poor, it may be necessary to treat the interior as a collection of separate well mixed spaces. Each space can communicate with every other space, as well as, the outside. To derive the multi-chamber continuity equation, we start with the same type of equation as for the single chamber case.

$$\left[\frac{dV_g}{dt} \right]_k = F_k - \left[\frac{dV_e}{dt} \right]_k \quad (20)$$

The subscript k denotes the k th chamber; hence, if there are N chambers there are N such equations.

The net amount of tracer that exfiltrates from each chamber is dependant not only on the total exfiltration but also on the infiltration from all the other chambers.

$$\left[\frac{dV_e}{dt} \right]_k = \sum_{j \neq k} \left[\frac{dV_e}{dt} \right]_{kj} - \left[\frac{dV^i}{dt} \right]_{kj} \quad (21)$$

where

$\left[\frac{dV_e}{dt} \right]_{kj}$ is the exfiltration from room k to room j

$\left[\frac{dV^i}{dt} \right]_{kj}$ is the infiltration from room j to room k .

This definition of air flows includes the inherent redundancy that infiltration into room a from room b is also exfiltration out of room b to room a :

$$\left[\frac{dV^i}{dt} \right]_{jk} = \left[\frac{dV_e}{dt} \right]_{kj} \quad (22)$$

We now introduce the concentration, much as we did before, as the ratio

of the volume of tracer-gas to the volume of the test space:

$$C_k = \frac{\left[\frac{V_g}{V_k} \right]_k}{V_k} \quad (23)$$

where

V_k is the volume of the kth chamber.

If we define the air flow, Q_{kj} , as the negative of the air flow from room j to room k,

$$Q_{kj} = - \left[\frac{dV^i}{dt} \right]_{kj} = - \left[\frac{dV^e}{dt} \right]_{jk} \quad \text{for } j \neq k \quad (24)$$

From these expressions we can rewrite the net exfiltration term,

$$\left[\frac{dV^e}{dt} \right]_k = \sum_{j \neq k} \left[Q_{jk} C_k - Q_{kj} C_j \right] \quad (25)$$

Since the total amount of air that flows into each room must be equal to the total amount of air that flows out, the total infiltration must equal the total exfiltration.

$$\sum_{j \neq k} Q_{kj} = \sum_{j \neq k} Q_{jk} \quad (26)$$

Up to now the diagonal elements of the infiltration matrix (Q_{kk}) have been undefined. The above expressions suggest a convenient definition for them; the element Q_{kk} is the total air flow either in or out of the kth space:

$$Q_{kk} = \sum_{j \neq k} -Q_{ji} = \sum_{j \neq k} -Q_{kj} \quad (27)$$

where

Q_{kk} is the total exfiltration out of room k.

This definition of the infiltration matrix has several interesting properties: all of the off-diagonal elements are negative and all of the diagonal elements are positive, making it a positive definite matrix; the sum of any row or any column is zero, which is an explicit statement of the fact that total amount of air flowing into each space is equal to the total amount flowing out.

The equation for the net exfiltration becomes,

$$\left[\frac{dv_e}{dt} \right]_k = -v_k \sum_j Q_{kj} C_j \quad (28)$$

which leads to the expression governing multi-chamber infiltration.

$$v_k \frac{dC_k}{dt} + \sum_j Q_{kj} C_j = F_k \quad (29)$$

The "Zeroth" Chamber - Outside

Thus far, we have implicitly been treating the outside as one of the N chambers in our multi-chamber derivation; it is, however, a very special chamber and merits special consideration. Treating the outside as a chamber of infinite volume means that the concentration of tracer-gas will always be zero, trivializing its continuity equation:

$$V_0 = \infty \quad (30.1)$$

$$C_0 = 0 \quad (30.2)$$

$$V_0 \frac{dC_0}{dt} = F_0 \quad (30.3)$$

where

C_0 is the concentration of tracer-gas outside

V_0 is the volume of outside and

F_0 is the tracer flow injected outside.

These equations contain no useful information and therefore can be eliminated from the multi-chamber equations without loss if care is taken to insure that the definition of the diagonal elements of the infiltration matrix (Q_{kk}) are properly defined. In the previous section we defined the diagonal elements of the infiltration matrix so that the sum of any row or column would be zero:

$$\sum_{k=0}^N Q_{kj} = 0 \quad \text{for all } j \quad (31.1)$$

$$\sum_{k=0}^N Q_{jk} = 0 \quad \text{for all } j \quad (31.2)$$

If we eliminate the zeroth chamber from the sums, the sums will no longer be zero but, rather, will yield the values of the infiltration and exfiltration from the outside to each chamber:

$$\sum_{k=1}^N Q_{kj} = -Q_{0j} \quad \text{for all } j \quad (32.1)$$

$$\sum_{k=1}^N Q_{jk} = -Q_{j0} \quad \text{for all } j \quad (32.2)$$

where

$-Q_{0j}$ is the infiltration from the outside to room j and

$-Q_{j0}$ is the exfiltration from room j to the outside.

We now stipulate the convention that all sums are to be taken from 1 to N , explicitly excluding the outside chamber. To recover the infiltration or exfiltration between a chamber and the outside, we can sum the appropriate row or column in the matrix.

Matrix Notation

The multi-chamber continuity equation can be put into matrix notation, but we must first define the volume matrix:

$$V_{kj} = V_k \delta_{kj} \quad (33)$$

where

δ_{kj} is the kronecker delta function.*

Now the continuity equation becomes,

$$\bar{V} \frac{d\bar{C}}{dt} + \bar{Q} \bar{C} = \bar{F} \quad (34)$$

where

\bar{V} , \bar{Q} are two dimensional matrices and

\bar{C} , \bar{F} are vectors (one dimensional matrices).

This notation offers great simplicity in expression, and we will use it whenever possible.

Mixing and the Volume Matrix.

In multi-chamber infiltration, all of the mixing problems (delay times, mixing functions, and effective volumes) exist for each chamber and can be handled in the same manner as in the single chamber case. However, there is one type of mixing that is peculiar to the multi-chamber problem: short-circuiting.

Short-circuiting occurs when flow that is injected to one chamber does not mix with the air in that chamber but, rather, flows directly into another chamber and adds to the concentration in that chamber. For example, this could happen if a small air current took part of the

*The kronecker delta is equal to 1 if $k=j$ and is equal to zero if $k \neq j$.

injected tracer and blew it into an adjacent room. Another way this could happen is if there were a leak in the tracer distribution system that allowed the gas to appear in one chamber when it was attributed to another.

Since the effect of short-circuiting is to increase the concentration in one chamber caused by flow in another, it will appear as an off-diagonal element in both the infiltration matrix and the volume matrix. The appearance of additional off-diagonal elements in the infiltration matrix is difficult to detect; since there are no off-diagonal elements in the volume matrix without short-circuiting, the appearance of any off-diagonal elements in the volume matrix can be attributed to short-circuiting. This fact can be used to find the amount of short-circuiting and, if the volume matrix is measured, correct for it. Conceptually, short-circuiting of a measured flow rate is equivalent to injecting a different flow without short-circuiting. This relationship allows the definition of an effective flow rate.

$$\bar{V} \frac{d\bar{C}}{dt} + \bar{Q} \bar{C} = \bar{F}_{eff} \quad (35)$$

where

\bar{F}_{eff} is the effective tracer flow.

We relate the effective flow to the actual flow by the short-circuiting matrix.

$$\bar{F}_{eff} = \bar{S} \bar{F} \quad (36)$$

where

\bar{S} is the short-circuiting (S) matrix.

Substituting the measured flow and short circuiting matrix in and multiplying through by the inverse of the S matrix,

$$\bar{V}_m \frac{d\bar{C}}{dt} + \bar{Q}_m \bar{C} = \bar{F} \quad (37)$$

where

\bar{V}_m is the measured volume matrix and

\bar{Q}_m is the measured infiltration matrix.

The measured quantities are related to the actual quantities and the S matrix.

$$\bar{V}_m = \bar{S}^{-1} \bar{V} \quad (38.1)$$

or,

$$\bar{S} \bar{V}_m = \bar{V} \quad (38.2)$$

and

$$\bar{Q}_m = \bar{S}^{-1} \bar{Q} \quad (39.1)$$

or,

$$\bar{S} \bar{Q}_m = \bar{Q} \quad (39.2)$$

Since the real volume matrix is diagonal, the off-diagonal elements of the product of the short-circuiting and measured volume matrices must be zero.

$$\sum_k S_{ik} \left[\bar{V}_m \right]_{kj} = 0 \quad i \neq j \quad (40)$$

This set of equations alone is not sufficient to determine the S matrix. We must make use of the fact that the total amount of tracer injected is the same regardless of any short-circuiting (i.e. the S matrix is normalized).

$$\sum_j S_{kj} = 1 \quad \text{for all } k \quad (41)$$

Once Eqs 41 and 42 have been used to find the elements of the short-circuiting matrix, Eq. 40 can be used to find the actual infiltration from the measured infiltration.

Measurement techniques

The continuity equation for multi-chamber infiltration has exactly the same form as that for single chamber infiltration. This suggests that the same type of measurement techniques could be used to find the infiltration.

Several authors^{12,13} have made multi-chamber calculations but very little field data has been taken. While each of the single chamber analysis schemes may be used for multi-chamber analysis, much more data must be taken to validate the measurement schemes. Because the number of unknown parameters scales as the square of the number of chambers. N^2 times as many independent data points must be taken to get the same results. In some cases, sufficient data may be acquired by increasing the length of time needed for the measurements but it is conceptually simpler to use N independent tracer-gases and measure the concentration of each gas in every chamber, thus giving the factor of N^2 more data without increasing the length of the experiment. The infiltration is a function of time; therefore, the increased length of the single gas experiment is likely to be prohibitive given that the quantity measured is changing during the course of the experiment.

Decay: In a multi-chamber decay all of the flows are set to zero.

$$\bar{C}(t) = e^{-\bar{A}t} \bar{C}_0 \quad (42)$$

where

$\bar{A} = \bar{V}^{-1} \bar{Q}$ is the infiltration rate matrix and

\bar{C}_0 is the initial set of concentrations

Care must also be taken in defining of the infiltration rate matrix; while all elements are well defined, only the diagonal elements have easily interpretable meanings: they are the rate of total infiltration

We have used a matrix as the exponent; this has meaning only through the context of an infinite series and cannot be expressed in simple terms otherwise.

from all spaces (including outside).

Constant Concentration/Constant Flow: In a constant concentration experiment, the concentration of gas in each space is held constant.

$$\bar{Q} \bar{C} = \bar{F} \quad (43)$$

This experiment cannot be done with only one gas, unless several completely independent runs are made. Using separate runs makes the rather poor assumption that the air flows will be the same for each run. In either case, we construct a concentration matrix and an injected flow matrix, whose columns in both cases are either different runs or different gases, and whose rows (as before) are different chambers and an injected tracer flow matrix having the same properties.

$$\bar{Q} \bar{C} = \bar{F} \quad (44)$$

Solving for the infiltration directly yields,

$$\bar{Q} = \bar{F} \bar{C}^{-1} \quad (45)$$

As can be seen from this expression, the requirement of independent runs or different gases are necessary to keep the concentration matrix from becoming singular.

In the constant flow case, the (diagonal) physical volume matrix is used as a correction term for the above expression.

$$\bar{Q} = \bar{F} \bar{C}^{-1} - \bar{V} \frac{d\bar{C}}{dt} \bar{C}^{-1} \quad (46)$$

where

\bar{V} is the physical volume matrix

A version of this technique is being used by British Gas.¹⁴

Long Term Average: Although long term average multi-chamber infiltration can be considered, it must be done with separate gasses because it is impossible to do several independent runs over such a long period of time. It is the inverse of the infiltration that is calculated, as

in the single chamber case.

$$\left[\bar{Q}^{-1} \right] = \bar{F} \left[\bar{C}^{-1} \right] \quad (47)$$

There is as in the single chamber case, a correction factor, k ; however, in the multi-chamber case, k will be a matrix and, without actual measurements, it is difficult to interpret the importance of this correction factor.

Continuous Flow: The continuous flow method uses the full solution to the multi-chamber continuity equation.

$$\bar{C}(t) = \bar{Q}^{-1} \bar{F} + e^{-\bar{V}^{-1} \bar{Q} t} \left[\bar{C}_0 - \bar{Q}^{-1} \bar{F} \right]$$

The single chamber algorithm could be adapted for use in the multi-chamber problem. In each chamber one and only one tracer-gas would be injected and it would be controlled using that diagonal element of the infiltration matrix as was done for the single chamber model. The simplex algorithm could be adapted to include the $3N^2$ unknown parameters in the above equation.

CONCLUSION

We have presented a spectrum of different types of infiltration measurement techniques. Each technique has certain advantages and disadvantages, and each technique is better suited for one type of task than another. Decay measurements are well suited for spot measurements; constant-flow measurements are well suited for medium-length, semi-automatic experiments; long term average measurements are good for low-cost low-to-medium accuracy data averaged over a period of time; and continuous flow is good for long-term, high-accuracy continuous infiltration measurements. Each type of measurement can, in principle be used in a multi-chamber mode; however, very little field data has been accumulated on multi-chamber infiltration.

Each technique handles the problems of mixing/effective volume in a slightly different way. The decay technique ignores the problem of effective volume and solves the mixing time problem by waiting; constant flow eliminates the mixing time and simultaneously minimizes the effective volume problem in steady-state as does the long-term average infiltration technique; and the continuous flow technique eliminates the effective volume problem by calculating it, and minimizes the mixing problem by having quasi-constant flow.

Infiltration-pressurization correlations are, potentially, the superior method for predicting infiltration loads and long term indoor air quality concerns. Such correlations involve a one-time set of measurements, for quantifying the structure leakage and terrain parameters. From these measurements the infiltration can be calculated at any time from readily accessible weather data.

In situations where the interior of a structure is divided into several communicating sub-sections it may be necessary to invoke a multi-chamber infiltration algorithm to analyze the air flows. We have developed the equations governing multi-chamber infiltration, and have indicated ways in which the single channel measurement techniques can be modified in order to incorporate multi-chamber features.

REFERENCES

1. J.B. Dick, "Experimental Studies in Natural Ventilation of Houses," J. Inst. Heat. Vent. Eng. 17, 420 (1949)
2. J.B. Dick & D.A. Thomas, "Ventilation Research in Occupied Houses," J. Inst. Heat. Vent. Eng. 19, 306 (1941)
3. J.B. Dick, "The Fundamental of Natural Ventilation of Houses," J. Inst. Heat. Vent. Eng., p. 123, (1950)
4. D.T. Grimsrud, M.H. Sherman, J.E. Janssen, A.N. Pearman, D.T. Harrje, "An intercomparison of Tracer Gases Used for Air Infiltration," ASHRAE Trans. 86, (1980), Lawrence Berkeley Laboratory Report, LBL-8394 (1979)
5. G. Reeves, M. McBride, C. Sepsy, "Air Infiltration Model for Residences," ASHRAE Trans. 85 Part 1, (1979)
6. A. Blomsterberg D. Harrje, "Approaches to Evaluation of Air Infiltration Energy Losses in Buildings," ASHRAE Trans 85, Part I:PH-79-10, (1979).
7. A.K. Blomsterberg, M.H. Sherman, D.T. Grimsrud, "A Model Correlating Air Tightness and Air Infiltration," Proc. Conf. Thermal Perf. Ext. Env. of Buildings, (1979)
8. D.K. Alexander D.W. Etheridge, "The British Gas Multi-cell Model For Calculating Ventilation," ASHRAE Trans. 86, Part I, (1979).
9. M.H. Sherman, D.T. Grimsrud, R.C. Diamond, "Infiltration-Pressurization Correlation: Surface Pressures and Terrain Effects," ASHRAE Trans. 85 Part II:DE-79-1, (1979)
10. M.H. Sherman, D.T. Grimsrud, "Infiltration-Pressurization Correlation: Simplified Physical Modeling," ASHRAE Trans 86 Part II,

(1980), Lawrence Berkeley Lab LBL-10163 (1980).

11. M.H. Sherman, D.T. Grimsrud, "Measurement of Infiltration Using Fan Pressurization and Weather Data," Proc. Air Infiltration Conference, Windsor, UK (1980), Lawrence Berkeley Lab LBL-10852 (1980)
12. D.T. Grimsrud, M.H. Sherman, R.C. Diamond, P.E. Condon, A.H. Rosenfeld, "Infiltration-Pressurization Correlations: Detailed Measurement on a California House," ASHRAE Trans. 85 Part I (1979), Lawrence Berkeley Laboratory LBL-7824 (1978).
13. F. Sinden, "Multi-chamber Theory of Air Infiltration," Build. Environ. 13, 21 (1978).
14. D.K. Alexander, D.W. Etheridge R. Gale, "Theoretical and Experimental Studies of Heat Loss Due to Ventilation," Proc. XXI Int. Cong. Building Services Eng. (1980)

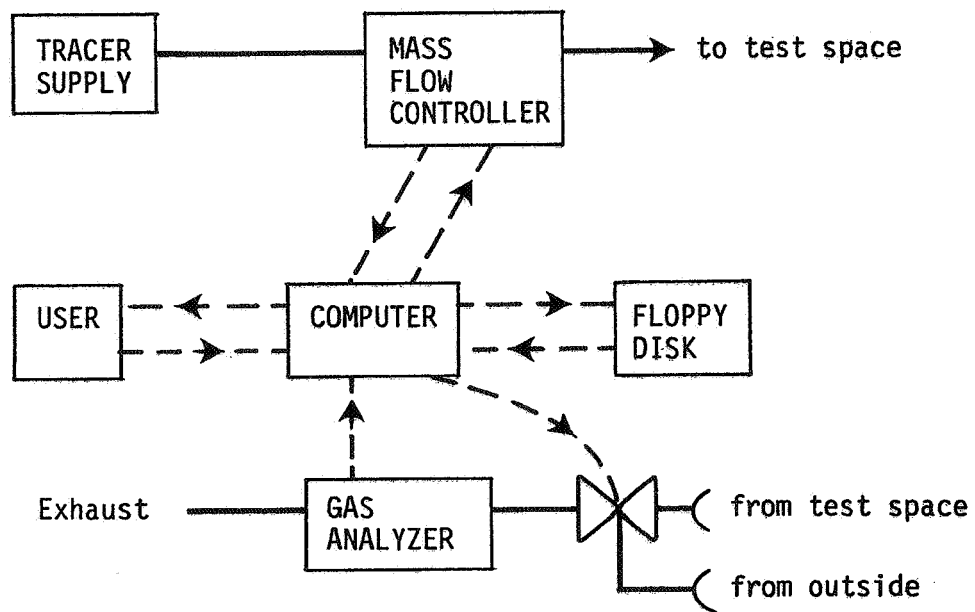
ACKNOWLEDGEMENT

The authors would like to thank Dave Krinkel for mothering the gas analyzers, Philip Strong for writing some of the computer software and finally, out group leader, Robert Sonderegger, for allowing us to build yet another infiltration measuring system.

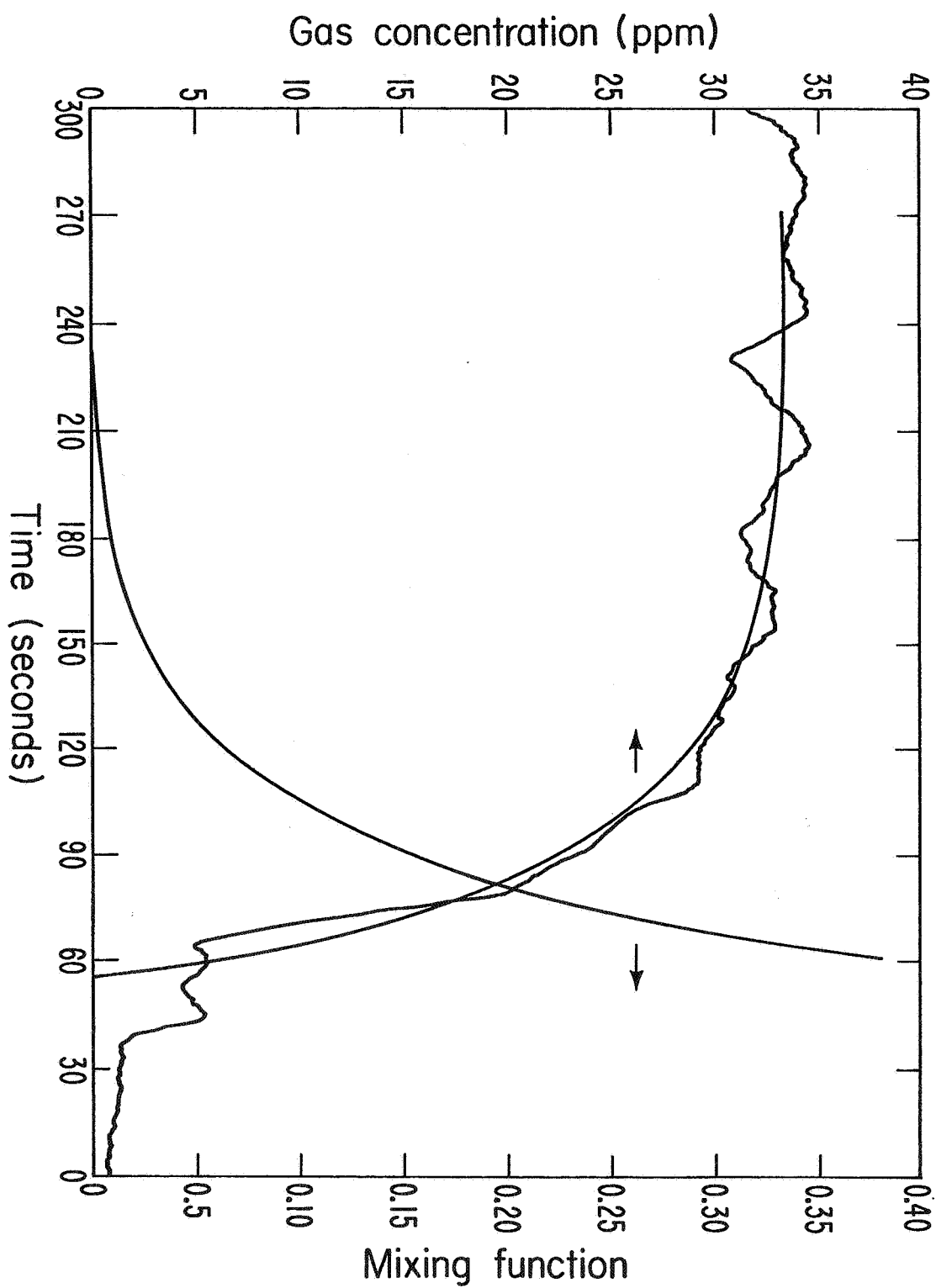
LIST OF FIGURES

- 1 The response of the concentration to a step function in flow is plotted vs. time. The flow was turned on at $t=0$ and the concentration recorded as a function of time. Also shown is the approximate mixing function for this situation. Note there are two scales.
- 2 Block diagram of the continuous flow infiltration system using a Z80 microprocessor, floppy disk, mass flow controller and gas analyzer.

AUTOMATED INFILTRATION SYSTEM



XBL 802-375



XBL 783-469

PAPER 3

**EXPERIMENTAL TECHNIQUES FOR
VENTILATION RESEARCH**

**D. K. ALEXANDER,¹
D. W. ETHERIDGE¹ AND R. GALE²**

**1. British Gas Corporation
London
UK**

**2. Segas
London
UK**

British Gas Corporation,
Research and Development Division,
Watson House,
Peterborough Road,
London, SW6 3HN

EXPERIMENTAL TECHNIQUES FOR VENTILATION RESEARCH

D.K. Alexander*, D.W. Etheridge* and R. Gale⁺

* British Gas, Watson House, London.

⁺ SEGAS, Central Laboratories, London.

1. INTRODUCTION

Ventilation has always been of interest to the Gas Industry, primarily for providing combustion air but more recently because of the desire for energy conservation. As a result of this British Gas has a continuing programme of research, and experimental techniques which have been used or developed during the course of this work form the subject of this paper. In addition, the opportunity is taken to comment on experimental techniques in general.

The paper is divided into the three main areas of experimental work, i.e. physical modelling, measurement of open areas and leakages, measurement of ventilation rates.

To be presented at AIC Conference "Instrumentation and Measuring Techniques", Cumberland Lodge, Windsor, October 1980.

2. PHYSICAL MODELLING TECHNIQUES

2.1 Pressure Distribution

The surface wind pressures on a dwelling are of considerable importance to an accurate ventilation prediction method. Rather than field measurements, which are held at the mercy of the weather, the pressure distributions are more easily derived from wind tunnel measurements on scale models. Provided that sufficient care is taken in the design of model and tunnel the results may be accurately applied to full scale (1,2). Attention must be given to the proper matching of the building model scales and wind profile and turbulence. British Gas, in a 2m x 1m wind tunnel, use a model scale of $1/200$ which also allows a great deal of the surrounding environment to be included. Wind profile and turbulence are modelled in a manner similar to that described in (3).

The most usual forms of presentation are dimensionless coefficients, relating surface pressure to a reference pressure and air speed. Much work has been done on generalising these coefficients for simple shapes and arrays (4). These have been obtained for rather idealised cases however and their use would therefore seem to be limited to more general long-term predictions. Higher accuracy in ventilation predictions, such as are desirable for monitoring test houses, will require measurements on a specific scale model.

In addition to the mean surface pressures, there has been increasing awareness of the need for the fluctuating pressures to be known. Pulsating airflows will produce an effective ventilation which could not be accounted for in a method assuming only steady conditions. Provided that the turbulence and the surroundings are correctly modelled, pressure fluctuations may also be determined in a wind tunnel. Uncertainties arise because of difficulties in providing a suitable constant reference pressure and because the measurements only indicate surface fluctuations. It is the fluctuations of pressure differences across openings which are really required and at present these can only be estimated.

In spite of the above difficulties, the determination of surface pressure distributions from wind tunnel models seems to be an established procedure.

2.2 Ventilation Rates

Several techniques for determining ventilation rates in models have been described, e.g. tracer decay methods used by British Gas (5, 6), anemometers (7) and calibrated openings (8). However, there has been less consideration given to the problem of applying the results to full-scale. This problem is very important because one must question the value of model tests if the results cannot be extended with confidence to full-scale conditions.

In (9) it was argued that ventilation arising through cracks is influenced by viscosity even at full-scale and therefore one would expect the scale effect of Reynolds number to be evident in model results. This was demonstrated by tests carried out on simple model windows. Even for the wind direction for which ventilation was due mainly to turbulent pressure fluctuations, there was evidence of the same effect. Although this behaviour was not evident at low wind speeds, thus indicating no strong dependence on Reynolds number (see the preliminary presentation of results in (10)), later examination indicated that the ventilation rates measured at these speeds were not due solely to pressure fluctuations (see (9)). This was a manifestation of another problem with models, namely that the flow rates under investigation are often small.

When the tests were carried out with sharp-edged holes, as expected the results showed little dependence on Reynolds number. The mean pressure difference across the windows $\overline{\Delta p}$ also showed little variation with Reynolds number and this is also to be expected because of the geometry of the model.

Recent full-scale studies in a house (11) using a novel fluctuating pressurisation technique indicated that the expected effect of viscosity was not present. This is rather surprising, because it is difficult to think of a physical mechanism which could eliminate the effect at low Reynolds numbers. A possible explanation is that the openings in the dwelling which was tested were predominantly of the purpose-provided type, so that even at the very low pressures the leakage was mainly comprised of flows with a constant discharge

coefficient.

As far as is known only one comparison has been made between model-scale and full-scale results. This was done for openings with sharp edges and one might therefore expect good agreement. In the preliminary presentation of results (5), good agreement was indicated, but a recent re-examination suggests that this was incorrect. The data was not properly non-dimensionalised (a criticism not confined to (5)) and when a proper comparison is made poorer agreement is found, as shown in Figure 1. The explanation for this lack of agreement probably lies with the pressure distribution. In the wind tunnel the surroundings of the building were not modelled, and it was not possible to model the wind turbulence accurately. Errors due to these factors could well be magnified because the openings were concentrated at two points on the building, thereby making extreme demands on the accuracy of the model pressure distribution. Another reason for the differences in Figure 1 is the fact that there were some adventitious openings in the full-scale building. However, the maximum allowance that can be made for this is to reduce the full-scale values by 25%.

To summarise all of the above, one must be pessimistic about the value of model-scale ventilation rates for providing full-scale data. For small cracks one is faced with the problem of the scale effect of Reynolds number. For sharp-edged openings which are concentrated at discrete points, an accurate pressure distribution is required. In both cases there is the additional difficulty of matching the model size and the turbulence length scales. Failure to do this introduces another scale effect. To achieve it however requires a very small model (at least $1/200$ scale) and this makes construction of the model very difficult and introduces problems of measuring ventilation rates.

3. MEASUREMENT OF OPEN AREAS AND LEAKAGES

Open areas and/or leakages are required for two basic reasons, (i) as a means of characterizing the ventilation potential of buildings or components, and (ii) to provide data for prediction methods.

Leakages are usually measured with a steady pressure across the component and a variety of equipment has been developed for this

purpose. The equipment currently in use by British Gas will be described in Section 3.4. Recently a novel alternating (AC) pressurisation technique has been used for determining the leakage of dwellings (11). It is claimed that this gives greater accuracy than the conventional DC technique at low pressures, because the noise introduced by external pressures (due to weather) can be eliminated. The leakage Q is not actually measured, but a value can be calculated from the pressure response of the structure at the driving frequency of the mechanical piston.

Although the above technique does not need a measurement of Q , it still requires measurement of very low pressures and this is often a source of error. The basic problem is that pressure differences encountered with natural ventilation are often very low, typically 2 Pa, and it can be argued that leakages should ideally be measured at this level.

There is however, a simpler alternative method for characterising the ventilation potential of components. It requires only one measurement of Q and $\overline{\Delta p}$, and this can be done at a pressure well above pressures induced by the weather. The result obtained however applies at very low pressures. The method relies on the fact that the geometry of a component is virtually independent of the flow rate passing through it and the pressure applied across it. Thus, if a parameter of the geometry is determined at a high flow rate, it will remain valid at all flow rates. The method is described in (10) and the geometric parameter is the open area A of the component, as determined from homogenous flow equations. Once A is determined, the flow rate Q at any steady pressure difference can be found from the flow equation. Whether or not the method can be generally applied to complete buildings remains to be seen, but it has been used with reasonable success for background leakage areas of rooms and this is encouraging.

3.1 Purpose-provided openings

Purpose-provided openings such as air vents and open windows are fairly easy to treat. There is little ambiguity about the definition of their open area, and indeed this can be measured with a ruler, i.e. mensuration.

3.2 Component Openings

For simple components, the open area can be obtained from mensuration, but in general pressurisation will be required. The crack flow equations described in (10) apply to only fairly limited types of crack, but it has been found that they can be used for the complex openings which are encountered in practice. This is illustrated in Figure 2. The fundamental point to note is that A is independent of pressure difference.

In contrast an effective orifice area A_E , which is defined by taking a constant value for the discharge coefficient, varies with Δp . Since the predicted flow rate is given by $Q = 0.6 A_E \sqrt{2 \Delta p / \rho}$, Fig.2 shows that a value of A_E measured at 20 Pa say, can considerably overestimate the flow rate at 2 Pa. As a ventilation characteristic, A_E is therefore unsatisfactory and needs to be used with caution.

3.3 Background Leakage Areas

Background leakage areas are all those not accounted for by the previous two categories. They are by definition those leakage areas left over when the purpose-provided and component openings have been sealed. Taken globally, for it would be difficult and perhaps pointless to treat them singly, the background areas of rooms may be characterised fairly well by an effective open area and crack-flow equations (10).

The data necessary to derive these parameters comes in the main from pressurisation measurements on, say, a room in a house. By themselves such measurements would produce the total open area of the room. Purpose-provided and component openings may be sealed but those background areas which communicate between interior spaces will still be included. These areas may account for considerable leakage but are not of direct relevance to fresh air entry.

To aid in determining the distribution of background areas necessary for accurate prediction methods,* techniques allowing a more direct measure of the parameters of interest are being investigated by British Gas. The total exterior leakage of a room, neglecting complications due to cavity walls, may be determined if

* the leakage distribution is an important part of the data required for "Vent", the British Gas method (17).

the rest of the building is balanced to the same pressure as the room under test. There will then be no flow to other interior spaces (leakage to adjoining houses may also be determined in this way). However, not all of the necessary information can easily be produced in this way. There are practical difficulties in distinguishing between external leakages through walls and through ceilings, or floors, but this needs to be done because the former will be more susceptible to wind pressures than to stack effect pressures.

A further technique, using a tracer gas in conjunction with pressurisation, has been developed. A tracer is injected into a communicating space, e.g. loft, to a constant concentration. The room under test is depressurized and the external leakage measured as described above. Now, however, the ratio of the steady-state tracer concentrations of the room and injected space gives the ratio of the leakages from the injected space (loft) and from the other areas (walls). This procedure is not much more complicated than the first and conceivably could be used to determine leakages to all communicating areas of a room. The technique may also be of use in determining the leakage characteristics of large buildings, where overall pressurisation may be difficult.

These techniques have been used successfully as shown in Figure 3, where the individual room leakage characteristics of a test house have been investigated.

3.4 Whole-House Leakage Characteristics

The whole-house leakage is the simplest and fastest quantity to measure and as such it provides the least information. The total leakage characteristic is generally measured at pressures large enough to overcome those generated by weather conditions. This is useful for purposes of comparisons, however the large pressures used may affect the relevance of the leakage measurement to ventilation characteristics.

The whole-house leakage is a global characteristic and as such would not seem to be a good basis of ventilation prediction, because no indication of the locations or communications of the measured leakage is given. For example, two houses with the same measured

leakage, one of which has all the open area on external walls, the other dividing the area between floor and ceiling, would conceivably have quite different ventilation characteristics even if sited side by side.

Figure 4 shows the results of a preliminary investigation of the relation between measured leakage and ventilation. Ventilation measurements were to be done in a number of identical houses, concurrent with a measurement in a control house. Thus the ventilation rate of a house, relative to the ventilation measured simultaneously in the control, could be compared to its leakage relative to the control house. Practical difficulties experienced in the measurement of ventilation in occupied houses, and in organising sufficient access precluded any definite conclusions. A number of the comparisons needed to be done with data from a regression model of the control house (this is felt to be reasonable as the model was produced from nearly 60 hours of measurements under the weather conditions experienced for all tests). There does not appear to be any useable relation between leakage and ventilation. It is felt that long-term experiments similar to this, comparing simultaneous measurements to eliminate the effect of weather, will be needed to determine any useful relationship between these two characteristics.

A further complexity in relating leakage and ventilation is the apparent variation with time of the whole-house leakage. As well as a possible seasonal variation there appears to be considerable changes in a building as it settles and ages from its "new" state. Recent tests on several nominally identical houses showed, as well as large variations between houses, an average increase in total leakage of 70% over the first two years of occupancy, with most of this change apparently occurring in the first year. As, unfortunately, the easiest and most convenient time to make such measurements is before occupation, the leakages measured may not reflect those found in occupied homes.

The leakage equipment used by British Gas has advantages in occupied houses. It is small, easily transported and set up and as such causes little disruption in use. A high-pressure/high-

volume centrifugal extractor is used, allowing an accurate conical inlet meter (12) and narrow flexible outlet ducting. Installation can be made through a small openable window. The equipment can be used as a module for leakier buildings (see Plate 1).

4. MEASUREMENT OF VENTILATION RATES WITH TRACER GAS

There are three main variants on the tracer gas theme, i.e. constant emission, tracer decay and constant concentration (13). Each method has strengths and weaknesses and each has suitable applications. The emphasis of our work has been on determining individual room ventilation rates and as such the constant concentration method has distinct advantages over the others. We have however made use of the other methods and these will be briefly discussed.

4.1 Constant Emission

In this method tracer gas is released at a fixed rate and after a suitable time lapse for the attainment of equilibrium the ventilation rate can be found from the tracer concentration. We have used the method to measure loft air change rates (14). CO₂ was used as the tracer and its concentration was sampled every minute. The average air change rate over 30 minute periods was found by averaging the concentrations.

4.2 Tracer Decay

The house is filled with a uniform concentration of tracer gas and the decay is monitored by discrete or continuous sampling at one or several points. For the measurement of whole-house ventilation rate, where the house is treated as a single cell, the method can give adequate results if the mixing in and between rooms is good. This mixing destroys information about the room rates and can influence the whole-house rate.

We have used a variation of the method to obtain simultaneous values of room ventilation rates and the whole-house rate. The difficulties which were encountered are described in (15). Although the method appeared to give reliable whole-house rates (it was possible to detect the effects of sealing windows), the room rates were much less reliable, and because these rates are

of considerable interest to us it was decided to develop a system (see Section 5) based on the constant concentration method.

4.3 Constant Concentration

In this method tracer gas is released so as to maintain a constant concentration in each room of the house. During any accounting period (usually 30 or 60 minutes) the amount of fresh air that enters a room is directly proportional to the amount of gas injected to maintain the required concentration.

There are several advantages in this method for whole-house and for individual room rates. Firstly, the concentration of tracer gas is uniform in all rooms so that cross flow between rooms does not influence the measurements. Secondly, there is no need for any subjective assessment of the role of the room as an outlet or inlet of fresh air, because the technique measures the amount of fresh air coming into each room. This includes ventilation arising from turbulent pressure pulsations. Thirdly, it is relatively straightforward to use multiple tracer gases to measure flow from cell to cell within the house. Fourthly, the method is very suitable for automation, and one can take advantage of this by developing a computer controlled system which enables continuous monitoring of ventilation and on-line analysis of results.

At British Gas we have developed such a system, known as "Autovent". The current version is shown in Plate 2.

5. DESCRIPTION OF THE AUTOVENT SYSTEM

The system consists of two networks of solenoid valves. One network of valves controls the sampling of air in each room, the other controls the injection of tracer gas to maintain the target level. The solenoid valves are activated by a command from the central computer logger which controls both the sampling and the injection sequences. The sampling lines are purged continuously to ensure that a fresh sample of room air reaches the analyser and all lines are of equal length to minimise differences in flow resistance. The rooms are sampled in sequence for 6 seconds each.

At the end of that period the analyser output is read by the computer and the injection period necessary to maintain the target concentration in that room is calculated. The relevant injection valve is then opened and the next room in the sequence is sampled. When the injection period has elapsed the computer closes the valve and stores the time for which the valve was open. Every half hour the results are summarised and the volume of air entering each room together with the relevant temperature and weather data is printed. A more detailed description of this system has been published in (16) and a full one is in preparation.

Mixing between the injected tracer gas and the room air is very important to the accuracy of the method. We adopt three measures to increase the effectiveness of mixing. Firstly, injection of gas into a room ceases six seconds before the room is next sampled. Secondly, a purge pump is used on the sample line to ensure a fresh sample, accurately reflecting the present state of the room, is available to the analyser. Thirdly, the injection lines are terminated in areas of high air speed, either near radiators or behind small mixing fans. These measures appear adequate in most circumstances where we have tested them by sampling room air at several points.

To illustrate the power and potential of the Autovent system, examples of its application are given in the following.

5.1 Continuous monitoring of ventilation

One advantage of continuous monitoring over discrete measurement is that it is possible to observe subtle variations due to wind speed and direction changes more quickly, more accurately and with less effort. Figure 5 shows some typical results obtained in an end-of-terrace house with all doors and windows sealed. The weather conditions and the corresponding changes in whole-house ventilation rate over nine consecutive 30-minute periods can be seen.

Another advantage of continuous monitoring of ventilation rates over long periods is that it is sometimes possible to isolate the effects of individual weather parameters. Figures 6 and 7 give two examples of this.

Figure 6 shows the effect of wind direction on the ventilation rate of a room in an end-of-terrace house. Also shown is the effect on the whole-house rate, which is much less pronounced.

Figure 7 shows the effect of wind speed on the whole-house rate for three wind directions, for two of which stack effect is clearly dominant.

Results like these illustrate the value of the 'Autovent' system for investigating the complex nature of house ventilation.

5.2 Multiple gas experiments

To illustrate this aspect of the system, we use the example of loft ventilation. The loft seems to be a very important route by which air can leave a house. Sealing some of the obvious leakage paths to a loft might make a significant contribution to energy conservation.

Using two tracer gases, we used N_2O and CO_2 , it is possible to measure simultaneously the whole-house ventilation rate, the loft ventilation rate and the proportion of air escaping from the house to the loft. Figure 8 shows loft air change rates as a function of wind speed and direction measured in a detached house. It is interesting that a strong directional effect was observed, with winds blowing directly at the roof tiles causing much higher ventilation rates. It was also found that the proportion of house air escaping through the loft depended on wind speed. In low winds, 80% escaped through the loft. This is probably because at low wind speeds the stack effect is dominant and acts on the cracks in the ceiling. As the wind increased, so the proportion of air leaving through the loft was found to decrease. At 5 m/s wind speed it was 40% of the total leaving the house.

Multiple gas experiments could be extended to measure the flow from or to any room or area within a house.

6. CONCLUSIONS

6.1 Wind tunnel models appear to be suitable for obtaining external pressure distributions. There are considerable problems however

associated with the measurement of ventilation rates in models. Such measurements are probably restricted to pure research rather than general design purposes.

6.2 Leakage measurements at steady high pressures are relatively easy to do, but they suffer from the disadvantage that they may not be very meaningful for natural ventilation which occurs at low pressures. High-pressure leakage characteristics can be used as a basis for comparison, but it remains to be seen whether they can be usefully correlated to natural ventilation rates.

6.3 Techniques for determining the low-pressure leakage characteristics of dwellings could prove valuable. The method for determining open areas developed by British Gas has proved useful for component areas, but has yet to be developed for complete buildings.

6.4 As a general rule, measured open areas should be independent of flow rate. This is particularly true when they are used as data for a prediction method. The prediction method developed by British Gas also requires the spatial distribution of background leakage areas to be specified. Methods for determining this have been devised with encouraging results.

6.5 For measurement of whole-house ventilation rates, techniques based on tracer decay, constant emission or constant concentration can be used. However, when simultaneous measurements of room ventilation rates are also required, the constant concentration technique is much superior.

6.6 The 'Autovent' system developed by British Gas is a computer controlled automatic ventilation monitoring rig based on the constant concentration technique. It has been used with considerable success for investigating the complex features of multi-cell ventilation, with single and multiple tracer experiments.

ACKNOWLEDGEMENTS

The permission of British Gas to publish this paper is gratefully acknowledged.

Some of the work described has been carried out by British Gas in dwellings at the Abertridwr test site, which is being monitored by UWIST under the sponsorship of the Housing Development

Directorate of the Department of the Environment. Their co-operation is gratefully acknowledged.

DWE/JW
18.6.1980

REFERENCES

1. L. Apperley, D. Surry, T. Stathopoulos and A.G. Davenport.
J. Ind. Aerod. 4, 207-228 (1979).
2. K.J. Eaton, J.R. Mayne and N.J. Cook. BRE CP 1/76 (1976)
3. N.J. Cook. Atmos. Env. 7, 691-705, (1973)
4. B.E. Lee, M. Hussein and B. Soliman. Sheffield University Report BS50 (1979).
5. J. Harris-Bass, B. Kavarana and P. Lawrence, Build. Serv. Engnr. 42, 106-111 (1974).
6. D.W. Etheridge and J.A. Nolan. Build. and Env. 14, 65-68 (1979).
7. J. Cockcroft and P. Robertson. Build. and Env. 11, 29-35 (1976).
8. R.E. Bilsborrow and F.R. Fricke. Build. Sci. 10, 217-230 (1975).
9. D.W. Etheridge and J.A. Nolan. Build. and Env. 14, 53-64 (1979).
10. D.W. Etheridge. Build. and Env. 12, 181-189 (1977).
11. M.H. Sherman, D.T. Crimsrud and R.C. Sonderegger. Lawrence Berkeley Lab. Rep. LBL-9162. Presented at DOE/ASHRAE Conference, Orlando, U.S.A., December 1979.
12. British Standard 848, 28-30 (1963).
13. J. Kronvall. "Airtightness - measurements and measurement methods". Swedish Council for Building Research, Stockholm (1980).
14. R. Gale. "The loft as an air escape route". Note presented at BRE Colloquium, Garston, U.K., April 1980.
15. D.W. Etheridge, R. Gale, M. Gell, L. Martin. Paper to be published in Applied Energy.
16. R. Gale, Gas Engng. and Management, 563 - 572, November 1979.
17. D.K. Alexander and D.W. Etheridge, ASHRAE Trans., Vol. 86, Pt. 2 (1980).

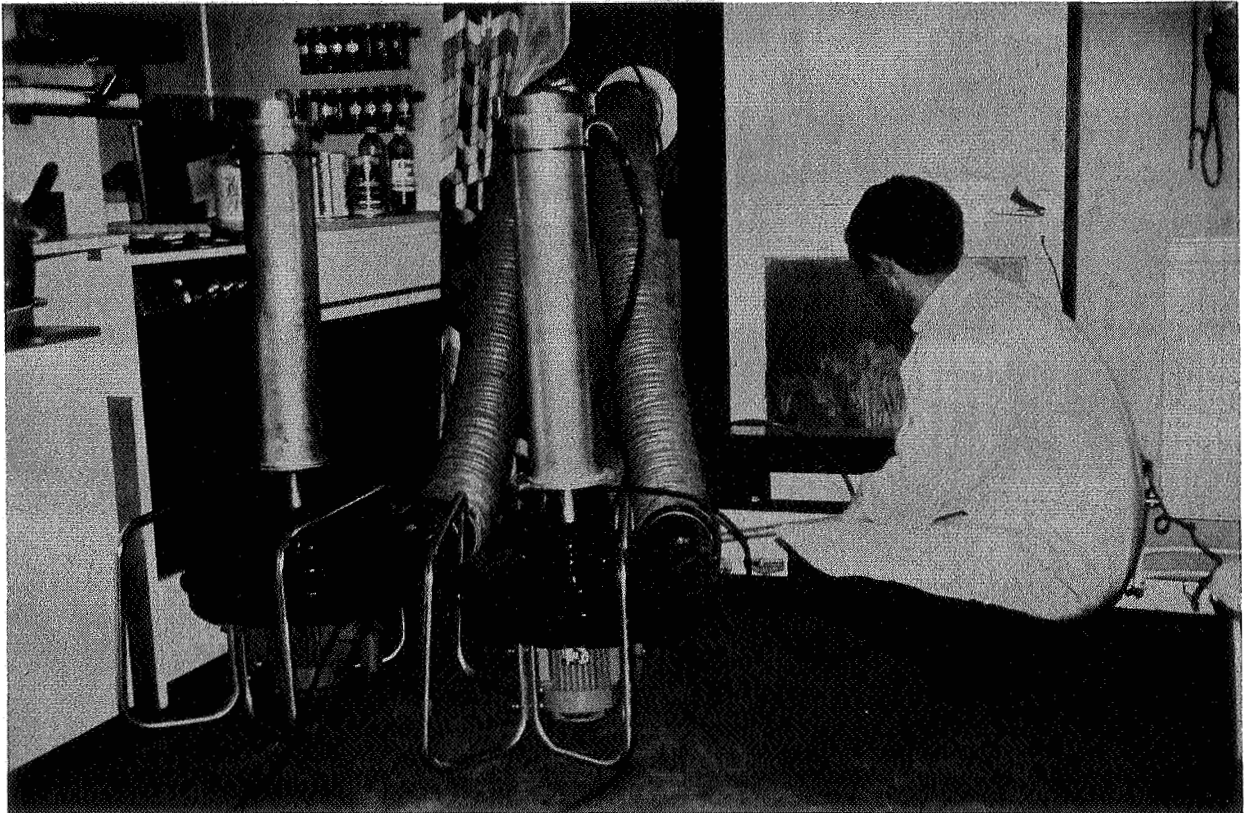


PLATE 1

PRESSURISATION EQUIPMENT DEVELOPED FOR WHOLE-HOUSE
LEAKAGE MEASUREMENT (AS SHOWN) AND FOR MEASUREMENT
OF LEAKAGE DISTRIBUTION.

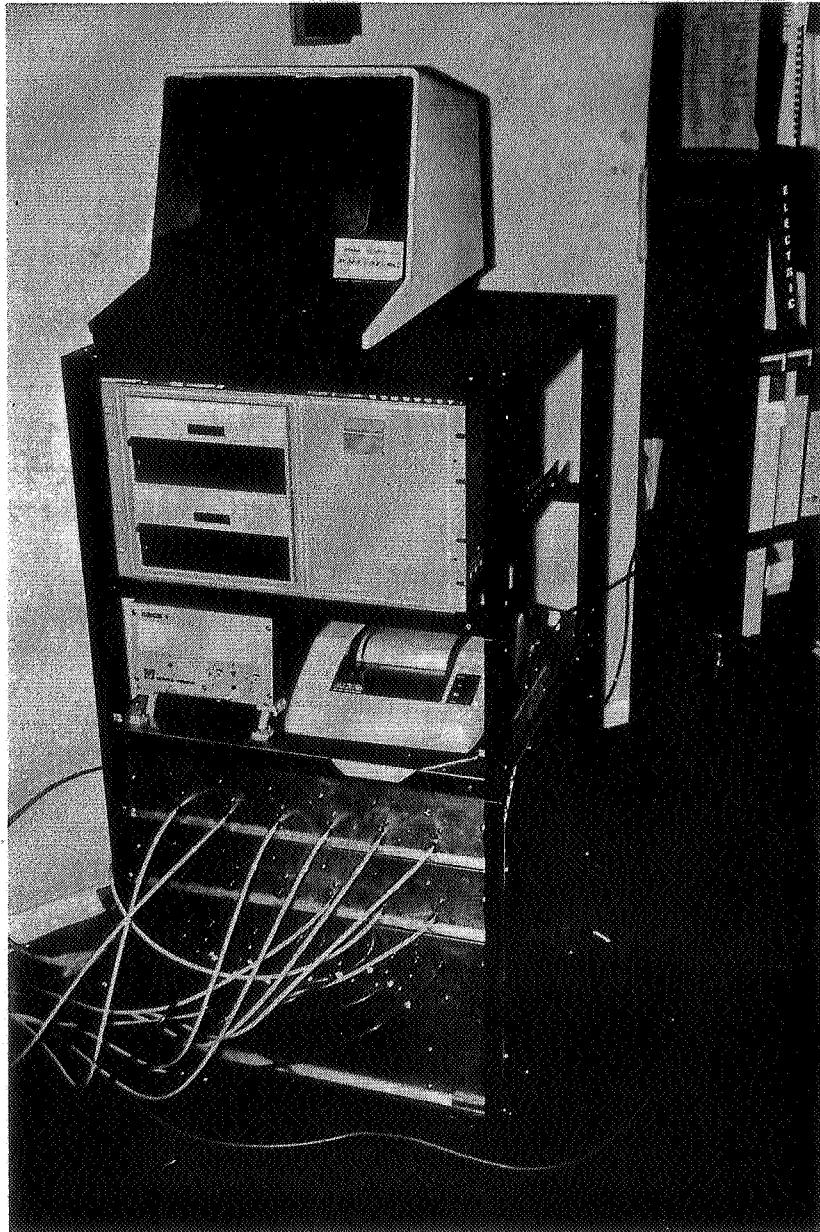
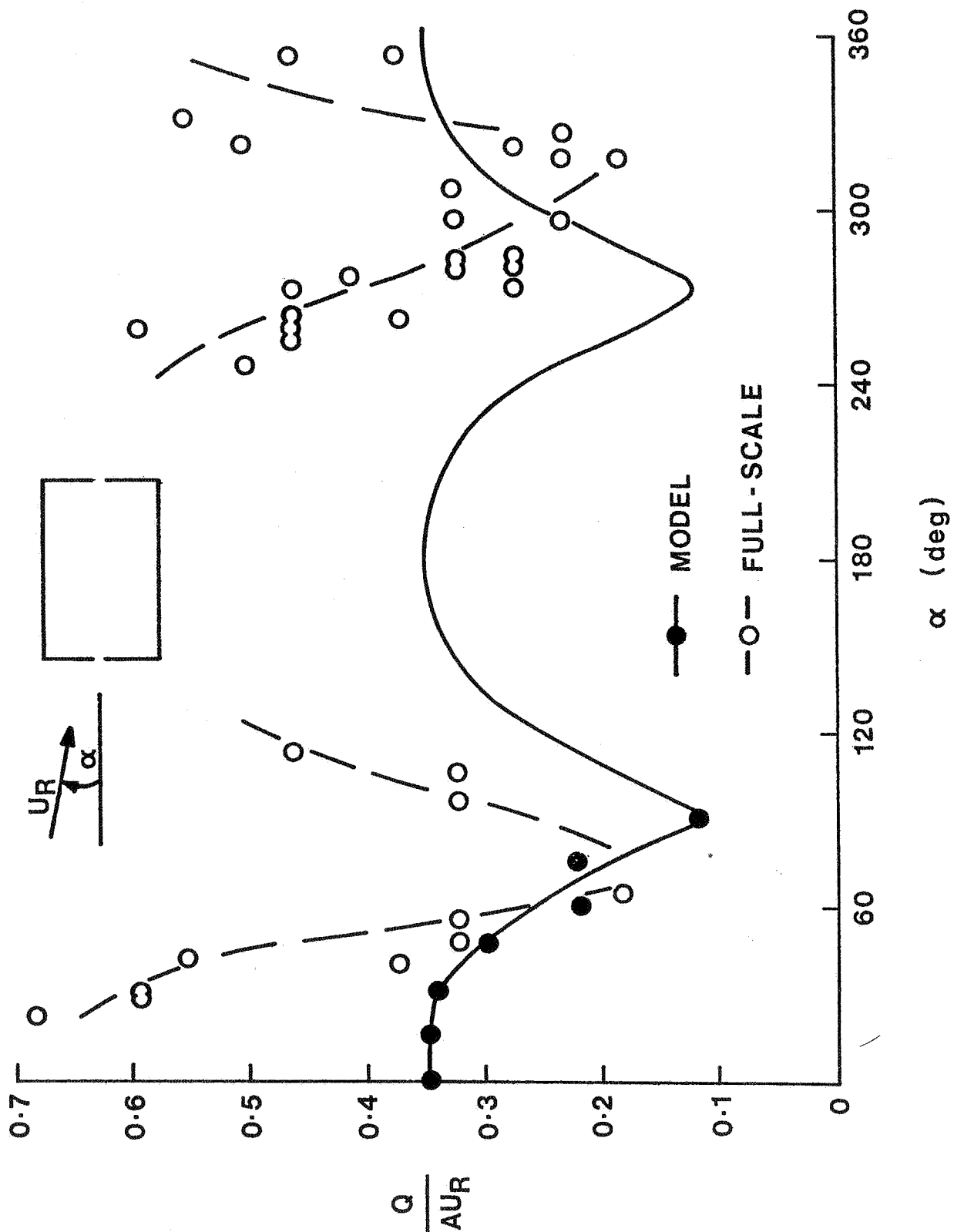
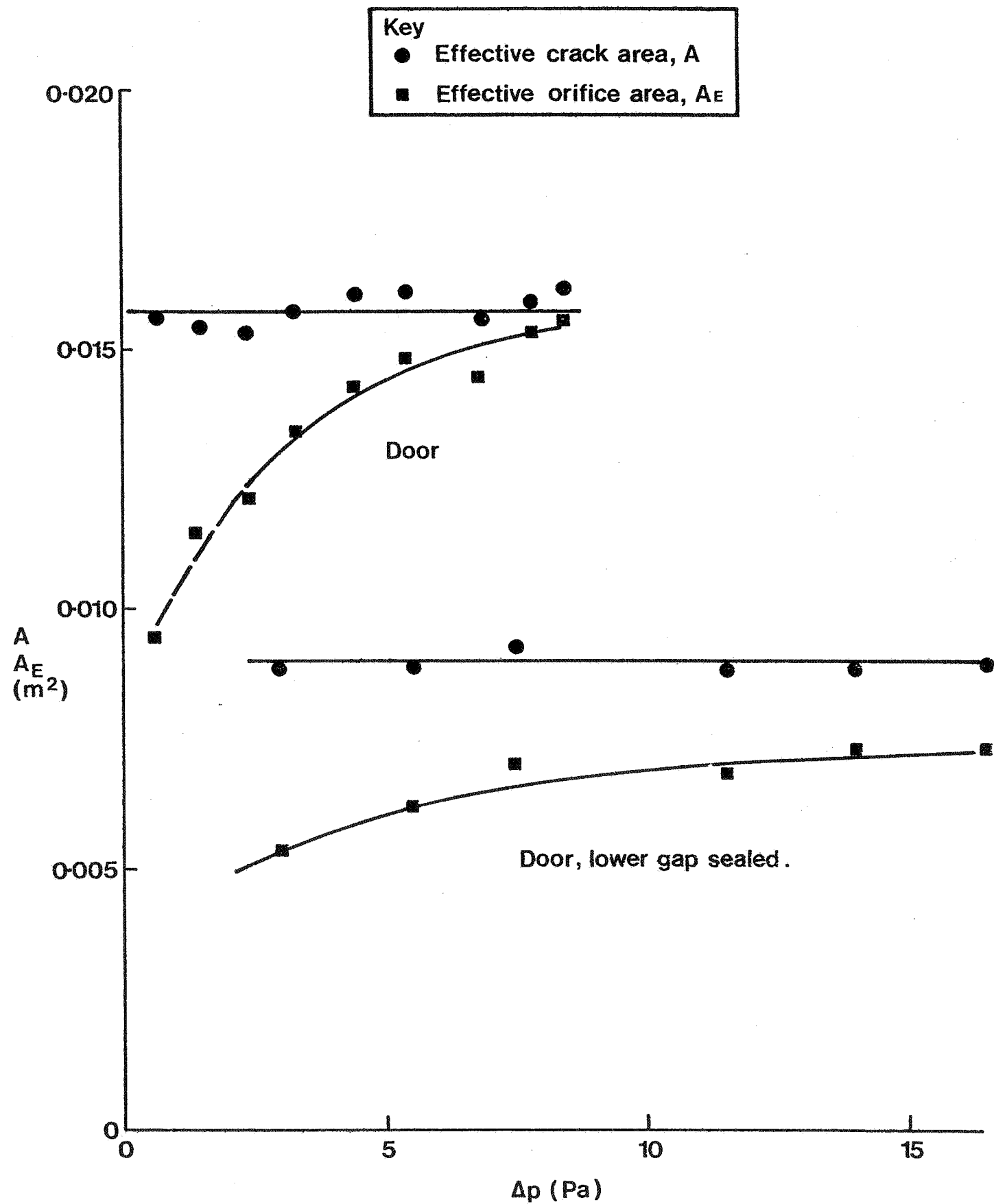


PLATE 2

'AUTOVENT' CONTROL AND ANALYSIS SYSTEM, DEVELOPED
FOR CONTINUOUS MONITORING OF VENTILATION RATES
(ROOMS AND WHOLE-HOUSE).

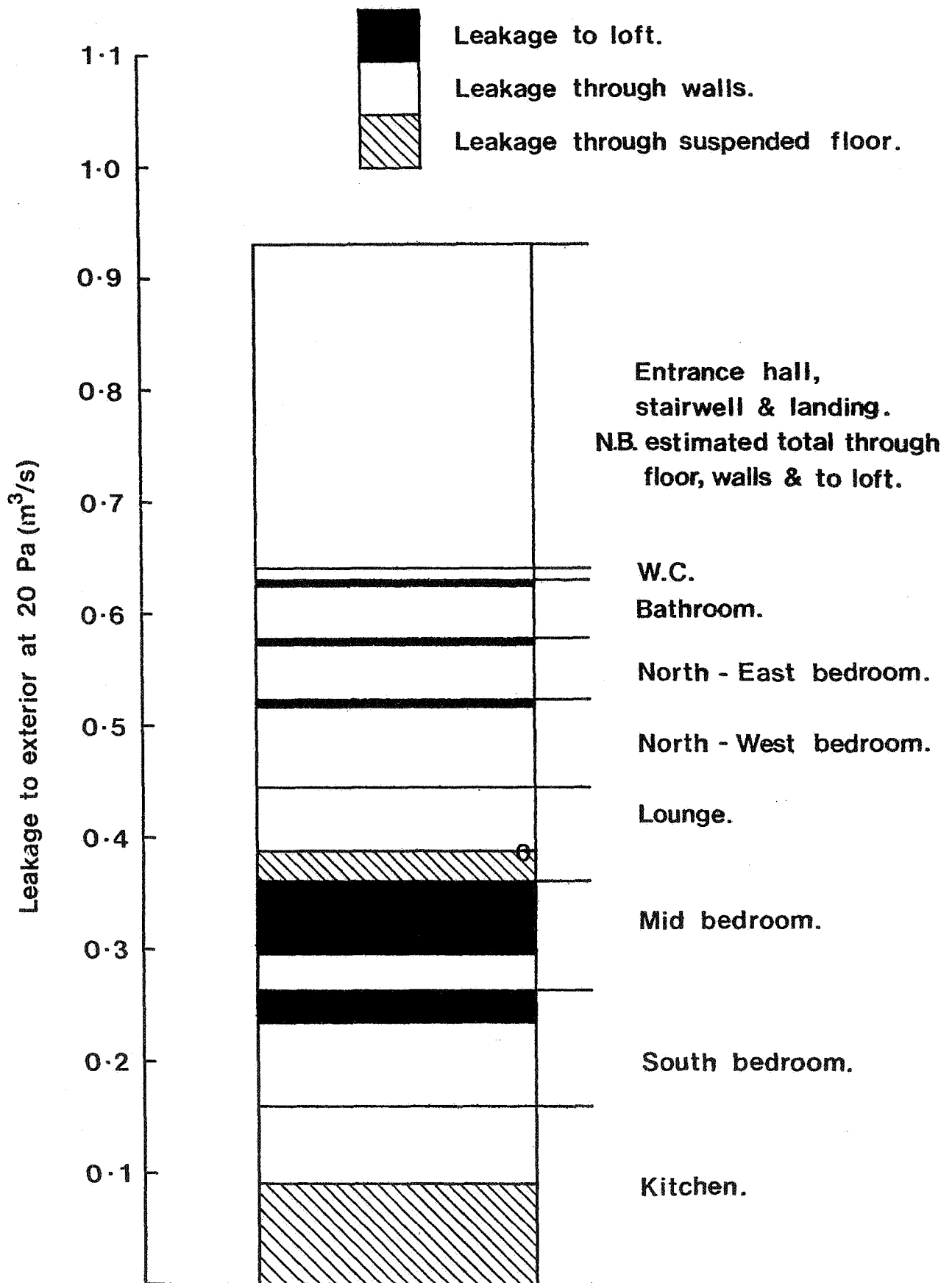


COMPARISON BETWEEN FULL-SCALE AND
MODEL-SCALE VENTILATION RATES
FOR A SINGLE-CELL STRUCTURE
WITH SHARP-EDGED OPENINGS



EFFECTIVE CRACK AND EFFECTIVE ORIFICE
AREAS DETERMINED FROM LEAKAGE TESTS

Fig.2

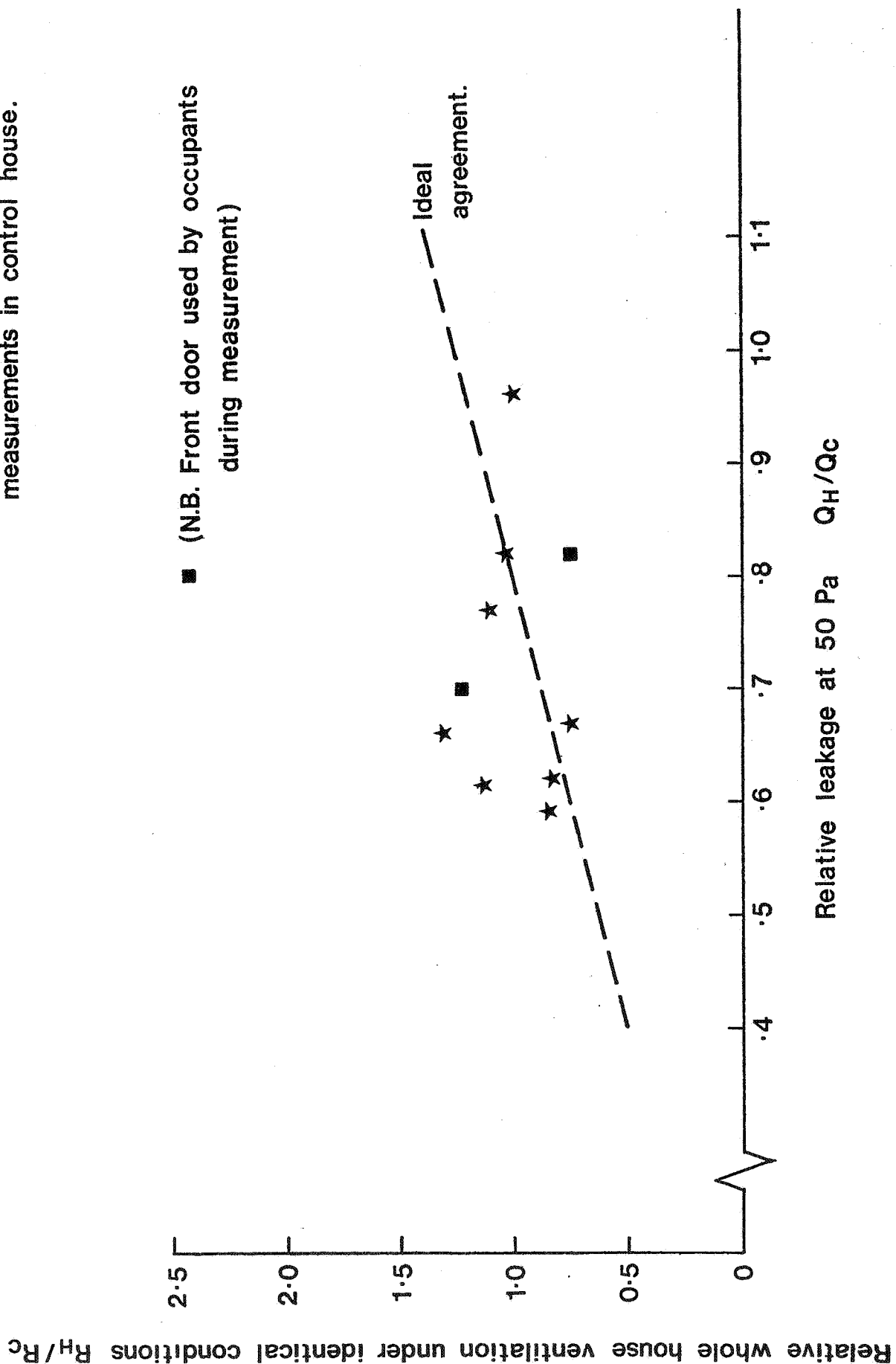


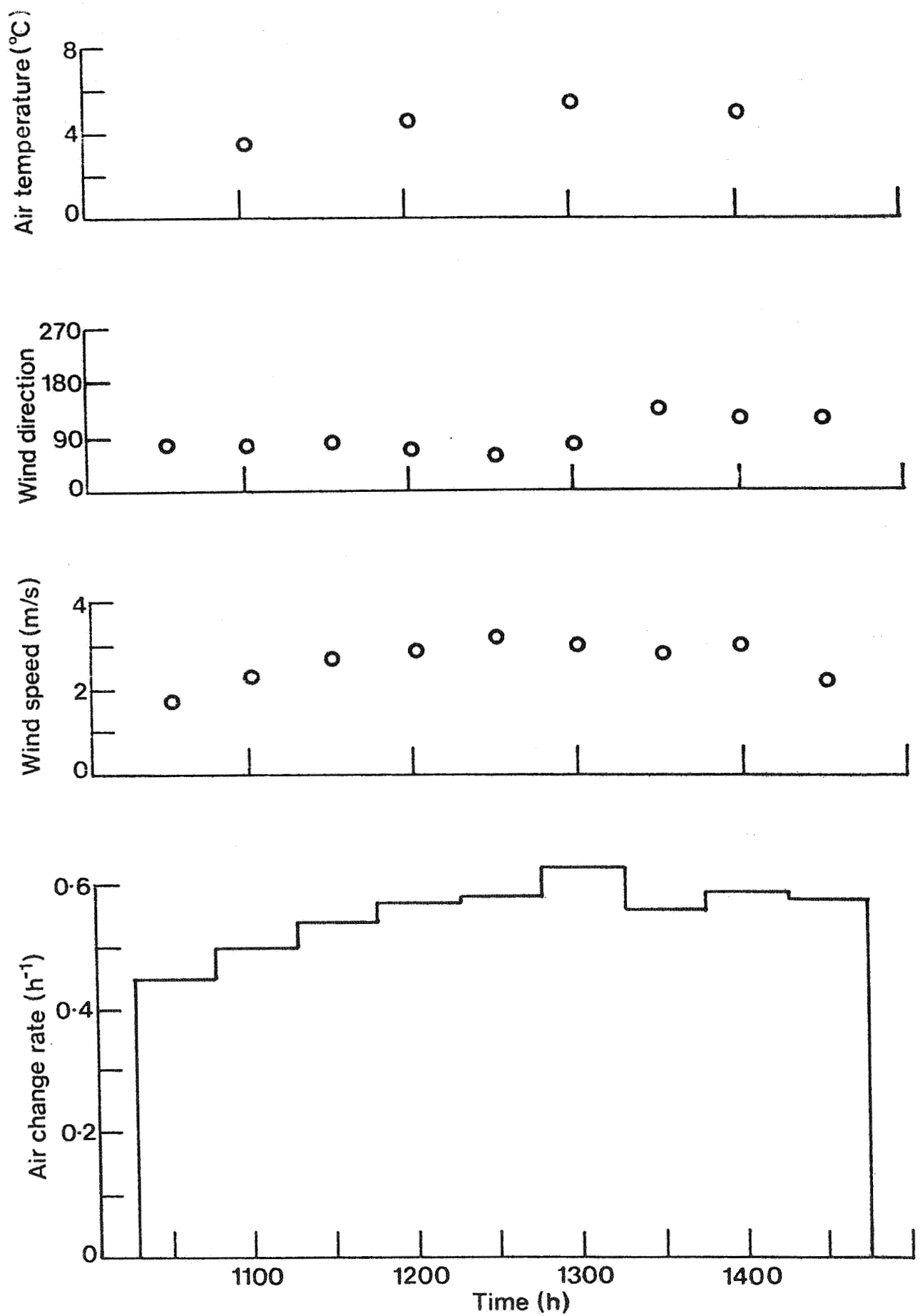
SPATIAL DISTRIBUTION OF LEAKAGE TO EXTERIOR MEASURED IN A DETACHED HOUSE.

INVESTIGATION OF POSSIBLE RELATION BETWEEN VENTILATION AND LEAKAGE.

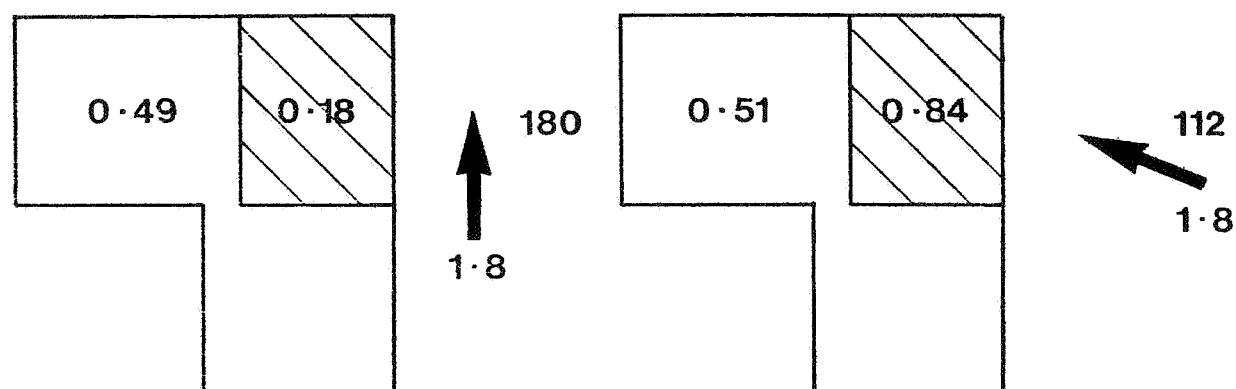
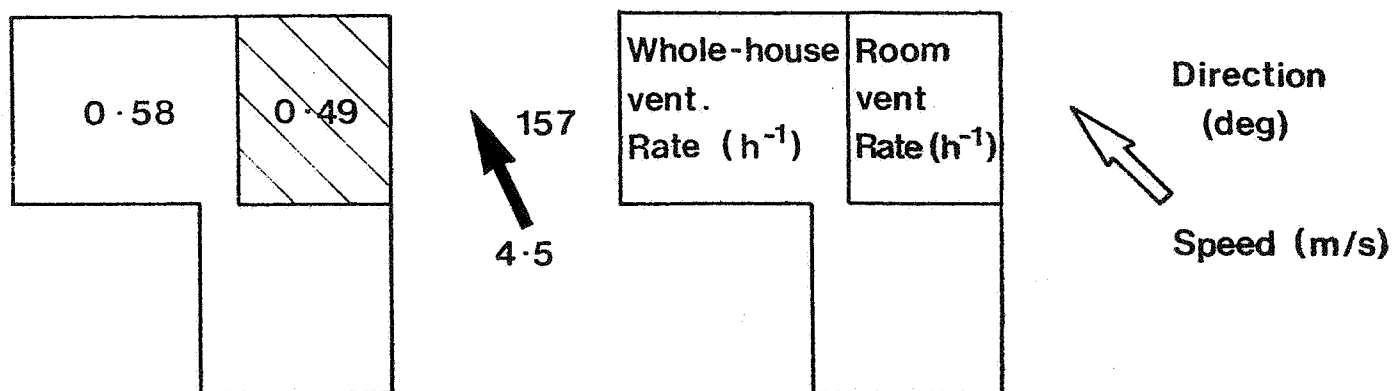
- R_c measured simultaneously with R_H
- ★ R_c estimated from regression on 1 week measurements in control house.

- (N.B. Front door used by occupants during measurement)

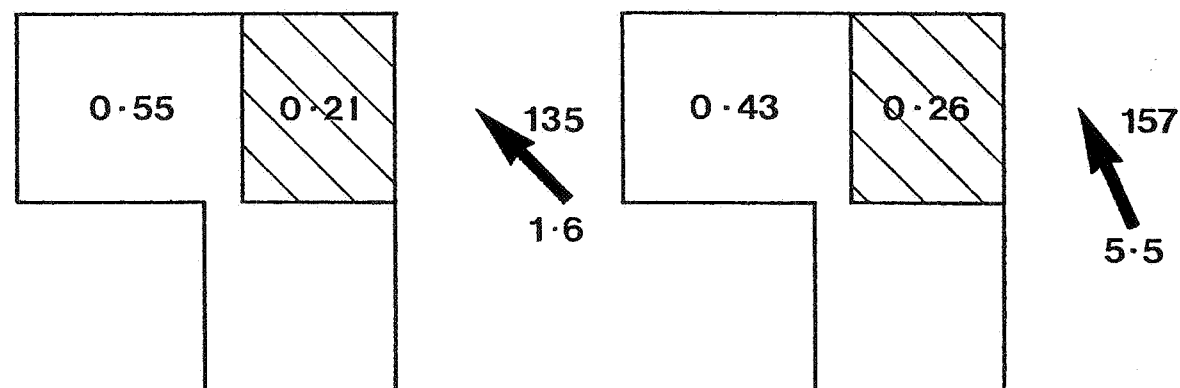




CONTINUOUS MEASUREMENT OF WHOLE-HOUSE
AIR CHANGE RATE WITH 'AUTOVENT', AND
CORRESPONDING WEATHER CONDITIONS

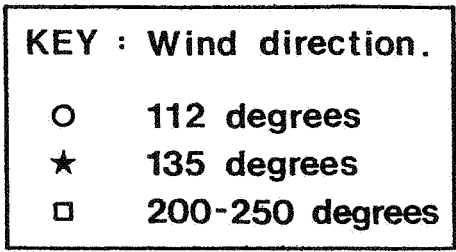


Internal doors opened

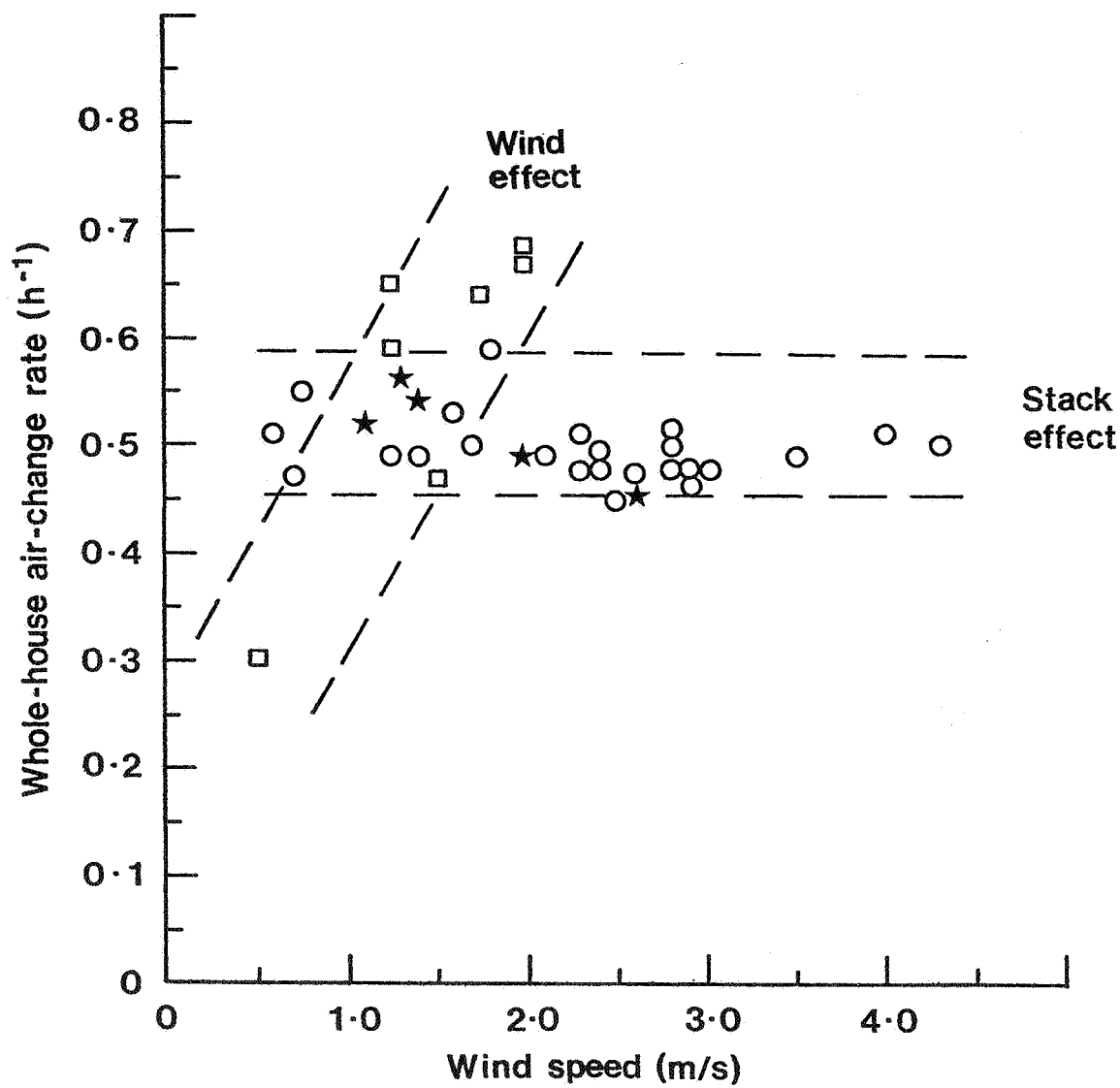


Internal doors closed

VARIATION OF WHOLE-HOUSE AND ROOM VENTILATION RATES WITH WIND SPEED AND DIRECTION ($12^{\circ}\text{C} < \Delta T < 16^{\circ}\text{C}$)



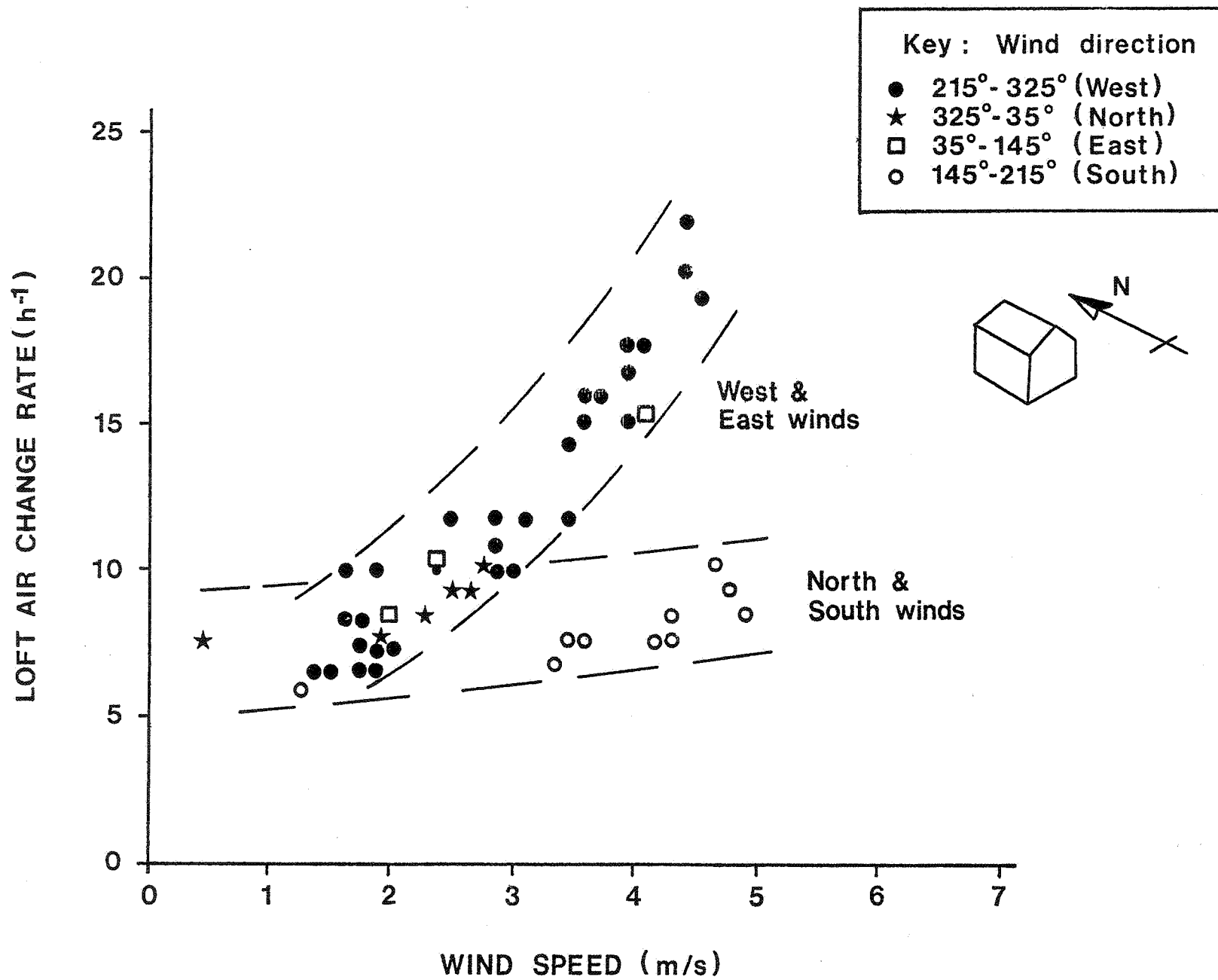
$$\sqrt{\Delta T} \approx 4.3 \text{ (3.3 for 200-250 degrees)}$$



WHOLE HOUSE VENTILATION: EFFECT OF WIND SPEED
FOR CONSTANT STACK EFFECT (0 DEGREES = BUILDING AXIS)

Fig. 7

VARIATION OF LOFT AIR CHANGE RATE WITH
WIND SPEED AND DIRECTION FOR A DETACHED HOUSE



PAPER 4

AN AUTOMATED AIR INFILTRATION MEASURING SYSTEM USING SF₆ TRACER GAS IN CONSTANT CONCENTRATION AND DECAY METHODS

**R. KUMAR,¹ A. D. IRESON² AND
H. W. ORR¹**

**1. National Research Council
Saskatchewan
Canada**

**2. National Research Council
Ottawa
Canada**

(Paper reproduced by kind permission of ASHRAE)

AN AUTOMATED AIR INFILTRATION MEASURING SYSTEM USING SF₆ TRACER GAS IN CONSTANT CONCENTRATION AND DECAY METHODS

R. KUMAR

A. D. IRESON

H. W. ORR

Associate Member ASHRAE

ABSTRACT

One method of measuring rate of air infiltration in buildings involves the use of small amounts of a tracer gas. The concentration of the gas, which is measured at regular intervals, provides the basis for evaluating the infiltration rate. In the following paper, two bases for such evaluations are discussed - the decay method and the constant concentration method.

A system is described which automatically operates a portable electron capture detector/chromatograph and measures parts per billion concentrations of sulphur hexafluoride (SF₆) in air. It samples air on a 1-min. cycle. In the decay method, the slope of concentration vs time on a semilogarithmic plot can be used to compute the infiltration rate. In the second method, the system injects SF₆ at the rate required to maintain the tracer gas at a fixed, predetermined level. The infiltration rate is proportional to the rate at which the tracer gas must be injected.

INTRODUCTION

The heat loss associated with air leakage through the enclosure of a typical detached house may be as much as 40% of the total heat loss. It is essential therefore to be able to estimate this component of the heat load with reasonable precision. But the variables, both physical and behavioral, that affect the phenomena of air infiltration and natural ventilation are not only numerous but also dependent on quantities that are difficult to measure and predict. Air infiltration can be caused by the passage of air through the cracks and other openings around windows and through walls, ceilings, roofs and floors of a building of any type; by the leakage in the air distribution system; by the need of the dwelling for combustion air for the heating system, etc. Each of these parameters can be influenced by the weather, the choice of building materials, the quality of the building construction, and the use of the building. By utilizing instrumentation that involves the direct measurement of air infiltration rates, it is possible to bypass the estimation and prediction difficulties. This paper deals with an automated approach to infiltration measurement using the tracer gas method, including principles of operation and design details, together with calibration procedure and preliminary field data on air infiltration.

R. Kumar, Division of Building Research, National Research Council of Canada, Saskatoon, Saskatchewan, Canada.

A.D. Ireson, Division of Building Research, National Research Council of Canada, Ottawa, Canada.

H.W. Orr, Division of Building Research, National Research Council of Canada, Saskatoon, Saskatchewan, Canada.

MEASUREMENT OF AIR INFILTRATION

(1) Decay Method

In the measurement of air infiltration by the decay method, a tracer gas is distributed in the air of a building and the decay in concentration is measured as a function of time. The theory of the method may be outlined briefly by considering the equation:

$$\frac{dc_i}{dt} = (c_o - c_i) \frac{V_1}{V_2} \quad (1)$$

where c_o and c_i are, respectively, the concentrations of tracer gas outside and inside the building at time t . V_1 is the rate at which air enters the building. It is also the rate at which air leaves the building unless there is a build-up or loss of pressure. V_2 is the ventilated volume of the building, and V_1/V_2 is the air infiltration rate expressed in air changes per unit time.

If the outside concentration of tracer is small enough to be neglected, Eq 1 may be reduced to:

$$\frac{dc_i}{dt} = -c_i \left(\frac{V_1}{V_2} \right) \quad (2)$$

Under conditions of perfect mixing, Eq.2 may be integrated to give:

$$\log_n \left(\frac{c_i}{c_{i_0}} \right) = - \left(\frac{V_1}{V_2} \right) t \quad (3)$$

or

$$\frac{V_1}{V_2} = - \frac{1}{t} \log_n (c_i / c_{i_0}) \quad (4)$$

where c_{i_0} is the initial indoor concentration of tracer gas. Since the equation involves the ratio of the tracer gas concentrations, any quantities proportional to the tracer gas concentration may be used to determine the air change rate. In practice, one usually selects an initial time, plots $\log_n(c_i/c_{i_0})$ against time, and determines the air infiltration rate from the slope of the line.

It should be noted here that the absolute value for concentration is not needed here, only relative values, since the ratio of concentrations is used in Eq 4. Hence the equipment does not need to be calibrated for concentration as long as the indication is linear. But the disadvantages of this method are: (i) it does not give continuous indication of infiltration rate; (ii) it is not a steady-state measurement, hence there could be problems involving the tracer due to its absorption and adsorption characteristics.

This method is limited to measuring infiltration rates for short periods since the initial amount of tracer is limited by maximum scale range of the detector/chromatograph. The period of measurement then is limited to the time required for the tracer to decrease in concentration from the initial maximum value to the minimum value limited by accuracy of measurement. If changes in air infiltration rate are slow, and there are no dead spaces, this is an acceptable method (1, 2).

(2) Constant Concentration Method

To overcome the problems inherent in the decay method, another method of measuring infiltration rate using a tracer gas was proposed by Orr (4). In this method the concentration of tracer gas is maintained at a fixed level.

For the measurement of air infiltration by the constant concentration method, a tracer gas is distributed in the air of a building to a certain concentration level. A sensing element is used to control the concentration of the tracer in the space. The amount of tracer gas required to maintain a constant concentration is then a direct function of the infiltration rate.

$$Q = cn$$

$$n = \frac{Q}{c} \quad (5)$$

$$n \propto Q \quad (6)$$

where Q - flow rate of tracer gas required to maintain a selective level, n = infiltration rate, flow rate per unit time, c = concentration in space (constant).

Advantages of the constant concentration method are that it is a steady-state mechanism and, hence, has no problems of adsorption and/or absorption. It gives an indication of infiltration rate in flow rate per unit time, which can be used for heat loss calculation without estimating the net internal space volume as for the decay method. The accuracy is dependent on measurement of the flow rate of the tracer gas and its concentration. The disadvantages of this method are that the flow control and its measuring apparatus are quite complicated. As a number of tracer gas injections is involved, thorough mixing of tracer gas and air can be more difficult to achieve than in the decay method with a single injection. Also, the absolute value of the concentration of tracer gas in space must be known.

In the present unit, constant concentration is achieved by controlling the number of injections of tracer gas of fixed quantity from the discharge unit. The air is sampled and the concentration is measured on a 2-1/2-min. cycle. The programmable calculator in the system can call up to 90 injections of tracer gas for the 2-1/2-min. period.

CHOICE OF A TRACER GAS

A wide variety of materials are being used as tracer gases. Of these, sulphur hexafluoride (SF_6) is particularly suitable for air infiltration studies involving continuous measurement and large buildings. The use of SF_6 was first reported as a tracer gas in 1965 (3). It has all of the desired properties of a tracer. It is inert, relatively non-toxic, colorless, odorless, tasteless, non-flammable, non-corrosive and thermally stable. It is not a normal background constituent of air. The six fluoride atoms in the molecule make the compound extremely sensitive to an electron capture detector.

There are certain problems which must be considered when using SF_6 as a tracer. The detector unit may require frequent calibration to maintain the desired accuracy. Also, because of the high sensitivity of the detector, minor leaks in regulators, valves and connections, which would go unnoticed in other gas measurement systems, are completely unacceptable when SF_6 is used as an indoor tracer. The measurements are in the form of chromatographic peaks which may require special equipment for automation and data processing.

AN AUTOMATED SYSTEM FOR MEASURING AIR INFILTRATION

The air infiltration measuring system is made up of three subsystems, as follows:

- 1) the programmable calculator,
- 2) the SF_6 discharge system,
- 3) the SF_6 measuring system.

The SF_6 discharge system and the SF_6 measuring system are controlled by the INPUT and OUTPUT instruction of the calculator. The control logic for both systems is housed in the unit named "INTERFACE", developed at the Division of Building Research (Fig.1).

(1) The Programmable Calculator

The Hewlett Packard 9815A is a desk-top programmable calculator. It features a built-in, high speed magnetic tape recorder that uses a data cartridge, a 16-character alphanumeric thermal printer, an auto-start switch, programming keys that double as special function keys, and two optional I/O channels.

The 9815A is used with a Hewlett Packard (HP) 98133A Binary-Coded Decimal

(B.C.D.) and an HP 98135A Interface Bus (IB). The B.C.D. interface connects the calculator to the DBR "INTERFACE" and the IB interface connects the calculator to the HP59309A ASCII digital clock.

(2) The SF₆ Discharge System

The discharge of SF₆ is controlled by two solenoid operated gas valves connected in series, as shown in Fig. 2. These two valves are normally closed. The volume of SF₆ to be discharged is trapped between two valves, D₁ and D₂. When the calculator requests a discharge, Valve D₁ opens for 0.1 sec, allowing the SF₆ between D₁ and D₂ to escape. After 0.1 sec, valve D₁ is closed, and both valves remain closed for the next 0.1 second. Valve D₂ is then opened for 0.1 sec. This allows SF₆ to fill the volume between valves D₁ and D₂. The discharge system is now recharged and is ready for the next discharge request.

The timing of the discharge sequence is controlled by a simple circuit. The SF₆ discharge sequence is always under control of the calculator OUTPUT instruction which can be triggered by the operator through the calculator keyboard or by the OUTPUT instruction itself.

There are two modes of control. One mode triggers the discharge sequence directly by outputting two control words in sequence. Each time the two output words are used, one volume of SF₆ is discharged. This discharge can be repeated every 0.9 sec. This mode can be used either for the constant concentration or the decay method.

The second mode controls the time interval between the automatic discharge of one volume of SF₆. This mode uses the calculator output word to program an interval timer, which triggers the discharge sequence circuit. The basic time interval is selected by the operator. The calculator output word can then multiply this time interval from 1 to 31 times, or stop the discharge altogether. This mode can be used for the decay method only.

(3) The SF₆ Measuring System

a) General Description of the System. The SF₆ measuring system is made up of four major components, as follows:

- i) The Ion Track Instruments Incorporated SF₆-Detector/Chromatograph, used as a gas chromatograph and detector unit;
- ii) A Newport 2000B/S-1 Digital Panel Meter with a voltage of 1.9999 VDC;
- iii) Part of the "INTERFACE";
- iv) An electro-pneumatic operated sample valve which replaces the sample valve of the chromatograph.

The SF₆ measuring system has two modes of operation. One mode used the calculator OUTPUT instruction to take a reading of the SF₆ concentration. This mode can be used either for the constant concentration or the decay method. The other mode is not under the control of the calculator. An interval timer in the "INTERFACE" is used to trigger the SF₆ measuring system. Time intervals from 1 to 15 min are available in 1-min steps. This mode can only be used for the decay method.

b) Operation of SF₆ Measuring System. The operation of the SF₆ measuring system is described, with reference to Fig. 3. The detector/chromatograph, as supplied, is manually operated. The system is automated by replacing the manually operated sample valve by an electro-pneumatically operated valve.

When the SF₆ measuring system is triggered by a calculator OUTPUT instruction, or by the internal interval timer, the sample valve control circuit operates the sample valve for 5 sec. The analogue output of the chromatograph, after the sample valve is operated, is shown in Fig. 4. The first peak represents the O₂ concentration reading and the second peak represents the SF₆ concentration.

The analogue output is digitized by a Newport digital panel meter. This digitized chromatograph output is made available to the calculator by the use of a READ instruction in the calculator.

The digitized chromatograph output is also made available to the auto SF₆ peak finding circuit. This circuit allows the calculator program to identify O₂ or SF₆ outputs of the chromatograph. This is done by changing the polarity of the data as seen by the calculator. All the digitized readings, from the time of the sample valve operation until the start of the SF₆ peak, are made to have a negative polarity. The start of the SF₆ peak changes the polarity of the readings, as seen by the calculator, to a positive value. The calculator can be programmed to look for positive readings and, in this way, can identify the SF₆ data.

The system is intended to be used for unattended operation. In the case of a power interruption, all the AC output control circuits are deactivated and must be manually reset to bring them back into operation.

INSTRUMENT CALIBRATION

(1) Laboratory Test

To determine the accuracy of the SF₆-detector/chromatograph, as employed in the tracer gas technique, tests were conducted with a glass tank having a volume of 0.0177 m³. A small fan was provided inside the tank for mixing air and tracer gas. A controlled rate of air, from a service line, was piped to an opening in the tank to obtain a predetermined rate of air input to the enclosure. SF₆/air mixture in the tank was allowed to leak out through a rubber tube connected to the tank. Both the constant concentration and decay methods were checked by this system. The schematic diagram of the experimental set-up is shown in Fig. 5.

Tests were conducted with different air flow rates of 0.2 to 9 air changes/hr. The results of these tests are shown in Fig. 6. The coefficient of correlation was found to be 0.99742 for the decay method, and 0.99671 for the constant concentration method. The average error was found to be only 1.5% for both methods.

It was evident from the tests that care should be taken how best to process field data. Tests have shown that changes in the sensitivity of the detector to SF₆ concentrations do occur. This is especially true in the warm-up period of the SF₆-detector/chromatograph. It can be avoided by starting the equipment half an hour before the test.

The tests have shown that the SF₆-detector/chromatograph, as used in the automated system, gives reliable results.

(2) Field Test

The air infiltration measurement system was tested in a 3-bedroom, experimental energy conservation house in Regina, Canada, using both the decay and the constant concentration methods.

For the decay method, SF₆ was introduced automatically into the furnace air recirculation fan at a selected SF₆ concentration level, and the build-up and decay of tracer in the house was measured from the sample extracted from the return air duct. For the constant concentration method, tracer gas was injected downstream of the furnace fan, and the sampling was done ahead of the fan. In both tests, the data were recorded on the magnetic tape cassette of the HP9815 calculator, and played back or printed on thermal printer paper.

The furnace fan was operated continuously during the experiment to achieve good mixing. Samples were taken from the return duct every 2 min. Several tests were conducted to check the reliability of the system. The results of one 2-hr test of the decay and constant concentration methods are plotted in Fig. 7. The agreement between these two methods is within normal experimental error. The computed values of air change rate per hour for the decay and constant

concentration methods were found to be 0.615 and 0.608, respectively. In several other tests, the results of the two methods agreed within 2%.

Tests were also conducted using the pressurization method, along with the decay method in a 2-story, 3-bedroom house located in Ottawa, Canada.

For the pressurization method, the air was exhausted from the house with a centrifugal fan and the drop in the inside pressure and, simultaneously, the air flow rate through the fan duct were measured with a laminar flow element. A detailed description of the experimental procedure is reported by Tamura (5). Several tracer gas tests using the constant concentration and decay methods were conducted at different air flow rates of 0.5 to 1.6 air changes/hr. The level of tracer gas concentration during the tests using the constant concentration method was maintained between 5 ppb to 20 ppb. Pressure difference across the walls of the house was also measured at 2 locations on each wall and across the ceiling of the 2nd floor to ensure that the direction of flow through the house enclosure was the same everywhere during the test conducted under moderate wind.

The furnace fan, of 0.436 m³/sec (4 air changes/hr) capacity, was operated continuously during the experiment to achieve good mixing. The results of pressurization and constant concentration measurements are plotted in Fig. 8, and the results of pressurization and decay measurements are plotted in Fig. 9. The average error was found to be only 5% for both methods.

The system operated satisfactorily for about 6 hr, but beyond this period a slight zero shift of the instrument occurred (less than 4%) which can be corrected simply by resetting the zero adjustment knob of the SF₆-detector/chromatograph. This problem has since been overcome by a change in the program to read and correct for the zero shift.

CONCLUSIONS

An automated system to measure air infiltration rates in buildings, using SF₆ as a tracer gas, was developed and checked both in the laboratory and in the field. It is made up of 3 main subsystems - the programmable calculator, the SF₆ discharge system, and the SF₆ measuring system. Concentration levels of SF₆ are maintained at the parts per billion level in the buildings, and are measured by a sensitive electron capture detector in conjunction with a gas chromatograph.

The system can be operated using either the decay or the constant concentration method. Air infiltration measurements in the laboratory and the field by both methods showed that the average error is only 1.5%. Repeated 6-hr-long, unattended operation has been achieved by both methods. Field tests in a house with the pressurization and tracer methods showed only 5% error in the air infiltration measurement results.

The conclusions on the automated air infiltration measuring system, laboratory and field calibration and operation from an instrument standpoint, have been favorable.

REFERENCES

1. ASHRAE Handbook and Product Directory, 1977 Fundamentals Volume, ASHRAE, Inc., New York, N.Y.
2. C.M. Hunt, D.M. Burch, "Air Infiltration Measurements in a Four Bedroom Townhouse Using Sulphur Hexafluoride as a Tracer Gas," ASHRAE Trans. Vol. 81, Part 1, p. 186, (1975).
3. G.F. Collins, F.E. Bartlett, A. Turk, S.M. Edmonds and H.L. Mark, "A Preliminary Evaluation of Gas Air Tracers," J. Poll. Cont. Assoc., 15, p. 109, (1965).
4. H.W. Orr, "Studies and Improvements to an Air-Infiltration Instrument," M.Sc. Thesis, University of Saskatchewan (1963).
5. G.T. Tamura, "Measurement of Air Leakage Characteristics of House Enclosures ASHRAE Trans., Vol. 81, Part 1, p. 202, (1975).

ACKNOWLEDGEMENTS

The authors wish to record their appreciation of the help of their colleagues, Dr. C.P. Hedlin, S.S. Tao and R.G. Nicholson, of the Prairie Regional Station of the Division of Building Research, during the investigation. The authors also wish to acknowledge the contribution made by G.T. Tamura, R.G. Evans and R. Plouffe, of the Energy and Services Section, during the tests conducted in Ottawa.

The work was carried out as part of the research program of the Division of Building Research, National Research Council of Canada.

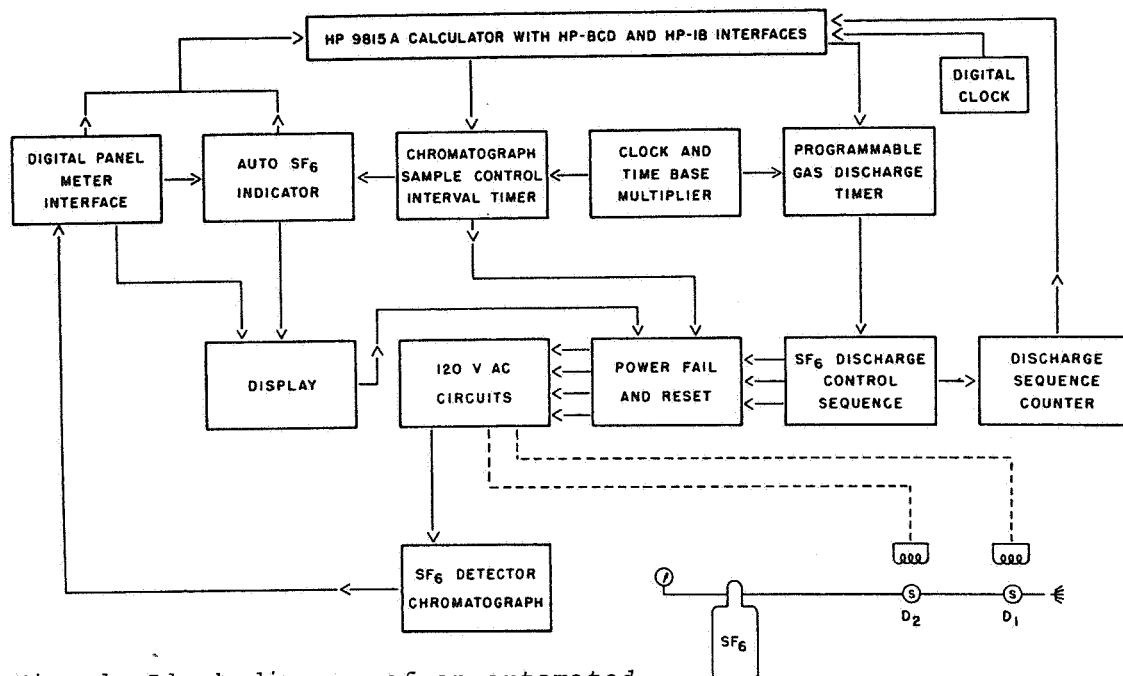


Fig. 1 Block diagram of an automated system for measuring air infiltration

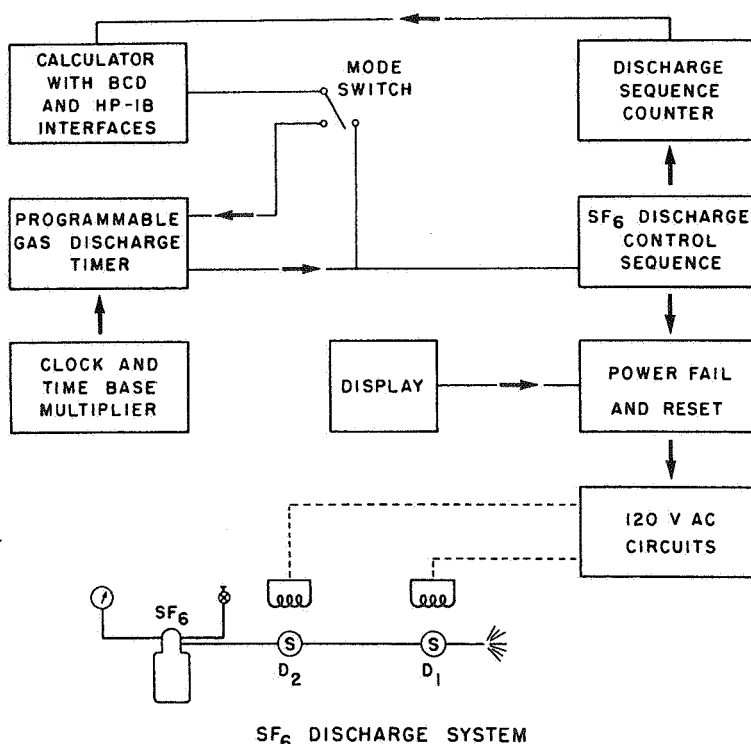


Fig. 2 Block diagram of SF₆ discharge system

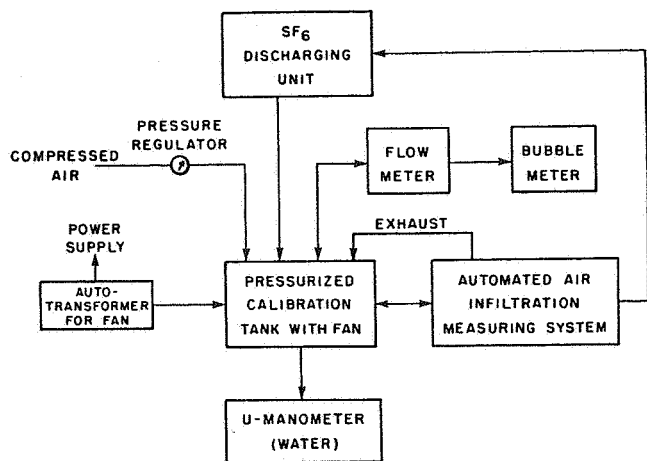


Fig. 5 Block diagram showing instruments used for calibration of an automated system for measuring air infiltration

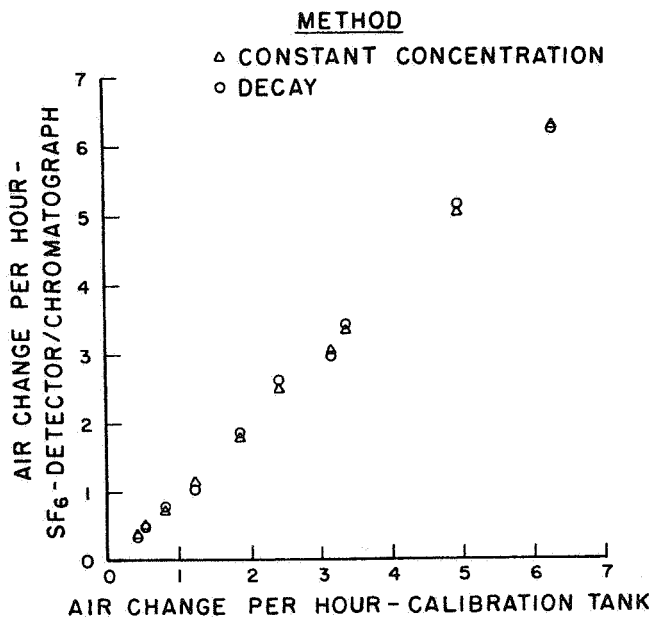


Fig. 6 Calibration tests on SF₆-detector/chromatograph

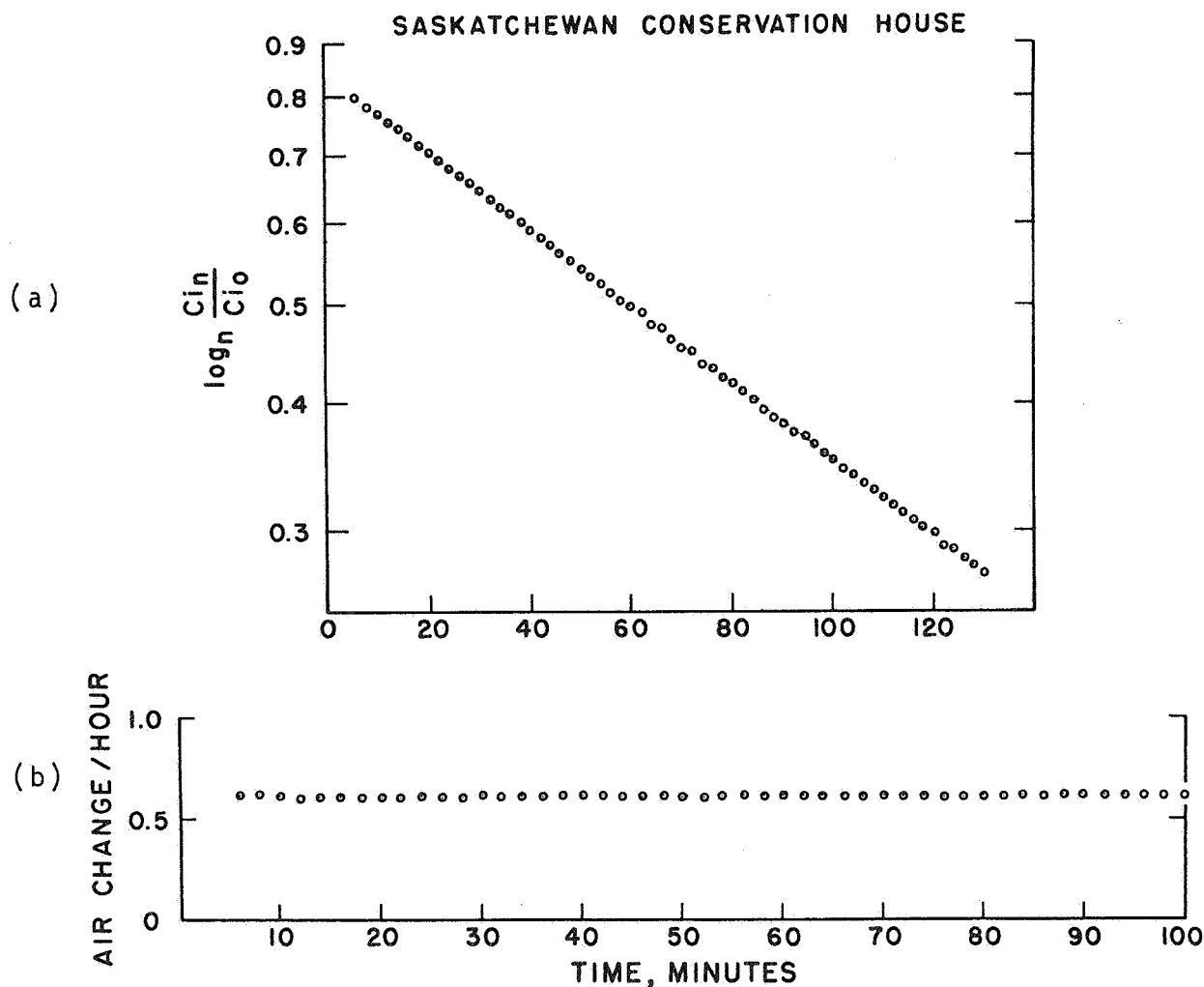


Fig. 7 Typical printout of magnetic cassette of air infiltration vs time: (a) Decay Method; (b) Constant Concentration Method

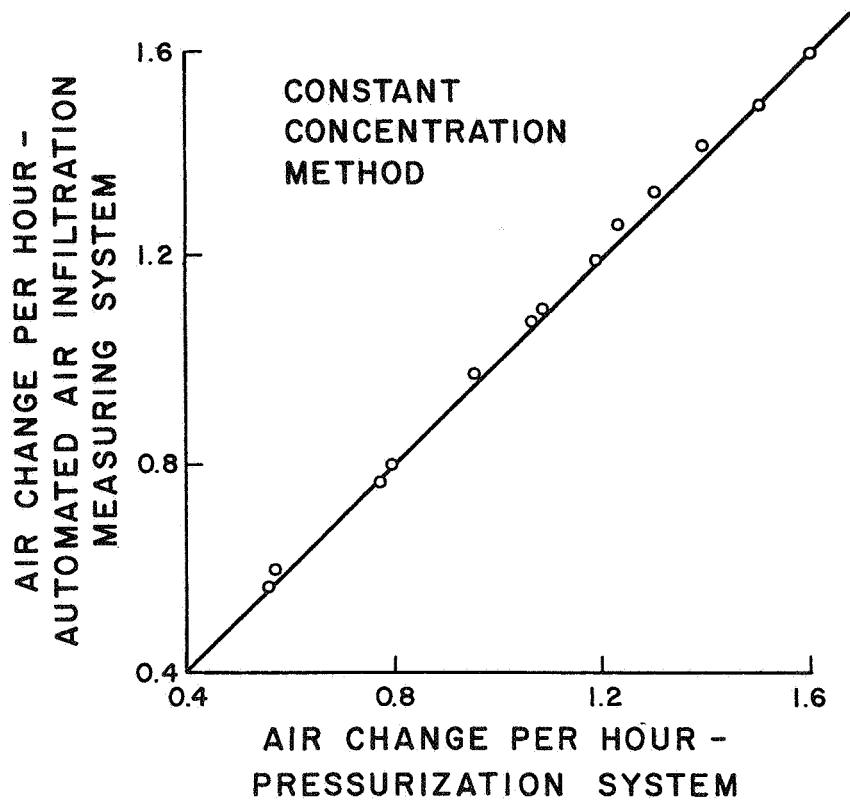


Fig. 8 Calibration tests on an automated air infiltration measuring system using SF_6 Tracer gas - Constant Concentration Method

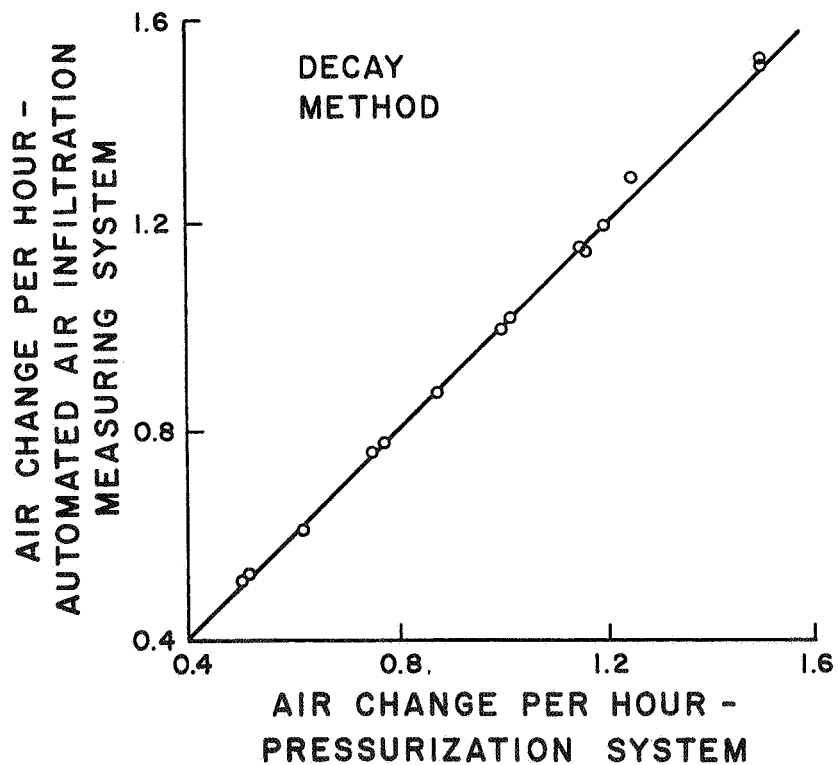


Fig. 9 Calibration tests on an automated air infiltration measuring system using SF_6 Tracer gas - Decay Method

DISCUSSION

JOHN A. HUGHES, Sr. Staff Mktg. Engr., Commonwealth Edison Co., Chicago, IL: Did you have a condensation problem with the vapor barrier on the cold side of the outside wall?

With the low heat loss-heat gain, does your heating-cooling system have a different cfm/capacity ratio than conventional equipment?

RANDALL P. TODD, Assoc. Engr., Duke Power Company, Seneca, SC: What SF₆ concentrations are being used and what is the detection range?

RAYMOND COHEN, Prof. of ME and Dir. of Herrick Laboratories, W. Lafayette, IN: In attempting to use SF₆ some researchers report difficulty with stability of the measuring system. Have you experienced this problem, and if so, how did you account for it?

Did you have difficulty with absorption of SF₆ into plastics, dead spaces, etc. in the building during the testing? Assuming that you took care of this problem with a steady-state instead of transient procedure, how long did you have to wait to reach steady state?

R. KUMAR, A.D. IRESON AND H.W. ORR: Responses not received in time for publication.

PAPER 5

**AUTOMATIC MEASUREMENTS OF
AIR CHANGE RATES (DECAY
METHOD) IN A SMALL RESIDENTIAL
BUILDING WITHOUT ANY FORCED-
AIR-HEATING SYSTEM**

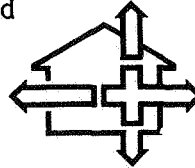
P. HARTMANN, H. MÜHLEBACH

**EMPA
Duebendorf
Switzerland**

AUTOMATIC MEASUREMENTS OF AIR CHANGE RATES (DECAY METHOD) IN A SMALL RESIDENTIAL BUILDING WITHOUT ANY FORCED-AIR-HEATING SYSTEM

P. Hartmann, H. Mühlebach

EMPA, Swiss Federal Laboratories
for Materials Testing and
Research,
Section 151,
CH 8600 Dübendorf,
Switzerland



Abstract

In this paper we describe an automatic measurement system for air infiltration and relevant influence factors, which is applicable to measurements in single rooms or in a group of connected rooms. This system works on the decay rate method and is controlled by a purpose-designed controller. The test data are evaluated by computer, but off-line. Recommendations in connection with different details of this system will be valid for tests in similar, relatively tight rooms.

In the last section, test data of long-term air infiltration measurements, correlations of this data with wind- and temperature-difference-data and finally a comparison with pressurization-test-data are given.

1. Introduction, Conditions for the Measurement System

After a period of different short-term-tests in Swiss buildings, there was a need to develop an automated air-infiltration measurement system which would allow long-term measurements without intensive manual control. A relatively tight budget imposed a tendency to cheap but well-adapted solutions for the different parts of the system.

A real lack of another Central-European institute with some experience in this field, forced us to evaluate many details in connection with the system by various small experiments.

The system should be able to do measurements in single rooms or in groups of some connected rooms (6 in maximum).

In connection with the test programme, some ambitious plans to simulate the buildings in comparison with intensive flow and pressure measurements could finally not be treated, but we were able to install a large number of sensors to measure necessary influence factors for the infiltration.

The planned infiltration measurement-system is adapted to typical Central-European buildings, which generally have the following characteristics:

- larger buildings are usually of solid-wall construction .
- single family houses are built as solid-wall or light-weight construction.
- windows, especially in new buildings, are relatively tight.
- additional ventilation systems are installed in internal toilets and sometimes in kitchens; otherwise they are ventilated by window-opening.
- open fireplaces in houses or apartments are uncommon.
- water-heating systems are very common (radiators, under-floor heating occur less frequently).

2. Concept of Measurement-System

The first two choices in connection with the system had to be the principle measurement-procedure and the type of tracer-gas to be used. At the planning stage we considered that we were not able to introduce a reasonable constant-concentration-control, so we decided to choose the decay method.

The choice of the tracer-gas type was influenced by our good experience with N_2O which we had gained in earlier years (see Ref 2). Usual test-concentrations for the available American type of analyser (Infra-red type, "Miran") are in the range of 10 to 20 ppm. Rather than employing systems with a very refined injection system (see Ref 12), or using on-line computer evaluation of data, we developed a relatively simple system with a purpose-designed controller for the injection and logging systems. A refined computer program for the evaluation of data avoids a lot of time-consuming work.

The system is presented in Figure 1 with its main parts:

controller, supply-system, analyser with scanner, data logging system for recording both gas concentration values and a large number of influence factors.

Figure 2 shows the instruments on a photograph, the analyser in the centre on the table, the controller at its left side, the scanner below the table.

Measurement procedure:

The procedure is not extraordinary but the method of choosing the different sequences may be of interest:

- The controller stops the analysis below a level of about 15% of the start-concentration.
- Adjusted volumes of test gas are injected in the different rooms and mixed by fans for about 10-15 minutes.
- Afterwards, the scanning and analysing procedure starts again in sequences of 5-10 minutes per sample.
- An analogue printer gives a visual display of the concentrations in different rooms; also the resulting concentration of each sequence is stored on a tape.

Evaluation of the data:

In connection with the design of this evaluation program, we spent some time devising a certain variety of evaluation procedures, making a comparison of the corresponding results. This program is able to calculate the following infiltration rates:

- of every sample location during the whole run or during a desired period.
- of a mean infiltration rate, taking into account all samples for a desired period.
- of a mean value including a weighting procedure, if the samples are selected from rooms with a certain variety of sizes.

The timing of evaluation and measurement procedure is chosen in such a way that all relevant data are printed a short period before the automated change to the next sample position.

Figure 3 shows an analogue print of a test run (notice the unusual direction of the time axis !). It is clearly visible that, although there is relatively good mixing at the beginning, there is quite a spread of concentrations in the different rooms of this house during the test period of some hours. Except for some special tests, which did not give a significant difference, we do not run the fans during normal tests, but evaluate the overall infiltration rate by weighting the values of the different rooms.

It may be of interest that manual evaluations and these automated evaluations of the data differ by a very small percentage, which is, in any case, in the range of other errors. Maximum deviations for single values of a test-run show 6%; mean deviations for a whole run are smaller than 2%.

During tests in the same house over a period of some months, the system worked quite well in nearly all conditions. If wind direction and wind velocity changed very much, the initial mixing was not good enough without some manual assistance.

3. Detail-evaluations in connection with the instrumentation set

This section seems to be reasonable in the context of a seminar on measurement technique; we hope to deliver some hints to other institutes starting similar experiments in the near future, especially in Central Europe. It will conclude with some general recommendations.

(a) Test gas characteristics

We did not find any indications of adsorption or absorption characteristics of usual building surface materials for our favoured test gas, N_2O . Therefore, we executed a certain number of long-term exposure tests of materials in closed-test-loop (for details, see Ref 2, p43). Test specimen included woodboard, gypsum-board, wallpaper, carpet, paint and plastic surfaces of different kinds. There is no evidence of adsorption/absorption for test-gas concentrations in the same range, as they are used in our experiments. Similar experiments are conducted with extremely long plastic tubes, which we used for sampling purposes.

Although we observed very small losses of gas per hour, they seemed to be generally due to fittings and valves (about 1%). These experiments nevertheless indicated the danger of leakages, especially for tubes with high concentrations of tracer-gas coming out of the pressure reservoir.

(b) Checking of the analyser

The manufacturer of the analyser recommends a test procedure in a closed circuit with a defined amount of test gas. Besides the procedure, which needs a lot of care, we developed another relatively simple laboratory procedure:

We were able to vary the infiltration rate in a 3 m^3 test box in a range of 1 to 10 a.c. per hour and to measure the air flow accurately ($\pm 1\%$). By measuring these infiltration rates a second time using the analyser, we

obtained a good test of its function (Figure 4). This checking procedure avoided any problems of temperature drift, which has to be considered when measuring in very small circuits.

(c) Injection system

Figure 5 illustrates an injection tube end. Each contains a slit, which is adjusted according to the volume of the room and closes itself very tightly as soon as the overpressure disappears. For the test gas we used only one magnetic valve with an adjustable opening-duration with a controlled small overpressure; all tubes to the injection ends had the same length.

Although this system is very much less refined than systems used by other institutes, it works reasonably under "normal" wind situations, as we mentioned before.

Recommendations

(i) Applicability of the system to different purposes:

Without contradicting the various discussions about advantages of a measurement system with constant level (see, e.g. Ref 3, Ref 7, et al), which seem to have been proven recently,

our system delivered, for a limited budget:

- accurate results for single rooms
- results with reasonable accuracy, e.g. repeatability, for groups of connected rooms with little internal resistances (usual in Swiss homes and apartments)
- indications of mean ventilation rates in buildings/flats with singular openings (may be one or two windows); refined measurements on these effects would need, e.g. a multiple-gas-system to detect internal flows.

(ii) The infra-red analyser as we use it does not need much recalibration (which seems to cause problems for other instruments), but it does need a "warming-up" time of more than one hour.

(iii) Painsstaking attention to all possibilities of leakage is seen to be very important, especially for tubes with high tracer-gas concentrations, maybe under pressure. Such leaks may occur after a longer period of tight running of the system, e.g. by ageing of tubes. As a consequence of some problems in this connection, we avoided placing injection tubes or gas reservoirs within the test rooms as much as possible and also paid attention to an eventual mixture of tracer leakage gas and inlet air of any room.

(iv) Evaluation system:

It is recommended to install a simple analogue registration device for the test-gas concentration in addition to any refined evaluation system. The displays provide the best way of supervising the performance of the system.

4. Test Results on Long Term Tests in a Single Swiss One-Family-House

Although test results have only secondary interest in this seminar, some results from our tests last winter would well fit into the data collections of other authors, where Central-European results are scarce.

A vertical section (Figure 6) shows the principle design of this building, which is nearly square. The surroundings of the building are relatively free; only its north facade is protected in the lower half by a slope at the back of the house. Prevailing winds are from the west-side/southwest-side, which have, as usual, some large windows. The building is a wooden, lightweight construction but protected on its outside by an overall styrofoam-insulation. The wooden windows have rubber gaskets (round form) and may be protected either by shutters or by roller blinds.

The following table gives a selection of main test results, which will be commented upon afterwards.

Results:

Variable	Conditions	Numbers
Leakage of elements	<ul style="list-style-type: none"> - windows (measured on site) - window (example, in lab.) - balcony doors - entrance door 	0.02 - 0.05 m ³ /m h Pa ^{2/3} 0.03 - " 0.03 - 0.1 " 0.5 - "
Leakage of buildings	<ul style="list-style-type: none"> - whole building, measured under overpressure and underpressure (similar results) - whole building at 50 Pa calculated from all known window gaps and leakages 	~1.5 h ⁻¹ at 50 Pa ~0.3 h ⁻¹

Although this experimental house (with same construction as series buildings of the manufacturer) was built with special attention, about 80% of infiltration happens through "unknown" gaps. Maybe another 20% of the air flows through gaps just around windows and doors. This fact shows how poorly the usual simple calculation rules, based on window gap lengths and leakage, work. Nevertheless, these rules are introduced in thousands of Central-European building laws. We hope that our Air Infiltration Centre will be able to provide refined new methods on such data sets.

References

- (1) Bargetzi, S., Hartmann, P., Pfiffner, I. : Messungen des natürlichen Luftwechsels in nichtklimatisierten Wohnräumen, Schweiz. Bauzeitung, Heft 14, 1977
- (2) EMPA, Bericht 34020, Luftwechselmessungen in nichtklimatisierten Räumen unter dem Einfluss von Konstruktions- und Klimaparametern , Dübendorf , Dez. 1977
- (3) Kumar, R., Ireson, A.D., Orr, H.W. : An automated air infiltration measuring system using SF₆ tracer gas in constant concentration and decay methods, ASHRAE Trans. 1979, 85, p. 385-395
- (4) Harrje, D.T., Grot, R. : Automated air infiltration measurements and implications for energy conservation, proceedings of the international conference on energy use management, Pergamon Press, New York , 1977, p. 457 - 464
- (5) Condon, P.E., Grimsrud, D.T., Sherman, M.H. and Kammerud, R.C.; An automated controlled-flow air infiltration measurement system, LBL , Berkeley, 1978
- (6) Alexander, D.K., Etheridge, D.W. and Gale, R.; Theoretical and experimental studies of heat loss due to ventilation, Heating Division, Watson House, British Gas, London (1979)
- (7) Gale, R.; Ventilation heat loss outside in, SEGAS, Central Laboratories, London, 1979
- (8) Kronvall, J. : Airtightness - measurements and measurement methods, Swedish Council for Building Research, Stockholm, 1980
- (9) Stewart, M.B., Jacob, T.R., Winston, J.G. : Analysis of infiltration by tracer gas technique, pressurisation tests, and infrared scans, Owens Corning, Granville, Ohio
- (10) Hitchin, E.R., Wilson, C.B. : A review of experimental techniques for the investigation of natural ventilation in buildings, Building Science, Vol.2, Pergamon Press, U.K., 1967
- (11) Sepsy, Jones, Mc Bride, Blancett : Air infiltration study for residential application, Ohio State University, Columbus (unpublished report)
- (12) Dumont, R.S., Figley, D.A. , Orr, H.W. : Comparative air - tightness levels in housing for six different locations in North America and Sweden , NRC, DBR, Ottawa, 1980 (Draft)

Figures

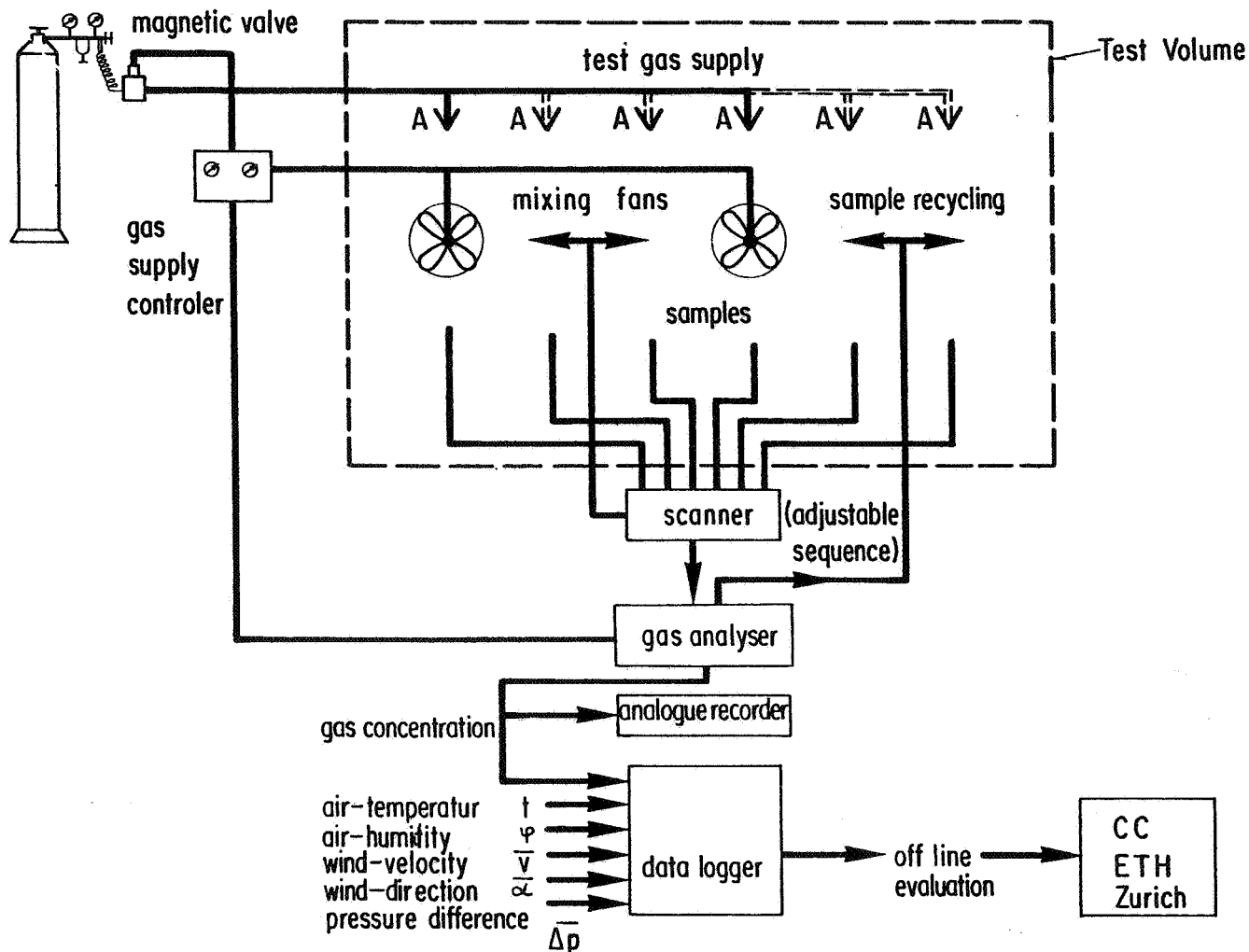


Fig. 1: System for automated decay-rate-tracer-gas-measurements

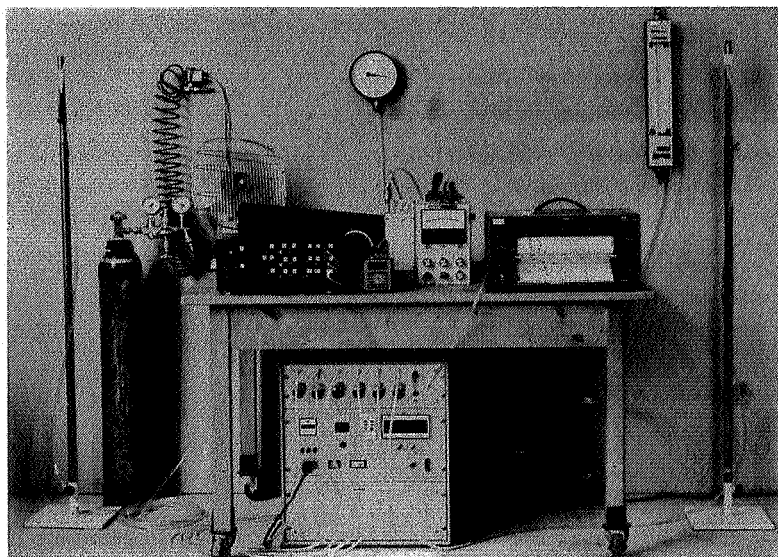


Fig.2 : Instruments for automated infiltration measurements

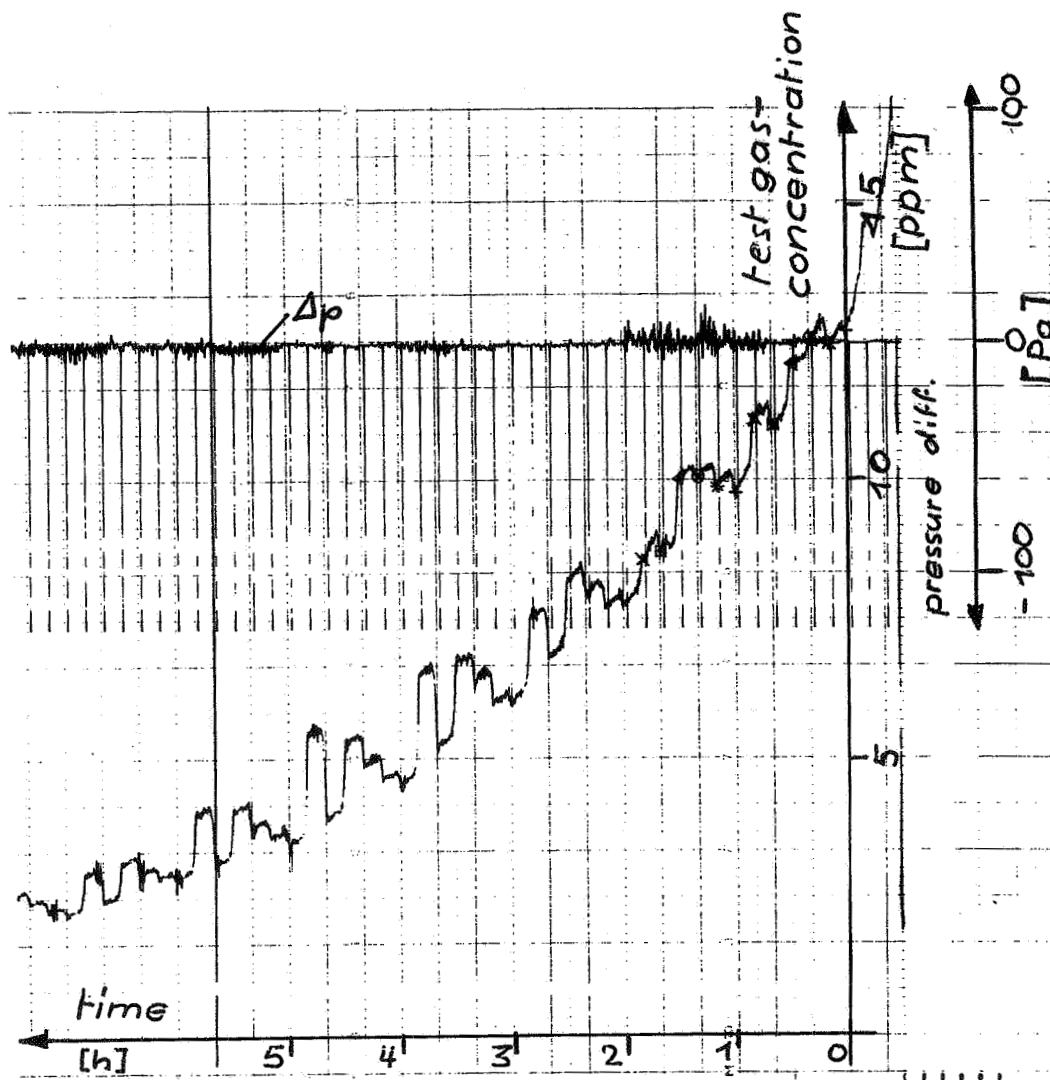


Fig.3 : Analogue print of tracer-gas concentration (6 different, automatically changed samples) and of the pressure difference over the main, wind opposed facade

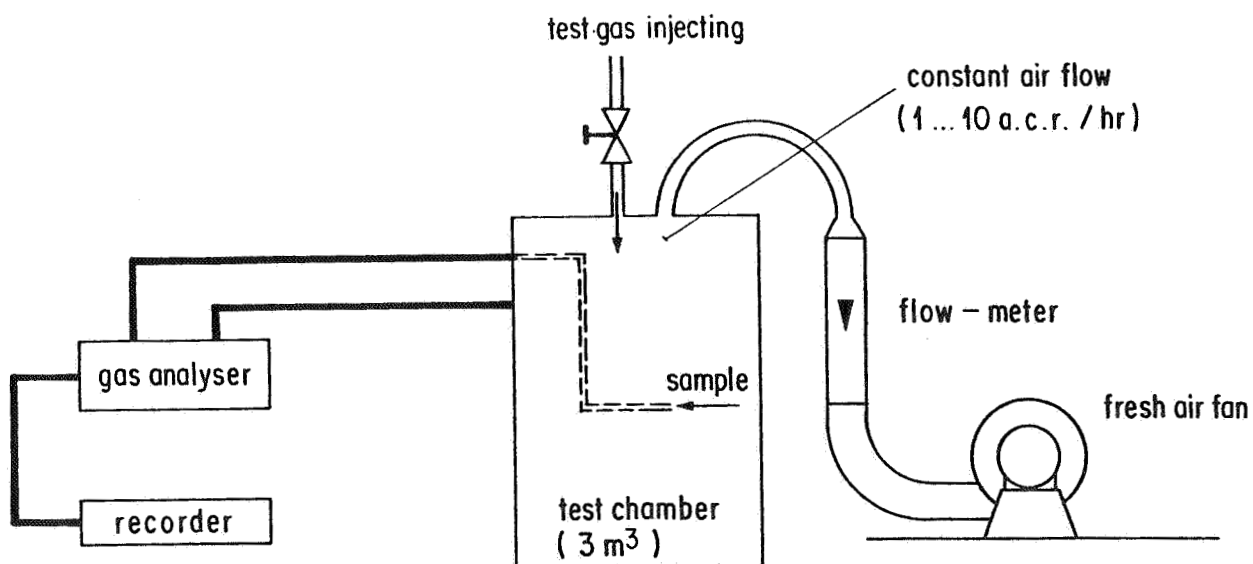


Fig. 4 : Checking equipment for gas analyser

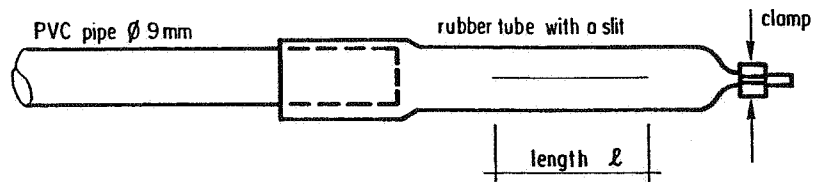


Fig. 5 : Injection tube with variable slit length, in order to adjust the injection flow to the volume of the corresponding room (detail A in Fig. 1)

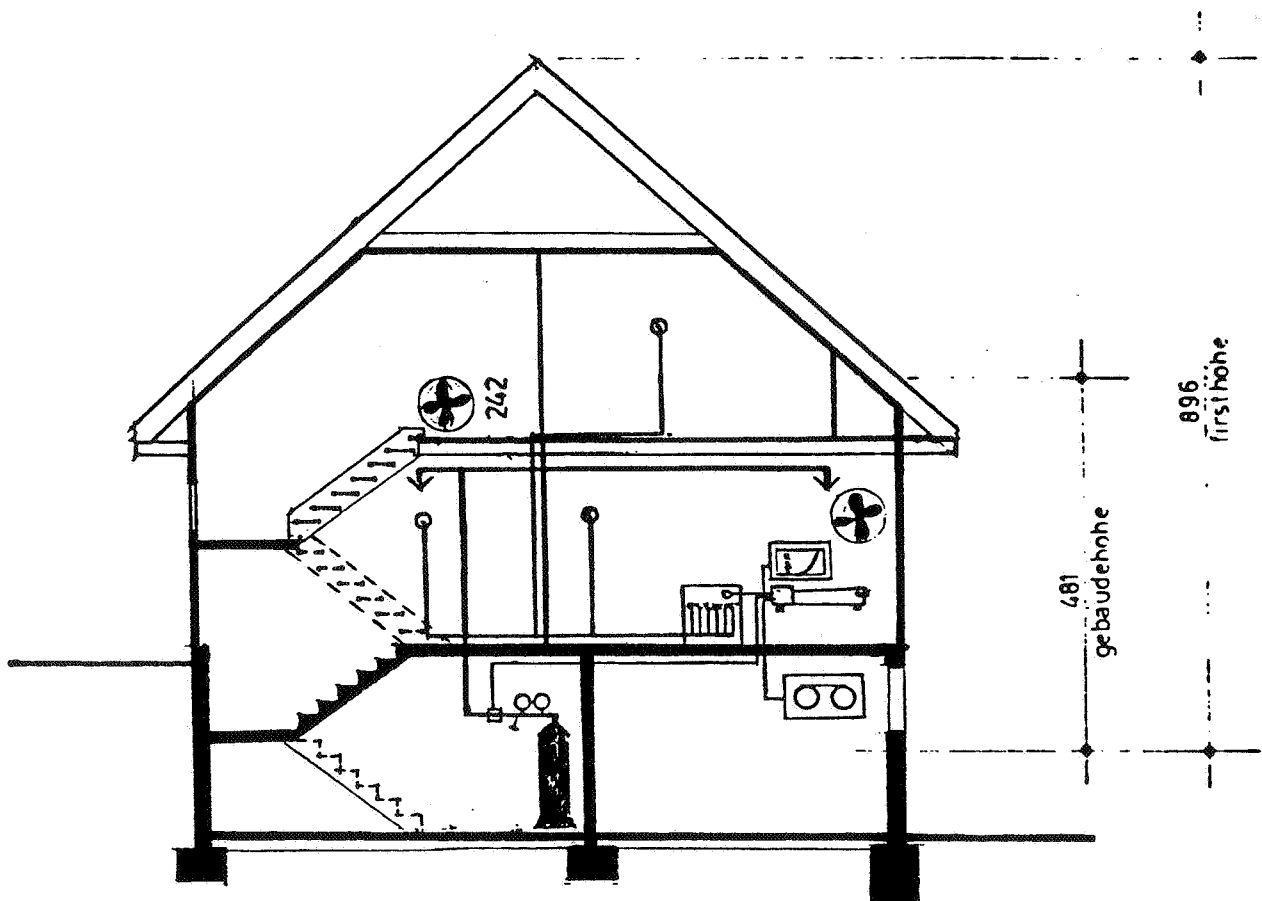


Fig. 6 Schematic vertical section through the test-building, including the main parts of the infiltration-instrumentation

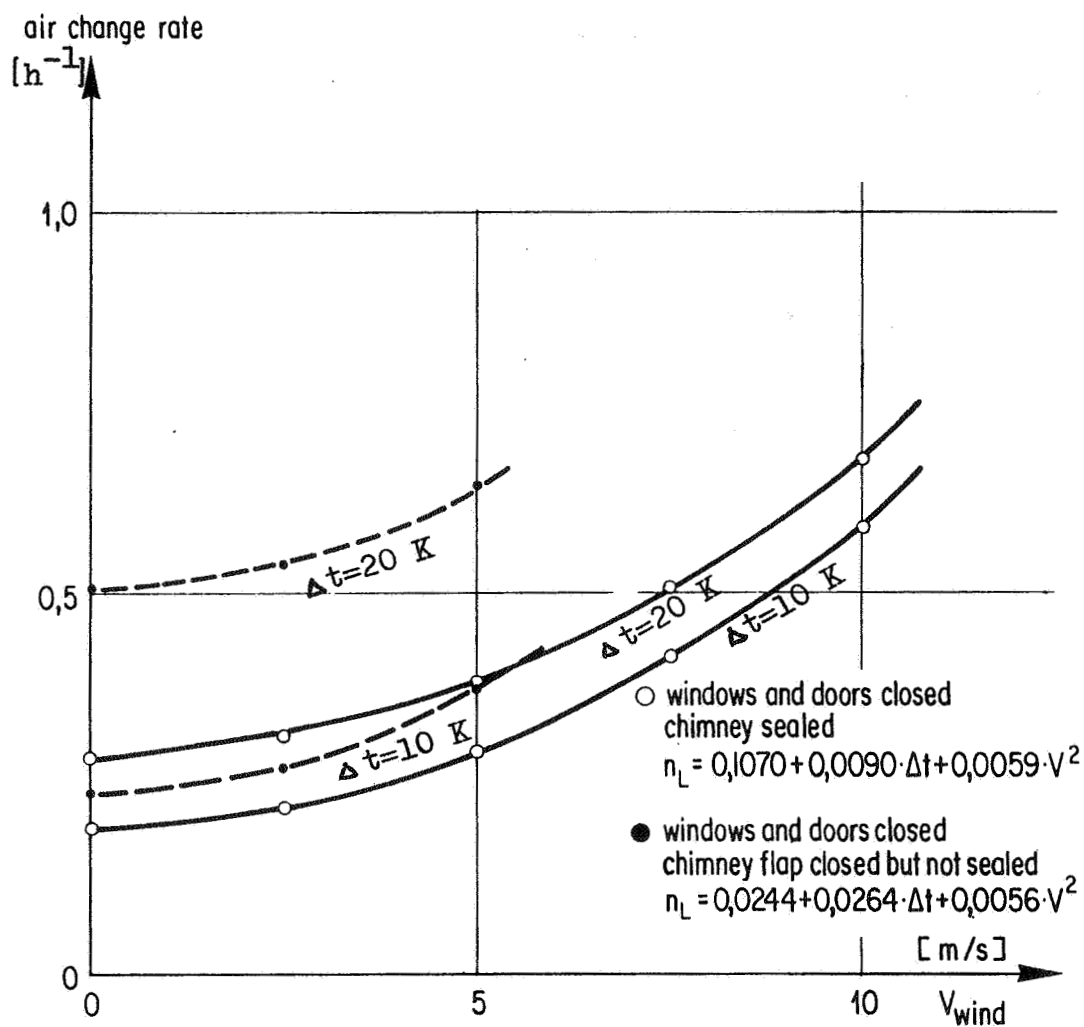


Fig. 7 Correlation of air-infiltration with wind-speed and temperature difference for the type of the test-building;

○ without an open fire-place

● with a fire place in the dining-room, with a closed, but not sealed flap

PAPER 6

**TRACER GAS AUTOMATED
EQUIPMENT DESIGNED FOR
COMPLEX BUILDING STUDIES**

**R. A. GROT,¹ C. M. HUNT,¹
D. T. HARRJE²**

**1. National Bureau of Standards
Washington
USA**

**2. Princeton University
New Jersey
USA**

For Presentation at
The First Air Infiltration Centre Conference
Instrumentation and Measuring Techniques
Windsor, England
October 6-8, 1980

**AUTOMATED AIR INFILTRATION MEASUREMENTS
IN LARGE BUILDINGS**

Richard A. Grot
Center for Building Technology
National Bureau of Standards
Washington, D.C. 20234

Charles M. Hunt
Center for Building Technology
National Bureau of Standards
Washington, D.C. 20234

David T. Harrje
Center for Energy and Environmental Studies
Princeton University
Princeton, NJ 08544

ABSTRACT

An automated air infiltration measurement system for large buildings is described. The system consists of a micro-computer, electron capture gas chromatograph, a ten port sampling manifold, and five tracer gas injection units. The system controls the injection and sampling of tracer gas in a multi-zone building, calculates the air infiltration rates of each zone, and measures the on-time of events such as HVAC fan operation, exhaust fan operation, and door/window openings. The measurements also include such analog variables as interior and exterior temperatures, wind speed, wind direction and pressure differentials across the building envelope. The data collected using the automated air infiltration system in large buildings will allow the determination of the relative importance of air leakage and forced ventilation on the energy requirements of the building, as well as evaluating the influence of meteorological conditions, HVAC fan operation, exhaust fan operation and exterior building pressure on the air leakage.

INTRODUCTION

It is generally assumed that the air exchange rate for large buildings is dominated by the requirements for ventilation of the building and that the air leakage into such buildings is only a small component of the total air exchange of the building. However, little data have been collected to verify that the air leakage in large buildings is indeed small, and that the ventilation rates that the building is experiencing under actual usage is that intended by the designers of the building and the designers of its HVAC system. Also, although the air leakage rate of a large building may be small compared to the ventilation requirements of the building, the energy requirements on the heating and cooling system imposed by air leakage in large buildings may be significant since such air leakage is uncontrollable and offers no opportunity for recovery of the energy lost. The parameters that influence air leakage in large buildings are also not well understood. It is not certain whether the air leakage is driven by the pressures induced by the operation of the mechanical system or by the natural driving forces of wind and temperature.

In an attempt to answer these questions, a project was started at the National Bureau of Standards under sponsorship of the U.S. Department of Energy to investigate the nature and causes of air infiltration in large buildings. The first building studied in this project was the 11-story administration building at the National Bureau of Standards in Gaithersburg, Maryland [1].

The air infiltration measurements initially made in the NBS administration building were accomplished using a semi-automated air infiltration measurement system [2-3]. The tracer gas was injected manually into the building. Tracer concentrations were measured using an electron capture gas chromatograph with the output recorded on a strip-chart. This system required large amounts of manual data reduction and required the frequent presence of technicians during the periods when measurements were being made. As part of the U.S. contribution to the International Energy Agency project to study the heating and cooling requirements of a large building near Glasgow, Scotland, the National Bureau of Standards was requested by the U.S. Department of Energy to provide the investigators of the Building Services Research Unit of the University of Glasgow^{*} with an automated air infiltration measurement system and to assist them in the operation and analysis of the data collected using the system.

The building being studied in the I.E. A. project is a four story, approximately 2.4 million cubic foot structure called the Collins Building and is located in Bishopbriggs, an outlying area of Glasgow. It is occupied by the Collins Publishing Company. It stands on open terrain with no immediately surrounding buildings, no external shielding, and on a grade so that there is one more exposed floor on the north side, than on the south. The building is serviced by four mechanical systems: one handling the basement, ground, first and second floors; a second handling the third floor; a third

^{*}This investigation is being conducted by Dr. Jeremy Cockcroft, now with Honeywell, Inc., and Neale Veech of the Building Services Research Unit of the University of Glasgow.

dedicated to the computer room; and the fourth used for the sports area.

The U.S. Department of Energy also requested that NBS provide a second air infiltration measurement system to be installed in a 26-story building called the Park Plaza Building in Newark, N.J. This building is occupied by Public Service Electric and Gas Company of New Jersey and is located in an urban environment.

It was decided that the automated air infiltration systems for application to these studies of energy usage in large buildings should be based on the automated air infiltration system previously developed and used in residences by Princeton University and NBS [3-4]. However, the new requirements on the measurement system (due to the complexity of the air handling system and multi-zone nature of large buildings) necessitated a more sophisticated design. It was decided that the most feasible approach was to incorporate a micro-computer in the measurement system, capable of being programmed to make the many decisions needed to properly handle the injection and sampling from several zones. This paper will describe this micro-computer based automated air infiltration measurement system.

Description of the Automated Air Infiltration System

The automated air infiltration system for large buildings is shown schematically in Figure 1. The system consists of a S-100 Buss micro-computer with two 5 1/4 inch dual-sided floppy disc drives, a 100,000 day real-time clock, a CRT terminal, a parallel printer, an electron capture gas chromatograph, a ten-port sampling manifold, five injection units, and an analog interface. The interfacing of the gas chromatograph, the sampling manifold and the injection units is accomplished through two specially designed S-100 interface cards: the S-100 air infiltration interface card, and the S-100 Buss octal A-C relay card. Figure 2 shows a block diagram of the interfacing of each component with the micro-computer. The micro-computer has a Z-80 based CPU (which operates at 4 MHZ), 64K of RAM memory, a disc controller and a dual serial/parallel I/O interface. It is programmable in Fortran, Z-80 assembly language, and Basic. Disc drive "A" of the computer is used for storage of the air infiltration programs and for "booting" the system. Disc drive "B" is used for data storage. Each has a capacity for storing 173k bytes of data. The resident disc operating system (on a PROM located on the disc controller card) was modified to allow for the automatic booting of the system and for the initialization of the air infiltration interface. Drivers for the real-time clock were added to the disc operating system so that the clock could be used through system calls.

The S-100 Buss air infiltration board controlled the capturing of the tracer gas peak and thus allowed the determination of the tracer gas concentration. A block design for this interface is given in Figure 3. This

interface board between the gas chromatograph and the S-100 Buss permits both software and hardware determination of the tracer gas concentration peak. The advantage of this flexibility is that in a system configuration where the computer is busy monitoring other variables, it is possible to output a short series of commands to the S-100 Buss air infiltration board. The peak detector will determine the tracer peak automatically, indicating to the computer when it has found the peak (usually about 25 seconds after initialization of the sequence). In a configuration in which the compiler is not busy with other functions, the peak can be detected by software. The software mode is more reliable and less sensitive to noise and adjustments to the gas chromatograph. The air infiltration board also has two 8-bit parallel output ports and can automatically control the activation of the rotary sample valve on the gas chromatograph, although in the configuration for large buildings this function is accomplished by a S-100 octal A-C relay card. The system has two S-100 Buss octal A-C relay cards. The block diagram for this card is given in Figure 4. These two cards control the sample value manifold, the injection units and the rotary sample valve on the gas chromatograph. They also serve as input ports for events data.

In the Collins Building, flow switches were installed in the HVAC and the exhaust fan systems. The output from these flow switches were connected to the event status ports on the S-100 Buss octal A-C relay cards. The interrupt service routine of the monitoring program would check the status ports each second to determine which HVAC system was operating and which exhaust fans were on. If the HVAC system of a zone was not operating, no injection of tracer into the zone was permitted.

The tracer gas selected for the study of air exchange in large buildings is sulfur hexafluoride. Although there are several suitable tracer gases for residential buildings, practical constraints limit the choice when dealing with volumes of one million cubic feet and more. One cannot truck in large quantities of tracer gas, rather the choice is to use a tracer which can be detected in concentrations as low as several parts per billion. For example, in a one million cubic foot building, the largest available cylinder of Nitrous Oxide would produce only 10 seedings of the building. The corresponding cylinder of sulfur hexafluoride would produce 10,000 seedings.

To minimize the size of the air infiltration measurement system, maximum use was made of the micro-computer cabinet. For example, the election capture gas chromatograph was removed from its standard cabinet, and the pneumatic rotary actuator was connected to the sample valve (Figure 5). The unit was then installed in the redesigned front panel in the micro-computer cabinet. The units power supply, in turn, was placed in the power supply section at the rear of the cabinet. In this way no additional space was required.

The 10 port sample manifold is shown in the photograph in Figure 6. It was designed so that it would fit in the rear of the computer cabinet, thus fully utilizing the cabinet space. The solenoids of the 10 port sample valve manifold were connected to the first octal A-C relay card and to the first two relays of the second octal A-C relay card. In any application in large buildings, auxiliary pumps must be added to the sampling system since the pump of the gas chromatograph is not designed to pull samples through the long lengths of tubing required by the building sampling network.

The injection units for a large building vary according to the size of the zone being seeded by the unit. For zones in excess of 300,000 ft³, the injection unit consists of an appropriately sized cylinder of tracer gas with a pressure regulator and leak-tight solenoid. For volumes less than 300,000 ft³ a specially designed injection unit consisting of a low pressure tank, a low pressure regulator and a zero leakage solenoid valve is required (see Figure 7). The maximum size of the tracer gas container is based upon maximum safe concentration of the tracer gas to which the occupant of the building could be subjected without harmful effects. That is

$$(Q_t/V_z) < C_{\max} \quad (1)$$

where Q_t is the quantity of gas contained in the injection unit tank, V_z is the volume of the zone served by the injection unit and C_{\max} is the maximum safe tracer concentration, usually taken to be a factor of three or more lower than the OSHA eight hour maximum concentration (i.e., 1000 ppm for SF₆).

Equation (1) is based on the assumption that the tank of tracer gas exhausted its contents instantly. In practice, the most likely mode of failure is a leaking injection valve. In that case, the flow controlling orifice would spread the leakage over an extensive period of time further limiting concentration build-up. Table 1 gives the parameters pertinent in the selection of the injection unit tank size for the four injection zones of the Collins Building. The estimated duration of each reservoir was

TABLE 1

PARAMETERS AFFECTING TANK SELECTION FOR ZONES OF COLLINS BUILDING

	Volume of Zone V_z	Injection Tank Size Q_t	Maximum Concentration Q_t/V_z	Estimated Duration of Tracer Supply
Zone Supplied by Main HVAC	$2.4 \times 10^6 \text{ ft}^3$	95 lb (1A cyl.)	245 ppm	~ 45 days
Zone Supplied by Third Floor HVAC	175,000 ft^3	10 lb (No. 3 cyl.)	360 ppm	~ 60 days
Computer Area	74,000 ft^3	1.3 lb	70 ppm	~ 22 days
Sports Area	68,000 ft^3	1.3 lb	80 ppm	~ 24 days

derived by assuming an injection of 100 ppb of tracer every three hours, 24 hours a day, seven days a week.

The 16-channel analog A/D interface card also deserves special mention. This card monitors such interior and exterior parameters as temperature, wind speed, wind direction and exterior building envelope pressure differentials.

Description of Software of Operating the Automated Air Infiltration Unit

A group of programs was developed for operating the automated air infiltration unit in large buildings. Two general subroutine libraries were written. The first library contained the interrupt related subroutines that were needed for controlling the injection of tracer gas, the determination of the status events, and the control of the sampling manifold. Although these subroutines were written in assembly language, they are all Fortran callable and thus allow the development of programs by those familiar with Fortran. The second library consisted of subroutines which did not depend on the interrupt feature of the micro-computer. Several diagnostic programs for testing the functioning of the major components of the hardware were also written and the program for the calibration of the electron capture detector was developed so that air sample bags of known tracer concentration could be used to obtain the coefficients C_0 and β of the equation:

$$C = C_0 [\ln (S/P)]^\beta \quad (2)$$

where S is the standing current P is the peak current, C is the concentration in ppb. For the gas chromatograph used in the systems installed in the Collins Building, the coefficients C_0 and β are approximately 80 ppb and 0.95 respectively.

Figure 8 shows a block diagram of the monitoring program for the Collins Building. Initially the program determines the parameters of the building, and then measures the initial concentration and injects tracer gas into the zones of the building.

The injection of tracer gas is controlled by the following considerations. In a large building with several interesting zones, it is desirable to keep the tracer gas concentrations of each zone approximately equal in order to minimize the error caused by the interchange of tracer between the zones. Also, in large buildings it is prudent to inject the tracer slowly into the ducts in order to ensure proper mixing. It was decided to design for an injection time of 5 minutes (about 4 times that used by the automated air infiltration system used in homes) and allow for possible injection times of up to 10 minutes. In order to insure that all zones at least started at approximately the same concentration level the injection time each hour was calculated from the following equations:

$$\frac{dC}{dt} = AIC + F \quad \text{during injection } (0 < t < t_0) \quad (3)$$

$$\frac{dC}{dt} = -AIC \quad \text{during mixing } (t_0 < t) \quad (4)$$

where AI is the air infiltration rate, C the tracer concentration and F the injection flow rate per unit volume.

The mixing period was specified as $\tau = 20$ minutes after the start of injection.

Equation (3) and (4) can be solved to yield the expressions:

$$C(t) = (C_0 - \frac{F}{AI}) e^{-AIt} + \frac{F}{AI} \quad 0 < t < t_0 \quad (5)$$

$$C(t) = [(C_0 - \frac{F}{AI}) e^{-AIt_0} + \frac{F}{AI}] e^{-AI(t-t_0)} \quad t_0 < t \quad (6)$$

If C_1 is the concentration at the end of the mixing period then:

$$C_1 = [C_0 - \frac{F}{AI} + \frac{F}{AI} e^{AI t_0}] e^{-AI\tau} \quad (7)$$

The concentration C_1 is chosen so that it lies in the linear range of the gas chromatograph as determined by the calibration curve of the electron capture detector. In the case of the system installed in the Collins building $C_1 \approx 120$ ppb. The initial concentration C_0 was chosen as the last measured concentration of the previous sample period. The injection time for each zone was then calculated by the following equation:

$$\begin{aligned} t_0 &= \frac{1}{AI} \ln \left[1 + \frac{AI}{F} (C_1 e^{AI\tau} - C_0) \right] \text{ if } 0 < t_0 < 10 \\ t_0 &= 0 \text{ if } C_1 e^{AI\tau} < C_0 \\ t_0 &= 10 \text{ if } t_0 \geq 10 \end{aligned} \quad (8)$$

The system then samples the zones once each ten minutes for the next 40 minutes. The air infiltration rates are determined by statistically fitting a semi-log curve

$$C = C' \exp(-AI\tau) \quad (9)$$

to each history of tracer concentration for each of the zones.

These data are then outputted to the discs and printer. Then the hourly cycle is repeated until the operator aborts the system.

Summary

The automated air infiltration measurement system described in this paper has proven to be capable of performing the complex tasks necessary for determining the air exchange rates in large buildings. Key components of the measurement system include: the micro-computer, the electron capture gas chromatograph, a ten port sampling manifold and five tracer gas injection units. How these components interact and the function each is performing have been discussed here in considerable detail. The programmed micro-computer is used: to control the injection of tracer gas, thus maintaining the building zones within chosen concentration limits; to selectively sample from the zones, thus accurately tracking the tracer gas concentration decay; and to store the resulting air exchange rate data on a floppy disc. The capacity of the micro computer allows storage of the event data (e.g. HVAC, fan operation and door/window openings), internal and external temperatures and the local weather data. With this vital information the air exchange rate measurements have that much more meaning, and thereby provide the basis for advancements in the understanding of the role of air infiltration in large buildings.

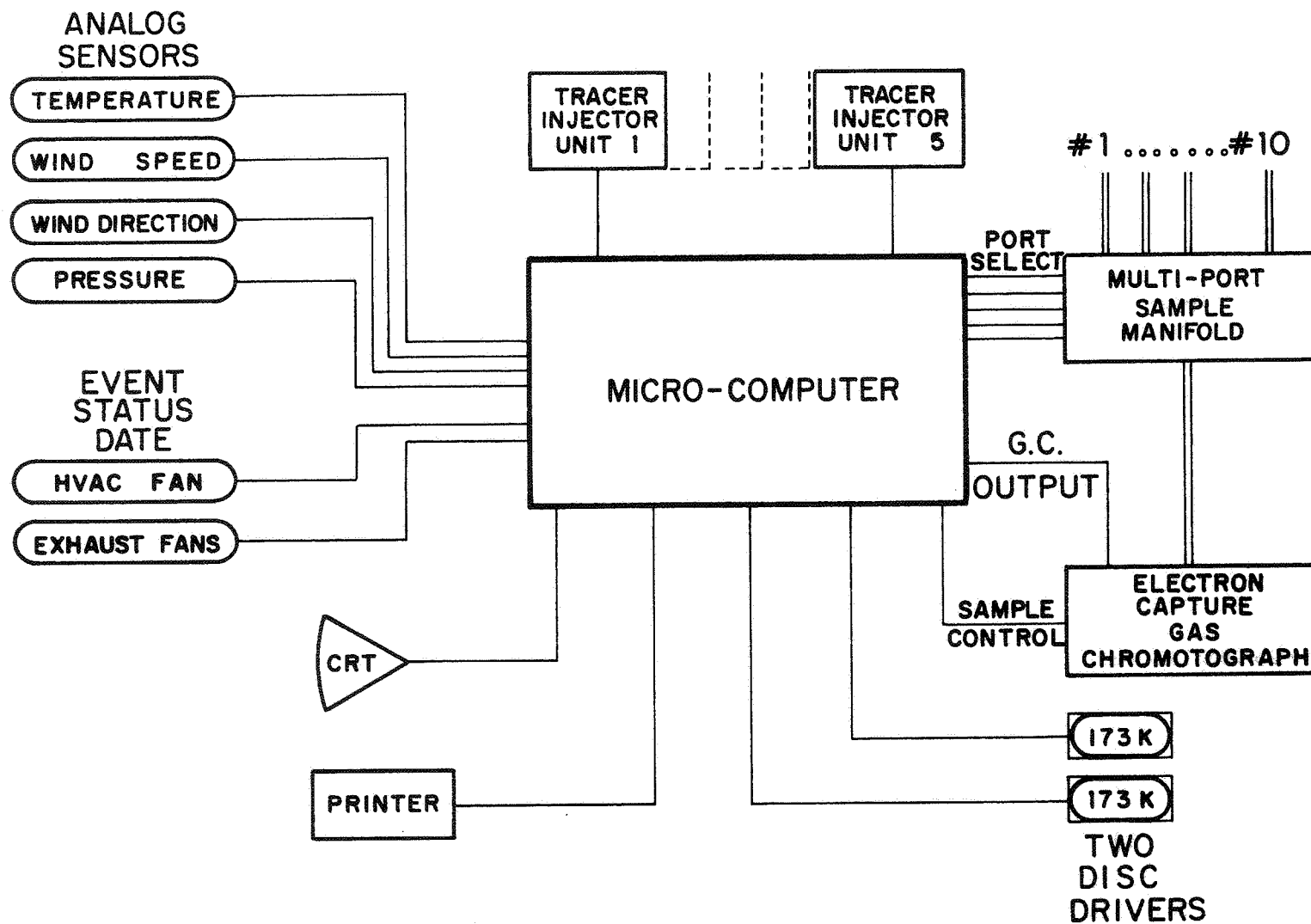
Although the initial application of this air infiltration measurement system has been in large multi-story commercial buildings, the built-in versatility allows wider application. For example, housing blocks with horizontal zoning and even tightly compartmentalized single-family houses often require air infiltration measurement systems with the capabilities described here. The compactness of the measurement system as illustrated in Figure 9 further aids its application potential in both large and small buildings.

Acknowledgements

The authors wish to acknowledge that the support for the measurement projects on large buildings described in this paper has been through the Building Division, Office of Building and Community Systems, U. S. Department of Energy. We also wish to acknowledge the contributions of Kenneth Gadsby, Princeton University, for his work on the design and calibration of the tracer gas injection systems.

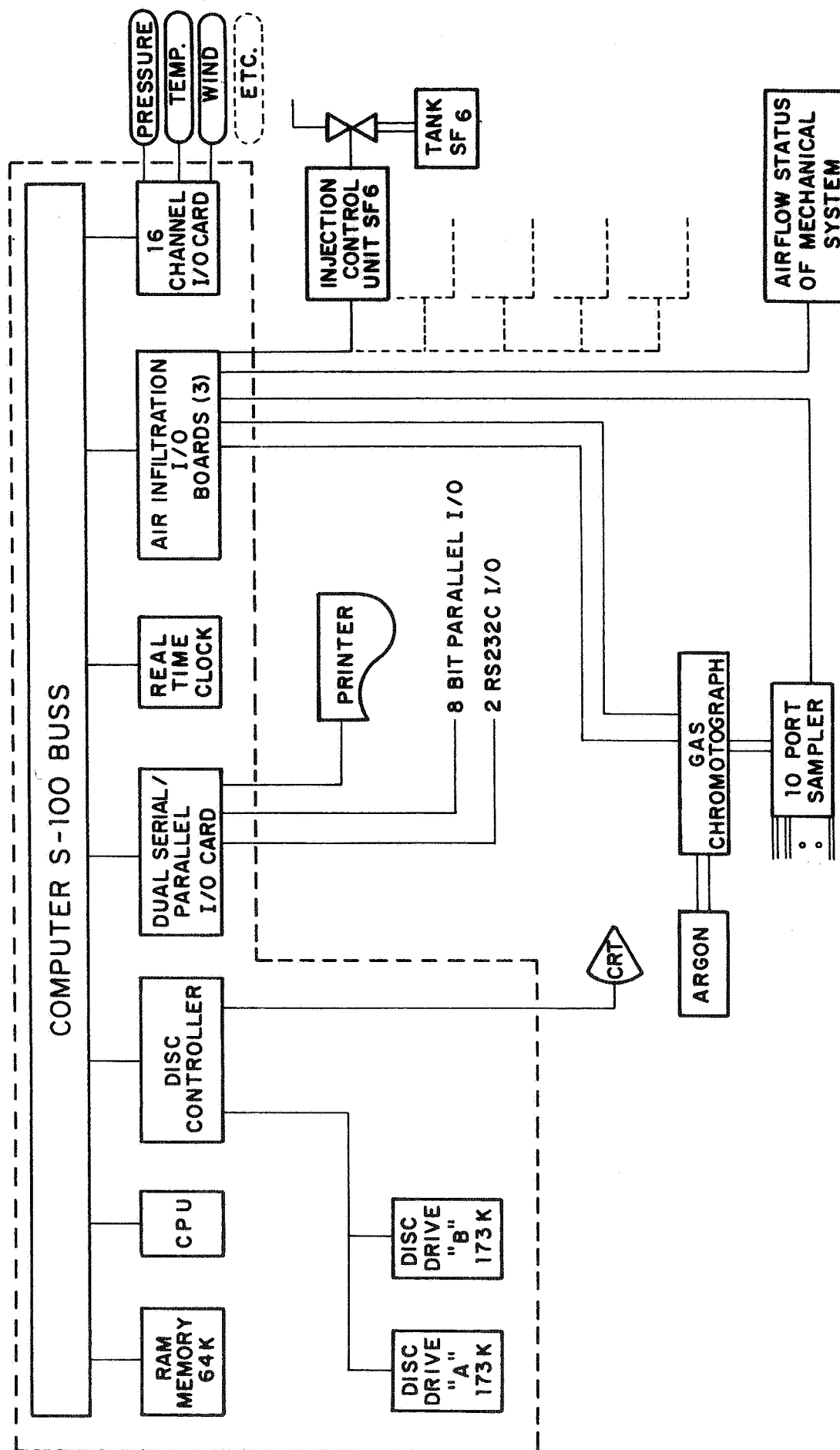
References

- [1] Hunt, C.M. and Treado, S.J., "Air Exchange Measurements in a High-Rise Office Building," Proceedings of the DOE-ASHRAE Conference on Thermal Performance of the Exterior Envelope of Buildings, Orlando, Florida, December 1979.
- [2] Hunt, C.M., and Treado, S.J., "A Prototype Semi-Automatic System for Measuring Air Infiltration in Buildings Using Sulphur Hexafluoride as a Tracer," National Bureau of Standards Technical Note 898, 1976.
- [3] Harrje, D.T., Hunt, C.M., Treado, S.J. and Malik, N., "Automated Instrumentation for Building Air Infiltration Measurements", Princeton University Center for Environmental Studies Report No. 13, 1975.
- [4] Harrje, D.T. and Grot, R. A. "Automated Air Infiltration Measurements and Implications for Energy Conservation," Energy Use Management , Proceedings of the International Conference, Vol. I, Pergamon, New York, 1977, pp. 457-464.



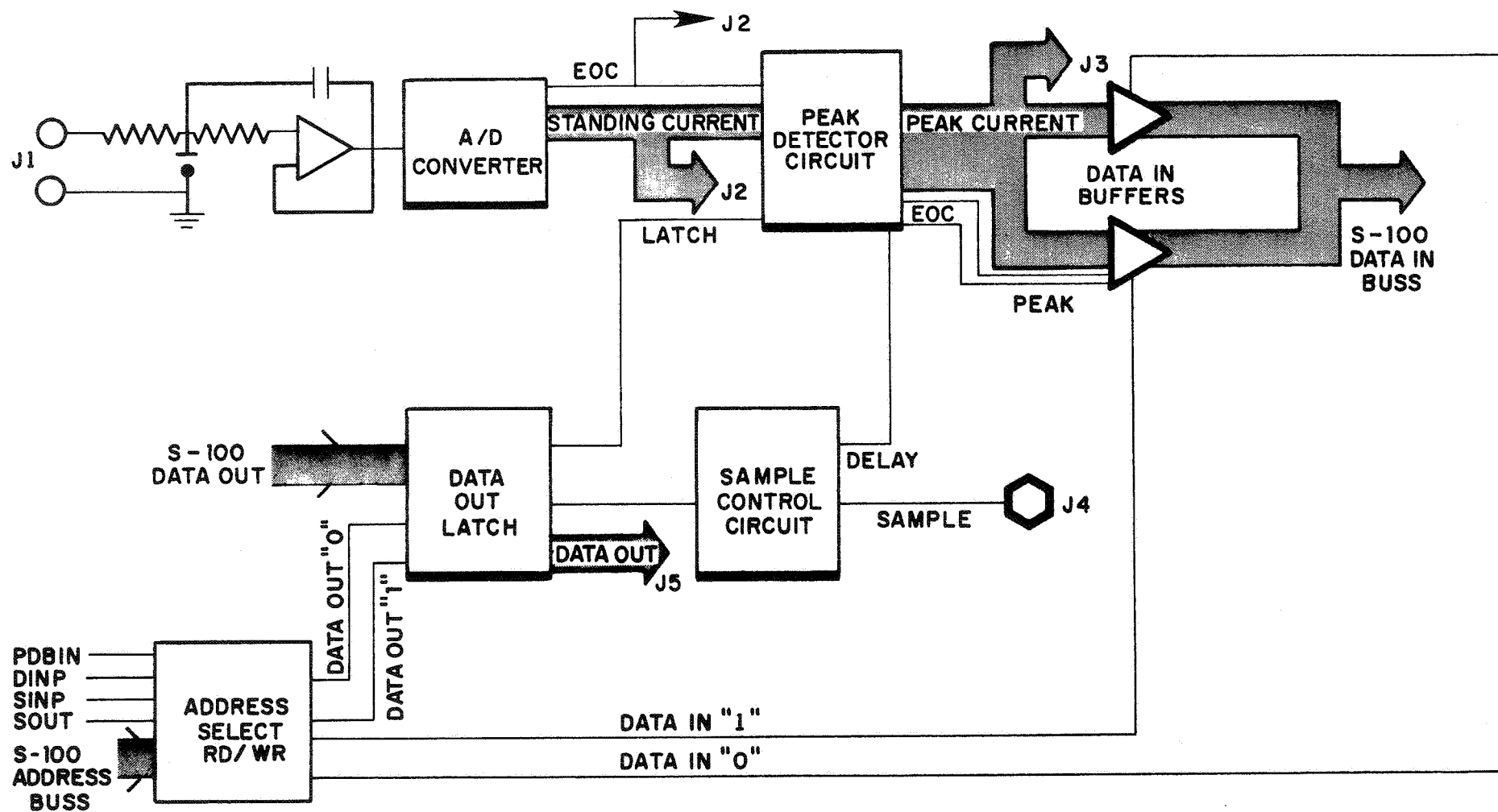
SCHEMATIC OF MAJOR COMPONENTS OF AIR INFILTRATION MEASUREMENT SYSTEM FOR LARGE BUILDINGS

FIGURE 1

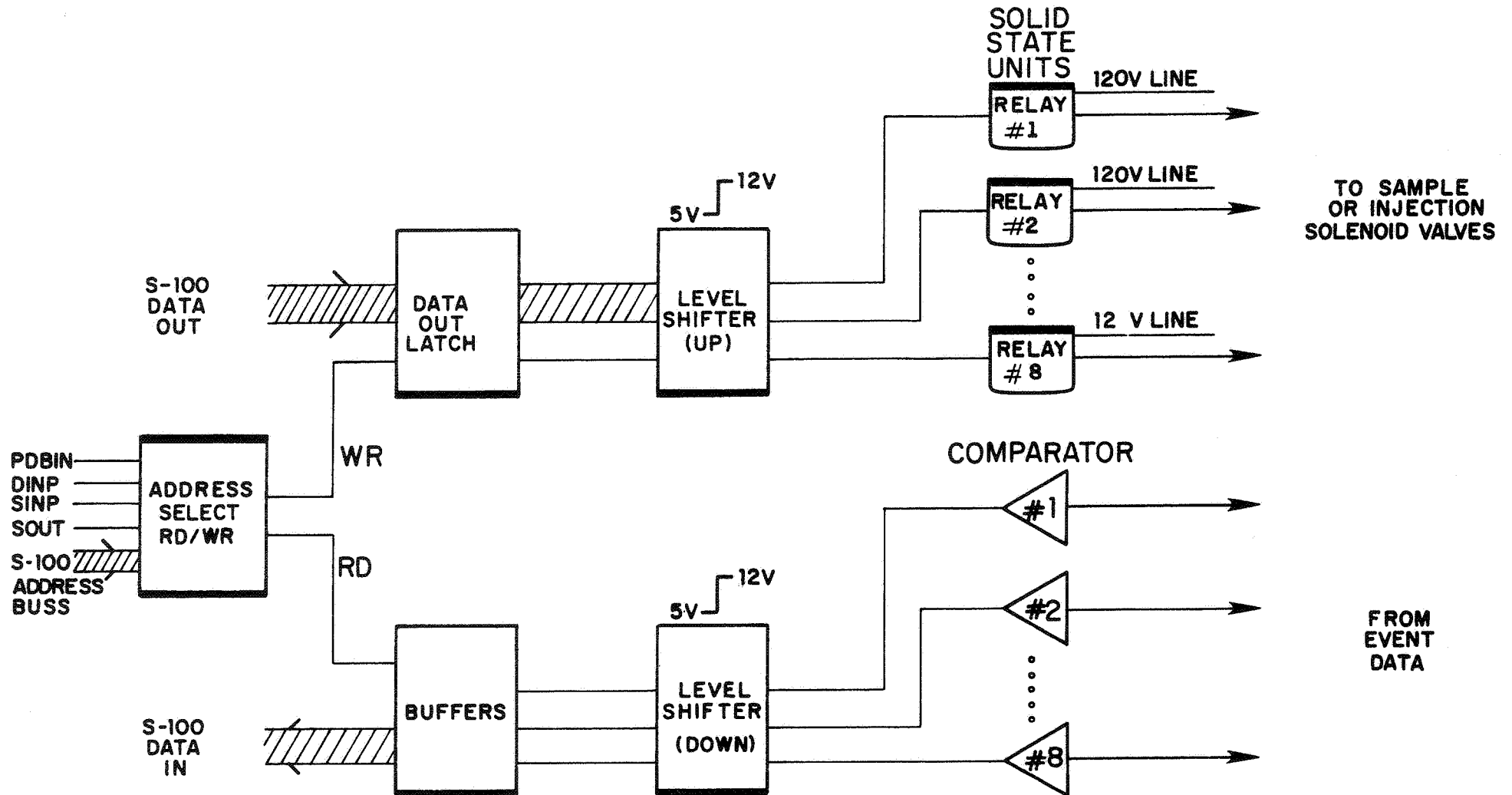


BLOCK DIAGRAM OF THE INTERFACING OF EACH COMPONENT WITH THE COMPUTER

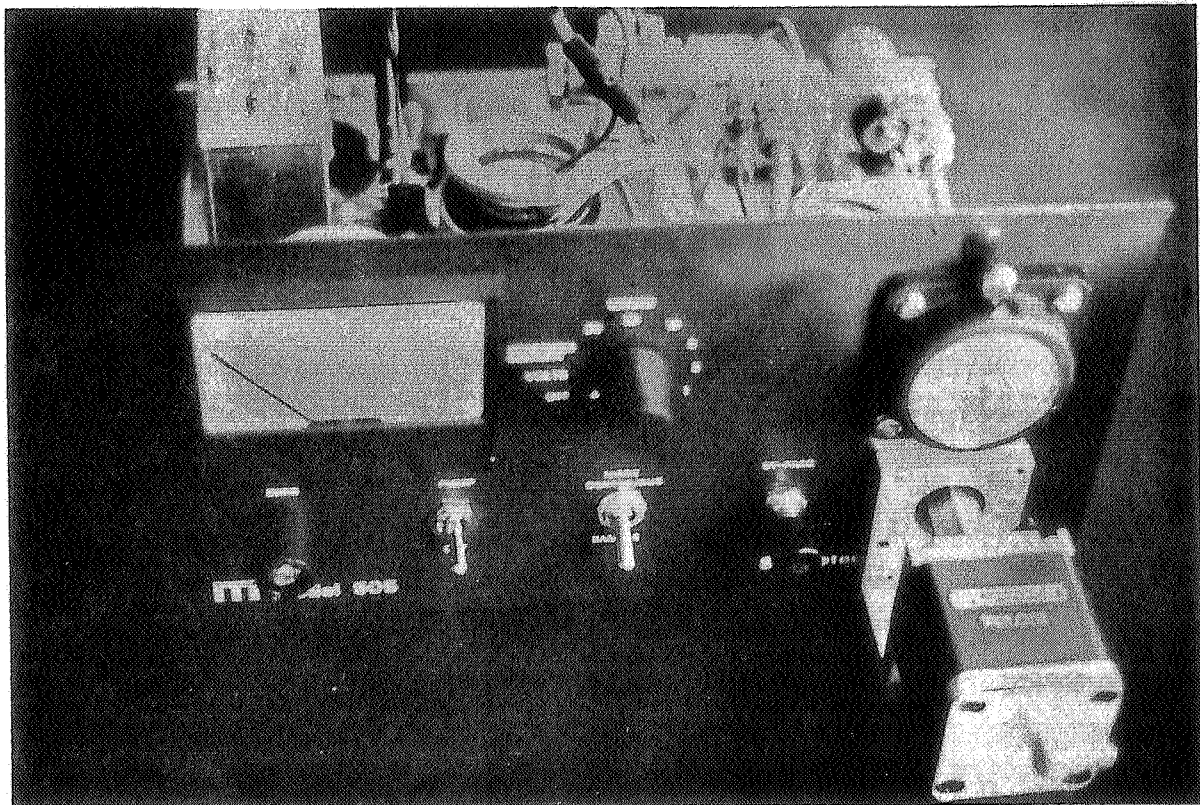
FIGURE 2



BLOCK DIAGRAM AIR INFILTRATION S-100 INTERFACE
FIGURE 3

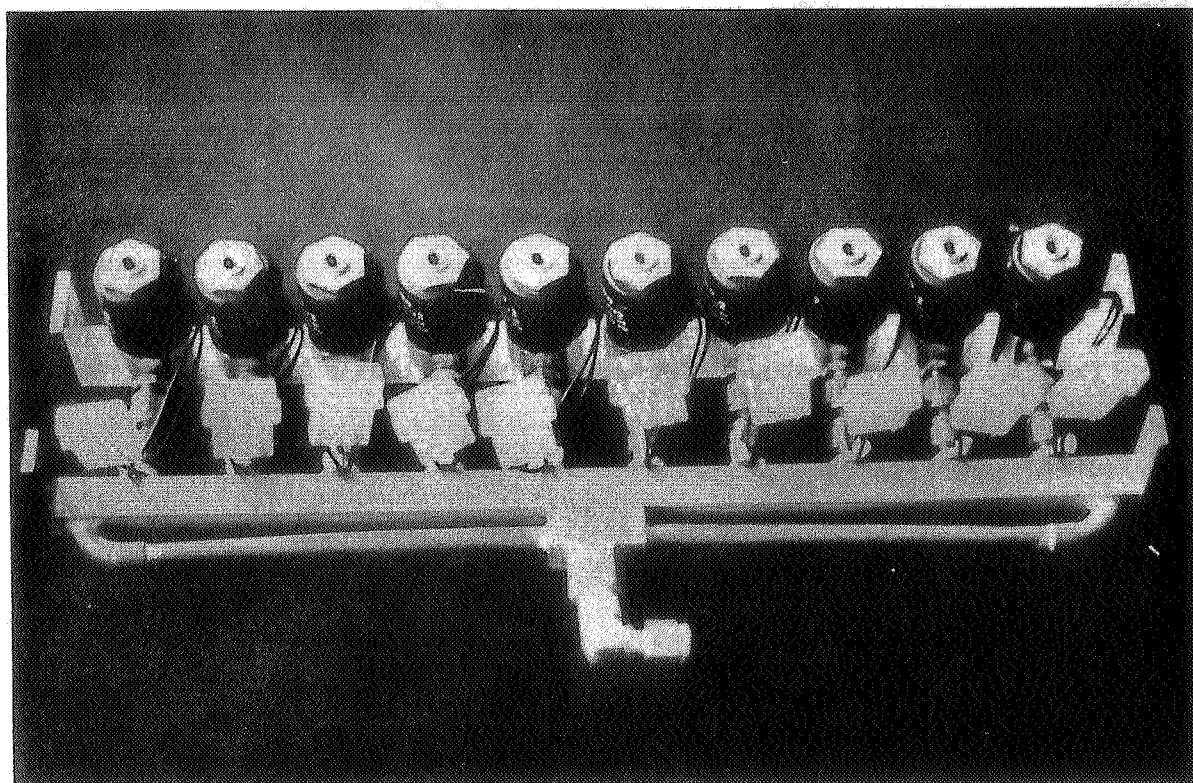


BLOCK DIAGRAM OF S-100 BUSS OCTAL A-C RELAY CARD
FIGURE 4



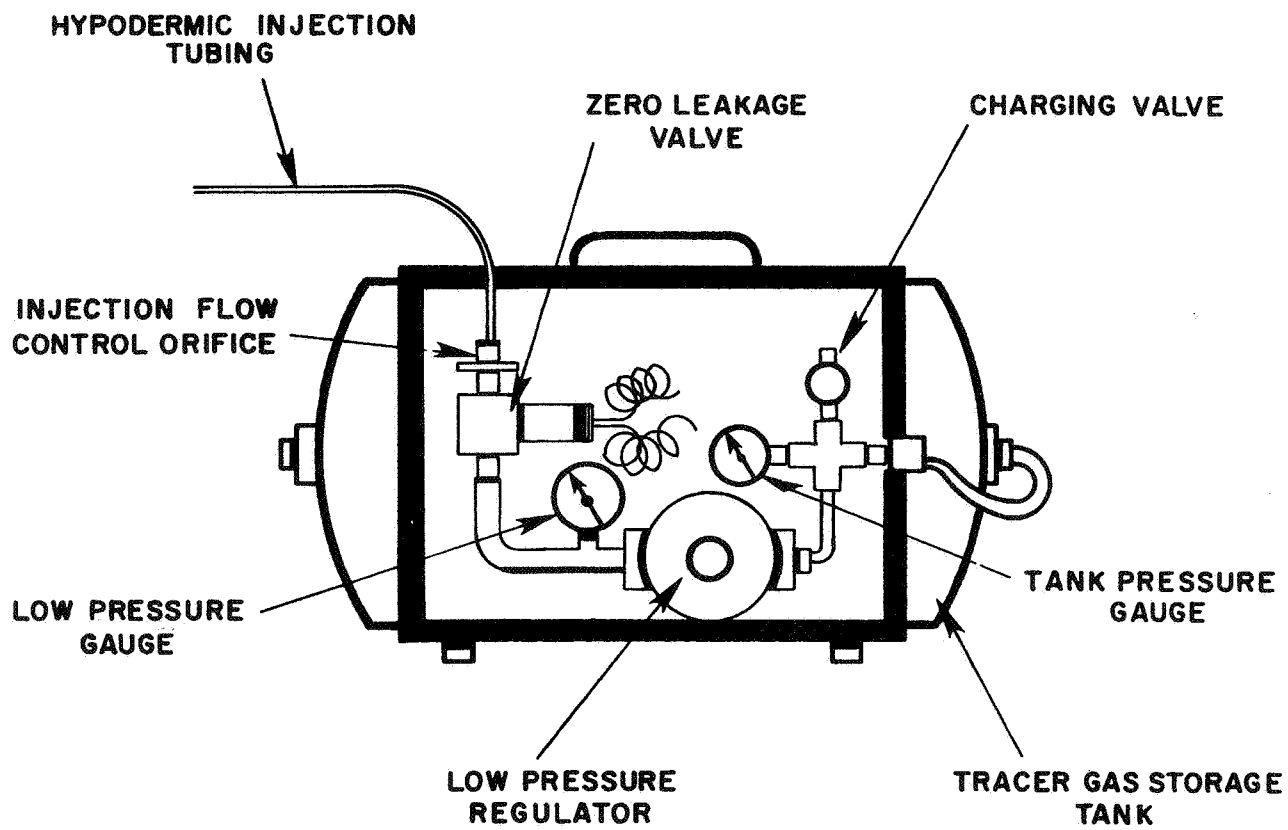
SF₆ DETECTOR USING AN ELECTRON CAPTURE GAS CHROMATOGRAPH
AND ROTARY VALVE ACTUATOR

FIGURE 5



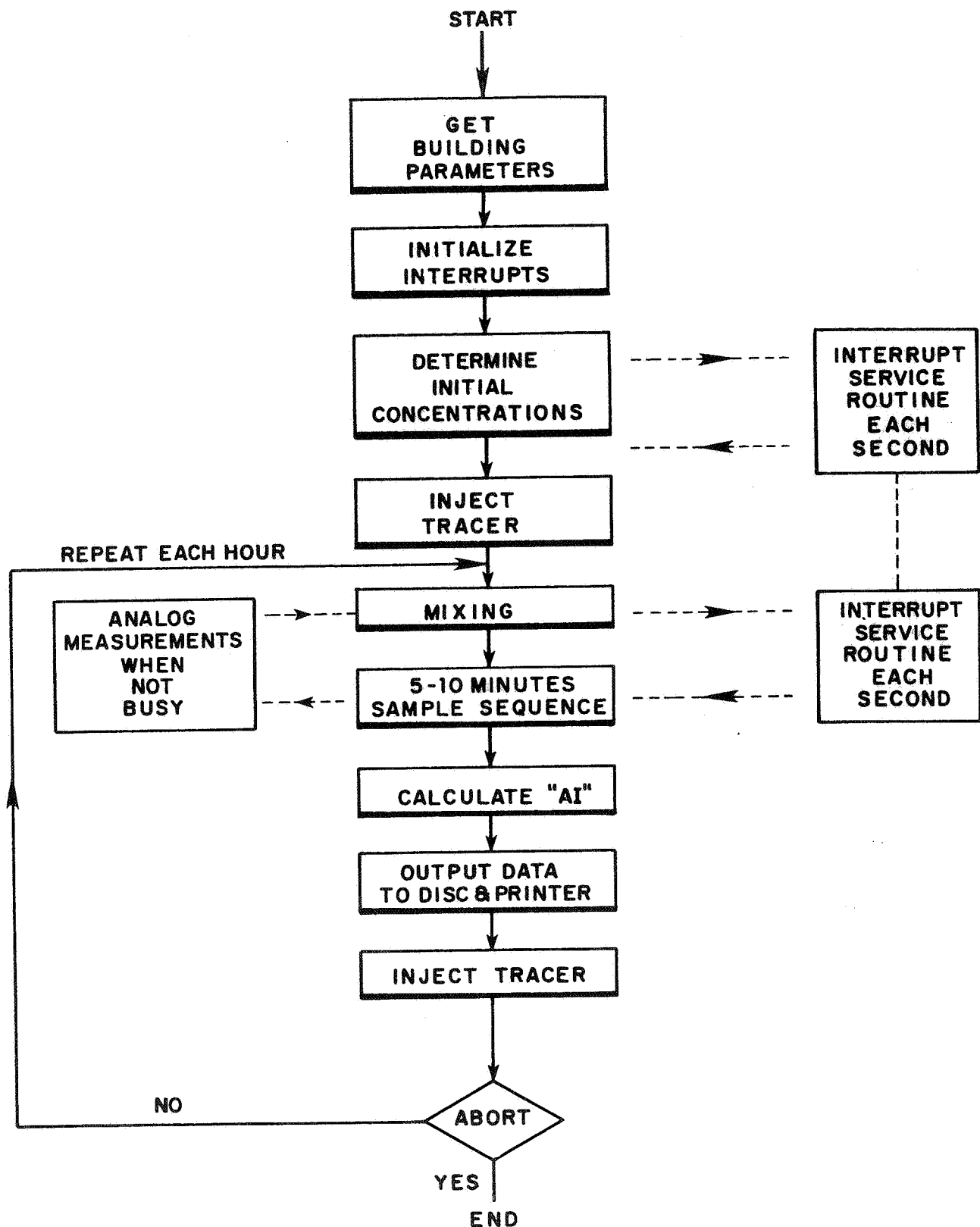
THE 10 PORT MANIFOLD USED FOR ZONE SAMPLING

FIGURE 6



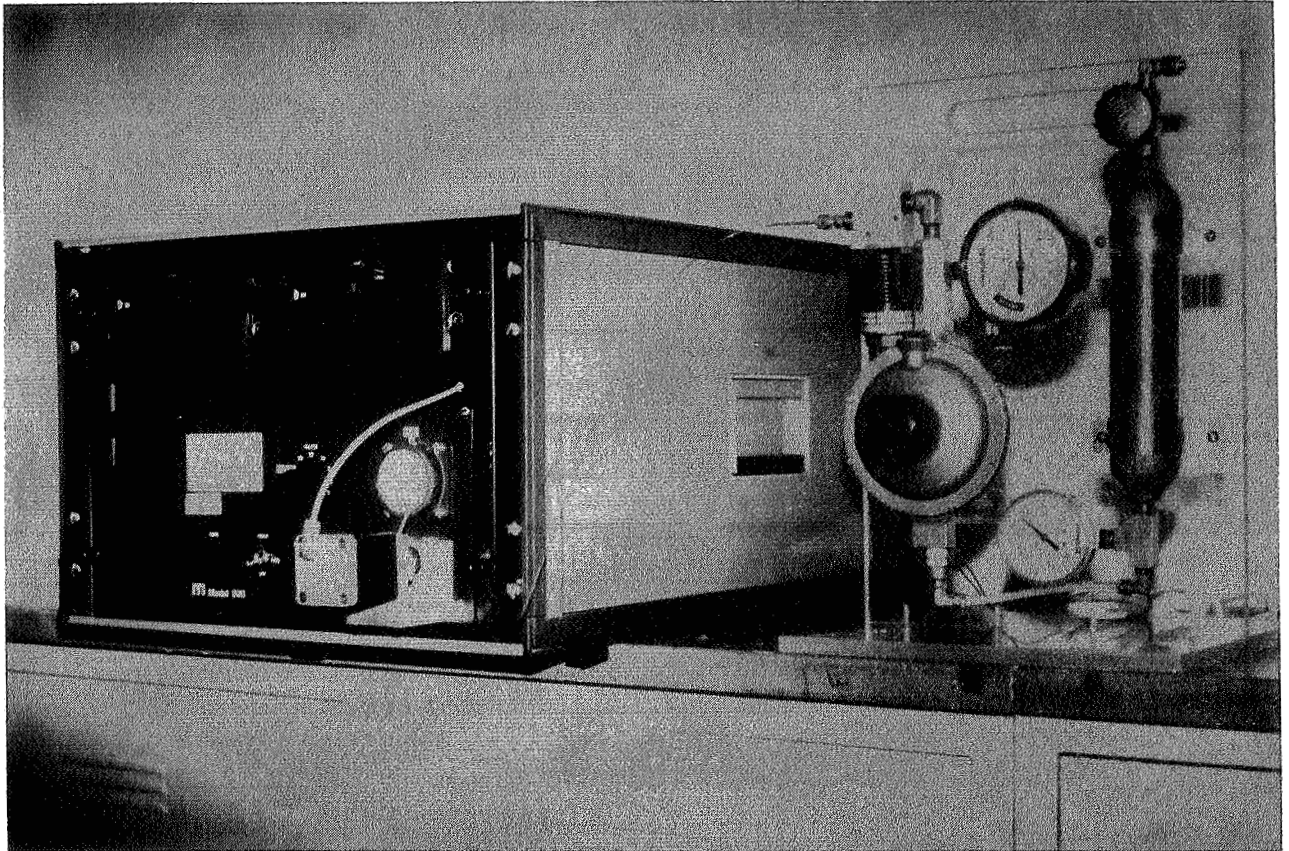
TRACER GAS INJECTION UNIT INCLUDING STORAGE TANK

FIGURE 7



SIMPLIFIED FLOW DIAGRAM FOR MONITORING AIR INFILTRATION
IN LARGE BUILDING

FIGURE 8



THE ASSEMBLED AUTOMATED AIR INFILTRATION MEASUREMENT
SYSTEM INCLUDING A SMALL ZONE TRACER GAS INJECTION SYSTEM

FIGURE 9

PAPER 7

**PROBLEMS AND CONSEQUENCES OF
THE PRESSURIZATION TEST FOR
THE AIR LEAKAGE OF HOUSES**

W. F. DE GIDS

**IMG-TNO
Delft
Netherlands**

PROBLEMS AND CONSEQUENCES OF THE PRESSURIZATION TEST FOR THE AIR LEAKAGE OF HOUSES

W.F. de Gids
Institute for Environmental Hygiene-TNO
P.O. Box 214
Delft
Netherlands

Contents

- Summary
- 1. Introduction
- 2. Description of the method
- 3. Problems
- 4. Measurements
- 5. Relation between pressurization results and infiltration rates
- 6. Relation between air leakage and energy losses due to infiltration
- 7. Conclusions
- 8. References

Summary

Research has been carried out on the problems and consequences of a measuring method for the determination of the air leakage of houses. From the research it has appeared that the pressurization test for the air leakage of houses can be used to compare houses on air leakage. Additional measurements on the distribution of air leakage over the building components are sometimes necessary. The relation between air leakage and infiltration and hence also the relation between air leakage and energy losses due to infiltration is not clear.

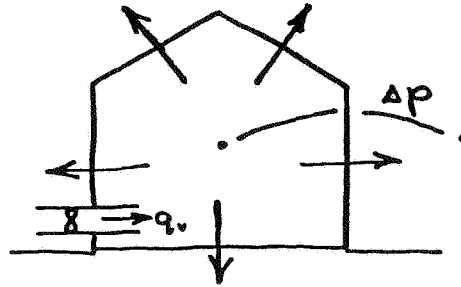
1. Introduction

Fan pressurization, blower door system, air leakage test, etc., all these are words to describe a test method for the air tightness of houses (see Refs. 1, 2, 3, 4 and 5). Infiltration losses become more important as houses are better insulated. One wishes to have a simple and less time-consuming method to quantify the air tightness of the building envelope. The important question arises whether the fan pressurization test is a reliable method in relation to occurring infiltration rates and energy losses due to this infiltration. This paper tries to give an overview on the problems and consequences of the pressurization test on houses.

2. Description of the method

A fan fixed in or on a "dummy door" pressurizes or depressurizes a house, in which all internal doors are open. The nominal value of this pressure is about 50 Pa. The pressure difference between inside and outside will be measured as a function of the air flow rate through the house (see Fig. 1).

Figure 1



In general this can be written as:

$$\Delta p = f(q) \dots\dots (1)$$

or more specifically:

$$\Delta p = (q/C)^n \dots\dots (2)$$

in which:

p=pressure difference

q=air flow rate

C=air leakage coefficient

n=flow exponent

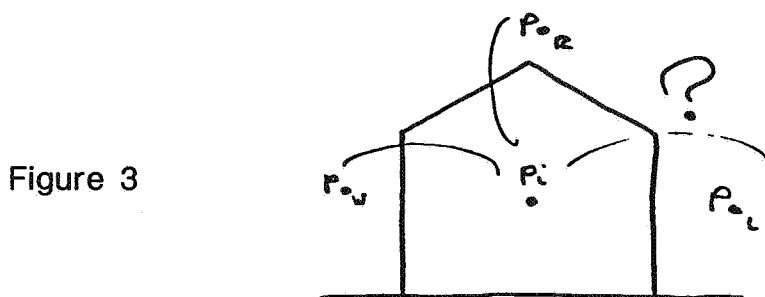
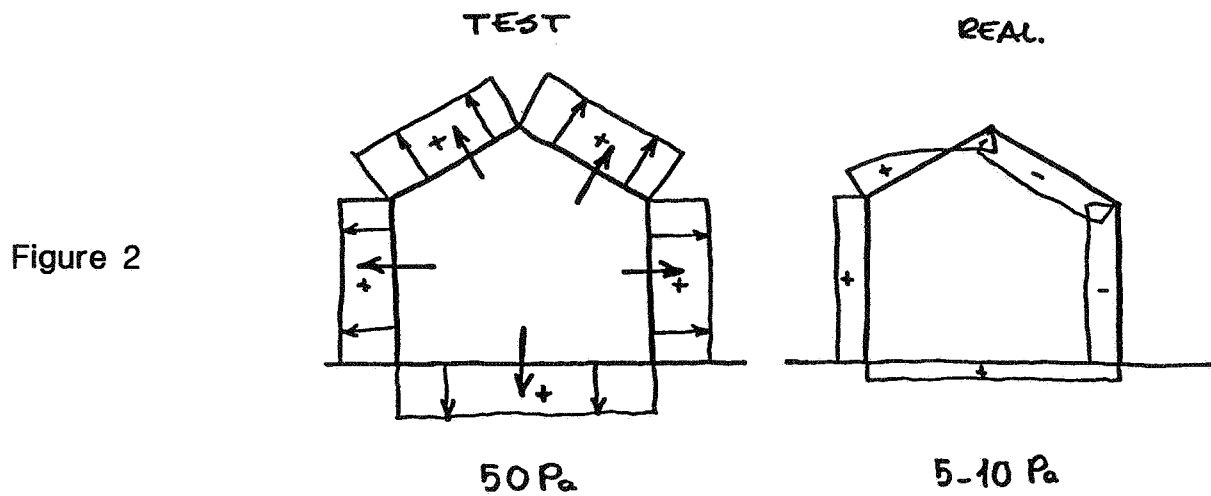
The air leakage coefficient is a function of a representative open area.

3. Problems

The following problems are associated with pressure tests:

- 3.1 There is a difference between the homogeneous pressure distribution over the building envelope during the test and the pressure distribution in reality. Also the pressure difference levels have an order of magnitude difference (see Fig. 2).

3.2 Where is the pressure difference measured ? More specifically:



Where should the outside pressure tap be placed during the measurements ? As one can imagine, due to wind and thermal forces, there is a difference in pressure between windward or leeward wall and roof (see Fig. 3).

This is one of the reasons to pressurize a house to about 50 Pa because, at that level, this influence is relatively small. But, even with 50 Pa pressure difference in a windy climate, there are enough circumstances under which accurate pressurization measurements are impossible.

3.3 The result of the pressurization test is an air flow rate at a certain pressure difference level. There is no quantitative information about the distribution of the leakages. Leakages to adjacent houses can play an important role (see Fig. 4).

3.4 In reality, the flow through cracks, caps, etc. can be laminar at some moments, at least at very low pressures, during the pressurization test at 50 Pa the flow will be more turbulent (see Fig. 5).

Figure 4

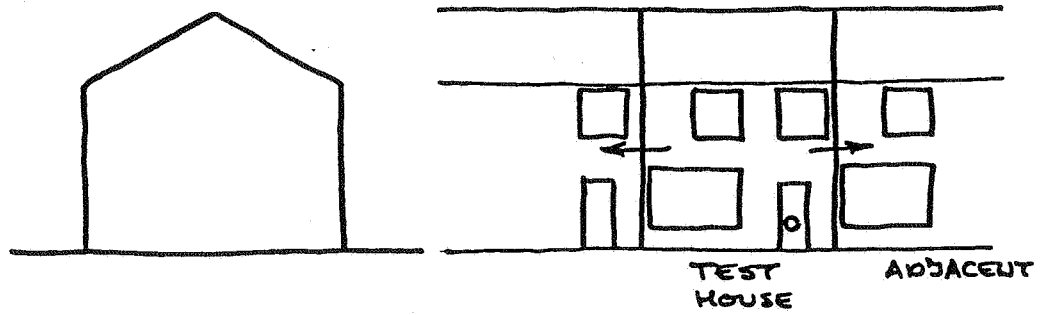


Figure 5

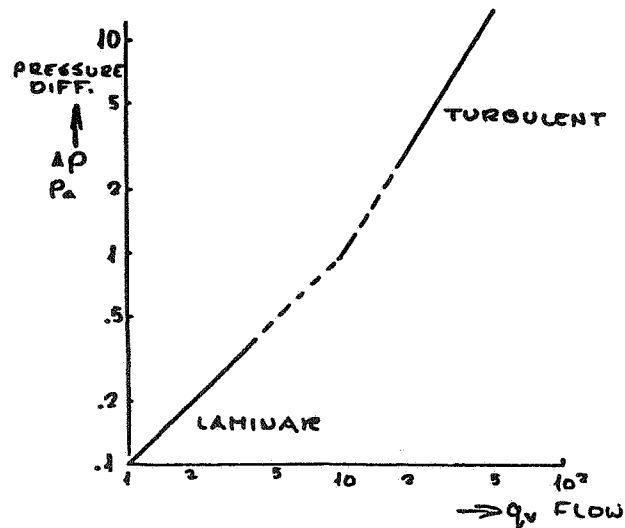
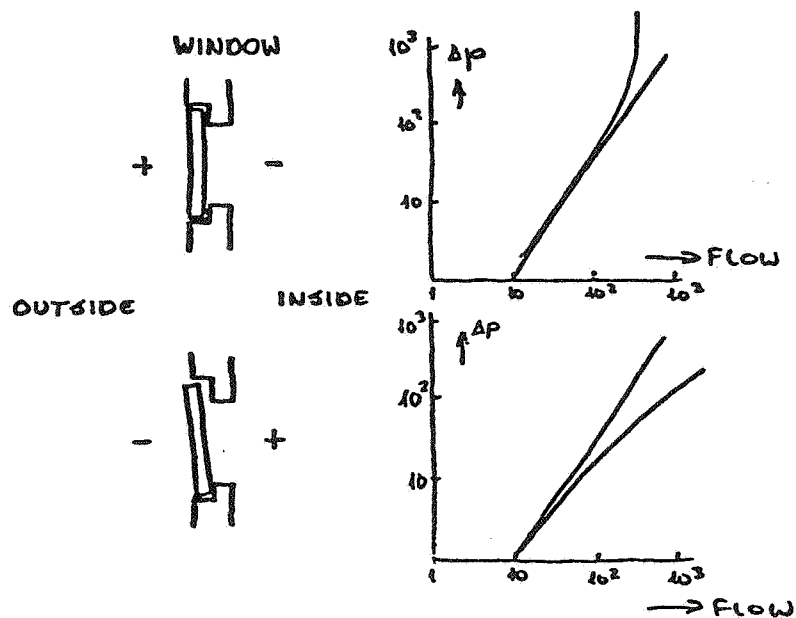


Figure 6



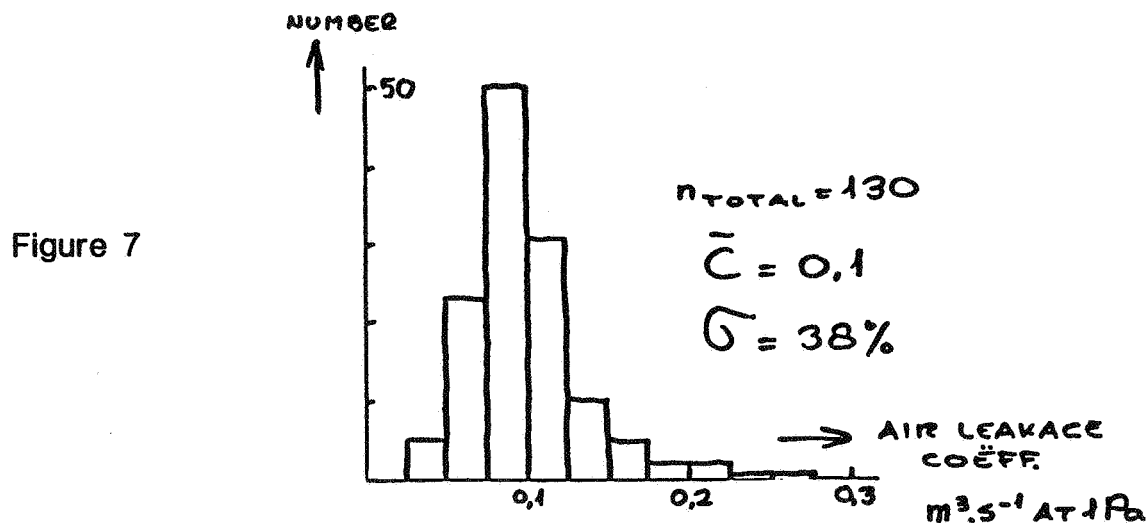
3.5 The possibility of changing air leakages by pressing open or sucking tight a window in its frame must be considered (see Fig. 6).

3.6 Replacing a door by a dummy changes the outside envelope of the house and so its air tightness a little.

To study these problems for the Dutch situation some measurements and calculations have been carried out (paragraph 5).

4. Measurements

4.1 The air leakage value of houses in the Netherlands.



A building co-operation carried out 130 (de)pressurization tests (see Ref. 6). A number of 130 cannot be statistically representative for 4.4 million houses, but all 130 can be qualified as typical houses for the Netherlands, normal price, size, building practice, etc. The results can be seen in Fig. 7. The mean air leakage value is 0.1 m³/s at 1 Pa with a standard deviation of 38%. These values are measured with all ventilation ducts open.

For comparison, Fig. 8 shows values of houses in other countries (see Refs. 7, 8 and 9).

The following remarks can be made:

- In Sweden some ventilation openings are blocked off during the test.
- The number of houses measured is too small to be representative for the total number of houses in other countries.

4.2 Distribution of air leakages over the building envelope.

In four houses the leakage of all components in the envelope were measured separately. Table 1 shows the results.

Table 1 : Distribution of air leakages over the envelope of houses.

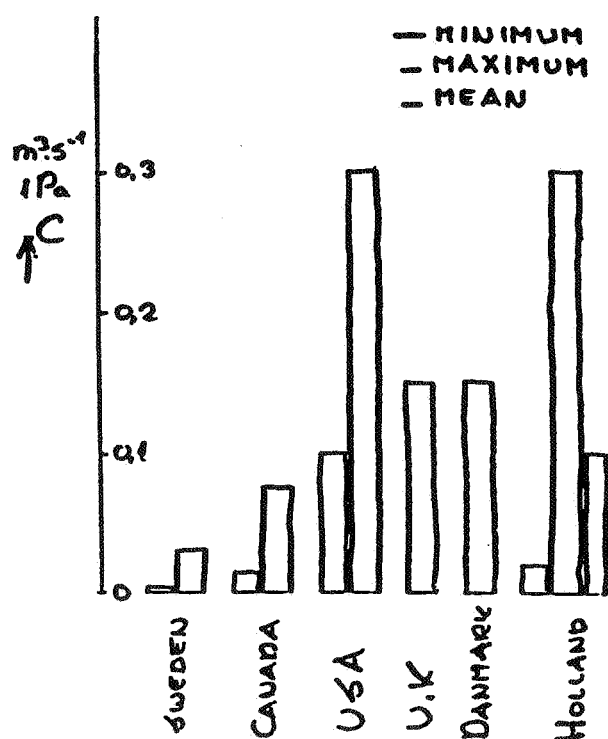
Houses	Components				
	Facades	Ducts	Roof and wall/roof connection	Unknown	Total dm ³ /s at 1 Pa
Apartments (concrete)					
1	42%	58%	x	-	22
2	17%	76%	x	7%	25
Single family houses (masonry)					
1	10%	27%	42%	21%	125
2	25%	27%	43%	5%	140

- not determined

x not relevant

The unknown air leakages may be the ground floor leakages, leakages to adjacent houses, etc.

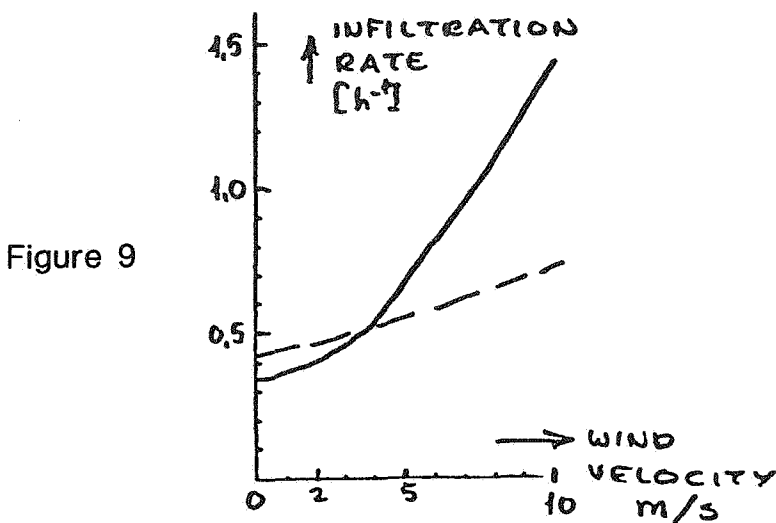
Figure 8



5. Relation between pressurization results and infiltration rates

A direct relation cannot exist due to the following reasons:

- Two houses with the same total air leakage can have different infiltration rates caused by:
 - another distribution of air leakages
 - another wind-environment
- Another problem is that the ratio between the air leakage co-efficient and the infiltration rate is not constant (see Fig. 9)



$$\text{RATIO } R = \frac{C}{a_2} \neq \frac{C}{a_5} \neq \frac{C}{a_{10}}$$

$$R = C/a_2 \neq C/a_5 \neq C/a_{10} \dots (3)$$

in which:

R=ratio

C=air leakage coefficient

a(i)=infiltration rate at i m/s
wind velocity

6. Relation between air leakage and energy losses due to infiltration

With a calculation model (see Ref. 10) in which all leakages can be simulated, calculations have been made to show an example of the influence of:

- the distribution of air leakages (see Fig. 10)
- the temperature distribution in the house (see Fig. 11)
- the wind climate or wind distribution (see Fig. 12)

From these figures it can be seen that:

- another distribution of air leakages can change the infiltration heat losses by up to 15%
- another temperature distribution can change the infiltration heat losses up to about 20%
- another wind climate can change the infiltration heat losses up to about 30%

These calculations have been carried out without changing parameters to any great extent.

Figure 10

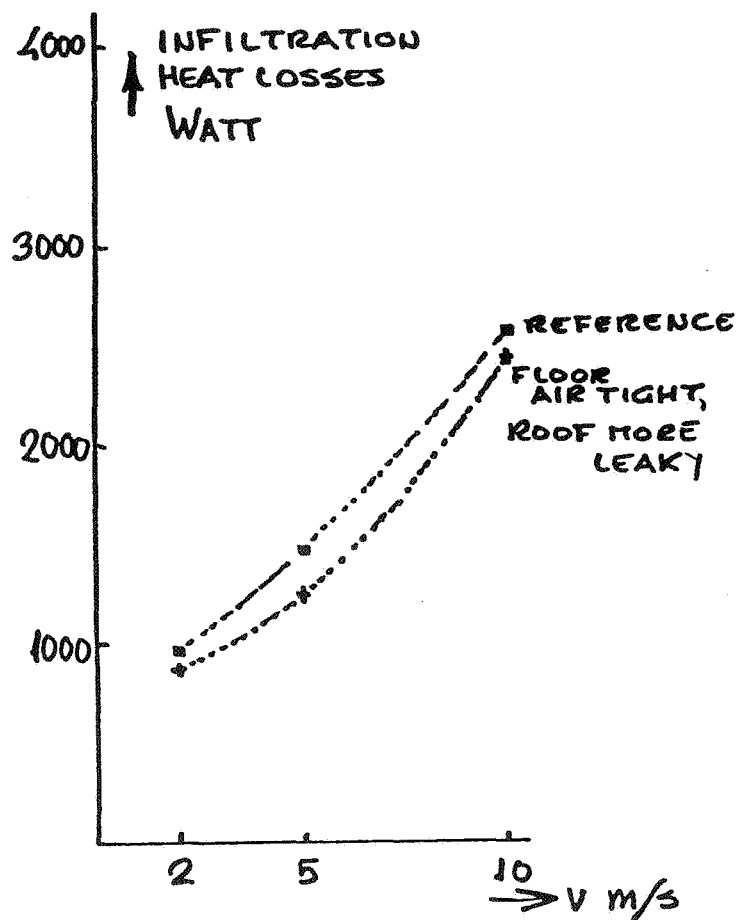


Figure 11

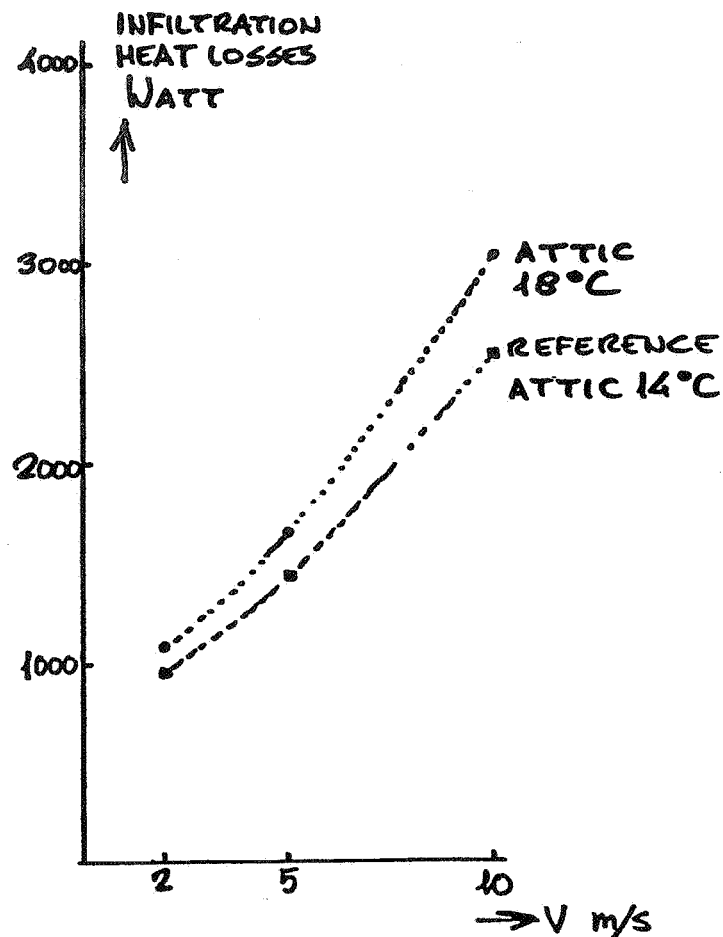
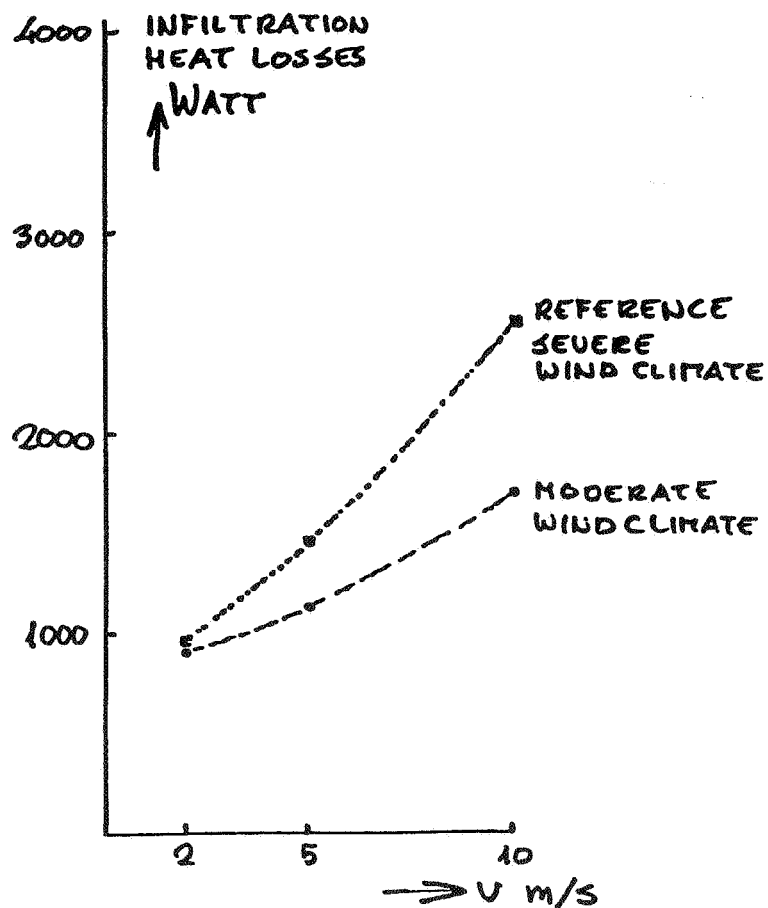


Figure 12



7. Conclusions

7.1 The pressurization test is a suitable method to compare houses on air leakage.

7.2 If the air leakage of a house does not meet a certain criterion, careful measurements on the distribution of air leakage are necessary to:

- make a final judgement
- know where to start with improvements

7.3 In some cases pressurization at the same time of adjacent houses can be necessary.

7.4 In single family houses in the Netherlands, the main important leakages are:

- the connection between walls and roof construction
- the ventilation- and flue-ducts

7.5 More industrial constructed houses with concrete elements seem to have less air leakage than traditional masonry houses.

7.6 Relations of air leakages with infiltration rates and energy losses due to infiltration are not clear.

8. References

1. Program plan infiltration in buildings.
International Energy Agency
Paris 1978
2. Kronvall, J.
Testing of houses for air leakage using a pressure method
ASHRAE, New York, 1978
3. Tamura, G.T.
Measurement of air leakage characteristics of house enclosures
ASHRAE, New York, 1975
4. Stricker, S.
Measurement of air tightness of houses
ASHRAE, New York, 1975
5. McIntyre, I.S. and Newman, C.J.
The testing of whole house for air leakage
Building Research Establishment, Risborough, 1975
6. Schippers, P.J. and de Jong, P.J.J.
Luchtdichtheid van woningen
Bouwfonds Nederlandse Gemeenten, Hoevelaken, 1978
7. Dumont, R.S.
Comparative airtightness levels in housing for six different
locations in North America and Sweden
8. Collet, P.F.
Boligers luftskifte
Byggeteknik, Tastrup, 1976
9. Warren, P.
Natural ventilation rates in modern housing
Building Research Establishment, Garston, 1977
10. de Gids, W.F.
Calculation method for the natural ventilation of buildings
IMG-TNO, Delft, 1977

PAPER 8

**THE APPLICATION OF RECIPROCITY
IN TIGHTNESS TESTING**

P. O. NYLUND

**Tyréns
Stockholm
Sweden**

THE APPLICATION OF RECIPROCITY IN TIGHTNESS TESTING

REPORT FOR THE AIC CONFERENCE, OCTOBER 1980

BY

PER OLOF NYLUND

TYRÉNS, SWEDEN

1. BACKGROUND

The problem of tightness in buildings is currently a very topical and important problem area. When people began to try and improve the energy status of houses they perhaps took too much notice of k values. More recently it has been seen that uncontrolled air-leakage is equally important - sometimes more so. One problem with such air-leakage is the difficulty in measuring quantity. Probably the most accessible method is to base the quantitative determinations of air-leakage on values achieved through tightness testing of the building shell and its sub-areas. In the case of small houses there is a method available today for carrying out such tightness testing on the whole house by using a separate test fan. However, for larger houses there is no method. During the last year, large office blocks have been tested in much the same way as small houses by using the existing fans. This method demands a considerable amount of work and is not always possible to carry out.

Invariably it is not possible to measure the tightness of a section of the facade by subjecting a room, or a limited section of the building, to a positive pressure. The large amount of leakage which thus occurs between dividing walls and joist structures is often too great to allow an acceptable result to be achieved.

The idea of applying the theory of reciprocity was developed in the work concerned with tightness testing of large office blocks, by deciding how the leaks are distributed throughout the sub-sections of the outer shell, irrespective of the size of the building.

The first measurement indicated that it was theoretically possible to use the reciprocity theorem in conjunction with refined tightness testing. The thesis was published in a paper "Draughts or ventilation"

in Byggnästaren 1977 no. 7-8. To quote an example, the method means that each room is pressurised in turn and the sum of the leakages is then measured thus indicating the true air leakage through the outer shell of the building.

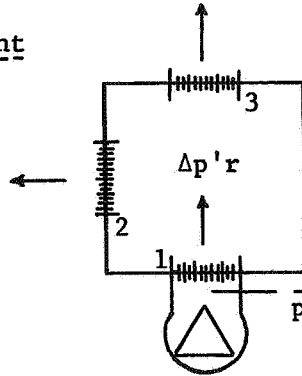
After carrying out theoretical studies, an experimental study was carried out in a laboratory. The experimental work was carried out by Sven Strand and published in a dissertation "Application of a reciprocity theorem in the tightness testing of buildings". Sven Strand Division of Building Technology, Royal Institute of Technology, Stockholm 1979. This report discusses the basic theory and an example of its application.

2. THEORETICAL derivation

The perviousness of a building's outer shell can be expressed in the form of a relationship between the flow through the outer shell and the pressure difference across the shell. In the case of a house, this relationship has the basic form of a function, $q = f(\Delta p)$, i.e. the air flow is a function of the pressure difference and this function can be written as $q = k(\Delta p)^\beta$, where k is a constant, Δp is the pressure difference and β is an exponential constant. For pure laminar air flow, $\beta = 1.0$ and in the case of pure turbulent flow, $\beta = 0.5$. The theoretical basis for the method is given below.

Laminar air flow, $\beta = 1.0$

First measurement



Assume that the room

in the figure is completely tight apart from three (1, 2 and 3) leakages.

Leakage 1 is subjected pressure \bar{p} . The pressure across 1 is then $\bar{p} - \Delta p'_r$,

where $\Delta p'_r$ is the pressure which occurs in the room. $\Delta p'_r$ is also the pressure drop across leakages 2 and 3. The flows through the respective leakages can be written as follows:

$$q'_1 = k_1(\bar{p} - \Delta p'_r)$$

$$q'_2 = k_2 \Delta p'_r$$

$$q'_3 = k_3 \Delta p'_r$$

The flow in through 1 is equal to the total flow out through 2 and 3.

$$q_1' = q_2' + q_3' \Leftrightarrow k_1(\bar{p} - \Delta p_r') = k_2 \Delta p_r' + k_3 \Delta p_r'$$

The equilibrium pressure in the room is then

$$\Delta p_r' = \frac{k_1 \bar{p}}{k_1 + k_2 + k_3}$$

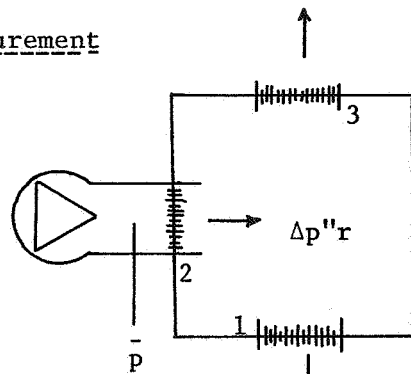
and the flows

$$q_1' = k_1 \left(\bar{p} - \frac{k_1 \bar{p}}{k_1 + k_2 + k_3} \right) = k_1 \bar{p} \left(1 - \frac{k_1}{k_1 + k_2 + k_3} \right)$$

$$q_2' = \frac{k_2 k_1 \bar{p}}{k_1 + k_2 + k_3}$$

$$q_3' = \frac{k_3 k_1 \bar{p}}{k_1 + k_2 + k_3}$$

Second measurement



Leakage 2 is now subjected to \bar{p} and using the analogy of the above:

$$\begin{aligned} k_2(\bar{p} - \Delta p_r'') &= \\ &= k_1 \Delta p_r'' + k_3 \Delta p_r'' \end{aligned}$$

The equilibrium pressure in the room is then

$$\Delta p_r'' = \frac{k_2 \bar{p}}{k_1 + k_2 + k_3}$$

and the flows

$$q_1'' = \frac{k_1 k_2 \bar{p}}{k_1 + k_2 + k_3}$$

$$q_2'' = k_2 \bar{p} \left(1 - \frac{k_2}{k_1 + k_2 + k_3}\right)$$

$$q_3'' = \frac{k_3 k_2 \bar{p}}{k_1 + k_2 + k_3}$$

It can thus be seen that $q_2' = q_1'' = \frac{k_1 k_2 \bar{p}}{k_1 + k_2 + k_3}$

The flow out through leakage 2 in the first test, as a result of the external load pressure \bar{p} , is therefore equal to the flow out through the leakage 1 in the second test for the same \bar{p} . This means that the flow through 3 in the first test is the difference between the measured flows through 1 in the first test and second test.

$$\therefore q_3' = q_1' - q_2' = q_1' - q_1''$$

Turbulent air flow, $\beta = 0.5$

In the same way as before we get the following:

First measurement

$$q_1' = k_1 (\bar{p} - \Delta p_r')^{0.5}$$

$$q_2' = k_2 (\Delta p_r')^{0.5}$$

$$q_3' = k_3 (\Delta p_r')^{0.5}$$

$$q_1' = q_2' + q_3' \Leftrightarrow k_1 (\bar{p} - \Delta p_r')^{0.5} = (k_2 + k_3) (\Delta p_r')^{0.5}$$

$$\Delta p_r' = \frac{k_1^2 \bar{p}}{k_1^2 + k_2^2 + k_3^2 + 2k_2 k_3}$$

$$q_1' = k_1 \sqrt{\bar{p} - \frac{k_1^2 \bar{p}}{k_1^2 + k_2^2 + k_3^2 + 2k_2 k_3}}$$

$$q_2' = k_2 k_1 \sqrt{\frac{\bar{p}}{k_1^2 + k_2^2 + k_3^2 + 2k_2 k_3}}$$

$$q_3' = k_3 k_1 \sqrt{\frac{\bar{p}}{k_1^2 + k_2^2 + k_3^2 + 2k_2 k_3}}$$

Second measurement

$$k_2 (\bar{p} - \Delta p_r'')^{0.5} = (k_1 + k_3) (\Delta p_r'')^{0.5}$$

$$\Delta p_r'' = \frac{k_2^2 \bar{p}}{k_1^2 + k_2^2 + k_3^2 + 2k_1 k_3}$$

$$q_1'' = k_1 k_2 \sqrt{\frac{\bar{p}}{k_1^2 + k_2^2 + k_3^2 + 2k_1 k_3}}$$

$$q_2'' = k_2 \sqrt{\bar{p} - \frac{k_2^2 \bar{p}}{k_1^2 + k_2^2 + k_3^2 + 2k_1 k_3}}$$

$$q_3'' = k_3 k_2 \sqrt{\frac{\bar{p}}{k_1^2 + k_2^2 + k_3^2 + 2k_1 k_3}}$$

For comparison's sake we can give the expressions for q_2' and q_1'' i.e.

$$q_2' = k_2 k_1 \sqrt{\frac{\bar{p}}{k_1^2 + k_2^2 + k_3^2 + \underline{\underline{2k_2 k_3}}}}$$

$$q_1'' = k_1 k_2 \sqrt{\frac{\bar{p}}{k_1^2 + k_2^2 + k_3^2 + \underline{\underline{2k_1 k_3}}}}$$

If $k_1 = k_2$, we get $q_2' = q_1''$

If $k_1 \neq k_2$ and if the difference is not too great we get

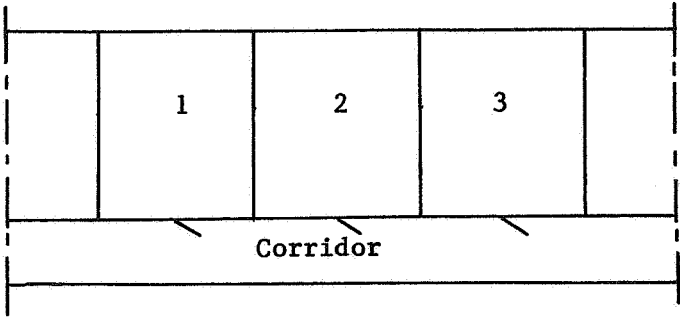
$$q_2' \approx q_1''$$

and therefore

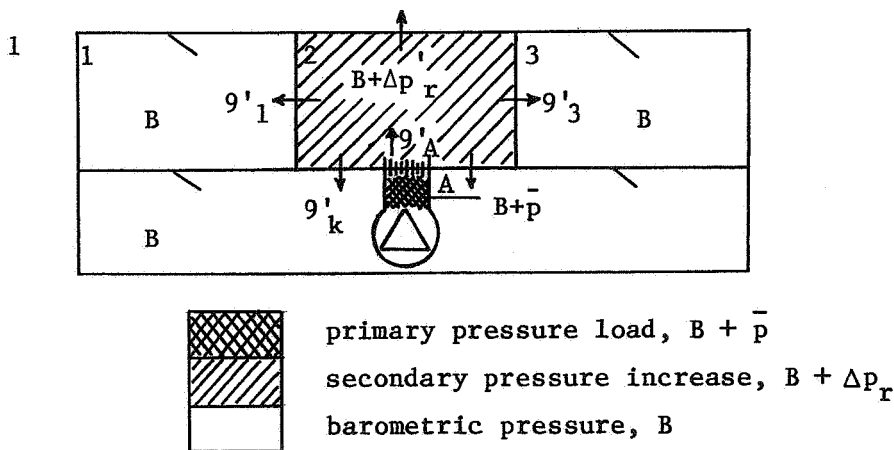
$$\underline{\underline{q_3' \approx q_1' - q_1''}}$$

3. AN APPLICATION EXAMPLE

On the basis of the previous derivations, the reciprocity theorem's application in practice can be illustrated in the following manner.



In this situation we assume a row of offices with offices 1, 2, 3, etc. and a corridor. For simplicity's sake we shall limit the example to one floor. The tightness of the external walls is to be calculated, i.e. the relationship between flow - pressure difference. The following procedure describes the method

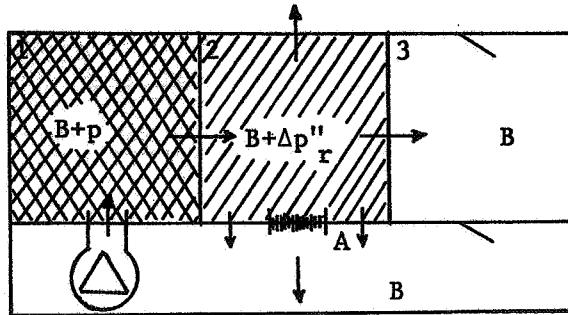


A is a calibrated flowmeter. This is subjected to pressure \bar{p} , wherein the pressure in room 2 assumes the value of $\Delta p_r'$. Flow q'_A through meter A is registered. There are three leakages, one to

room 1, one to room 3 and one to the corridor. The flow through the shell to be calculated is

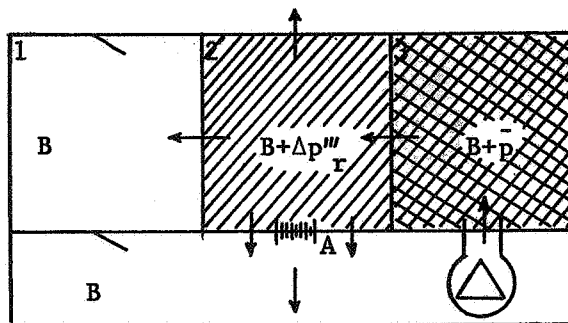
$$q' = q_A' - q_1' - q_3' - q_k' \quad (1)$$

2.



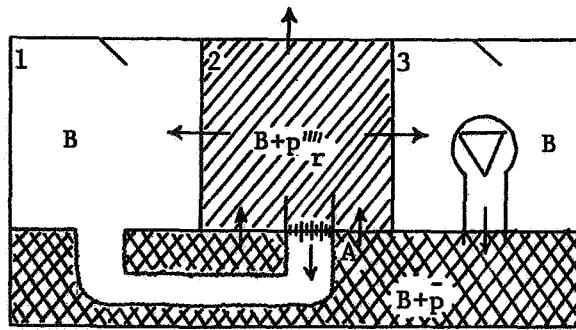
If we subject room 1 to \bar{p} and measure p_r'' we get from the calibration curve for the flowmeter A a value of q_A'' which, according to the derivations, is approximately q_1' .

3.



In the same way as above, room 3 is subjected to positive pressure \bar{p} , $\Delta p_r'''$ is measured and we get $q_A''' \approx q_3'$

4.



In order to determine the final leakage, the corridor is subjected to \bar{p} , $\Delta p_r''''$ is measured and we get $q_A'''' \approx q_k'$. In this case A has been connected to a tube which, for the purposes of the test, has a negligible flow resistance, and which is connected to room 1. From this we get the pressure drop across A as $\Delta p_r''''$

5. Equation (1) now gives the load to be calculated

$$q' = q_a' - q_A'' - q_A''' - q_A''''$$

When tightness testing large houses it is best to use the existing ventilation fans and subject the whole building to positive or negative pressure. The pressure difference across the external walls and the flow in the main ducts is registered.

When it is not possible to carry out such measurement - the ventilation system may be a self-exhausting system for example - it is possible to use the method described and work through room by room in order to get a measurement of the building's total tightness. Of course, the method is equally applicable for several leakages, i.e. on several floors. The method above is applied in order to correct for these leakages. It is best to regard the method as a means of carrying out random tightness checks of localised external wall sections, preferably in combination with a total test using the "existing fan system".

PAPER 9

**TIGHTNESS AND ITS TESTING IN
SINGLE AND TERRACED HOUSES**

P. O. NYLUND

**Tyréns
Stockholm
Sweden**

TYRENS
TECHNICAL MEMORANDUM
1979:5

TIGHTNESS AND ITS TESTING IN
SINGLE AND TERRACED HOUSES
PER OLOF NYLUND

Special Reprint From "Byggnästaren 5, 1979"

SUMMARY

TIGHTNESS AND ITS TESTING IN SINGLE AND TERRACED HOUSES

By Per Olof Nylund

The Swedish regulations give recommended tightness values for buildings of 3 changes per hour for single houses, 2 changes for other housing with not more than two stories and 1 change per hour for taller buildings. These values are measured at a pressure differential between outside and inside of 50 Pa.

Houses are tested by sealing ventilation ducts and the like and replacing the door with a panel having a reversible fan and a manometer connected to the outside by a hose through the panel. The house is tested for air flow through the fan at differing positive and negative pressure differentials.

For terrace houses the air leaks through walls facing the outside or cavities leading to the outside as well as through walls partitioning spaces with air at the same temperature. Because this leakage does not waste energy the authorities allow leakage of 3 changes per hour in terraced houses having party walls of a timber structure.

The leakage to or from terraced houses can be measured and allowed for if the houses adjoining the one being measured are sealed and the pressure differentials in them registered at the same time as in the house being tested. If the houses are very similar, correction can be made after testing one of them. If dissimilar all three must be measured as test houses.

The tube leading to the outer air from the manometer can be passed through an elbow bend from a wash basin or bath. The fan can be connected to a ventilation duct thus obviating replacing the front door with a special board and measuring the front door together with the rest of the house.

This method could be used generally. From energy and ventilation viewpoints it would seem that the air change factors for terraced houses ought to be the same as for single houses.

TIGHTNESS AND ITS TESTING IN SINGLE AND TERRACED HOUSES

The comments in the Swedish Building Regulations give recommended values for tightness in buildings. The values refer to results achieved during tightness testing in accordance with pressure test method SP 1977:1.

The following air change rates are given:

small detached houses and linked houses, 3.0 changes/h

other dwelling houses with a maximum of two floors, 2.0 changes/h

dwelling houses with three or more floors, 1.0 changes/h

These values, or perviousness factors, relate to an air change rate at a pressure difference of 50 Pa between internal and external air pressure. The values can be regarded as standards which, indirectly, can form the basis for calculating the ventilation and air leakage through the structure.

The corresponding energy losses comprise the energy consumed to heat the incoming cold air to room temperature which is later lost with the outgoing air. It is therefore important that the standard obtained during pressure testing refers to the air which goes from the inside to the outside or from the outside to the inside as a result of positive air pressure and negative air pressure testing respectively.

First a recapitulation of tightness testing of small detached houses.

TESTING SMALL DETACHED HOUSES

Figure 1 gives a schematic illustration of how positive pressure testing is carried out in a detached house. This is done by using a test fan, connected in series with a flowmeter, which supplies air at positive pressure to the building through an opening, normally in sheet material, which temporarily replaces the door during pressure testing. All the air which passes through, past the fan and through the flowmeter, also passes out through the structure. While the flow is being measured the pressure is also registered on a manometer which is affected on one side by the internal air pressure and on the other side by the external air pressure via a tube which is passed through the panel in the door. By varying the

speed of the fan and measuring the flow at different pressures, a leakage curve is obtained which indicates the relationship between the pressure difference and the flow. Then by reversing the fan and evacuating the building a leakage curve which relates to negative pressure testing of the building is obtained in the same way. The values for the leakages, both in and out respectively, at a pressure difference of 50 Pa are noted as is the mean value, the latter being the value to be compared with the standard requirement. (If the external temperature differs significantly from room temperature during testing, a correction is made on the basis of the difference in density.)

TESTING TERRACED HOUSES

Figure 2 illustrates testing in three adjacent terraced house flats A, B and C. Let us assume that we are carrying out a positive pressure test on the middle flat (B). Part of the air pumped in leaks out directly through the external envelope, i.e. walls and roof. A further amount leaks out through the party walls and out into the open if there are gaps inside the party walls. These two types of leakages have been designated with a 1 in the diagram. More air leaks through the party walls and into the adjacent flats - flow routes, number 2 in the diagram. The leakage measured during testing is therefore comprised of leakage type 1 in the diagram, which must be counted in the result for the building's tightness and leakage of type 2, which must not be counted.

The requirement for tightness in terraced houses has therefore been recently modified in relation to the figure of 2.0 changes/h given in the introduction. The following is an extract from Planverkets 38, aktuellt 4-1978 (Newsletter No. 38, 4-1978 published by the National Swedish Board of Physical Planning and Building):

It should be observed that in the result obtained from testing air leakage, in accordance with test method SP 1977:1, the result also comprises the proportion of air leakage which can be related to parts of buildings adjacent to areas with the same temperature unless particular correction for the values obtained is carried out. This leakage cannot normally be considered to constitute any real energy loss. In terraced houses this can apply to the party walls.

in cases where party walls have a construction which is somewhat pervious, for example certain types of framework walls, and correction for leakage through these is not carried out, it can be considered acceptable for the time being that the air leakage can amount to 3.0 changes/h in flats in the group "Other dwelling houses with a maximum of 2 floors".

In reality the modification means that the requirement of 2.0 changes/h is retained for terraced houses with party walls of stone material and is increased to 3.0 changes/h when the walls are of wood. The values relate to results from pressure testing without the elimination of, or correction for, leakage through party walls.

There are, however, ways of approaching the problem of obtaining a relevant figure during pressure testing, i.e. a perviousness factor which does not include leakage through party walls.

ELIMINATION OF LEAKAGE BETWEEN PARTY WALLS

One method of eliminating leakage routes (2) is to provide the flats on either side with fans which maintain the same pressure as the air in the flat being tested. This method is, however, very complicated. Even if we can assume that we have access to three fans and replace the doors in all three flats with sheet material, it would be necessary to synchronise all three fans so that the pressures in the flats were identical for a series of in/out pressure difference measurements carried out at the given flow rate supplied to the middle flat.

This measurement procedure is hardly acceptable for practical pressure testing purposes.

Instead of eliminating the leakage between the party walls, it is possible to make an appropriate correction.

CORRECTION FOR LEAKAGE BETWEEN PARTY WALLS

The principle is quite simple. It has been verified through scale tests in the laboratory, tested in practice and is at present being standardized in Sweden.

Let us assume that we are carrying out a positive pressure test on middle flat (B) using the same procedure as for a detached house. We obtain a leakage curve at varying pressure drops and take particular note of the leakage value at a positive pressure of 50 Pa. The fan is then switched off and the pressure allowed to drop to equilibrium with the external air pressure. One of the two people engaged in pressure testing goes into the adjacent flat (A) which has been prepared in the same way as the measurement flat, i.e. by taping-up or closing the ventilation ducts. In flat A, a manometer is used to measure the magnitude of the resulting pressure difference when the pressure in the measurement flat (B) is raised from zero (or equilibrium pressure equal to the outside air pressure) to an excess pressure of 50 Pa. What needs to be done in flat A is to zero the manometer, when the fan is switched off in measurement flat B, and then to read off the pressure increase obtained in A when the pressure in measurement flat B amounts to 50 Pa. Communication by telephone or walkie-talkie is necessary between the two flats for this task. The same procedure is repeated, this time by registering the pressure increase in flat C, when the pressure is increased from 0 to 50 Pa in measurement flat B.

In order to simplify the description of the correction method we shall assume that the three flats are equally airtight. In this case no more measurement or registration than that previously discussed is necessary.

There is nothing to prevent the use of the same correction method even if the tightness in the flats differs. It is however necessary to repeat the procedure discussed first with flat A as the measurement flat, and then with flat C as the measurement flat. In both cases the rise in pressure in the adjacent flats is recorded when the pressure is increased from 0 to 50 Pa in the measurement flats.

It is assumed that diagram 3 shows the leakage curve Q_{measured} which was registered during pressure testing of flat B. From the curve we can obtain a value for the total measured leakage at 50 Pa positive pressure. This leakage is designated $Q_{50, \text{measured}}$. We assume that we have measured the pressure increase P_A when we measured the pressure change in the adjacent flat. From the measured leakage curve we can obtain the necessary correction term Q_{pA} .

The corrected value for the leakage can be derived and expressed as follows:

$$Q_{50, \text{ corrected}} = Q_{50, \text{ measured}} - Q_{pA} - Q_{pB} + \text{remainder.}$$

The remainder can be calculated from the measurement values obtained.

In all probability it will be possible to carry out sample tightness tests in detached houses by selecting a flat at random and merely registering the pressure changes in adjacent flats. However, the relationship must be studied in more detail by systematic field investigations before the method can be accepted as a complement to the pressure testing methods for measuring tightness in terraced flats drawn up by the National Swedish Institute for Materials Testing.

The most significant disadvantage of the method described is that it includes the measurement of small pressure differences - between the measurement flat and adjacent flats - and it may be necessary to limit the method to occasions when the prevailing wind is slight or non-existent.

EXAMPLES OF THE MAGNITUDE OF LEAKAGE THROUGH PARTY WALLS

As an example of the magnitude of leakage, the results from pressure testing of terraced houses administered by AB Folkhems in Sollentuna are given.

In the middle flat a change rate of 2.0 changes/h at 50 Pa was measured. The corrected value was 1.5 changes/h. In an end-of-terrace flat, the corresponding values were 1.8 and 1.5 changes/h respectively.

SIMPLIFIED PROCEDURES FOR REGISTERING INTERNAL/EXTERNAL PRESSURE DIFFERENCES

In the introduction it was noted that the registration of the difference between external and internal air pressure is carried out with manometers which, on one side, are connected to the internal air pressure and the other via a tube which is inserted through a temporary panel in the external envelope and which is in contact with the external air pressure.

When it is necessary to register the pressure change in adjacent flats it is obviously inconvenient to have to place an extra panel in the door opening purely to introduce a tube connected to a manometer. There is an easy way of avoiding this complication by passing a tube through the water trap of a sink or toilet to achieve contact with the external air pressure through the ventilation opening. (This is assuming that the ventilated pipe is not fitted with a non-return valve.)

Using the method discussed for registering pressure in the building in relation to a ventilation pressure reference, it is possible to eliminate sheets in the external doors completely, even in the measurement flat. This is assuming that we connect the fan, with which we extract or supply air to one of the house's ventilation ducts. This is particularly simple when testing during a production stage. In this way there is the minor advantage of having external doors with their inherent perviousness as part of the house's total tightness.

PERVIOUSNESS FACTORS FOR SINGLE AND TERRACED HOUSES

In the introduction it was noted that the standard - perviousness factor obtained from relevant tightness tests in accordance with the pressure test method - can form a basis for calculating ventilation and air leakage. The perviousness factor is one of the parameters which, in a quite complicated interaction, is decisive for ventilation and natural ventilation and thus the associated energy losses. (Natural ventilation means the air leakage in and out through the building structure, i.e. the air change which does not go through the ventilation system.)

Even if the interaction between the structure's perviousness, the effects of wind and temperature, and the ventilation system is complicated, it is still possible to consider in principle that

- the amount of natural ventilation in a push-pull system is linearly dependent on the perviousness factor

- the total ventilation for a supply air system is linearly dependent on the perviousness factor

- the natural ventilation for an exhaust air system increases in proportion to the perviousness factor, but not linearly.

In the long term it is necessary to relate the tightness requirements for detached houses to the type of ventilation system. In order to do this, it is necessary to expand the basis of knowledge from practical and theoretical development work.

At the moment it is important that there should be a balance between the requirements for both detached houses and terraced houses on the basis of current knowledge. The way in which perviousness factors for the two categories relate to each other so that "justice is done" depends on the criteria we have. For example:

On the basis of production conditions.

On the basis of specific energy consumption.

On the basis of ventilation requirements.

The basis for this argument is that the air change rate of 3.0 for small detached houses can be considered reasonable at the moment.

PERVIOUSNESS IN TERRACED HOUSES - PRODUCTION CONDITIONS

Terraced houses with framework walls between flats provide roughly the same, or somewhat better, conditions as for detached houses with the same design technology in relation to achieving tightness, measured without correction for leakage between party walls.

Terraced houses with party walls of stone material provide somewhat better conditions and should mean a lower value for the perviousness factor.

Using this argument we arrive at values which agree quite well with those recommended by the National Swedish Board of Physical Planning and Building and the newsletter referred to above.

PERVIOUSNESS IN TERRACED HOUSES - FROM AN ENERGY POINT OF VIEW

Another basis for achieving balance is that the specific energy consumption, i.e. the energy consumption per m^3 of building volume, should be the same for both house types. This provides the motivation for having the perviousness factor for terraced houses, after correction for leakage through party walls, equal to that of detached houses, i.e. 3.0 changes/h. This should also lead to a higher value for terraced houses than for detached houses if the tightness testing and perviousness factor is indicated without correction for leakage to adjacent flats.

PERVIOUSNESS IN TERRACED HOUSES - FROM A VENTILATION POINT OF VIEW

Natural ventilation is permissible in both detached houses and terraced houses. Such houses must not be too airtight.

If we make allowance for this and assume that the conditions for ventilation should be the same for both categories of houses, we arrive at the same result as was the case of the energy aspect. The perviousness factor for terraced houses, without correction for leakage to adjacent flats, should be set higher than for detached houses.

SUMMARY

The test method described for correcting for leakage through party walls in terraced houses could be developed relatively soon to a routine which is manageable for measurement technicians. Perviousness factors for terraced houses, after correction for side leakage through party walls, should be set to the same level as for small detached houses.

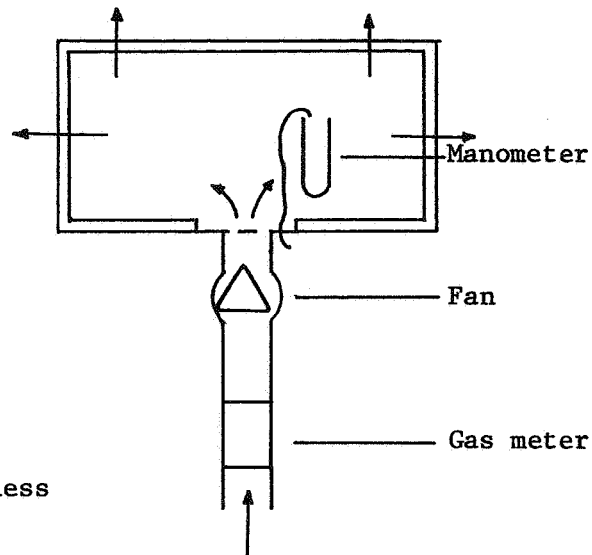


Figure 1. Tightness testing of small detached houses.

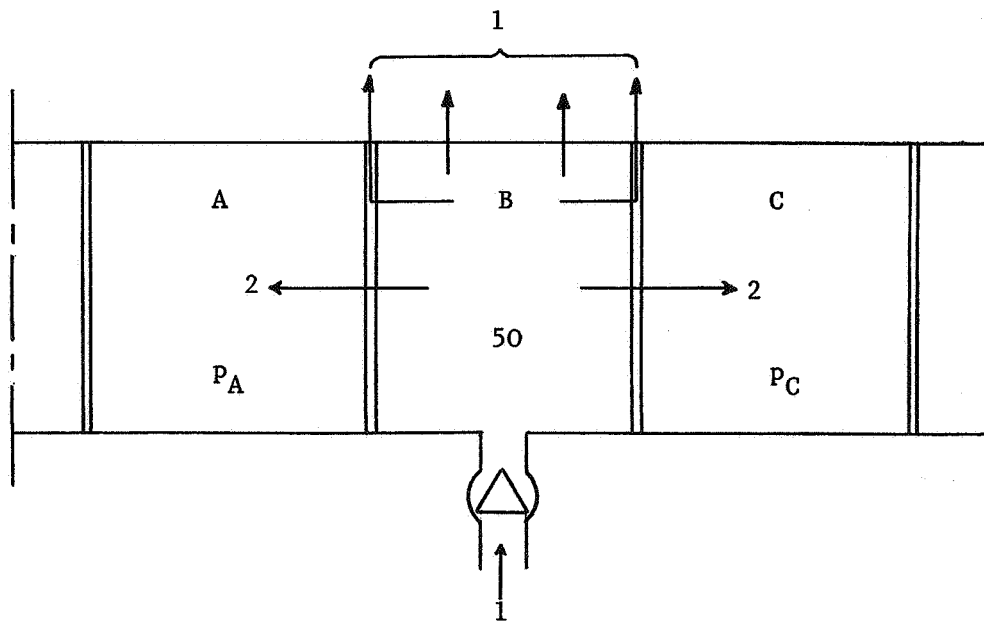


Figure 2. Tightness testing in terraced houses. Pressure measurement for correction with reference to leakage flows 2 in the figure.

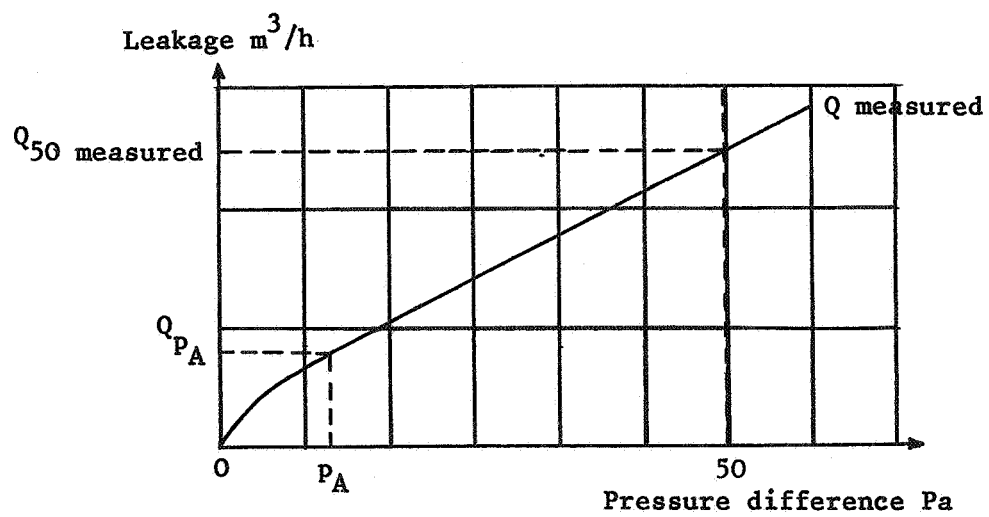
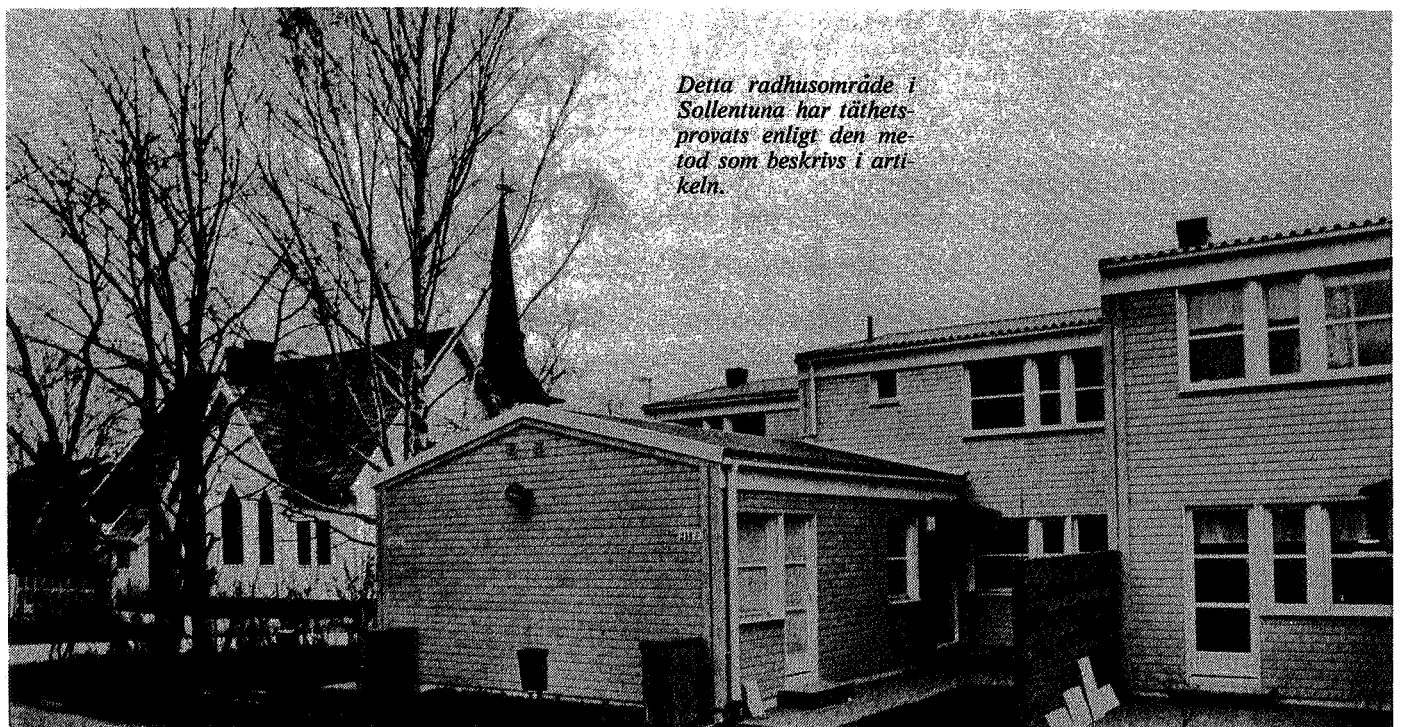


Fig. 3. Leakage curve and magnitude of correction term.



This terraced house area in Sollentuna has been tightness tested in accordance with the method described in the article.

PAPER 10

**AIR LEAKAGE MEASUREMENTS OF
THE EXTERIOR WALLS OF TALL
BUILDINGS**

**C. Y. SHAW, D. M. SANDER AND
G. T. TAMURA**

**National Research Council
Ottawa
Canada**

(Paper reproduced by kind permission of ASHRAE)

No. 2280

C.Y. SHAW

Associate Member ASHRAE

D.M. SANDER

Associate Member ASHRAE

G.T. TAMURA

Member ASHRAE

AIR LEAKAGE MEASUREMENTS OF THE EXTERIOR WALLS OF TALL BUILDINGS

Air leakage into and out of a building occurs mainly through cracks formed at the mating surfaces of the various exterior wall components. It contributes to the heating, cooling, and moisture loads of a building and is therefore of interest to the designer for calculating the energy requirements of air conditioning systems. Also, air movement inside a building resulting from air leakage through the exterior walls not only spreads odors but, in the event of fire, contributes to the spread of smoke and toxic gases.¹ The design of buildings and air handling systems to prevent undesirable air movement requires knowledge of the air leakage characteristics of exterior walls as well as those of various interior separations.

The conventional methods of estimating the rate of air infiltration are described in Chapter 25 of the ASHRAE Handbook of Fundamentals.² They are the air change and the crack methods, both of which depend to a great extent on the judgment and the experience of the designer. Air leakage data for windows, doors, and simple frame and brick walls are given in Ref. 2; these data are based on laboratory studies. There is no information on the air leakage characteristics of contemporary wall constructions such as curtain walls and spandrel panels with fixed glazing. It is difficult, therefore, for a designer to make a reliable estimate of the infiltration heat loss and gain, which continue to be the most uncertain component of the calculated total heating and cooling loads.

C.Y. Shaw is Asst Research Officer, and D.M. Sander and G.T. Tamura are Research Officers, all with National Research Council, Ottawa, Canada. This paper was prepared for presentation at the ASHRAE Spring Conference, Minneapolis MN, May 3-5, 1973.

Air tightness of exterior walls depends not only on the wall design and materials used, but also on the workmanship and condition of various joints after weathering, both of which are difficult to duplicate in the laboratory. Only a relatively small section of an exterior wall can be tested in the laboratory, consequently a more realistic indication of the air tightness values of exterior walls would be obtained from tests performed on whole buildings. A test method was developed, therefore, to measure the air leakage characteristics of the exterior walls of existing buildings; four tall buildings in the Ottawa area were selected for this study. This paper describes the test method used and presents the results of air tightness measurements obtained for these buildings.

APPROACH

The air leakage characteristics of a building enclosure as a whole can be obtained by pressurizing the building with the supply air system and recording the supply air flow rate and the resultant pressure differentials across the enclosure. To obtain the air leakage characteristics of the typical wall area, however, it is necessary to isolate it from the non-typical wall areas such as those of the mechanical, ground and basement floors. This could be accomplished by sealing all leakage openings other than the exterior walls but, because of the number, size, and location of openings involved, this method of isolation is impractical for most buildings. An alternative method was developed, therefore, to determine the air leakage characteristics of a typical wall area.

Consider the idealized building enclosure shown in Fig. 1. The enclosure consists of three parts: the part enclosed

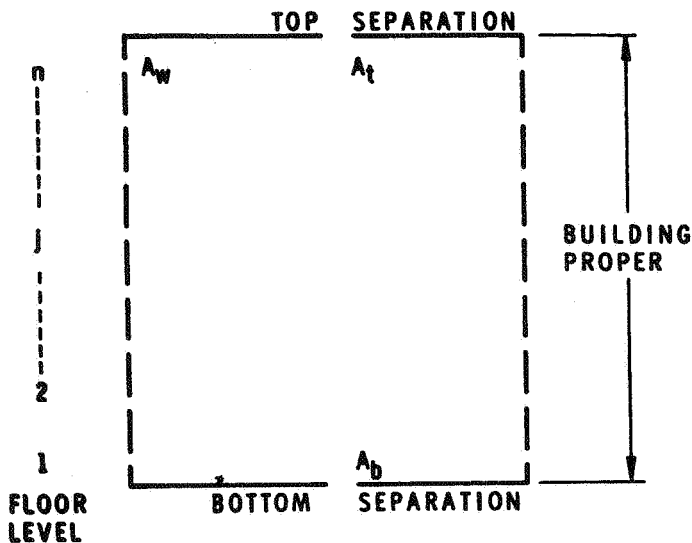


Fig. 1 Mathematical model

by the typical wall area of floors 1 to n ; the top separation; and, the bottom separation. If outside air is introduced into the building proper, pressures inside are increased and hence, air flows out through the exterior walls and the bottom and top separations.

Under steady state conditions the total outside supply rate equals the air leakage rate through exterior walls plus air leakage rate through bottom separation plus air leakage rate through top separation.

$$\text{thus } Q = A_w \left[\sum_{j=1}^n (\rho \Delta P_w)_j^{X_w} \right] + A_b (\rho \Delta P_b)^{X_b} + A_t (\rho \Delta P_t)^{X_t} \quad (1)$$

where

- Q = the total fresh air supply rate
- X = flow exponent
- A = flow coefficient
- ΔP = pressure difference
- ρ = air density
- n = the total number of floors with typical wall construction

and subscript

- w = exterior wall
- b = bottom separation
- t = top separation

The values of Q , ΔP_w , ΔP_b and ΔP_t can be measured. By obtaining several sets of these measured values it is possible to evaluate the coefficients A_w , A_b and A_t and the exponents X_w , X_b and X_t in Eq (1).

APPLICATION

So far only a simple model of a building has been considered. The building proper, i.e., the part enclosed by the typical wall area, is usually connected to the ground, basement, and top mechanical floors by a number of vertical

shafts, e.g., elevator, stair and service shafts, and air ducts. Because of these interconnections, the pressure differentials across the top and bottom separations must be defined carefully.

A typical building of about twenty-five stories is often served by an air conditioning system located on the top mechanical floor. The return and exhaust ducts are usually connected directly to the outside at the top. Elevator and service shafts may also have leakage openings connected directly to the outside at the top. Air can flow, therefore, from the building proper directly to the outside at the top through these shafts as well as into the mechanical floor and from there to outside. The pressure differential across the top separation has been defined as the difference in pressure between the top typical floor (the floor below the top mechanical floor) and the outside at mid-height of the top mechanical floor.

The basement and ground floor areas are usually served by an air conditioning system located in the basement, in which case no air ducts would connect the building proper to these areas. The only inter-connections would be the stair wells, and the elevator and service shafts that terminate either at the ground or basement floors. There is no direct connection from the building proper to the outside at the bottom. Therefore, the pressure differential across the bottom separation is defined as the difference in pressure between the first typical floor (the floor above the ground floor) and the average of the ground floor and basement pressures.

CALCULATION TECHNIQUE

Eq (1) is a nonlinear equation in six unknowns. These six unknowns can be estimated by a trial and error technique used in conjunction with the method of least squares. The calculation procedure is as follows:

- 1 Choose combinations of flow exponents with values between 0.5 and 1 (as this is the range of accepted values.)^{2,3}
- 2 Use the method of least squares to obtain the flow coefficients and calculate the standard error of estimate for each combination of the flow exponents.
- 3 Select the values of the flow exponents and associated flow coefficients that give the lowest value of the standard error of estimate. These values are taken as the solution to Eq (1).

The rate of air leakage through the exterior wall for a given pressure differential can then be estimated by the following equations:

$$Q_w = A_w \sum_{j=1}^n (\rho \Delta P_w)_j^{X_w} \quad (2a)$$

or

$$q_w = \frac{A_w}{D} (\rho \Delta P_w)^{X_w} \quad (2b)$$

where,

Q_w = the total wall air leakage rate in cfm

q_w = the wall air leakage rate per unit area in cfm/sq ft

D = the total exterior wall area per story in sq ft

ρ = the air density in lb/cu ft

ΔP_w = the pressure difference across the wall in in. of water

Eq (1) shows that the division of the total air leakage rate into three components depends upon the values of pressure differentials across each separation. If those values are the same, the rate of air leakage through the exterior wall cannot be separated from the air leakage through the top and bottom. One way to ensure that they will be different is to conduct the tests when the outside temperature is lower than the inside temperature, thus producing stack action which will result in pressure differentials across the walls that will vary from the bottom to the top of the building. They can then be superimposed on those caused by the outside air supply into the building. Also, to ensure that stable pressure readings are obtained, measurements should be made during calm wind conditions.

VALIDATION OF THE METHOD

An ideal method of testing the accuracy of the proposed method would be to apply it to a building that has a known air leakage characteristic; this is not possible because air leakage characteristics are not known. A building with specified air leakage characteristics can, however, be simulated by using a digital computer.⁴ Simulated test data can thus be obtained and the proposed method applied and verified.

The model selected for test is that of a twenty-story building, shown in Fig. 2, which includes a basement and a top mechanical floor. It contains three vertical shafts representing the return and exhaust air mains of the air handling system and an elevator shaft. Specific values of air leakage characteristics were used for the model and, with the aid of a digital computer, pressure differential and air leakage rate across each separation were computed.

Three conditions were considered:

Case I

The flow exponents for the exterior walls, floor and shafts were 0.5. Computations were carried out with fresh air supply rates of 0 to 70,000 cfm in 10,000 cfm increments with an outside temp of 25F and an inside temp of 75F.

Case II

Same conditions as Case I except that all leakage openings in the top separations were sealed off.

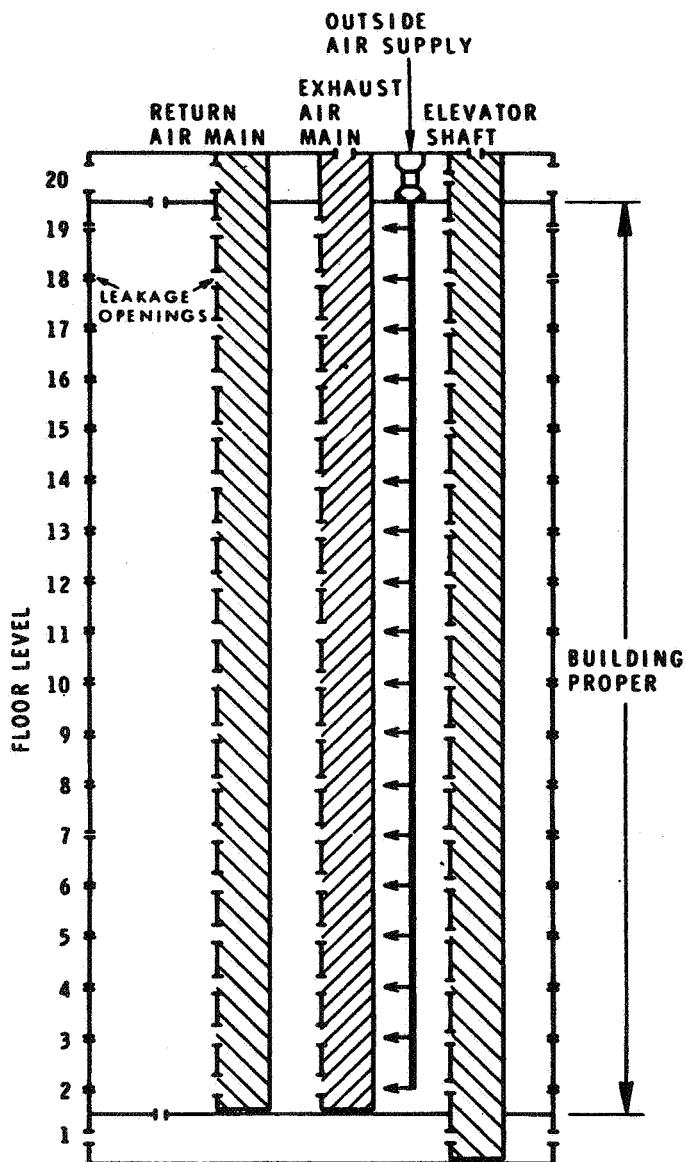


Fig. 2 Computer-simulated building

Case III

Again, same conditions as Case I except that the flow exponent for the exterior walls was 0.66.

The proposed method permits selection of the combination of flow exponents and their associated flow coefficients that give the best estimate of the overall leakage characteristics of the building enclosure as a whole. The minimum standard errors of estimates were found to be 146, 696 and 164 cfm for Cases I, II and III, respectively, indicating that the selected combination of flow exponents gave a close estimate of the specified overall leakage characteristics.

Flow exponents and coefficients of the exterior walls obtained from the proposed method were found to give a

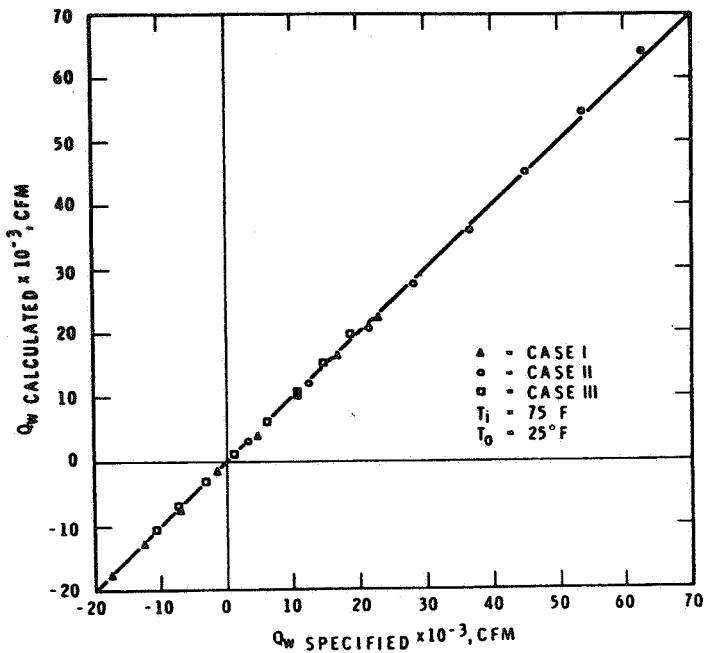


Fig. 3a Calculated exterior wall air leakage rate vs specified exterior wall air leakage rate

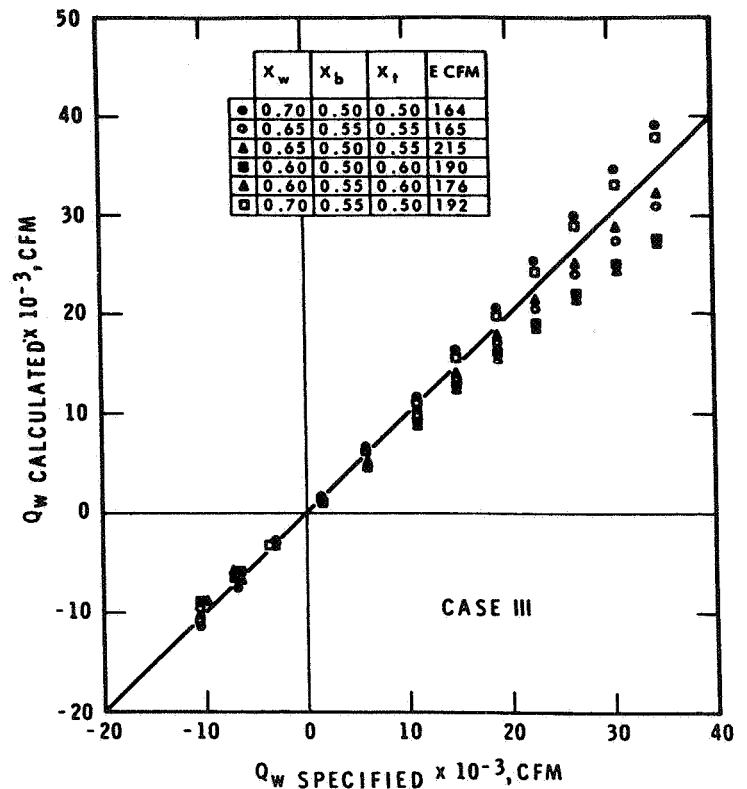


Fig. 3c Calculated exterior wall air leakage rate vs specified exterior wall air leakage rate for various standard errors of estimate

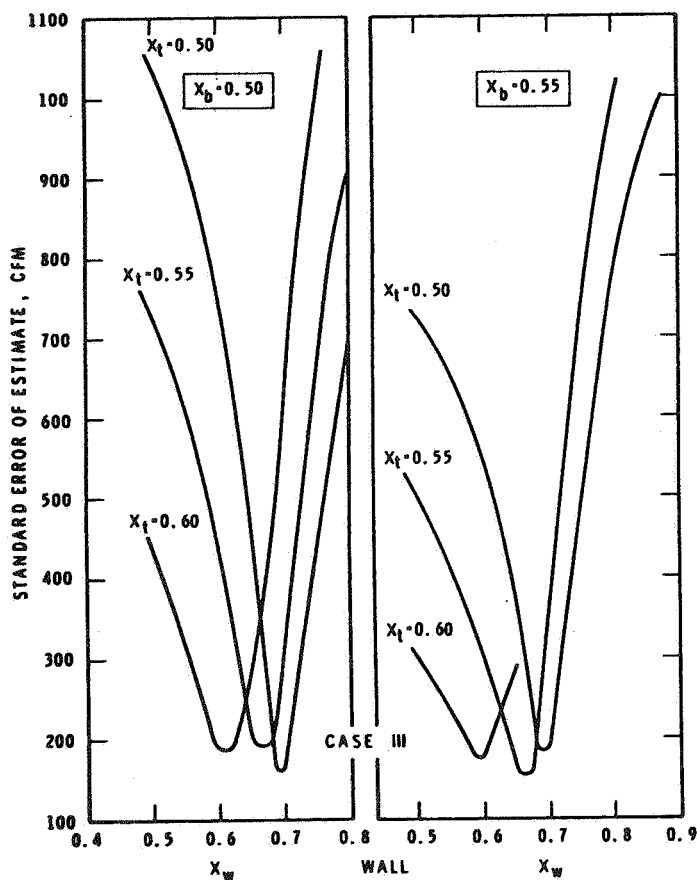


Fig. 3b Standard error of estimate vs flow exponent for wall

good estimate of the air leakage characteristics of the exterior walls. The calculated wall air leakage rates were plotted against the specified wall air leakage rates as shown in Fig. 3a. The results show that the calculated wall air leakage rates lie within $\pm 10\%$ of the specified wall air leakage rates.

Because the standard error of estimate is related to the overall air leakage rates, the minimum standard error of estimate may not necessarily give the best indication of the wall air leakage rate. To investigate this, wall exponents were plotted against the standard error of estimate for different combinations of exponents for the bottom and top separations. A graph for Case III is shown in Fig. 3b, with flow exponents in the top separation of 0.5, 0.55 and 0.60 and in the bottom separation of 0.5 and 0.55. The graph indicates that, with fixed values of flow exponents for the bottom and top separations, the standard error of estimates for different combinations of flow exponents shown in Fig. 3a varies from 164 to 215 cfm, with variation in the exterior wall flow exponent of from 0.6 to 0.7. The minimum standard error of estimate is obtained with flow exponent of 0.50 for the bottom separation, 0.50 for the top separation and 0.70 for the exterior wall. The assigned value of flow exponent for Case III is 0.66.

TABLE I
DESCRIPTORS OF TEST BUILDINGS

	Building A	Building B	Building C	Building D
Height	151	220	247	253
No. of floors above ground (excluding lobby and mech. floor)	9	13	20	20
Floor dimensions (ft)	166 x 210	88 x 140	126 x 146	75 x 93
Typical Floor height (ft)	13	11	10.6	10.5
Volume above ground (cu ft)	5,095,000	2,459,000	4,509,000	1,704,000
Outside wall area per typical floor (ft ²)	9,776	5,016	5,757	3,920
Typical window size (ft)	8.5 x 7.9	3.8 x 6.9	2.6 x 6.5	4.7 x 4.5
No. of windows per typical floor	56	64	104	44
Roof area/net outside wall area	.61	.25	.23	.12
Total outside wall area above ground level (including area of the exterior walls of the top mech. floor)	112,700	103,700	134,400	82,900
Windows	Fixed double glazing in aluminum	Openable double glazing in aluminum (normally locked)	Fixed double glazing	Fixed double glazing
Wall construction	5-in. PEAC panel 8-in. Tile 2-in. Rigid insulation with vapour barrier Air space 6-in. Tile 3/4-in. Plaster	Precast concrete panel backed with 2-in. rigid insulation	Precast concrete panel Air space 1-in. Rigid insulation 1/2-in. Cement rendering 6-in. Block wall 3/4-in. Plaster	(1) Wall 2-in. Hollow steel panel Air space Rigid insulation 20-in. Concrete (2) Corners 4-in. Face brick 2-in. Rigid insulation 12-in. Poured concrete

The exterior wall air leakage rates calculated with flow exponents and their associated flow coefficients corresponding to the minimum standard error of estimates given in Fig. 3b are plotted against the specified air leakage rates in Fig. 3c. The graph shows that the flow exponent and associated flow coefficient corresponding to the minimum standard error of estimate of 164 cfm does not give the best estimate of the specified wall leakage rates. The best estimate is obtained with standard error of estimate of 215 cfm. Although the flow exponents corresponding to the minimum standard error of estimate do not necessarily give the best estimate of the wall air leakage rates, as shown in Fig. 3a and 3c, they do give an adequate estimate. Also, where the wall leakage characteristics are not known, as in the case of real buildings, the use of minimum standard error of estimate serves as a criterion for the selection of the flow exponents and coefficients.

- 1 All auxiliary air handling systems were shut down.
- 2 All fans of the return and exhaust systems were shut down.
- 3 To obtain uniform pressurization in the building proper, stair doors were kept open except for those on the basement, ground and mechanical floors.

FIELD MEASUREMENTS

Air leakage characteristics of the exterior walls of four tall buildings designated as Buildings A, B, C and D (Figs. 4, 5, 6 and 7) were determined using the proposed method. These buildings all have a full basement below grade and a mechanical floor at the top. Descriptions of the building are given in Table I. Pressure differentials across the exterior walls and bottom and top separations were measured for various rates of fresh air supplied under the following conditions:

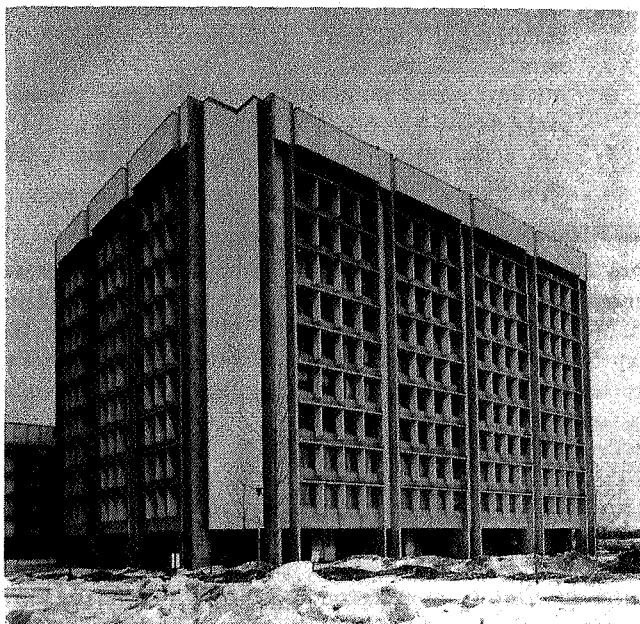


Fig. 4 Building A

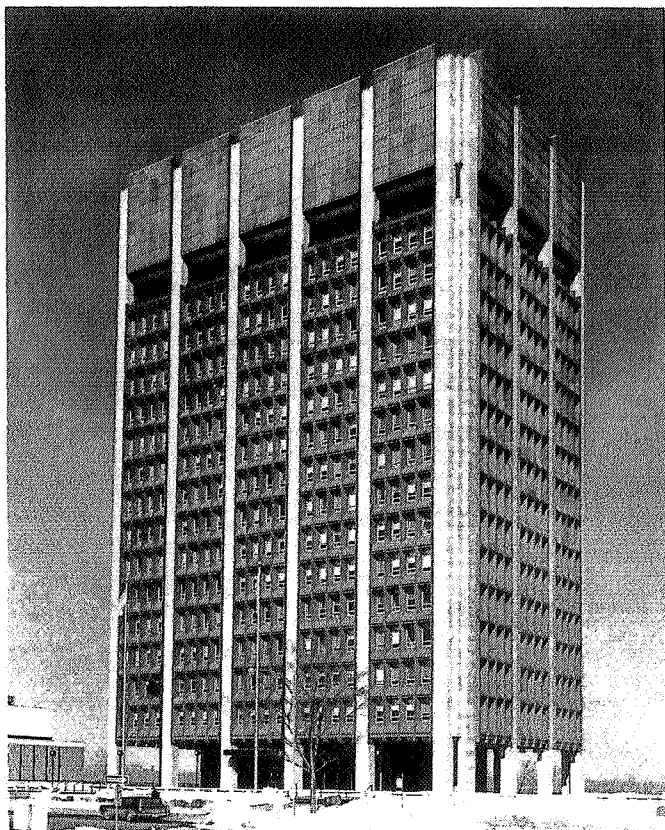


Fig. 5 Building B

- 4 Main entrance doors and elevator and stair doors at the basement, ground floors, and the top mechanical floors were kept closed during the test.
- 5 To minimize the effect of wind pressures on the buildings all tests were conducted during relatively calm conditions.
- 6 All tests were conducted when the outside temperature was at least 20 F below the inside temp.
- 7 All tests were conducted during unoccupied periods.

INSTRUMENTATION

Fresh air supply rates were measured using total pressure averaging tubes⁵ and their associated static pressure taps installed in the main supply air ducts at positions as far away from the duct bends as practicable. Based on laboratory tests,⁵ the accuracy of this flow rate measuring device was found to be better than $\pm 6.5\%$ of the actual flow rate for air velocities of from 600 to 1400 fpm. Pressure differentials were measured with a pressure recording instrument located on the top mechanical floor. One side of the meter was connected to the roof top pressure tap which served as a reference pressure; the other side of the meter was connected to a pressure selector switch. From the pressure selector switch, 3/16 in. plastic tubes were installed vertically in a stair shaft terminating at various floor spaces and also to the outside at ground level. The sensitivity of the

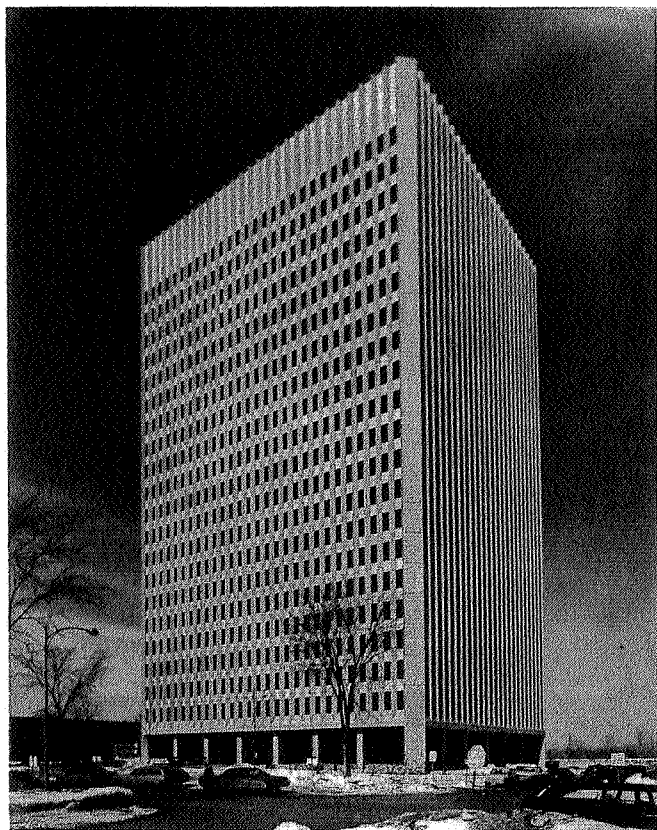


Fig. 6 Building C

pressure transducer is 0.002 in. of water. The schematic diagram of the installation is shown in Fig. 8a.

Pressure differences across the various separations can be calculated from the pressure meter readings as follows:

- (a) Pressure difference across the exterior wall at the j th level (Fig. 8b)

$$\begin{aligned}\Delta P_{wj} &= P_{ij} - P_{oj} \\ &= \Delta P_{Mij} - (h - h_j)(\rho_o - \rho_i) \\ &= \Delta P_{Mij} - [h(\rho_o - \rho_i) - h_j(\rho_o - \rho_i)] \\ &= \Delta P_{Mij} - [\Delta P_{Mog} - h_j(\rho_o - \rho_i)] \\ &= \Delta P_{Mij} - \Delta P_{Mog}(h - h_j)/h\end{aligned}$$

where

- P_i, P_o = inside and outside gauge pressures
 $\Delta P_{Mi}, \Delta P_{Mo}$ = meter readings associated with P_i and P_o respectively.
 ΔP_{Mog} = meter reading associated with outside pressure at the ground level.
 h and h_j = vertical distances as shown in Figs. 8a, 8b.

- (b) Pressure difference across the bottom separation

$$\Delta P_b = P_{i1} - \left(\frac{P_{b1} + P_{b2}}{2} \right) = \Delta P_{Mi1} - \left(\frac{\Delta P_{Mb1} + \Delta P_{Mb2}}{2} \right)$$

(c) Pressure difference across the top separation.

$$\Delta P_t = P_{in} - P_{o(n+1)} = \Delta P_{Min} - \Delta P_{Mon} + (\rho_o + \rho_i) H$$

where

H = the distance between the centers of the n^{th} and the mechanical floors ($n+1^{th}$ floor).

Subscripts

l, n = first and top typical floors,
b1 and b2 = the ground floor and basement,
M = meter reading.

RESULTS AND DISCUSSIONS

The flow coefficients and flow exponents that describe the air leakage characteristics of the various separations were obtained for the four buildings and are given in Table II. Also given in this Table are values of the standard error of estimate that indicate that the measured and estimated overall air leakage rates are in good agreement. This does not imply that the same degree of accuracy in the estimates of the exterior wall air leakage rates was obtained. It has been shown, however, that the proposed method estimates the wall air leakage rate to within $\pm 10\%$ for the computer-simulated building. It would be expected, therefore, that if the standard error of estimate is small, reasonable accuracy of the estimate of wall leakage characteristics would be obtained.

The total air leakage rates for the test buildings are given in Fig. 9. The total air leakage rates are expressed in

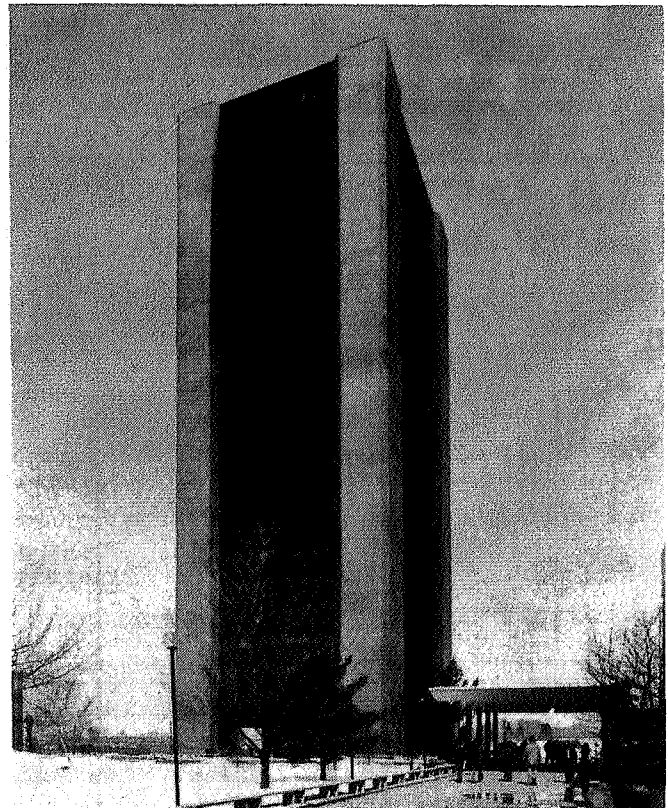


Fig. 7 Building D

TABLE II
FLOW COEFFICIENTS AND EXPONENTS

Test Buildings		A	B	C	D
Building proper	A_w	67600	12800	25200	14500
	X_w	0.70	0.5	0.75	0.65
Bottom separation	A_b	688800	33400	85900	6900
	X_b	0.7	0.7	0.5	0.5
Top separation	A_t	141300	154200	645000	184100
	X_t	0.6	0.5	0.7	0.5
Total outside wall area from ground to the roof levels (sq ft) (D_1)		112700	103700	134400	82900
Exterior wall area per typical floor (sq ft) (D)		9776	5016	5757	3920
Standard error of estimate (cfm)		8900	1310	1190	1130
		for	for	for	for
		130000	45000	160000	47500
		$0 < Q < 120000$	$0 < Q < 40000$	$0 < Q < 100000$	$0 < Q < 47000$

Governing Equations

$$\begin{aligned} \text{Over-all air leakage rate (cfm/sq ft)} & \quad \frac{Q}{D_1} = \frac{1}{D_1} \left\{ A_w \sum_{i=1}^n (\rho \Delta P_i)^{X_w} + A_b (\rho \Delta P)^{X_b} + A_t (\rho \Delta P)^{X_t} \right\} \\ \text{Wall air leakage rate (cfm/sq ft)} & \quad q_w = \frac{1}{D} A_w (\rho \Delta P)^{X_w} \\ \text{Standard error of estimate (cfm)} & \quad E = \left\{ \sum (Q_{\text{measured}} - Q_{\text{calculated}})^2 / (\text{No. of samples} - 3) \right\}^{1/2} \end{aligned}$$

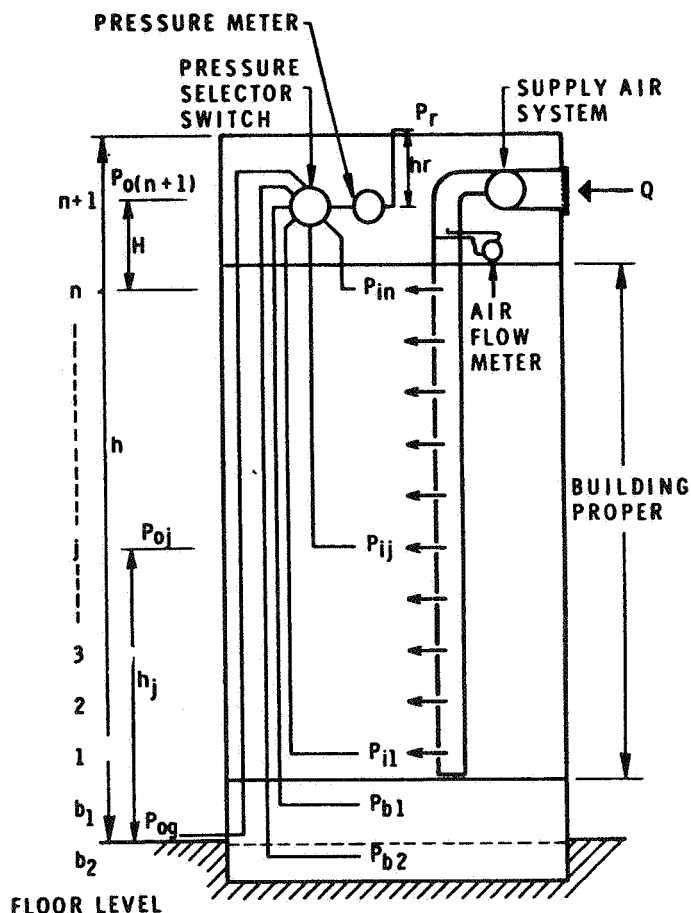


Fig. 8a Arrangement of test equipment

cfm/sq ft of outside wall area above ground level and include the area of the exterior walls of the top mechanical floor. The air leakage rates for the test buildings ranged from 0.5 to 1.1 cfm/sq ft of outside wall area at pressure difference of 0.3 in. of water.

Fig. 9 shows that the overall air leakage rate of Building A is considerably higher than that of the other buildings. This building differs from the other buildings in that it has two conveyor shafts with large openings to each floor which serve as an additional interconnection between the building proper and the basement as well as the mechanical floor. Also, there is a large tunnel to a nearby building from the basement. It is to be expected that these interconnections contributed to the high value of overall leakage rate for this building.

The measurements of overall leakage characteristics for three tall buildings including Building B were reported in 1967 by Tamura and Wilson.⁶ The overall air leakage rates of these buildings varied from 0.5 to 0.8 cfm/sq ft of outside wall area at 0.3 in. of water and are within the range of those given in Fig. 9. This figure also shows the overall air leakage characteristics of Building B obtained prior to 1967. During the time between the two tests, an attempt was made to improve the exterior wall tightness of Building B by sealing the cracks and openings in the corners, behind the induction units and other locations. This

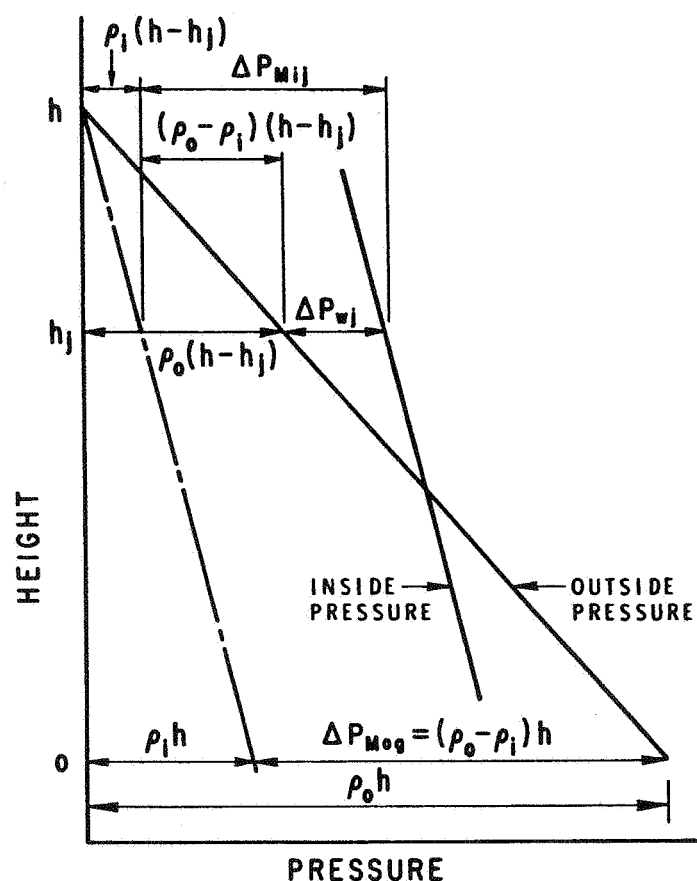


Fig. 8b Pressure difference across an exterior wall

partly explains the lower value of air leakage rate for the recent test

The air leakage characteristics of the exterior wall of the four test buildings are given in Fig. 10 in terms of cfm/sq ft of the total typical wall area. The exterior wall air leakage rates of these buildings varied from 0.25 to 0.48 cfm/sq ft at a pressure difference of 0.3 in. of water. The exterior wall air leakage rates of the four buildings were found to be from 30 to 55% of the overall air leakage rates. The air leakage characteristics of a 13 in. unplastered brick wall given in Ref. 2 is also plotted in Fig. 10. It appears that the exterior walls of the test buildings have about the same permeability to air as an unplastered brick wall.

It is difficult to identify all the leakage openings in the exterior wall of a building from either inspection of the wall construction or the architectural drawings. Also, air tightness of a wall section depends on the quality of workmanship as much as on the wall design and is therefore difficult to predict. The test results presented in this paper give some indication of the wall air leakage characteristics that can be expected for modern high-rise buildings.

SUMMARY

A test method was developed to determine the air leakage characteristics of the exterior walls of a building. The

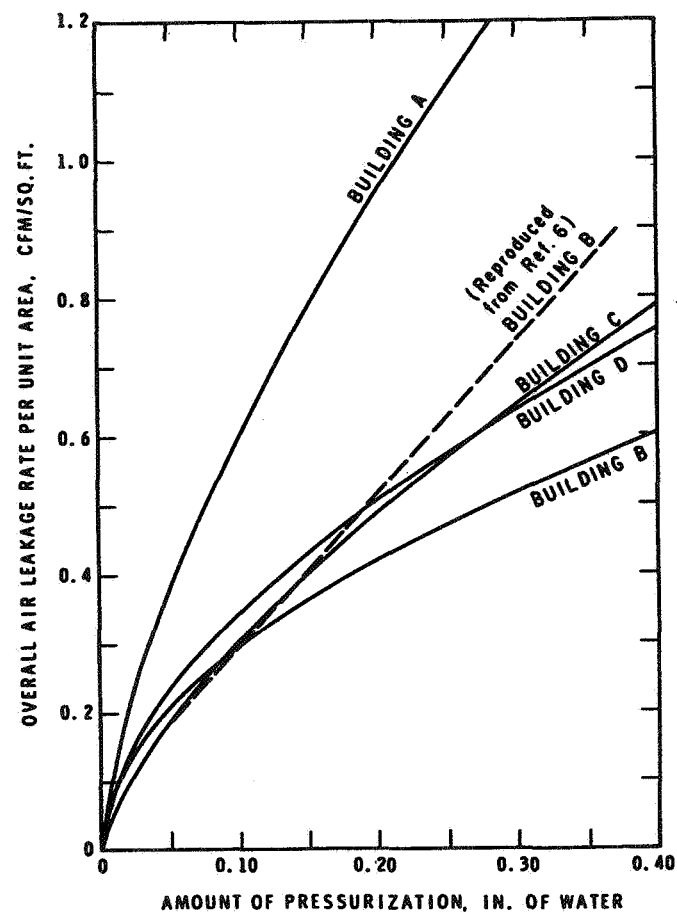


Fig. 9 Overall air leakage rate per unit area vs building pressurization

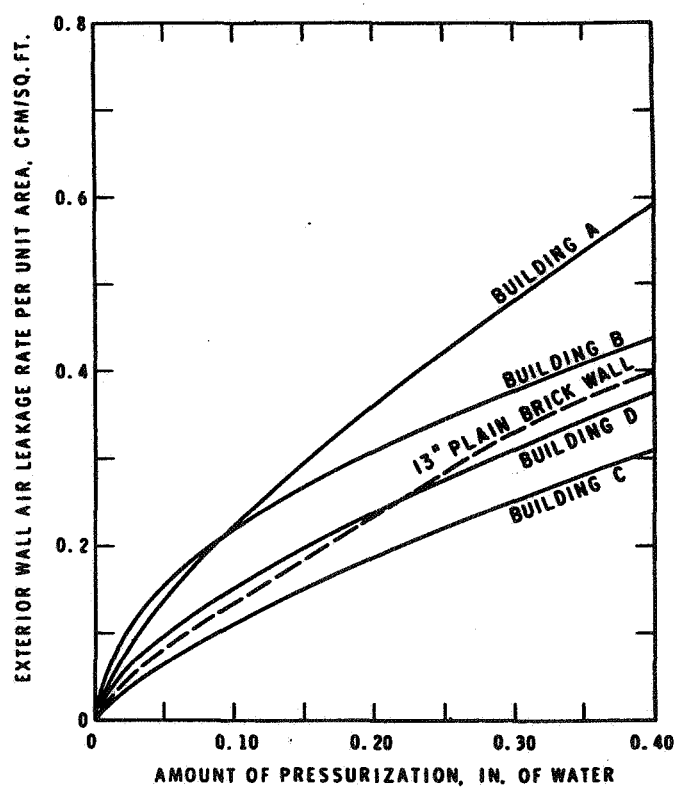


Fig. 10 Exterior wall air leakage rate per unit area vs building pressurization

validity of the method was checked using a computer-simulated building with specified air leakage characteristics. Good agreement was obtained between the calculated and specified wall air leakage rates. Using this method the exterior wall air leakage characteristics of the four test buildings were obtained. The test results indicate that the exterior walls of these buildings allow relatively high air leakage, their air leakage characteristics being similar to those obtained from laboratory tests of a 13 in. unplastered brick wall.

ACKNOWLEDGEMENTS

The authors are indebted to the Department of Public Works and Carleton University for cooperation in making this study possible; also to the operating personnel of the four test buildings for their assistance during the tests. The authors also wish to acknowledge the assistance of R.G. Evans in the field tests and in the processing of the test data.

This paper is a contribution from the Division of Building Research, National Research Council of Canada, and is published with the approval of the Director of the Division.

REFERENCES

1. Tamura, G.T., Computer Analysis of Smoke Movement in Tall Buildings, ASHRAE TRANSACTIONS, Vol. 75, 1969.
2. ASHRAE Handbook of Fundamentals, Chapter 25, 1967.
3. Sasaki, J.R., and A.G. Wilson, Air Leakage Values for Residential Windows, ASHRAE TRANSACTIONS, Vol. 71, II, 1965.
4. Tamura, G.T., and A.G. Wilson, Building Pressures Caused by Chimney Action and Mechanical Ventilation, ASHRAE TRANSACTIONS, Vol. 73, II, 1967.
5. Ma, W.Y.L., The Averaging Pressure Tubes Flowmeter for the Measurement of the Rate of Airflow in Ventilating Ducts and for the Balancing of Airflow Circuits in Ventilating Systems, of Inst of Heating and Ventilating Engrs, Feb. 1967.
6. Tamura, G.T. and A.G. Wilson, Pressure Differences Caused by Chimney Effect in Three High Buildings, ASHRAE TRANSACTIONS, Vol. 73, II, 1967.

PAPER 11

**STUDIES ON EXTERIOR WALL AIR
TIGHTNESS AND AIR INFILTRATION
OF TALL BUILDINGS**

G. T. TAMURA AND C. Y. SHAW

**National Research Council
Ottawa
Canada**

(Paper reproduced by kind permission of ASHRAE)

STUDIES ON EXTERIOR WALL AIR TIGHTNESS AND AIR INFILTRATION OF TALL BUILDINGS

GEORGE T. TAMURA, P.E.
Member ASHRAE

CHIA Y. SHAW, P.E.

One of the functions of the exterior walls of buildings is to separate outdoor elements from the inside environment. Building envelopes are not normally completely air tight and they permit some flow of air into and out of them through joints and cracks in the wall fabric. This leakage of air contributes to heating and cooling loads and must be taken into account in any energy analysis of buildings and design of HVAC systems.

Infiltration rates depend primarily on the air leakage characteristics of exterior walls and to a lesser extent on those of interior separations such as floor construction, interior partitions and various service shafts. A reliable prediction of the infiltration rates of multi-storey buildings is hampered, at present, by the scarcity of information on the actual air leakage characteristics of exterior walls.

The National Research Council of Canada has taken measurements of the air leakage characteristics of the exterior walls of eight multi-storey office buildings located in Ottawa, Canada. Varying in height from 11 to 22 stories, with curtain wall construction and fixed glazing, they were built during the sixties and early seventies. The results of the measurements are reported in this paper. A method for calculating infiltration rates caused by stack action has been developed and is applied to heat loss calculations using the measured wall leakage values.

EXTERIOR WALL MEASUREMENTS

The results of air leakage measurements of the exterior walls of four multi-storey buildings were reported by Shaw, Sander and Tamura.¹ This project was subsequently expanded to include four additional buildings, using the same test method (Table 1). Briefly, it involved pressurizing all typical floor spaces between the ground floor and the top mechanical floor, using 100% outside air for the central supply air systems with return and exhaust systems shut down. Supply air rates were varied and the concomitant pressure differences across the pressurized enclosure recorded. To ensure stable pressure differences across the building enclosure, the tests were conducted during unoccupied periods and when there was little or no wind.

Under steady-state condition the rate of supply of outside air equals the sum of the air leakage rates through the exterior walls of typical floors, bottom and top separations (Fig. 1). It can be expressed as follows:

$$Q_s = C_w \sum_{j=1}^N (A_w \Delta P_w^{n_w})_j + C_b A_b (\Delta P_b)^{n_b} + C_t A_t (\Delta P_t)^{n_t} \quad (1)$$

G.T. Tamura, Division of Building Research, National Research Council of Canada, Ottawa, Canada.
C.Y. Shaw, Division of Building Research, National Research Council of Canada, Ottawa, Canada.

where

Q_s = total outdoor air supply rate, cfm

n = flow exponent

C = flow coefficient, cfm/(sq ft)(in. of water)ⁿ

ΔP = pressure difference, $P_i - P_o$, in. of water

P_i = inside pressure, in. of water

P_o = outside pressure, in. of water

A = area, sq ft

N = total number of floors with typical wall construction

subscripts

w = exterior wall

b = bottom separation

t = top separation

The values of Q_s , ΔP_w , ΔP_b and ΔP_t can be measured. By obtaining several sets of these values it is possible to determine the values of flow coefficients C_w , C_b and C_t and the flow exponents n_w , n_b and n_t , defining air leakage characteristics of the three separations. Details of test methods and data analysis are given in Ref 1.

TEST RESULTS

The values of flow coefficient and exponent, as defined in Eq 1 for the eight test buildings, are given in Table 2. Using these values, the over-all air leakage rates in terms of cfm per sq ft of outside wall area vs pressure difference were plotted on Fig. 2. These values, which include the air leakage rates through the top and bottom as well as through the exterior walls, are useful in estimating the supply air rates required for pressurizing a building. It should be noted that leakage values of the top separation, given in Table 2, include leakage flows through the closed exhaust dampers at the top of the return and exhaust systems (shut down during the tests).

The dependence of the exterior wall air leakage rates on pressure difference is shown in Fig. 3. These air leakage rates varied from 0.12 to 0.48 cfm per sq ft of wall area at a pressure difference of 0.30 in. of water pressure and constituted from 20 to 55% of the over-all air leakage rates of the test buildings. These values are well above the standard² specified by the National Association of Architectural Metal Manufacturers (NAAMM): 0.06 cfm per sq ft of wall area at the same pressure difference. The exterior facades of three of the test buildings, D, E and H, were constructed of metal panels; those of the remaining test buildings were of precast concrete panels. As the wall materials are relatively impermeable to air, it is probable that the air leakage rates depended mainly on the design of wall joints and the way they were put together. Buildings F and H, which were constructed with close supervision of workmanship on wall jointing to minimize air infiltration, gave the lowest leakage rates; and where joint seals appeared inadequate, remedial measures were taken.

CALCULATION OF INFILTRATION RATE CAUSED BY STACK ACTION

Air infiltration in a building is caused by both wind and stack action. The calculation of infiltration rates caused by wind is quite complex, for the wind pressure distribution over the surface of a building depends on wind speed and direction, building shape and the nature of the surrounding terrain, including adjacent buildings. The literature on wind pressures on actual and model buildings in boundary-layer wind tunnels is extensive. Pressure measurements have been made primarily to develop data for structural load calculations and not for infiltration calculations, which require more detailed data on wind pressures both horizontally and vertically. If wind pressure data for a building are available, infiltration rates caused by both wind and stack

action can be calculated with the aid of a digital computer and an appropriate mathematical model.^{3,4,5}

The infiltration rates caused by stack action alone, which tends to govern the infiltration rate of a multi-storey building during cold weather, can be calculated relatively easily. The derivation of the equation is as follows:

Theoretical pressure difference across exterior walls caused by stack effect is given by ⁶

$$\Delta P = 0.52 p h \left(\frac{\Delta T}{T_i T_o} \right) \quad (2)$$

where

p = barometric pressure, lb/sq in.

h = vertical distance from neutral zone, ft

positive sign above neutral zone

negative sign below neutral zone

ΔT = temperature difference, $T_i - T_o$, F

T_i = absolute temperature inside, R

T_o = absolute temperature outside, R .

The neutral zone is the level at which inside and outside pressures are equal. Eq 2 indicates that ΔP and ΔT have the same signs for all locations above the neutral zone and, conversely, opposite signs below the neutral zone. Thus there will be infiltration through the walls of the lower storeys and exfiltration through the walls of the upper storeys when the temperature inside the building is higher than the air temperature outside. This means that air flows upward within the building during the winter months. The flow pattern is reversed during the summer months when the air temperature outside is higher than that inside.

Actual pressure difference depends on the resistances to flow of both the exterior and interior separations. It is less than the theoretical pressure difference indicated by Eq 2 because of the resistance to air movement associated with interior components such as partitions, floor constructions and walls of vertical shafts. The upward flow caused by stack action during cold weather takes place from floor to floor through openings in the floor construction and through vertical shafts. It can be expected that most upward flow will occur in the vertical shafts because their resistance (friction losses) will be considerably less than that associated with floors, which act as resistances in series. For this discussion, therefore, the floor construction is considered to be air tight.

With this assumption, the theoretical pressure difference given by Eq 2 is that between outside the building and inside a shaft at the same level. It is distributed across the exterior walls, interior partitions and the walls of vertical shafts. The manner of distribution depends upon the resistance of each of these separations in relation to that of the combined resistances at the same level. If the resistances of the exterior and interior separations are uniform from floor to floor, the ratio of actual (exterior walls) to theoretical pressure differences will be constant for the whole height of a building.

Eq 2 can be modified to take this into account

$$\Delta P = 0.52 \gamma p h \left(\frac{\Delta T}{T_i T_o} \right) \quad (3)$$

where

γ = ratio of actual to theoretical pressure difference.

If the exterior wall is much tighter than the interior separations, the value of γ will approach unity; if it is much looser, the value of γ will approach zero. The values for γ determined experimentally for a few multi-storey office buildings ⁷ ranged from 0.63 to 0.88.

The rate of airflow through an infinitesimal area of the exterior wall is given by

$$dQ_w = C_w dA_w (\Delta P)^{n_w} \quad (4)$$

where

dQ_w = air leakage rate through an area dA_w of the exterior wall, cfm

C_w = flow coefficient, cfm/(sq ft)(in. of water) ^{n_w}

n_w = flow exponent

Combining Eq 3 and 4 gives

$$dQ_w = C_w [0.52 \gamma p h \left(\frac{\Delta T}{T_i T_o} \right)^{n_w} S dh] \quad (5)$$

where

S = perimeter of the building, ft.

For a building with a constant cross-sectional area and a uniform distribution of leakage openings with height, an equation for the total air infiltration rate can be obtained by integrating Eq 5 from the ground level to the neutral zone. The neutral zone level can be expressed as βH where β is the ratio of the height of the neutral zone and the building height H in ft.

Thus,

$$Q_w = C_w S [0.52 \gamma p \left(\frac{\Delta T}{T_i T_o} \right)^{n_w} \frac{(\beta H)^{n_w + 1}}{n_w + 1}] \quad (6)$$

where

Q_w is the total rate of infiltration for the whole building.

As this equation assumes a wall with a uniform air leakage characteristic, a separate infiltration heat loss calculation using Eq 3 and 4 should be made for the exterior walls of the ground floor since their air leakage values tend to be higher than those of other floors.

INFILTRATION HEAT LOSSES CAUSED BY STACK ACTION

From Fig. 3, air leakage values for a tight, average and loose wall were assigned arbitrarily for heat loss calculation. A flow exponent, n_w , of 0.65 was assumed for these walls (it varied from 0.50 to 0.75 for the test buildings). The flow coefficients were assumed as follows:

Wall Tightness	Air Leakage Rate, cfm/sq ft at 0.3 in. water	Flow Coefficient, C_w cfm/(sq ft)(in. water) ^{0.65}
NAAMM	0.06	0.13
tight	0.10	0.22
average	0.30	0.66
loose	0.60	1.30

These values will probably apply to exterior walls of curtain wall construction with fixed glazing but not to exterior walls of masonry construction. Measurements on one building⁸ of the latter construction indicated that its leakage rates are considerably higher than those shown on Fig. 3.

The equation for infiltration rate, Eq 6, can be simplified for practical purposes by assuming the following: $\gamma = 0.80$, $p = 14.7$ psia, $T_i = 530R$, $n_w = 0.65$, $\beta = 0.50$. Substituting these values in Eq 6

$$Q_w = 0.00974 C_w S \left(\frac{\Delta T}{T_o} \right)^{0.65} (H)^{1.65} \quad (7)$$

The sensible heat load due to infiltration is given by ⁸

$$Y = 1.08 Q_w \Delta T \quad (8)$$

where

Y = sensible heat loss, Btu/hr

Substituting Eq 7 in Eq 8 gives

$$Y = 0.0106 C_w S \left(\frac{1}{T_o} \right)^{0.65} ([\Delta T]H)^{1.65} \quad (9)$$

The latent heat loss when indoor humidity ratio is to be maintained at a constant level is given by ⁹

$$Z = 4800 Q_w (W_i - W_o) \quad (10)$$

where

Z = heat required to increase moisture content of infiltration air from W_o to W_i , Btu/hr

W_i = humidity ratio of indoor air, pounds of water per pound of dry air

W_o = humidity ratio of outdoor air, pounds of water per pound of dry air

Substituting Eq 7 in Eq 10 gives

$$Z = 50.9 C_w S \left(\frac{\Delta T}{T_o} \right)^{0.65} H^{1.65} (W_i - W_o) \quad (11)$$

Infiltration rates were calculated for the four air leakage values and various building heights using Eq 7, expressed in air changes per hour and assuming a floor plan 150 ft sq. A temperature difference of 70 F was assumed between indoor and outdoor air. The results of these calculations (Fig. 4) indicated that air change rates increase with building height as well as with increasing wall leakage values.

These values may be compared with the outdoor air requirement for ventilation. ASHRAE STANDARD 62-73 ¹⁰ gives the minimum required ventilation air without tempering or filtering as 15 cfm per person for general office space (0.15 cfm per sq ft, based on 10 persons per 1000 sq ft of floor area). This represents 0.9 air change per hour. As this value is much higher than the values shown on Fig. 4, it appears that air infiltration by itself will not usually satisfy the ventilation requirement.

The sensible and latent infiltration heat losses were calculated using Eq 9 and 11, assuming an indoor-outdoor temperature difference of 70 F, a humidity ratio for indoors of 0.0047 lb of water per lb of dry air (70 F, 30% RH) and one for outdoors of 0.0006 lb of water per lb of dry air (0 F, 80% RH). The results of the calculation given in Btu per hour per square foot of wall area are shown in Fig. 5 for various building heights. For this example, the latent heat losses are 28% of the sensible heat losses.

In Fig. 6, the infiltration heat losses (sensible plus latent) are compared with the total heat losses through the exterior walls (infiltration plus transmission). The over-all U value was assumed to be 0.30, with values of 0.15 for the insulated walls and 0.55 for double-glazed windows, which constituted 40% of the total wall area. Transmission heat loss was 21.0 Btu/(hr) (sq ft) at a temperature difference of 70 F. For a building with an average wall leakage value, the percentage of total heat loss contributed by air infiltration varied from 22 to 46% for building heights of 200 to 1000 ft, respectively; these values are reduced to 9 to 22% for buildings with relatively air-tight walls. As infiltration heat losses increase with building height, the significance of air tightness for walls of tall buildings is apparent.

The ventilation requirement for general office space of 15 cfm of outdoor air per person demands an outdoor air supply of 0.56 cfm per sq ft of outside wall area, assuming a floor dimension of 150 by 150 ft and floor height of 10 ft. Using Eq 8 and 10, the heat loss (sensible plus latent) was 53.6 Btu/(hr)(sq ft) of wall area at a temperature difference of 70 F

and humidity ratio, indoors, of 0.0047 lb of water per lb of dry air and, outdoors, of 0.0006 lb of water per lb of dry air. This heating load imposed by ventilation air has been compared with those of transmission and infiltration through a wall of average air tightness in Fig. 7. It may be seen that the ventilation heating load is the largest component of the total heating load (infiltration plus transmission plus ventilation). For a 200-ft high building it constitutes 67% of the total heating load, whereas infiltration heating load is only 7%. ASHRAE Standard 62-73 permits reduction in the ventilation air to 5 cfm per person (0.05 cfm per sq ft of floor area) if the air is tempered and filtered. This reduction in ventilation air results in heat losses due to ventilation and infiltration of 40 and 12% of the total heat loss, respectively. During unoccupied periods with no ventilation air, the infiltration heat loss is 22% of the total for walls of average air tightness and 9% for tight walls.

These calculations recognized stack action alone at a given inside-outside temperature difference. It is probable that infiltration rates of tall buildings depend primarily on stack action during cold weather and average wind velocity. The infiltration rates calculated in the previous examples would have been somewhat higher if wind action had also been considered. A complete analysis would involve integration of heat losses over the seasons, taking into account both wind and stack action.

HEAT LOSSES CAUSED BY BUILDING PRESSURIZATION

HVAC systems are sometimes designed and operated to minimize air infiltration, particularly at the entrance level, by means of building pressurization. Its effect is to increase the inside pressures and thereby lower the level of the neutral zone. If the neutral zone is lowered to ground level, air infiltration is eliminated but air exfiltration is increased. The required rate of supply of outside air to achieve this can be calculated from Eq 6; for this, the value of β , the ratio of the neutral zone height to building height, is taken as unity. The ratio of total exfiltration rate with pressurization ($\beta = 1.0$) to infiltration rate without pressurization ($\beta = 0.5$) is about 3.2; i.e., the outside supply air rate required to pressurize a building fully is 3.2 times the infiltration rate. This value would be greater if the exfiltration rate through the top of the building were also considered. Reducing infiltration rate by pressurization incurs a high heating cost penalty. It is more economical to pressurize the ground floor only, provided the ground floor enclosure is reasonably air tight.

CONCLUSIONS

1. The air leakage rates of the exterior walls of eight test buildings varied considerably, with values of 0.12 to 0.48 cfm per sq ft of wall area at a pressure difference of 0.30 in. of water. They were much above that specified by an industry standard of 0.06 cfm per sq ft of wall area at the same pressure difference.
2. For a wall with average air tightness and U value of 0.30 Btu/(hr)(sq ft)(F), the percentage of total heat loss through the walls contributed by infiltration during cold weather varied from 22 to 46% for building heights of 200 to 1000 ft, respectively; these values are reduced to 9 to 22% for buildings with relatively air-tight walls. They indicate the necessity of assuring relatively air-tight walls for tall buildings.
3. Air infiltration alone cannot be relied upon to provide an adequate amount of outdoor air for ventilation of buildings with curtain wall construction and fixed glazing. The heating load caused by ventilation air was found to be a major component of the total heating load.
4. Reducing air infiltration by mechanically pressurizing a building can mean a high heating cost penalty.

REFERENCES

- 1 C.Y. Shaw, D.M. Sander, G.T. Tamura, "Air Leakage Measurements of the Exterior Walls of Tall Buildings," ASHRAE TRANSACTIONS, vol 79, part 2, 1973, pp. 40-48.
- 2 National Association of Architectural Metal Manufacturers, Metal Curtain Wall Manual, Specifications, pp. 4-9, December 1962.
- 3 P.J. Jackman, "A Study of the Natural Ventilation of Tall Office Buildings," Journal of the Institute of Heating and Ventilating Engineers, vol 38, August 1970, pp. 103-118.
- 4 R.E. Barrett and D.W. Locklin, "Computer Analysis of Stack Effect in High-Rise Buildings," ASHRAE TRANSACTIONS, vol 74, part II, 1968, pp. 155-169.

- 5 D.M. Sander and G.T. Tamura, "Simulation of Air Movement in Multi-Storey Buildings," presented at Second Symposium on the Use of Computers for Environmental Engineering Related to Buildings, Paris, 13-15 June 1974.
- 6 ASHRAE HANDBOOK OF FUNDAMENTALS, Chapter 19, "Infiltration and Natural Ventilation," 1972.
- 7 G.T. Tamura and A.G. Wilson, "Pressure Differences Caused by Chimney Effect in Three High Buildings," ASHRAE TRANSACTIONS, vol 73, part II, 1967, pp. II. 1.1 - II. 1.10.
- 8 G.T. Tamura and A.G. Wilson, "Pressure Differences for a Nine-Storey Building as a Result of Chimney Effect and Ventilation System Operation," ASHRAE TRANSACTIONS, vol 72, part I, 1966, pp. 180-189.
- 9 ASHRAE HANDBOOK OF FUNDAMENTALS, Chapter 21, "Heating Load," 1972.
- 10 ASHRAE STANDARD 62-73, "Standards for Natural and Mechanical Ventilation," 1973.

ACKNOWLEDGEMENTS

The authors are indebted to the Department of Public Works, Carleton University, and Campeau Corporation for cooperation in making this study possible; also to the operating personnel of the test buildings for their assistance during the tests. The authors wish to acknowledge the assistance of R.G. Evans in the field tests and in the processing of test results. This paper is a contribution from the Division of Building Research, National Research Council of Canada, and is published with the approval of the Director of the Division.

TABLE 1

Description of Test Buildings

Building	A	B	C	D	E	F	G	H
Year constructed	1970	1964	1970	1971	1968	1973	1974	1974
Year tested	1970	1971	1971	1971	1974	1974	1974	1974
No. of typical floors	9	17	20	20	21	16	25	20
Floor plan (ft x ft)	166x210	88x140	126x146	75x93	83x158	83x183	123x143	126x146
Floor height (ft)	13	11	10.6	10.5	10.4	10.6	10.6	10.6
Wall area per floor (sq ft)	9,776	5,016	5,766	3,528	5,013	5,656	5,639	5,766
Window area (% wall area)	38	33	30	26	35	52	26	40
Window type	Fixed sealed double glazing	Openable sealed double glazing (key locked)	Fixed sealed double glazing	Fixed sealed double glazing	Fixed sealed double glazing	Fixed sealed double glazing	Fixed sealed double glazing	Fixed sealed double glazing
Wall construction	Precast concrete 8-in. tile 2-in. insulation air space 6-in. tile plaster	Precast concrete panel 2-in. insulation	Precast concrete panel air space 1-in. insulation 1/2-in. cement 6-in. concrete block plaster	Metal panel air space 2-in. . insulation 20-in. concrete	Metal panel 2-in. insulation	Precast concrete panel 1-in. insulation	Precast concrete panel 1-in. insulation	Metal panel 2-in. air space 3.5-in. insulation

TABLE 2

Flow Coefficients and Exponents of Test Buildings

Test Building	Outside Wall		Bottom Separation		Top Separation	
	C_w	n_w	C_b	n_b	C_t	n_t
A	1.12	0.70	3.21	0.70	0.85	0.60
B	0.69	0.50	0.44	0.70	3.42	0.50
C	0.62	0.75	1.27	0.50	5.69	0.70
D	0.76	0.65	0.27	0.50	7.20	0.50
E	0.48	0.50	0.21	0.70	4.35	0.50
F	0.30	0.50	1.01	0.50	2.38	0.50
G	0.84	0.65	0.11	0.70	6.82	0.65
H	0.20	0.50	6.55	0.70	2.90	0.50

C_w in cfm/(sq ft of wall area)(in. of water) n_w

C_b in cfm/(sq ft of floor area)(in. of water) n_b

C_t in cfm/(sq ft of floor area)(in. of water) n_t

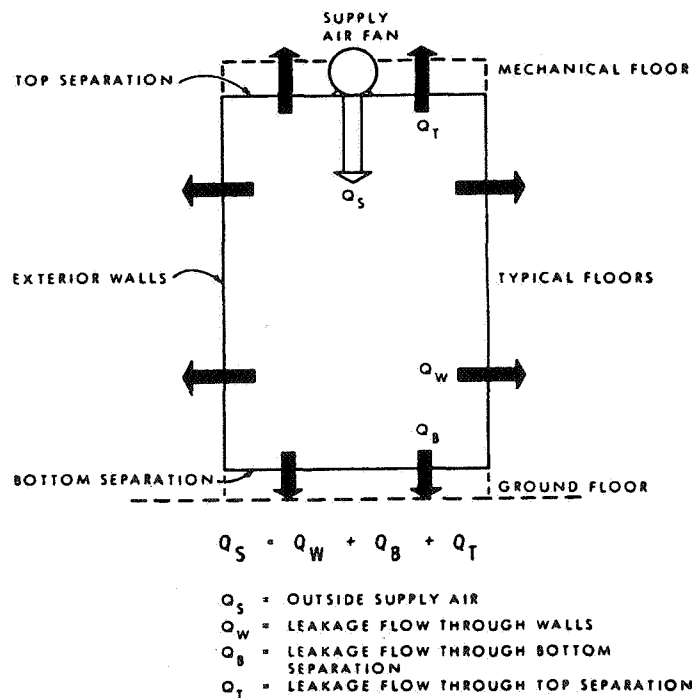


Fig. 1 Flow balance under wall leakage tests

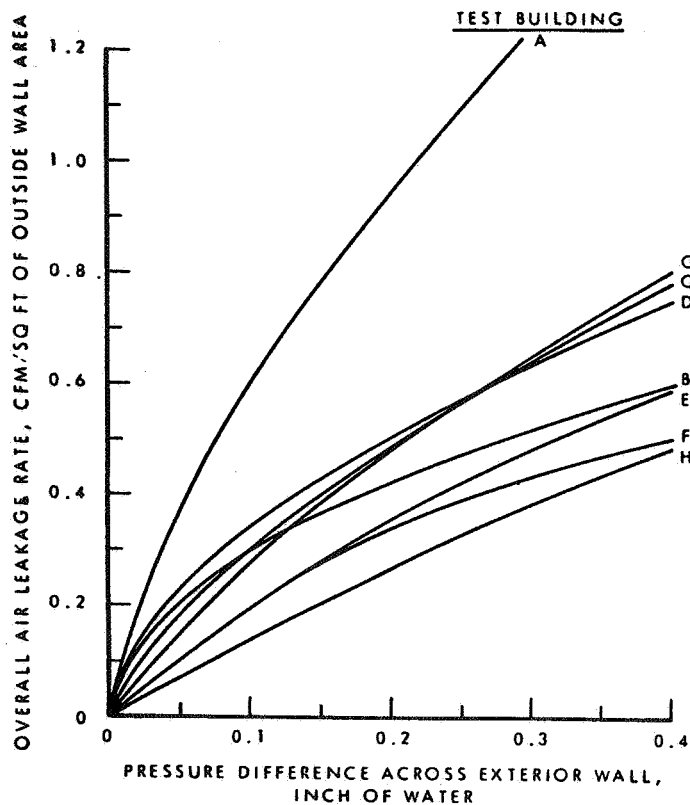
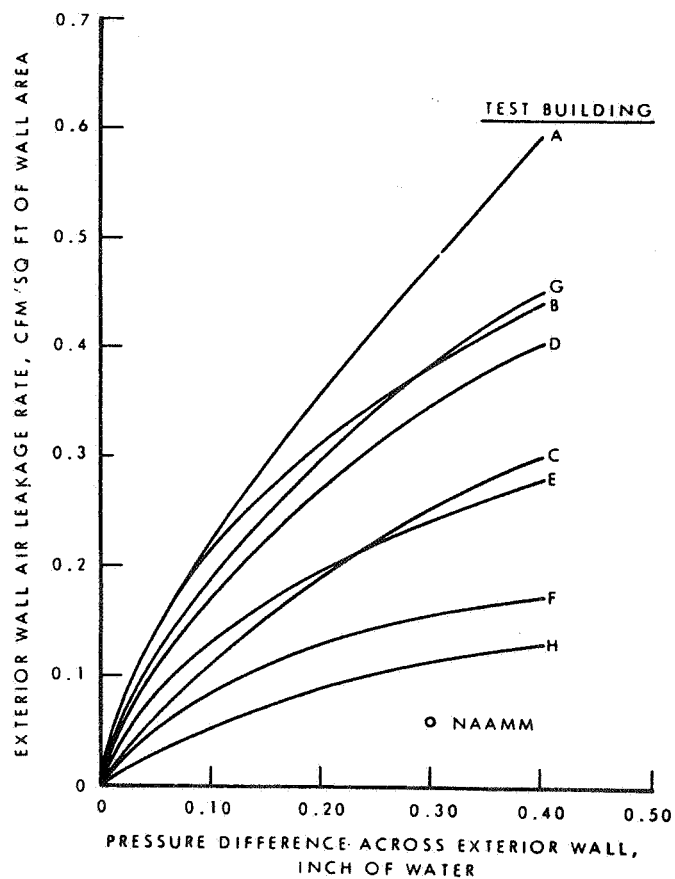


Fig. 2 Over-all air leakage rates of pressurized enclosure

Fig. 3 Air leakage rates of exterior walls



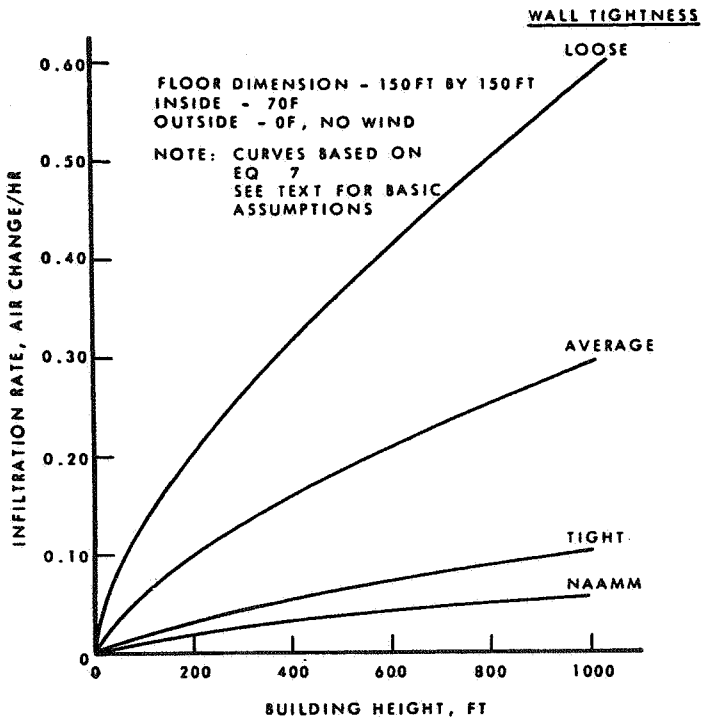
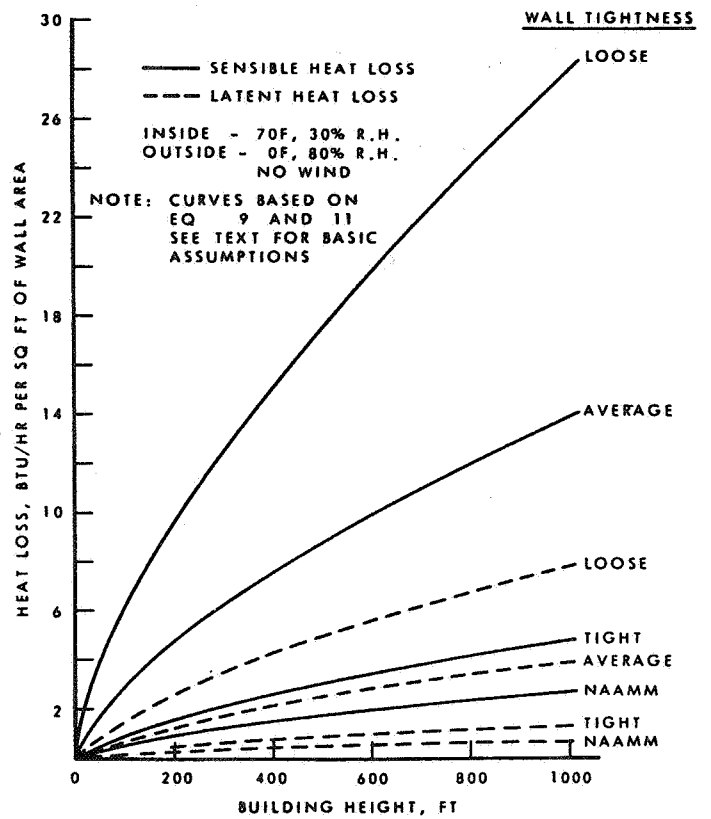


Fig. 4 Infiltration rate vs building height

Fig. 5 Sensible and latent heat losses caused by infiltration



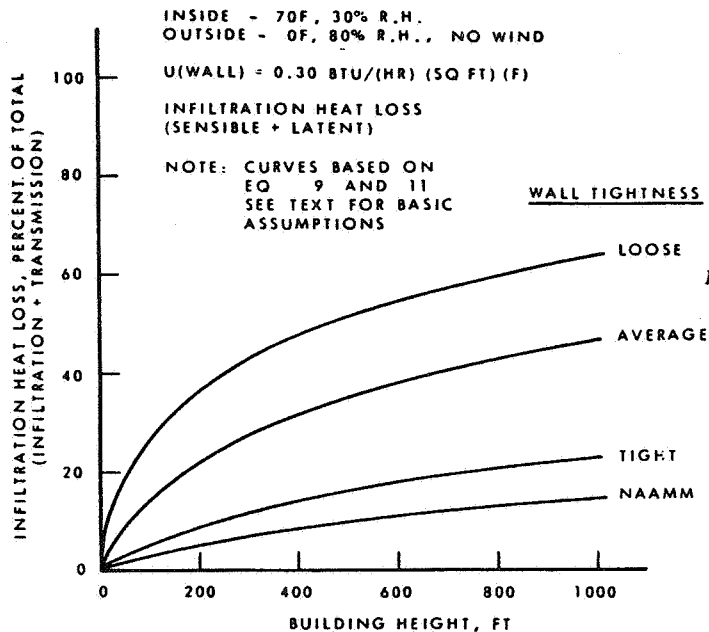
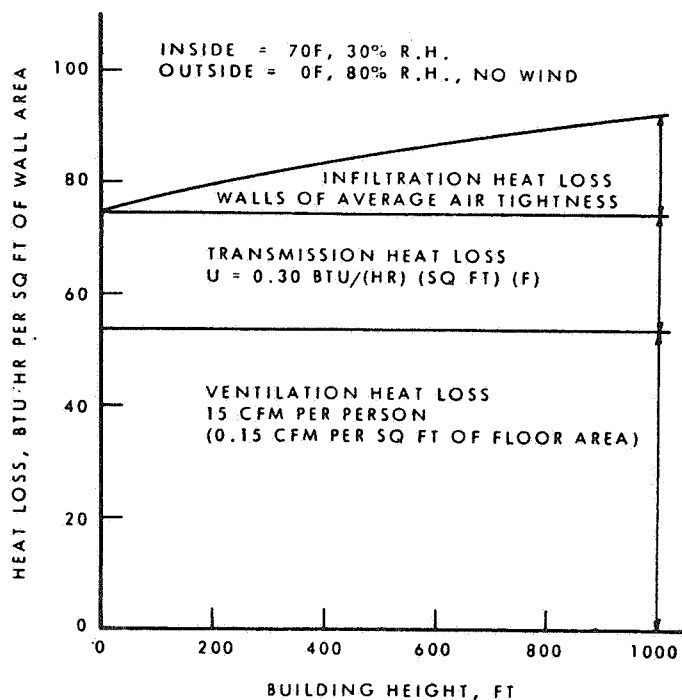


Fig. 6 Comparison of infiltration heat loss with transmission heat loss

Fig. 7 Comparison of ventilation heat loss with infiltration and transmission heat losses



DISCUSSION

DAVID T. HARRJE, Senior Research Engineer and Lecturer, Princeton Univ., Princeton, NJ: Has there been any attempt to use the central shaft with blowing downward at the neutral line to attempt to benefit both the upper and lower portions of the building through reduced air infiltration?

TAMURA: Computer studies on this approach to reduce infiltration are given in a paper entitled "Building Pressures Caused by Chimney Action and Mechanical Ventilation" by A.G. Wilson and myself (ASHRAE TRANSACTIONS, vol. 73, Part II, 1967). The reduction of pressure differences across the exterior walls would depend on the recirculation rate and the internal resistance of a building; inside pressures of a building with a low internal resistance will not be altered significantly to affect the pressure differences across the exterior walls.

It should be recognized that if both infiltration and exfiltration are eliminated by this means, then the pressure differences caused by stack action would be transferred from the exterior walls to the walls of vertical shafts which can give rise to difficulties in operating elevator and stair doors. It is probable that effective operation of this system with changing condition of wind and stack action would be difficult. The preferred approach to minimize infiltration is by constructing outside walls that are relatively air tight rather than by using ventilation fans as suggested or for building pressurization.

RONALD N. JENNER, NASA, Hampton, VA: In regards to infiltration due to wind on low-rise building, what does your study show?

TAMURA: It was stated that infiltration rates of high rise buildings depend primarily on stack action during cold weather and average wind velocity. It is expected that the effect of wind action compared to that of stack action would be greater for low-rise buildings than for high-rise buildings; that due to stack action, however, it should not be neglected as field studies indicate that even for houses its effect is significant.

PAPER 12

**AIR TIGHTNESS AND AIR
INFILTRATION OF SCHOOL
BUILDINGS**

C. Y. SHAW AND L. JONES

**National Research Council
Ottawa
Canada**

(Paper reproduced by kind permission of ASHRAE)

AIR TIGHTNESS AND AIR INFILTRATION OF SCHOOL BUILDINGS

C.Y. SHAW L. JONES

INTRODUCTION

Schools, as a group, are the third largest users of energy in buildings in Canada. The Division of Building Research, National Research Council of Canada therefore welcomed the opportunity in the autumn of 1975 to participate with the Carleton Board of Education in a program to reduce energy use in schools.

A major problem encountered initially was the lack of data on air infiltration for school buildings. A program of air leakage measurements in schools was therefore carried out. Results of the measurements were then applied to a simplified model of a school building, from which air infiltration and its contribution to total heating consumption could be calculated.

SELECTION OF TEST SCHOOLS

Eleven test buildings were selected from a total of 56 elementary schools, based on their 1975 energy consumption (1). Of the eleven schools, five were considered to have average consumption, three to have high consumption and the remaining three to have low consumption (Fig. 1). A brief description of the tested schools is given in Table I.

TEST METHOD

The air leakage characteristics of school buildings were measured by means of the pressurization method. The fan used was a vane axial type with a variable-pitch blade that can be adjusted manually to obtain flow rates between 0 and 23 m³/s (0 to 50,000 cfm). The fan intake was connected by several lengths of 0.9 m (3 ft) diameter duct to an entrance door replaced for the tests by a plywood panel (Fig. 2).

Air flow rates were measured upstream of the fan intake using total pressure averaging tubes (2) for high air flow rates and an orifice plate for low air flow rates. The pressure differences across the exterior walls were measured at the middle of each wall near the ground. A portable pressure meter consisting of a diaphragm-type pressure transducer (static error band of 5% full scale) and a digital voltmeter were used. To minimize wind influence on the pressure measurements all tests were conducted with a meteorological wind speed lower than 15 km/h (9.3 mph) (3).

Most tests were conducted under suction conditions, partly because air infiltration occurs with buildings under this condition, but also because of the need to avoid any possible damage to furniture and discomfort to occupants. For comparison, two schools were tested under both suction and pressurization.

The buildings were tested with the air-handling system in operation and with it shut down. With the system on, an initial reading of pressure difference across the exterior walls was taken with the test fan shut down and its intake sealed. This reading, which is the amount of pressurization resulting from imbalance between outside air supply and exhaust air rates of the

C.Y. Shaw and L. Jones, Research Officers, Energy and Services Section, Division of Building Research, National Research Council of Canada. K1A 0R6

air-handling systems, was then subtracted algebraically from the pressure difference readings obtained with the test fan operating. All schools except School C operated under suction pressures ranging from -2 to -35 Pa (-0.008 to -0.14 in. of water).

The air leakage rates through air intake and exhaust openings, openable windows, and doors were obtained by comparing the over-all air leakage rates taken before and after they were sealed. Because of difficulties in sealing, only schools with centralized air-handling systems were tested. As well, joints between window or door frames and walls were not sealed so that any leakage there was considered as part of the air leakage through the walls.

In addition, air leakage tests were made in School J in both June and December to discover whether leakage varied with season.

EXPERIMENTAL RESULTS

The over-all air leakage rates per unit area of exterior walls and their corresponding pressure difference are shown in Fig. 3 and 4 for air-handling system either operating or shut down. The results vary from 0.0024 to 0.006 m³/s·m² at a pressure difference of 25 Pa, (0.43 to 1.2 cfm/ft² at 0.1 in. of water). These figures also show that, in general, the operation of the air-handling systems had little effect on over-all air leakage rate when pressure differences were lower than 50 Pa (0.2 in. of water).

Examination of the limited air leakage data (Fig. 3 and 4) indicated that there was no meaningful relation between total energy consumption (Fig. 1) and the measured air leakage rate. The variation in air leakage from school to school could not be explained by wall construction because all were similar in design (see Table I). Investigation of the construction of the school with the highest leakage value (School D) revealed, however, a large number of unsealed openings around the roof joists at the exterior wall, suggesting that poor workmanship and lack of concern for sealing can lead to high air leakage. In addition, the air leakage rate measured in June at School J was within 2% of the leakage rate measured there in December, suggesting that, for this particular school, crack width did not vary with outside temperature.

Fig. 5 indicates that with the air-handling systems shut down 15 to 43% of the over-all air leakage can be attributed to the air intake and exhaust openings and the remainder to the walls, of which openable windows and doors of two schools contributed up to 4 and 10%, respectively (the percentage areas of openable windows and doors to the total wall area are about 2 and 2.5%, respectively).

Tests were conducted on two schools to investigate the difference in air leakage rates with a building under suction and pressurization. Comparison of the over-all air leakage rate measured under the two conditions was made with the air-handling systems both in operation and shut down; in the latter case, with the air intake and exhaust openings sealed and unsealed. Fig. 6, which shows the results for School B (the more extreme of the two schools), indicates that the difference in over-all air leakage rates between suction and pressurization is minimum with the air-handling systems shut down and the duct openings sealed. If the duct openings are unsealed, the over-all air leakage rate obtained under suction, with the air-handling systems in operation, is about 10% higher than it would be under pressurization; the reverse is true with the air-handling system shut down.

GENERALIZATION OF AIR LEAKAGE DATA

The air leakage data measured in the eleven schools were used to define three classes of building construction: loose, average and tight (Fig. 7). The air leakage characteristics were defined using the following equation:

$$q = C (\Delta P)^n \quad (1)$$

where

q = over-all air leakage rate per unit area of exterior walls, m³/s·m² (cfm/ft²)

C = flow coefficient, m³/s·m²·(Pa)ⁿ (cfm/ft²·(in. of water)ⁿ)

ΔP = pressure difference across exterior wall, Pa (in. of water)

n = flow exponent

The common flow exponent for the three classes was found to be about 0.65 by curve fitting; the corresponding flow coefficients were:

Class	Flow Coefficient, C	
	$\overset{0.65}{\text{m}^3/\text{s}\cdot\text{m}^2 \text{ (Pa)}}$	$\overset{0.65}{\text{cfm}/\text{ft}^2 \text{ (in. of water)}}$
Tight	3.0×10^{-4}	2.1
Average	5.0×10^{-4}	3.5
Loose	7.0×10^{-4}	4.9

These flow coefficients are based on the air leakage values for schools with air-handling systems off. They can be applied to other conditions (air-handling systems on and building under pressurization) for load and energy calculations without introducing significant errors.

AIR INFILTRATION RESULTING FROM WIND AND STACK EFFECT

Using the method described in Ref. 4, air infiltration rates for a simplified model of a school building were calculated at various combinations of wind speed and ambient air temperature. The school model (1) (see Appendix A) consists of two independent parts: a single-storey classroom block and a two-storey high open hall (gymnasium) comprising 90 and 10% of the total floor area, respectively. The intake and exhaust openings of the air-handling systems were assumed to be located at the roof level.

The air leakage paths in each wall were lumped into five equally-sized openings located at equal intervals in the vertical direction. Ventilation openings were represented by a single opening located in the roof. The corresponding flow coefficients were calculated from Eq 1 assuming 70 and 30% of the total air leakage value for walls and roof, respectively. Wind was assumed to act normally to the long wall. The surface pressure coefficients were derived from the measurement of pressure distributions on a cubic model in a suburban boundary layer (5). These coefficients increase almost linearly with height from 0.46 to 0.64 for the windward wall and are approximately constant, with values of -0.25, -0.54 and -0.6 for the leeward wall, the two side walls, and the roof, respectively.

The calculated air infiltration rates are shown in Fig. 8 as a function of wind speed at the roof and inside-outside temperature difference. Wind speed at the roof level of an isolated school can be approximately related to the meteorological wind speed by the equation (6):

$$V = B H^{1/3} V_s \tag{2}$$

where

- V is wind speed at roof level, km/h (mph)
- H is building height, m (ft)
- V_s is the wind speed at 10 m (32.8 ft) above the ground measured by the Meteorological Service, km/h (mph)
- B is a constant and is equal to 0.142 and 0.211 for Imperial and S.I. units, respectively.

Using Eq 2, the relation between the roof level wind speed and the meteorological wind speed thus assumed were:

$$V = 0.33 V_s \text{ for classroom block}$$

$$V = 0.42 V_s \text{ for hall}$$

The contribution of stack effect to air infiltration was shown to be quite significant, even for a single-level building. This is illustrated by the results for the classroom block (see Fig. 8) where the air infiltration resulting from stack effect for an inside-outside temperature

difference of 55.6°C (100°F) is approximately the same as that from a 15 km/h (9.3 mph) wind at the roof level (45 km/h or 28 mph meteorological wind speed).

EFFECTS OF AIR INFILTRATION ON ANNUAL ENERGY CONSUMPTION

The annual heat consumption for the school model was calculated both with and without air infiltration, using the Meriwether Energy Analysis Series. A brief description of the building model and the conditions used for heating load calculations is given in Appendix A. The annual heating loads were calculated for various combinations of mean annual wind speed acting normally on the long wall and ambient air temperature between -17.8°C and 23.9°C (0°F and 75°F). The values of air infiltration rates were obtained from Fig. 8, which is based on walls of average air tightness.

The calculated annual heat consumption, using 1974 Ottawa weather data for various mean annual wind speeds at roof level, is shown in Fig. 9. The contribution of air infiltration to the total annual heat consumption is illustrated in Table II, assuming a mean annual wind speed of 16 km/h (10 mph), the Ottawa average (7). It indicates that the proportion of heat consumption attributed to air infiltration is about 29%.

The use of annual average wind speeds in energy analysis will tend to underestimate heat consumption because air infiltration rate varies non-linearly with wind speed (Fig. 8), and because wind speed is generally higher in winter than in summer. A separate method of calculating the contribution to annual heating load from air infiltration, using three years of hourly weather data for Ottawa, resulted in values 4 to 7% higher than those using annual mean wind speeds; monthly loads varied from 2 to 13%.

CONCLUSION

The calculated flow coefficients for the eleven schools, assuming a flow exponent of 0.65, vary from 3.0×10^{-4} to $7.0 \times 10^{-4} \text{ m}^3/\text{s} \cdot \text{m}^2 (\text{Pa})^{0.65}$ (2.1 to 4.9 cfm/ft² (in. of water)^{0.65}). Tests on four of the buildings showed that with the air-handling system off, 15 to 45% of over-all air leakage could be attributed to flow through the intake and exhaust system openings.

Tests conducted at pressure differences below 50 Pa (0.2 in. of water) showed no significant difference in the air leakage rates when the buildings were tested under either suction or pressurization

The large variation in air leakage values could not be explained by the wall design of the schools; it was probably caused by variation in workmanship during construction and by the number of openings associated with the air-handling system.

Air infiltration rates calculated for a model school building indicated that those due to stack action are significant even for single-storey buildings. Air infiltration is also shown to be a major contributing factor to annual heat consumption.

REFERENCES

1. Jones, L., "Calculating Energy Budgets for New Schools." To be published.
2. Ma, W.Y.L., "The Averaging Pressure Tubes Flowmeter for the Measurements of the Rate of Airflow in Ventilating Ducts and for the Balancing of Airflow Circuits in Ventilating Systems," J.I.H.V.E., Feb. 1967, pp. 327-348.
3. Tamura, G.T., and Shaw, C.Y., "Studies on Exterior Wall Air Tightness and Air Infiltration of Tall Buildings," ASHRAE TRANSACTIONS, Vol. 82, I, 1976, pp. 122-134.
4. Sander, D.M., "Fortran IV Program to Calculate Air Infiltration in Buildings," DBR Computer Program No. 37, May 1974, NRCC.
5. Baines, W.D., "Effects of Velocity Distribution on Wind Loads and Flow Patterns on Buildings," Proceedings, Symposium 16, Wind Effects on Buildings and Structures, Vol. 1, June 1963, pp. 198-225.
6. Shaw, C.Y. and Tamura, G.T., "The Calculation of Air Infiltration Rates Caused by Wind and Stack Action for Tall Buildings," ASHRAE TRANSACTIONS, Vol. 83, II, 1977.
7. Hourly Data Summaries, Dept. of Transport, Meteorological Branch and later Dept. of the Environment, Atmospheric Environment Service, various dates from May 1967 to March 1974.

ACKNOWLEDGEMENT

The authors are indebted to the Carleton Board of Education for cooperation in making this study possible; and to the custodial personnel of the test schools for their assistance during the tests. They gratefully acknowledge, also, the contribution of G.T. Tamura and G.P. Mitalas in the preparation of this paper; and the assistance of R.G. Evans in the field tests and of G.L. Johnson in the computer programming.

This paper is a contribution from the Division of Building Research, National Research Council of Canada, and is published with the approval of the Director of the Division.

TABLE 1
Description of Test Schools

School	A	B	C	D
Year tested	1976	1976	1976	1976
Year constructed	1970	1971	1965	1973
Floor area, m ² (ft ²)	2694 (29 000)	1858 (20 000)	3771 (40 600)	3493 (37 600)
Floor height, m (ft)	4.3 (14.0)	4 (13.0)	3.4 (11)	3.8 (12.5)
Volume, m ³ (ft ³)	11 495 (406 000)	7361 (260 000)	12 644 (446 600)	13 307 (470 000)
a. Exterior wall area, m ² (ft ²)	1175 (12 651)	1136 (12 234)	1875 (20 183)	1610 (17 330)
Window type	fixed and openable sealed double glazing	fixed and openable sealed double glazing	fixed and openable sealed double glazing	fixed and openable sealed double glazing
Window area/wall area	0.106	0.077	0.178	0.137
Openable window/wall area	0.018	0.012	0.06	0.026
Typical wall construction	15.24 cm autoclaved cellular concrete 1.6 cm drywall	10.2 cm face brick air space 5.1 cm rigid insulation 20.3 cm concrete block	10.2 cm face brick air space 5.1 cm rigid insulation 20.3 cm concrete block	10.2 cm face brick 5.1 cm foam insulation 20.3 cm concrete block
Number of exterior doors	Vestibule No vestibule		2 double	
b. Ratio of adjusted door area to wall area	5 single, 5 double	4 single, 4 double	3 single, 4 double	15 single, 4 double
HVAC system	#2 oil, centralized all-air H/V systems	#2 oil, centralized all-air H/V systems	electric, localized roof exhausters and convectors	#2 oil, centralized all-air H/V systems

Notes: a. Including Windows; b. A 50% reduction in area is allowed for door with vestibule or similar arrangement.

TABLE 1 (Cont'd)

School	E	F	G	H
Year tested	1976	1976	1976	1976
Year constructed	1957	1952	1968	1965
Floor area, m ² (ft ²)	3689 (39 711)	3093 (33 300)	5388 (58 000)	5156 (55 500)
Floor height, m (ft)	3.8 (12.5)	3.7 (12.0)	3.7 (12.0)	4 (13.0)
Volume, m ³ (ft ³)	14 054 (496 388)	11 314 (399 600)	19 706 (696 000)	20 427 (721 500)
a. Exterior wall area, m ² (ft ²)	2102 (22 630)	1256 (13 516)	1967 (21 179)	1613 (17 369)
Window type	fixed sealed double, openable sealed double and single glazing	fixed sealed double, openable sealed double and single glazing	fixed and openable sealed double glazing	fixed and openable sealed double glazing
Window area/wall area	0.248	0.299	0.096	0.221
Openable window/wall area	0.143	0.054	0.014	0.016
Typical wall construction	10.2 cm face brick 2.5 cm air space 2.5 cm rigid insulation 20.3 cm concrete block	10.2 cm face brick air space 2.5 cm rigid insulation 20.3 cm concrete block	10.2 cm concrete block 2.5 cm air space 2.5 cm rigid insulation 20.3 cm concrete block	10.2 cm face brick 2.5 cm air space 3.8 cm rigid insulation 15.2 cm concrete block
Number of exterior doors	Vestibule No vestibule			
	1 single, 1 double 7 single, 3 double	1 single 2 single, 4 double	1 single, 4 double 2 single, 2 double	1 single, 2 double 1 single, 5 double
b. Ratio of adjusted door area to wall area	0.013	0.016	0.010	0.016
HVAC system	#2 oil, centralized all-air H/V systems with unit ventilator in perimeter room	#2 oil, localized exhausting systems and hot-water convectors	#2 oil, centralized all-air H/V systems and unit ventilator in perimeter room	#2 oil, localized all-air H/V systems and hot-water convector in perimeter room

Notes: a. Including Windows;

b. A 50% reduction in Area is allowed for door with vestibule or similar arrangement.

TABLE 1 (Cont'd)

School	I	J	K
Year tested	1976	1976	1976
Year constructed	1968	1972	1968
Floor area, m ² (ft ²)	2620 (28 200)	3003 (32 331)	3219 (34 650)
Floor height, m (ft)	3.8 (12.5)	4 (13.0)	3.8 (12.5)
Volume, m ³ (ft ³)	9980 (352 500)	11 900 (420 303)	12 263 (433 125)
a. Exterior wall area, m ² (ft ²)	1241 (13 357)	1365 (14 695)	1815 (19 536)
Window type	fixed and openable sealed double glazing	fixed sealed domes, fixed and openable sealed double glazing	fixed sealed domes, fixed and openable sealed double glazing
Window area/wall area	0.104	0.062	0.102
Openable window/wall area	0.032	0.008	0.040
Typical wall construction	10.2 cm face brick	10.2 cm split block face	10.2 cm face brick
	2.5 cm air space		5.1 cm foamed insulation
	2.5 cm rigid insulation	5.1 cm air space	
	20.3 cm concrete block	15.2 cm concrete block and foamed in place insulation	20.3 cm concrete block
Number of exterior doors	Vestibule	3 single, 2 double	14 single, 1 double
	No vestibule	8 single, 4 double	2 single, 3 double
b. Ratio of adjusted door area to wall area	0.024	0.016	0.014
HVAC system	#2 oil, localized exhausting systems and hot-water convectors	gas, centralized all- air H/V systems with roof-top A.H. units	#2 oil and electric centralized all-air H/V system with convector or unit ventilator in perimeter room

Notes: a. Including Windows; b. A 50% reduction in area is allowed for door with vestibule or similar arrangement.

TABLE 2
Contribution of Air Infiltration to Annual Heat
Consumption in Ottawa for $V_s = 16$ km/h

Wind Speed at Roof, km/h	Annual Heat Consumption, GJ/m ² /Annum	
	No Infiltration	Average Infiltration
Classroom 5.3	0.28	0.36
Hall 6.7	1.19	1.69
Total = 90% Classroom + 10% Hall	.38	0.49
% Total Heat Consumption Attributed to Infiltration = 29%		

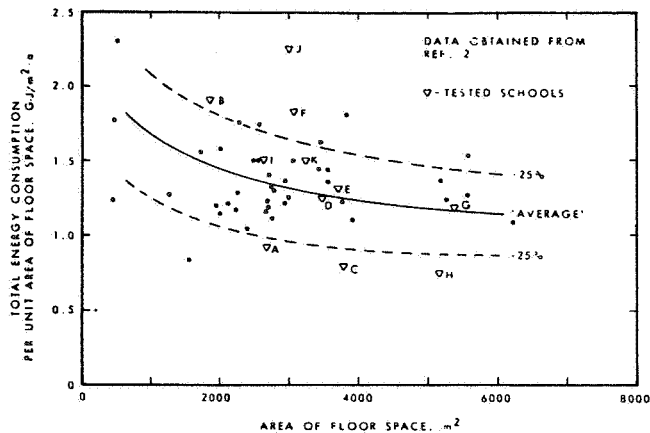


Fig. 1 1975 annual total energy consumption of the elementary schools under the Carleton Board of Education

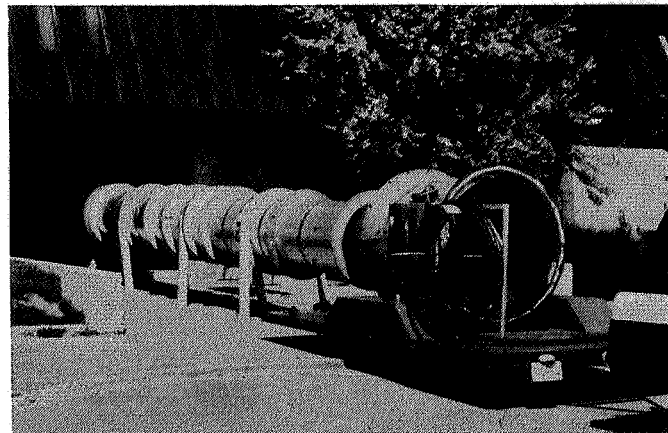


Fig. 2 Building test setup showing exhaust fan and duct connection

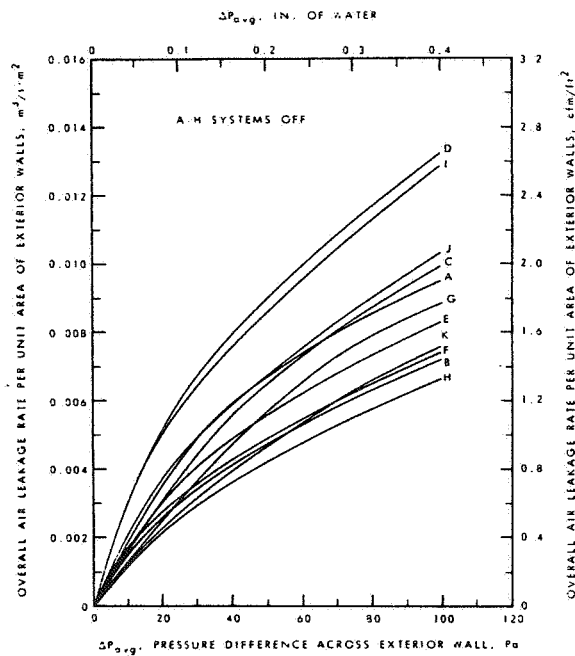


Fig. 3 The overall air leakage rates for schools with their air handling systems shut off

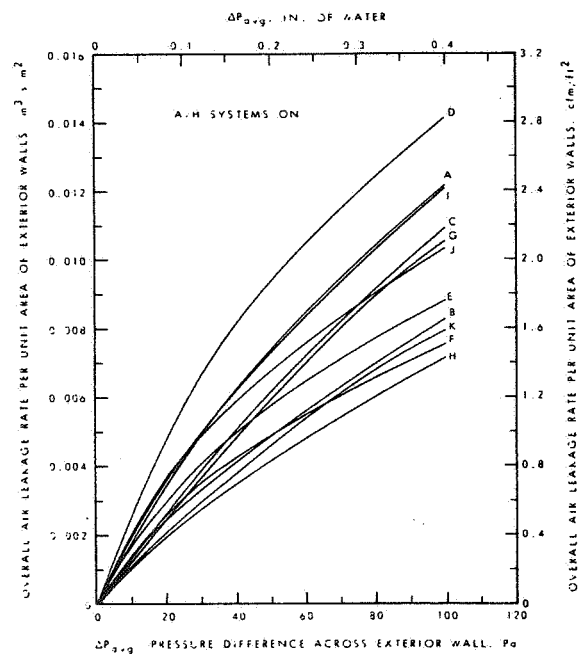


Fig. 4 The overall air leakage rates for schools with their air handling systems in operation

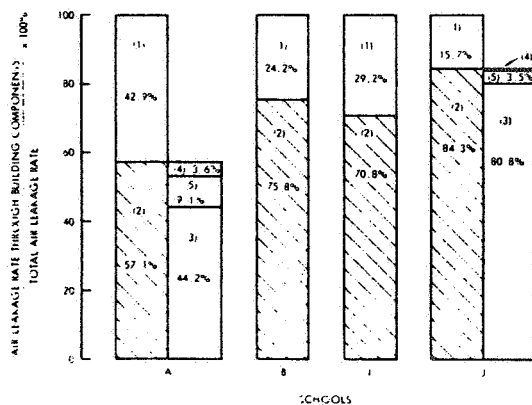


Fig. 5 The contribution of building components to the overall air leakage rate

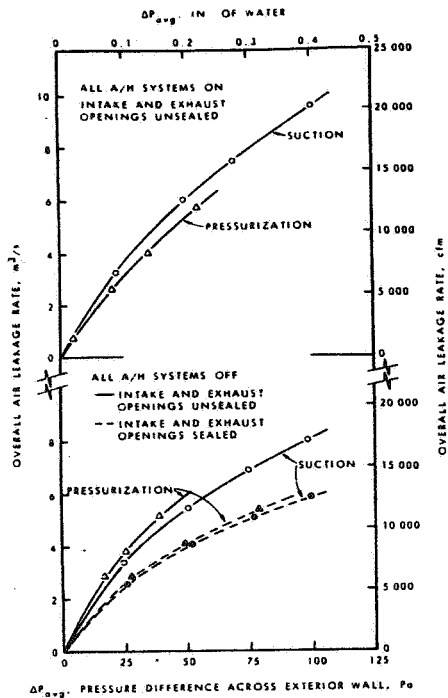


Fig. 6 The effect of pressurization or suction on the air leakage rate of School B

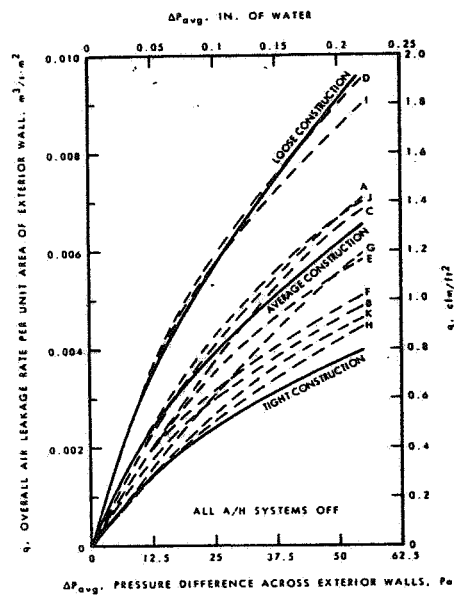


Fig. 7 The generalized overall air leakage values for school buildings

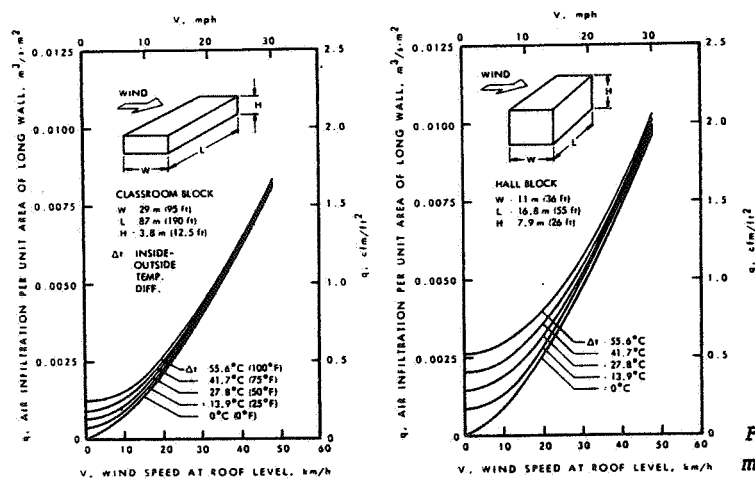


Fig. 8 Air infiltration rate of a model school of average air tightness

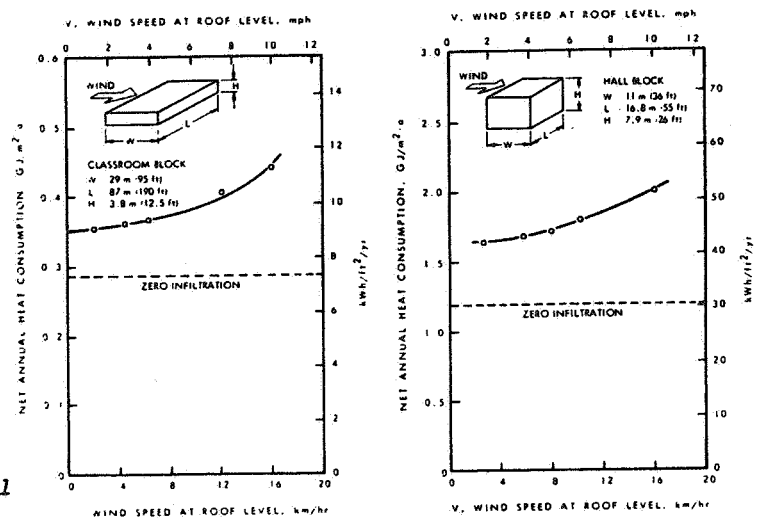


Fig. 9 Net heating load of a model school with average air tightness

School Model

Size	Over-all area 1800 m^3 ($20,000 \text{ ft}^2$) Dimensions: Classroom Block $87 \text{ m} \times 29 \text{ m}$ ($190 \text{ ft} \times 95 \text{ ft}$), 2.74 m (9 ft) floor to ceiling, 3.8 m (12.5 ft) over-all height Hall $16.8 \text{ m} \times 11 \text{ m}$ ($55 \text{ ft} \times 36 \text{ ft}$), 6.4 m (21 ft) floor to ceiling, 7.9 m (26 ft) over-all height
Orientation	Major axis runs SW to NE
Construction	Over-all Transmittances: Wall $1.28 \text{ W/m}^2 \text{ K}$ ($0.225 \text{ Btu/h ft}^2 \text{ F}$) Roof $0.34 \text{ W/m}^2 \text{ K}$ ($0.06 \text{ Btu/h ft}^2 \text{ F}$) Glazing: Class - 25% of external wall (as viewed from inside), double-glazed with internal blind Hall - unglazed "Medium Weight Construction"
Environmental Condition	Temperature: Class - 22.2°C (72°F) Hall - 20°C (68°F) 5.5°C (10°F) set-back during unoccupied period Ventilation: $2.36 \text{ (dm)}^3/\text{s}$ person (5 cfm) equivalent to: Class - $0.0072 \text{ (dm)}^3/\text{s m}^2$ (0.085 cfm/ft^2) Hall - $0.0211 \text{ (dm)}^3/\text{s m}^2$ (0.25 cfm/ft^2) Lighting: Electrical load: class - 12 W/m^2 (1.12 W/ft^2) hall - 19 W/m^2 (1.77 W/ft^2)
HVAC System	Class - terminal re-heat with scheduled supply air temperature Hall - constant volume variable temperature No mechanical cooling
Operation	School assumed to be used through an academic year for normal school use plus evening school. Plant operated 6 a.m. to 10 p.m. weekdays; lighting and occupancy rates reduced by ~50% in the evenings.

DISCUSSION

JAMES E. WOODS, Assoc. Prof., Iowa State Univ., Ames, IA: You have reported that infiltration may account for about 30% of the annual energy consumption, based on your computer modelling. Have you verified these results with actual annual fuel data (energy consumption)? What was the actual fuel consumption (annual)?

L. JONES, C.Y. SHAW: No, we have not been able to verify our computer calculations with field data. We doubt very much if such verification can be made.

DAVID T. HARRJE, Sr. Resch. Engr., Princenton Univ., Princeton, NJ: Since these tests in schools covered a wide range of construction and ventilation systems, was there any attempt to use tracer gas to evaluate relative contributions?

JONES, SHAW: No. However, we hope to be able to use a tracer gas technique to measure the air infiltration rate for schools in the future.

WILLIAM RUDROY, Prof., Univ. of Pittsburgh, Dept. of Mech. Engr., Pittsburgh, PA: Would you comment on the comparable infiltration when individual unit ventilators are used in each classroom compared to a central HVAC system.

JONES, SHAW: Based on the results presented in the paper, we could find no meaningful relationship between air leakage and HVAC systems.

MARTIN ALTSCHUL, Energy Conservation Eng., University of Virginia, Charlottesville, VA: Since you found no correlation between air leakage and window area, were you able to correlate the infiltration to other factors (i.e., type of construction, building age, type of HVAC system)?

JONES, SHAW: No, we were not able to discern any definite correlations.

CLAYTON A. MORRISON, Assoc. Prof., Univ. of Florida, Mech. Eng. Dept., Gainesville, FL: Please use English units as an alternative so that practicing engineers will readily have a feel for what you wish to communicate.

JONES, SHAW: Both SI and Engineering Units were used in the paper.

G.H. GREEN, Prof. of Mech. Eng., Univ. of Saskatchewan, Saskatoon, Sask., Canada: Can you clarify how you distinguished between energy losses due to infiltration and those due to mechanical ventilation in your yearly studies of energy consumption?

JONES, SHAW: Ventilation and infiltration rates for the calculation of energy consumption are entered as separate values in the Meriwether Program--hence, by calculating energy consumption first with an infiltration rate as described and then with zero infiltration, we were able to say that infiltration was responsible for about 29% of the heating consumption for the example quoted.

GREEN: Where there have been reductions in the quantity of ventilation air in schools (i.e., the Carlton School Board), the reduction in energy consumption in buildings has been about 30% or more. Could you comment on this?

JONES, SHAW: Reduction in energy consumption will undoubtedly accompany lower ventilation rates, although the percentage savings will obviously vary from building to building.

PAPER 13

**METHODS FOR CONDUCTING SMALL-
SCALE PRESSURIZATION TESTS AND
AIR LEAKAGE DATA OF MULTI-
STOREY APARTMENT BUILDINGS**

C. Y. SHAW

**National Research Council
Ottawa
Canada**

(Paper reproduced by kind permission of ASHRAE)

METHODS FOR CONDUCTING SMALL-SCALE PRESSURIZATION TESTS AND AIR LEAKAGE DATA OF MULTI-STOREY APARTMENT BUILDINGS

DR. C.Y. SHAW, P.Eng.

ABSTRACT

An experimental study has been made to develop methods for conducting small-scale pressurization tests to determine the air leakage characteristic of multi-storey apartment buildings where a full-scale air leakage measurement cannot always be performed. These methods require the use of a portable fan for developing a suction or pressure inside a test chamber which is sealed around the perimeter of a test area such as the exterior wall of a room or a window. To minimize the lateral air leakage due to air movement in the cavities of a wall construction, the pressure in the test chamber is balanced with those in the surrounding rooms.

Applying these methods, the air leakage rates through the exterior walls were measured in five buildings ranging from 5 to 20 storeys high. Air leakage rates through major leakage sources were also measured in selected buildings to determine their contribution to the total leakage of wall assemblies. In addition, the overall air leakage rate was measured in a 5-storey building with the entrance door to each apartment unit open and closed to investigate the influence of corridor walls on the overall building air leakage characteristic.

INTRODUCTION

High-rise apartments represent a large group of buildings whose heating demands make up a major part of their annual energy consumption and where substantial savings can be achieved by applying appropriate energy conservation measures. Without exception, however, a major problem encountered in evaluating various conservation measures is the lack of air leakage characteristics of these buildings for heating load prediction. Therefore, the Division of Building Research, National Research Council of Canada, initiated a program in the spring of 1978 to conduct air leakage measurements for this type of building. The results are presented in this paper.

A high-rise apartment is different from other types of tall buildings in that it is divided into small units connected by a common corridor on each floor, and it is normally serviced by a common ventilation system for supply of fresh air into the corridors and exhaust air from each unit. Owing to the limited capacity of the ventilation system and the large building volume, the usual pressurization method for measuring the overall air leakage rate cannot be applied. Thus, there is a need for methods that can be applied to measure the air leakage rate through part of a building shell, such as the exterior wall of a room or a window. Field studies were conducted to develop such methods and, applying these methods, air leakage data for five apartment buildings (see Table 1) were obtained. In addition, the overall air leakage rate of a 5-storey building was measured using a large fan mounted on a trailer.

TEST METHOD

Fig. 1(a) shows the experimental set-up for measuring the air leakage rate through an entire wall assembly of a room (Direct Method). As shown, a portable fan with a maximum capacity of 200 l/s at 2000 Pa (424 cfm at 8 in. of water) was used for this purpose. The fan intake was

C.Y. Shaw, Research Officer, Energy and Services Section, Division of Building Research, National Research Council of Canada, Ottawa, Ontario K1A 0R6.

connected to an airtight test chamber by a duct of about 3 m (9.8 ft) in length and 0.2 m (8 in.) in diameter. The test chamber was made of plywood panels covered with polyethylene sheets and was sealed around the perimeter of the test wall with tapes. To facilitate sealing the top, the test chamber was slanted towards the wall.

The air flow rates of the fan were adjusted with a manual damper and measured with a laminar flow element (MERIAM LFE ELEMENT; accuracy of 5% of measured values). The pressure difference across the middle of the wall was measured with a diaphragm-type pressure transducer (static error band of 5% full scale) and a digital voltmeter. The pressures in the test chamber and the adjacent rooms were balanced with fans (Fig. 1(b)) to minimize the flow of leakage air through the four boundaries of the test area into the test chamber. The flows through these balancing fans were also controlled by individual manual dampers. As shown in Fig. 1(b), a minimum of four balancing fans were required for wall air leakage tests.

The air leakage rate through a wall assembly can also be obtained by measuring the air leakage rate through each component that makes up a wall. For an apartment building, they are usually windows, balcony doors, window sills, and floor-wall joints. Two methods, Direct and Indirect, can be used either independently or jointly for the purpose. Fig. 2 shows the arrangement required to apply the Direct Method. They are very similar to the one for walls, except for the size of the test chamber and the requirement for pressure balancing. It was found that a heavy-duty shop vacuum cleaner would have enough capacity to meet the flow requirements and also to produce the head required by the laminar flow element. Except for balcony doors and windows, the pressure in the test chamber and that in the test room should be properly balanced with a portable fan to minimize lateral air leakage. The experimental set-up for the Indirect Method is identical to that shown in Fig. 1(a). The air leakage rate through one particular component is obtained by comparing the flow rates measured before and after it is sealed.

In addition, an overall air leakage test was conducted on Building A using the method developed for schools¹. The fan used was a vane axial type with variable pitch blades that can be adjusted manually to obtain flow rates between 0 and 23 600 l/s (0 and 50 000 cfm). The fan intake was connected by a duct of about 15 m (49.2 ft) in length and 0.92 m (3 ft) in diameter to an entrance where the door was replaced by a plywood panel. All inside stair doors were kept open during the tests to allow a free flow of air from the floor spaces to the fan.¹ Air flow rates were measured upstream of the fan intake using total pressure averaging tubes.¹ The pressure differences across the four exterior walls were measured at the middle of each wall at three levels using the same pressure transducer.

Most tests were conducted under the suction condition. For comparison, some components were tested both under suction and pressurization. To minimize wind influence on pressure measurements, all tests were conducted when the meteorological wind speed was lower than 15 km/h (9.3 mph)².

VALIDATION OF TEST METHOD

A series of validation tests was conducted to verify the test methods and to demonstrate the necessity of pressure balancing. The result of validation tests for the Direct Method for measuring wall air leakage is shown in Fig. 3. It indicates that the air leakage values of the wall assembly of Building C obtained by the Direct Method is within 5% of that obtained by summing the independently measured air leakage values of the floor-wall joint, window and window sill of the same wall. Likewise, as shown in Fig. 4, an agreement in results within 15% was also obtained for validation tests on floor-wall joints and window sills.

In conducting the air leakage test, the pressure in the test chamber was balanced either with that in the adjacent rooms or with that in the test room by adjusting the air flow rate of the balancing fan. It was found that even with a manual damper, these pressures could be balanced within ± 2.5 Pa (0.01 in. of water) without difficulty.

The effect of pressure balancing is illustrated in Fig. 4 showing the air leakage rates through both the window sill and the floor-wall joint. It indicates that a substantial reduction in the air leakage rate resulted from pressure balancing which reduced the lateral air leakage into the test chamber via the cavities in the wall. This hypothesis is at least partially supported by the fact that the air leakage rate obtained with pressure balancing is within 15% of that by the Indirect Method (Fig. 4). The effect of pressure balancing was further investigated by conducting air leakage tests on the floor-wall joint of Building M where the air leakage rate through the carpet could be eliminated. Fig. 5, which gives the results of four tests, indicates that when the pressures were balanced, identical air leakage rates were

obtained before and after removing the carpet (Curves 1 and 2). If, however, the pressures were not balanced, an increase in the air leakage rate was observed, the amount of increment depending on whether the carpet was removed from the floor (Curves 3 and 4). The differences between Curves 4 and 3, and between Curves 3 and 2 are approximately the air leakage rates through the carpet and other sources (e.g., window sill as indicated by the heavy dotted line).

Finally, the effect of pressure balancing between test chamber and adjacent rooms is illustrated in Fig. 6. The results indicate that the air leakage through a wall assembly measured without pressure balancing brings about an increase in flow up to 73% (Building T) of that with pressure balancing. An inspection of the test rooms indicated that Buildings T and M were the only two whose partition walls were penetrated by heating pipes. Since these walls were used as the two side panels of the test chamber in these tests, the openings around the heating pipes of Building T, which could not be properly sealed, were mainly responsible for the large increase in the air leakage rates.

RESULTS AND DISCUSSIONS

Applying the developed test methods, air leakage rates through wall assemblies were measured in five apartment buildings. Except for Buildings A, M and T, the exterior walls of two rooms of each building were tested for air tightness. The air leakage characteristics of windows of the five buildings and those of the sliding glass balcony doors of one additional building (Building W) were also studied. Also, the overall air leakage rate of the entire building was measured in Building A with the entrance door to each apartment unit open and closed. These results were analyzed and presented for opaque walls consisting of window sills and floor-wall joints, the sliding glass balcony doors, and windows including window frame-wall joints. Fig. 7 shows the air leakage data of the opaque walls. Their values vary not only from building to building with similar wall design (e.g., Buildings C and V), but also vary from room to room in the same building. Also shown in this figure is the air leakage characteristics of a 33-cm (13-in.) unplastered brick wall obtained from the ASHRAE Handbook of Fundamentals³. It indicates that, except for Building M, the air leakage values of the opaque walls of the test buildings are within $\pm 50\%$ of that of the unplastered brick wall.

The air leakage rates through the four types of windows are shown in Fig. 8(a) and 8(b). In this paper, the air leakage through a window frame-wall joint is credited to the window instead of the wall. The reasons are twofold: firstly, it will considerably reduce the work in field testing and secondly, it is more appropriate to do so in modeling air leakage characteristics of buildings. Air leakage values of windows as shown in Fig. 8(a) and 8(b) vary widely from building to building. Even in the same building these values can be different by a factor of 2. There is no clear evidence to indicate that one window design gives a tighter window than another. Nor is there any correlation between air leakage characteristics and ratio of openable area to total window area (e.g., Building T with fully openable windows has a lower leakage rate than Building A, which has partially openable windows).

ASHRAE Standard 90-75 on energy conservation in new building design⁴ recommends that the maximum air leakage rate through windows should be $0.77 \text{ l/s}\cdot\text{m}$ at 75 Pa (0.5 cfm/ft at 0.3 in. of water). This value does not include the air leakage through a window frame-wall joint whereas the measured values in our study did include this leakage. Even so, one-third of the 17 test window units (including window frame-wall joints) had air leakage values below the suggested limit, suggesting that it is possible to design, manufacture, and install windows to meet the leakage specification of the Standard.

Tests were also conducted on three buildings to investigate the difference in air leakage characteristics under suction and pressurization. It was found that for floor-wall joints, there was no appreciable difference in the test results whereas for windows, the air tightness value obtained under one condition was, at most, 12% higher or lower than the other.

Fig. 9 shows the air leakage rates of the eight residential-type sliding glass doors (excluding frame-wall leakage²). As shown, there are 6 out of 8 doors whose air tightness values are lower than the $2.5 \text{ l/s}\cdot\text{m}^2$ at 75 Pa (0.5 cfm/ft^2 at 0.3 in. of water) maximum recommended by ASHRAE Standard 90-75. All these doors are double doors with the outer door acting as a storm door. Hence, tests were also conducted with the outer door open to study the effect of the storm door. The results indicate that with both doors closed, a reduction in the air leakage rate (ranging from 15% to 32%) was obtained.

The contribution of major building components to the total air leakage rate of wall assemblies was studied in selected buildings. Fig. 10 shows that at a pressure difference of 75 Pa (0.3 in. of water), windows including window frame-wall joints can be the main contributing

component which may account for as high as 70% of the total leakage. Next are floor-wall joints and window sills which can account for 50% and 30% of the total air leakage respectively. The air leakage rate of the ceiling joint was measured in one building (Building M) as this is the only building having smoothly plastered ceilings. As shown, there was no measurable air leakage through the ceiling joint of this building.

Finally, the overall air leakage rate was measured in Building A with the entrance door to each apartment unit open and then closed. As shown in Fig. 11, there is no appreciable difference in the overall air leakage rate whether the door is open or closed. Fig. 11 also shows that the overall air leakage characteristics of Building A are similar to the average air leakage values of the 7 tall office buildings, all having open floor arrangements².

CONCLUSIONS

Air leakage characteristics of the exterior walls of multi-storey apartment buildings can be obtained by conducting small-scale pressurization tests using the methods outlined in this paper. These methods were validated by comparing the overall leakage values and the sum of the independently obtained component leakage values.

It was found that air leakage rates through opaque walls were similar to those of a 33-cm (13-in.) unplastered brick wall obtained from laboratory tests. It was also found that one-third of the 17 windows tested as installed met the 0.77 l/s·m of sash crack at 75 Pa (0.5 cfm/ft at 0.3 in. of water) maximum value recommended by ASHRAE Standard 90-75. The air leakage data of the 8 balcony doors tested as installed indicated that three-quarters of them also met the requirement of the 2.5 l/s·m² at 75 Pa (0.5 cfm/ft² at 0.3 in. of water) maximum air leakage rate recommended by the same Standard.

Air leakage rates through various building components were measured in selected buildings. The results indicated that floor-wall joints, windows, and window sills are the three major air leakage sources in exterior walls. The results obtained from one building indicated that there is no measurable leakage through ceiling joints.

Opening or closing the entrance door to each apartment unit was found to have no effect on the air tightness values of Building A. This finding suggests that the air leakage rates of apartment buildings are mainly governed by the resistance of the exterior walls. Further studies are required in this area.

REFERENCES

1. Shaw, C.Y. and Jones, L., "Air Tightness and Air Infiltration of School Buildings," ASHRAE Transactions 1979, Vol. 85, Pt. 1.
2. Tamura, G.T. and Shaw, C.Y., "Studies on Exterior Wall Air Tightness and Air Infiltration of Tall Buildings," ASHRAE Transactions 1976, Vol. 82, Pt. 1, p. 122-134.
3. ASHRAE HANDBOOK of Fundamentals, Table 3, Chap. 21, 1977, ASHRAE, Inc., N.Y.
4. ASHRAE Standard 90-75, "Energy Conservation in New Building Design," 1975, ASHRAE, Inc., N.Y.

ACKNOWLEDGEMENTS

The author is indebted to A. Zdanowicz of the Ontario Housing Corporation, F. Monopoli and W. Forrester of the University of Ottawa, and the Board of Directors of the Ambleside I for granting permission to conduct the tests, and to the managers of the test buildings for their assistance during the tests. The author wishes to thank Dr. D.G. Stephenson and G.T. Tamura for their valuable comments during the review of this paper. The author also wishes to acknowledge the assistance of R.G. Evans and Miss R. Plouffe in the field tests.

This paper is a contribution of the Division of Building Research, National Research Council of Canada and is published with the approval of the Director of the Division.

TABLE 1 Description of Test Buildings

Building	A	C	M	T	V
Year Constructed	1978	1978	1965	1972	1978
Year Tested	1978	1978	1978	1978	1978
Height (Storeys)	5	10	20	15	12
Dimensions of Test Wall Assembly m (ft.)	3.14 W x 2.44 H (10.3 x 8.0)	3.05 W x 2.44 H (10.0 x 8.0)	1.88 W x 2.41 H (6.17 x 7.92)	4.34 W x 2.48 H (14.25 x 8.13)	3.02 W x 2.41 H (9.92 x 7.92)
Dimensions of Test Window m (ft.)	1.52 W x 1.22 H (5.0 x 4.0)	1.62 W x 1.62 H (5.33 x 5.33)	0.91 W x 1.42 H (2.98 x 4.67)	3.94 W x 1.37 H (12.92 x 4.5)	1.93 W x 1.57 H (6.33 x 5.15)
Window Type	Fixed and Openable; Sealed Double Glazing	Fixed and Openable; Sealed Double Glazing	Openable; Sealed Double Glazing	Openable; Sealed Double Glazing	Fixed and Openable; Sealed Double Glazing
Openable/ Total Window Area	50%	38%	100%	100%	63%
Wall Construction	10.2 Cm (4 in.) Clay Brick, 15.3 Cm (6 in.) Conc. Block, Parging, Bldg. Paper, 8.9 Cm (3.5 in.) Batt Insulation, Vapour Barrier, Gypsum Board	22.9 Cm (9 in.) Conc. Brick, 5.1 Cm (2 in.) Rigid Insulation, Dry Wall	Outer Shell: 15.3 Cm (6 in.) Clay Brick - for main wall; or 10.2 Cm (4 in.) P/C panel - for wall below window Inner Shell: Parging, Bldg. Paper 5.1 Cm (2 in.) Batt Insulation, Vapour Barrier, Plaster	15.3 Cm (6 in.) Pre-poured Conc. Spandrel Panel, 5.1 Cm (2 in.) Insulation, Vapour Barrier, Dry Wall	10.2 Cm (4 in.) Face Brick, 10.2 Cm (4 in.) Conc. Block, Parging, 6.4 Cm (2.5 in.) Rigid Insulation, Gypsum Board

Note: Bldg. W is not included as it was tested for balcony door only

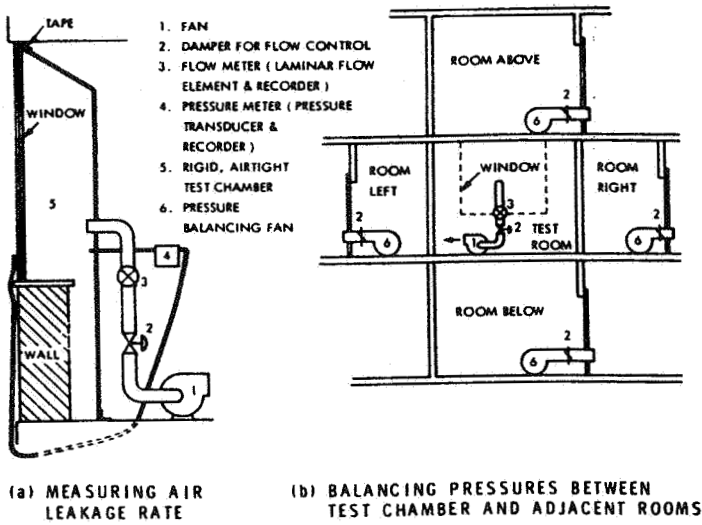


Fig. 1 Experimental set-up for measuring air leakage rate through wall assembly

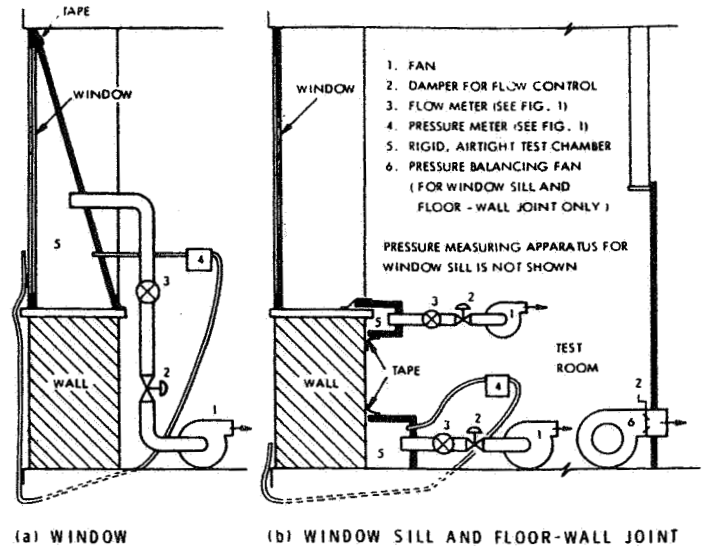


Fig. 2 Experimental set-up for air leakage rate through building components

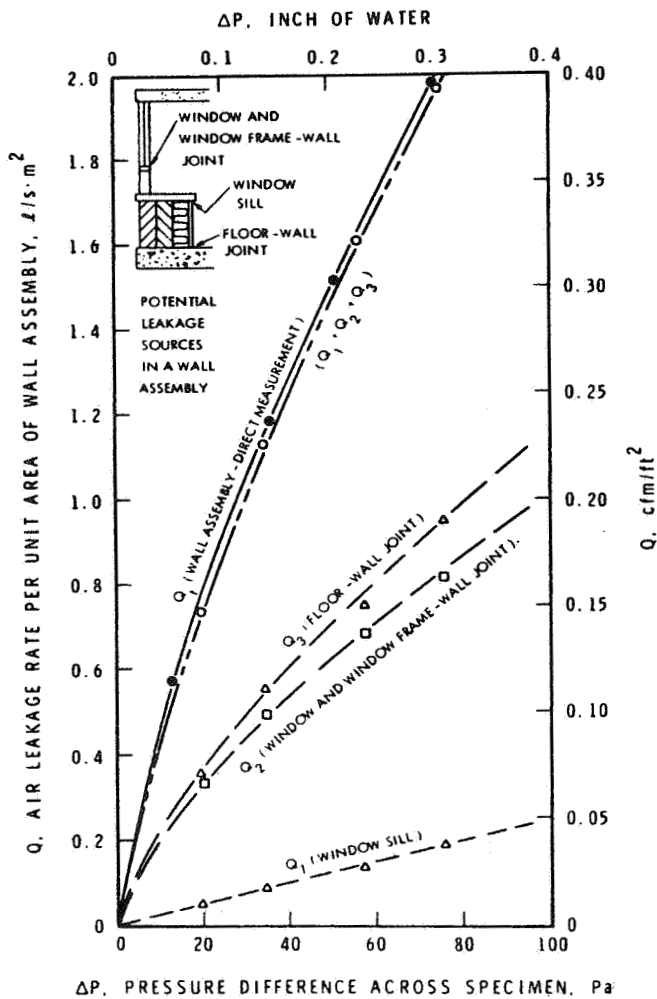


Fig. 3 Comparison of air leakage rates through wall assembly of Building C obtained by direct measurement and measurements of building components

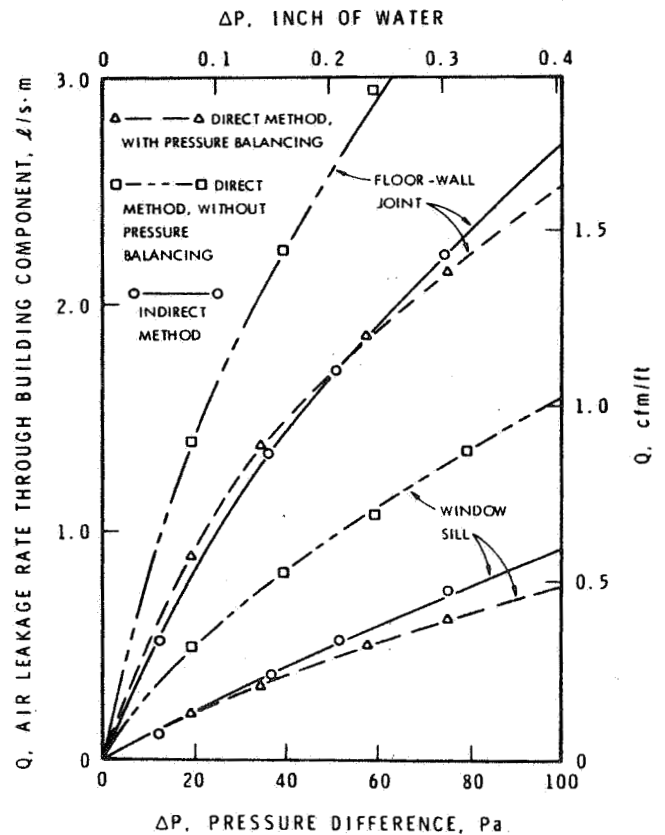


Fig. 4 Comparison of air leakage rates through window sill and floor-wall joint of Building C obtained by Direct and Indirect Methods

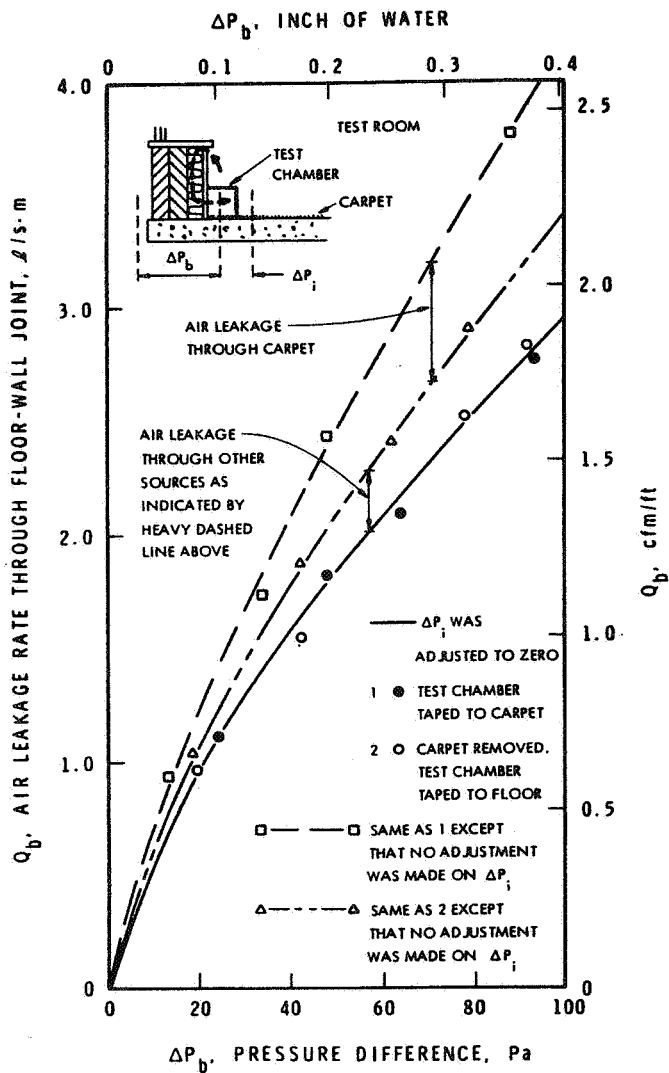


Fig. 5 Effect of pressure balancing on air leakage rates

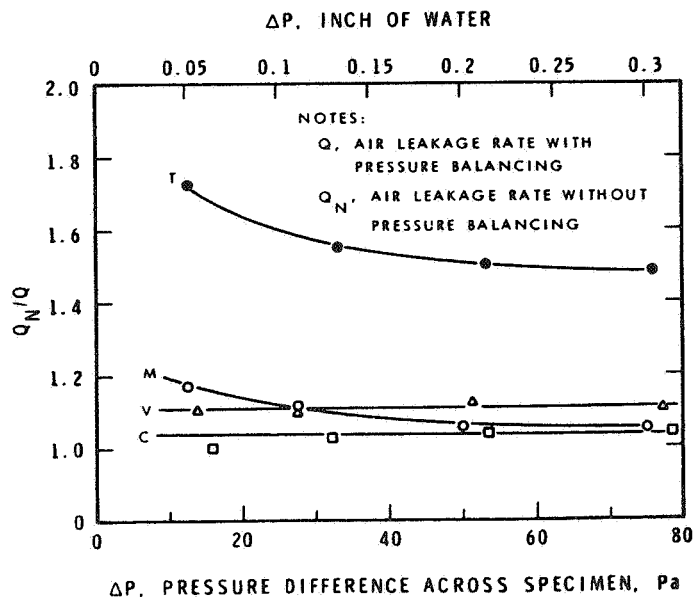


Fig. 6 Effect on air leakage rates with and without pressure balancing

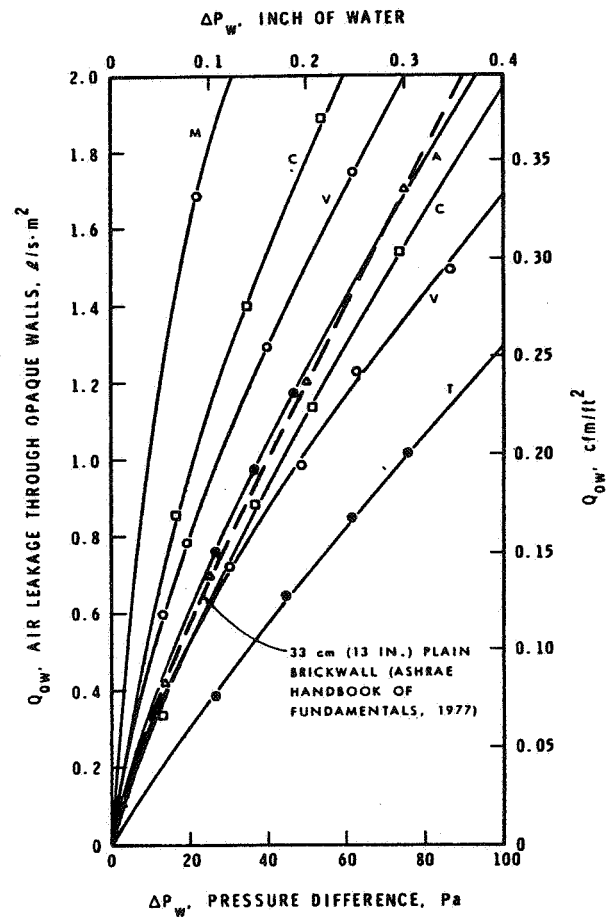


Fig. 7 Air leakage rates through exterior walls excluding windows and doors

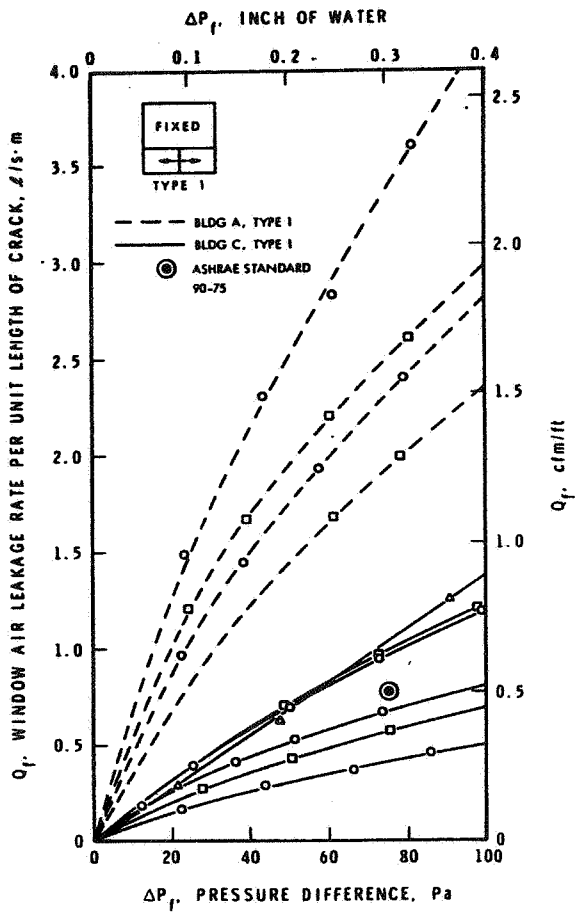


Fig. 8(a) Air leakage rates through windows including window frame-wall joints (Buildings A and C)

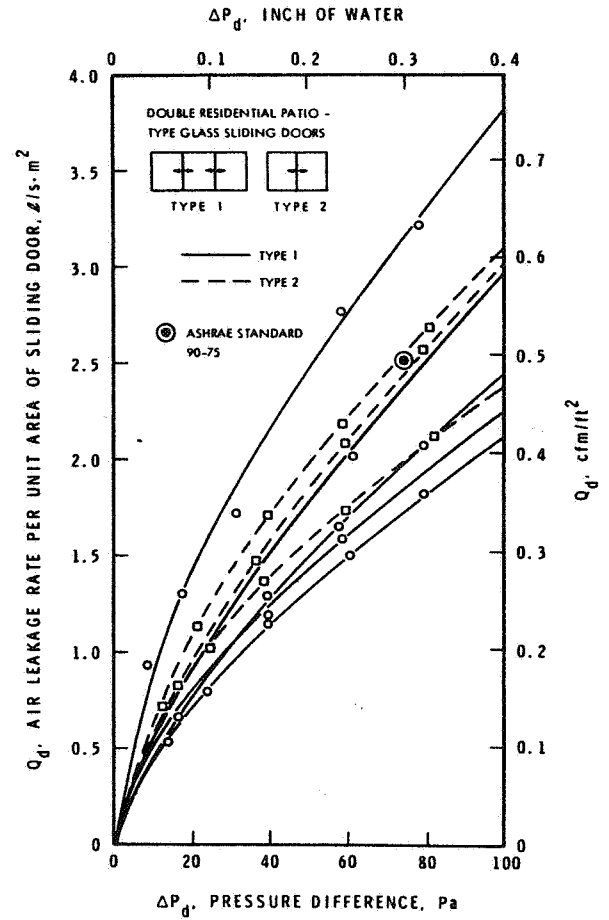


Fig. 9 Air leakage rates through balcony sliding doors

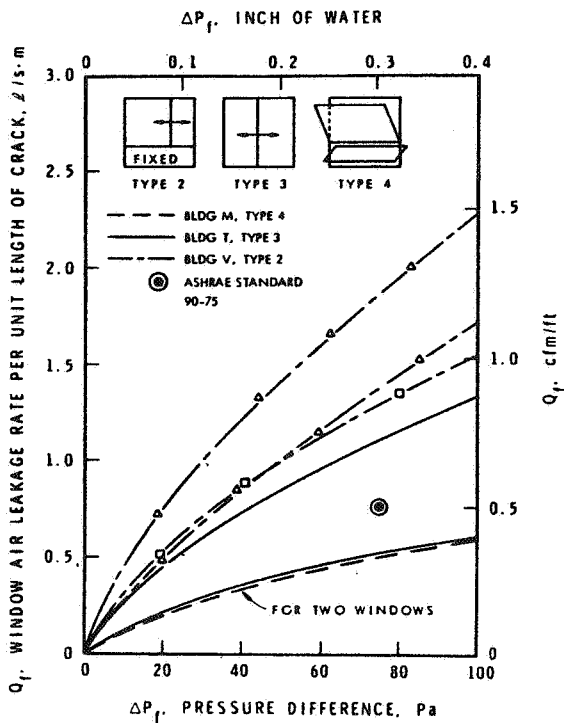


Fig. 8(b) Air leakage rates through windows including window frame-wall joints (Buildings M, T and V)

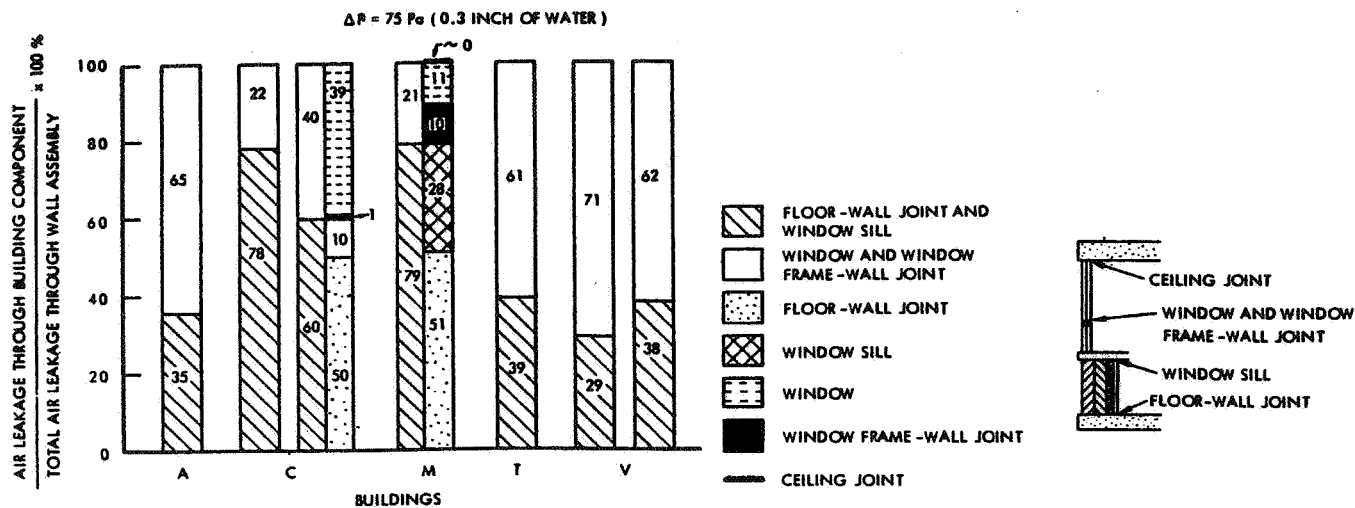


Fig. 10 Contribution of various building components to total air leakage rate

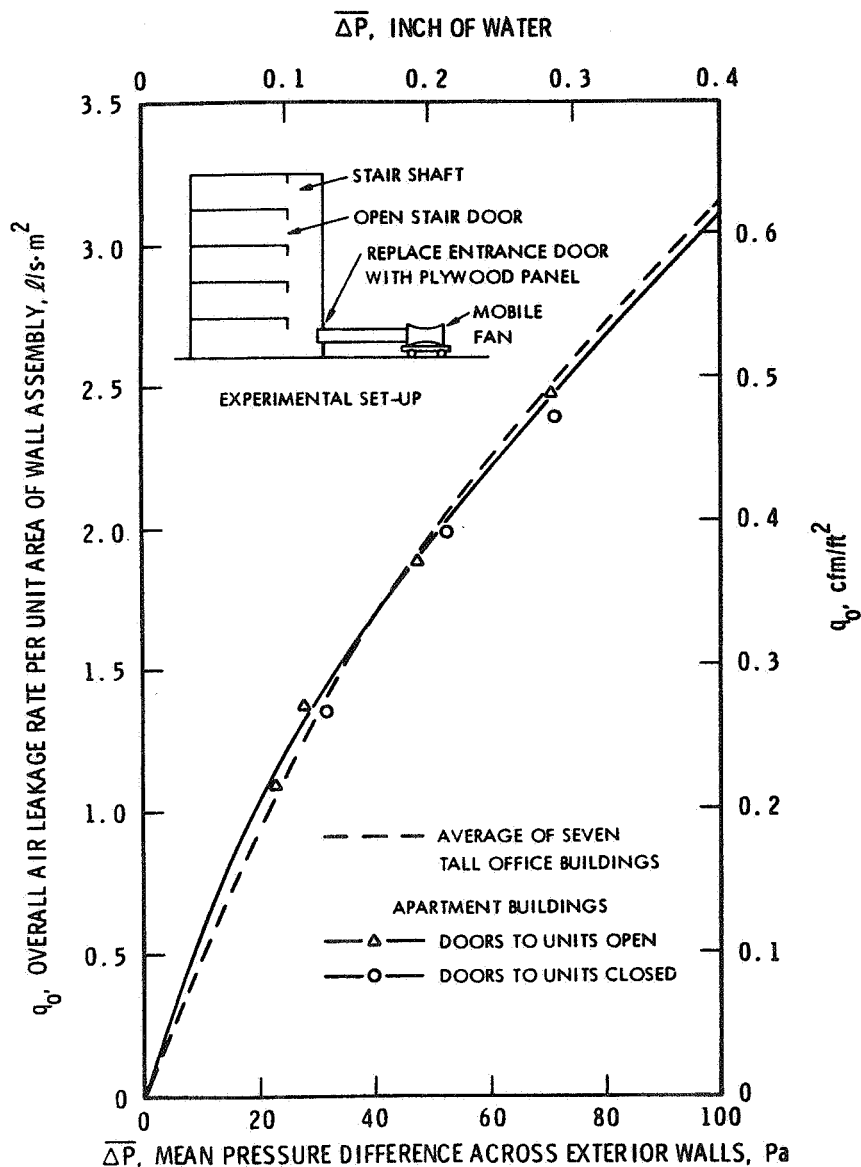


Fig. 11 Overall air leakage rates per unit area of wall assembly of Building A

PAPER 14

**CORRELATING PRESSURIZATION
AND INFILTRATION RATE DATA —
TESTS OF AN HEURISTIC MODEL**

J. KRONVALL

**Lund Institute of Technology
Sweden**

CORRELATING PRESSURIZATION AND INFILTRATION RATE DATA - TESTS OF AN HEURISTIC MODEL.

J Kronvall, Lund Institute of Technology, Div of Building Technology,
Lund, Sweden.

1 BACKGROUND

In many countries we now have some years of experiences of testing houses for airtightness using the pressurization/depressurization technique. The main purpose of the test in most cases has been a performance control of the air tightness of the house. It was expected, however, that in future the test result should give an estimate of the infiltration rate of the building too. For example in a paper from 1978 (1) the author claims that: "To make such a relationship reliable many measurements on different types of houses with both the pressurization- and tracer gas methods must be made and reasonable corrections for the wind- and temperature influence of the tracer gas measurements must be found".

Since then, valuable contributions to the knowledge of these matters have been given, see for example (2), (3)! It is, however, quite obvious that there cannot exist a simple relationship (for example via a coefficient) as the test result from one of the tests is not dependent on the prevailing weather conditions while the other certainly is dependent on them.

2 CALCULATION MODELS

The problem of correlating pressurization data to infiltration data is very complex and almost all the present knowledge of air infiltration and even more should preferably be used. For the treatment of the problem you use measurement results from two most different measurement methods, with a series of measurement and interpretation problems. Furthermore you want to make a mathematical analysis based on these measurements and have to make a number of sometimes quite dubious assumptions.

The building may be considered to be a part of a system which consists of acting forces, an airleaking building and a ventilation system.

Fig 1.

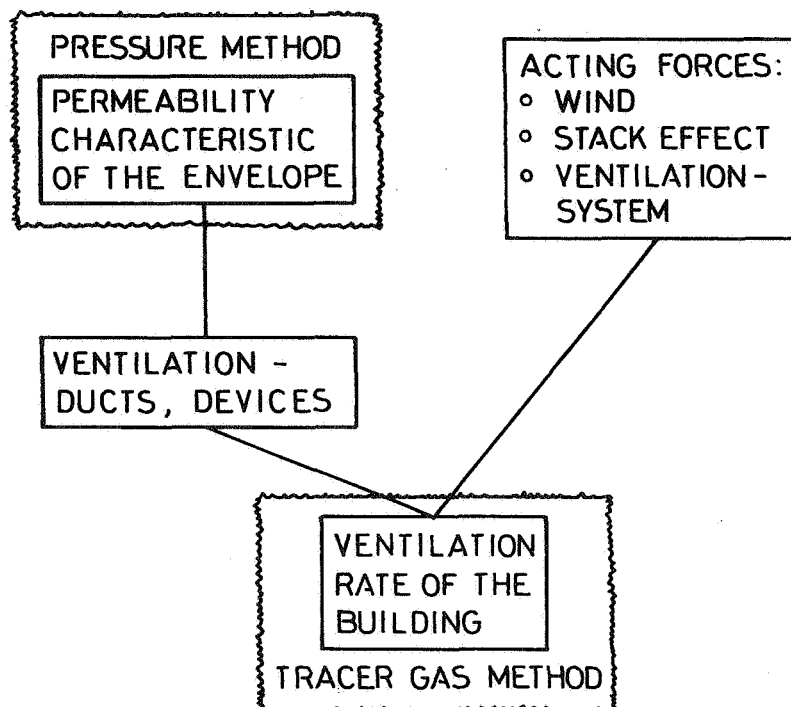


Figure 1.

Two characteristics may be settled by testing - a permeability characteristic of the envelope with the pressurization test and the ventilation rate of the building at the prevailing weather conditions (wind and temperature difference) when the test is carried out.

The test methods themselves introduce errors in a calculation model. Both accuracy and precision of the test methods should be taken into account. These matters have been discussed in (4) where it is stated that the probable error of the pressurization test according to Swedish practice is less than 4% when using electrical manometers and a recorder and 8% when using liquid manometers. The probable error of the tracer gas test depends heavily on the measurement time (decay measurement) but can for reasonable measurement times ($\approx 1,5$ h at a ventilation rate of 0,2 ac/h) be around 5%. The figures given above refer to measurement accuracy only. Matters influencing precision - that is the proba-

bility of obtaining the same measurement value on some other occasion - are not taken into account. For the pressurization test such matters are:

- o weather dependence (limitations are stated in the method description)
- o ageing durability of the tightness behaviour of the envelope.

For the tracer gas test the following factors are influencing the measurement precision:

- o the weather (wind and temperature differences)
- o the degree of "perfect" mixing of the tracer gas
- o the degree of fluctuation of wind speeds.

The last factor in fact initiates the question of the validity of the measurement. Do we in other words measure the quantity we want information about or do we perhaps measure something (quite) different? However, this may be more of interest from the ventilation effectiveness point of view than that of energy aspects.

One way of analysing the problem is to compare a value of the ventilation rate calculated with a calculation model - for example according to (5) - with a measured value. This procedure is outlined in figure 2.

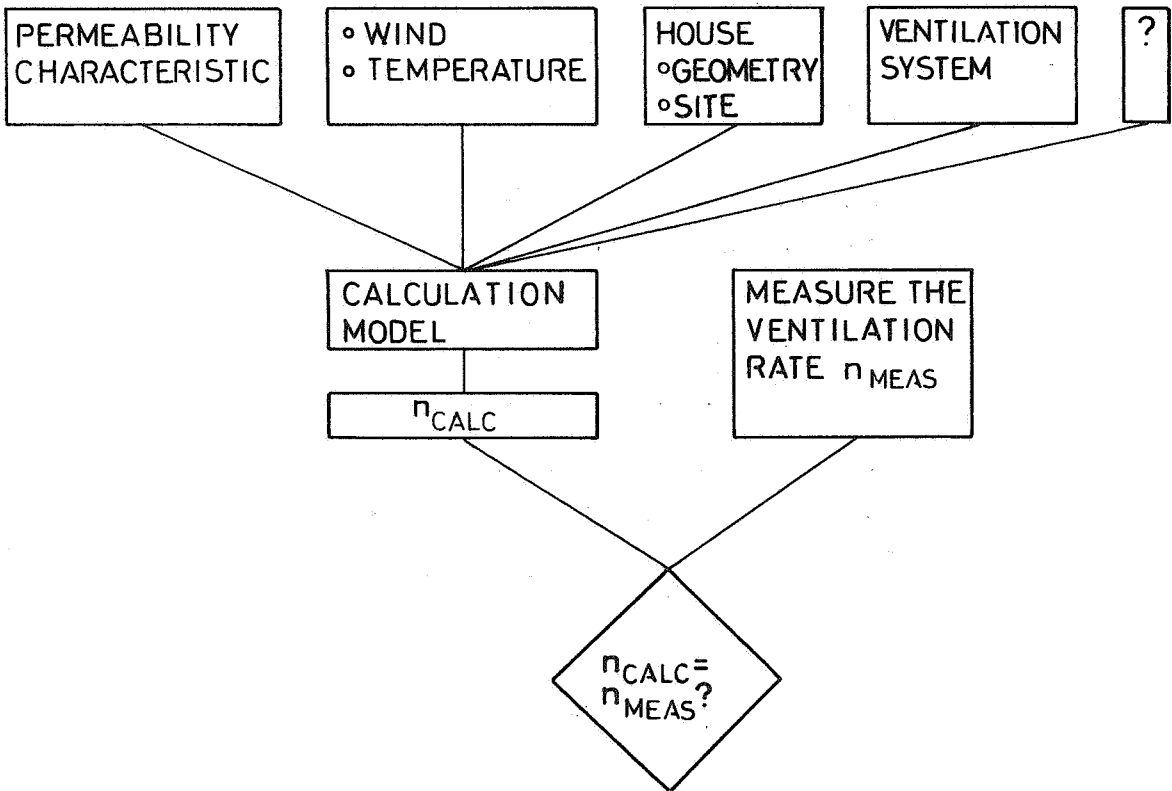


Figure 2. Comparing calculated and measured ventilation rate. Principal sketch.

Such an analysis must be based on detailed knowledge of the input factors.

Doing such a procedure for a number of different houses over and over again should, according to my opinion, teach us a lot of the mechanisms of air infiltration in a most effective way. It should help us to get a feeling for the sensitivity of the system to changes in various input parameters.

Being aware of the difficulties (and costs) of this procedure and in the absence of a fully developed calculation model a more heuristic approach is going to be discussed below. The principle of the method is shown in figure 3.

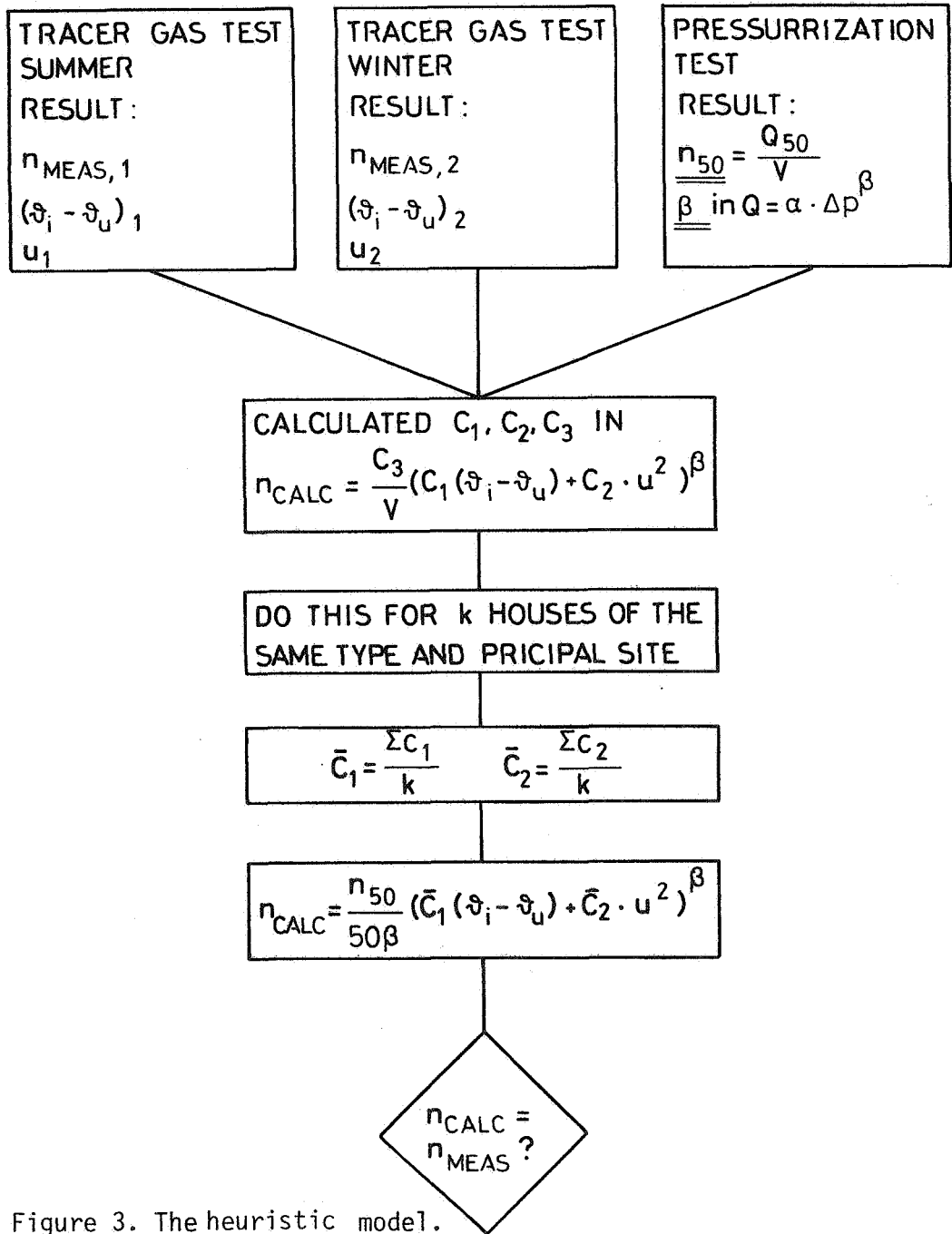


Figure 3. The heuristic model.

In words this means that you start with a pressurization test value and tracer gas test values from two very different weather conditions - preferably summer and winter. Such values should be available for at least some tens of houses of the same type and principal site.

The measured values are "forced" into the model

$$n_{\text{CALC}} = \frac{C_3}{V} (C_1(\vartheta_i - \vartheta_u) + C_2 u^2)^\beta \quad (1)$$

which is based upon

$$Q = \alpha \cdot \Delta p^\beta \quad (2)$$

By identification it is obvious that:

$$Q = n_{\text{CALC}} \cdot V; \text{ the ventilation flow; infiltration or exfiltration} \quad (3)$$

$$\alpha = C_3 \quad \text{a flow coefficient} \quad (4)$$

$$\Delta p = \underbrace{(C_1 (\vartheta_i - \vartheta_u))}_{\text{STACK EFFECT}} + \underbrace{C_2 u^2}_{\text{WIND}} \quad (5)$$

In (1) to (5)

n_{CALC} = calculated air change rate, ac/h

V = building volume, m^3

ϑ_i = indoor temperature, $^{\circ}\text{C}$

ϑ_u = outdoor temperature, $^{\circ}\text{C}$

u = wind velocity at a reference point, m/s

C_1 = model coefficient, Pa/K

C_2 = " , $\text{Pa}/(\text{m/s})^2$

C_3 = " , $(\text{m}^3/\text{h})/\text{Pa}^\beta$

C_3 and β are obtained from the pressurization test:

$$\frac{C_3}{V} = \frac{n_{50}}{50^\beta} \quad (6)$$

where

n_{50} = resulting leakage divided with the volume of the house at pressurization to 50 Pa, ac/h

β = flow exponent in the relationship $Q = \alpha \cdot \Delta p^\beta$ fitted to the measured values.

C_1 and C_2 are solutions to the following equation system where $n_{MEAS,1}$ and $n_{MEAS,2}$ stand for measurement values of the ventilation rate at two occasions.

$$n_{MEAS,1} = \frac{n_{50}}{50^\beta} (C_1 (\vartheta_i - \vartheta_u)_1 + C_2 u_1^2)^\beta \quad (7)$$

$$n_{MEAS,2} = \frac{n_{50}}{50^\beta} (C_1 (\vartheta_i - \vartheta_u)_2 + C_2 u_2^2)^\beta \quad (8)$$

Thus:

$$C_1 = \frac{\frac{n_{MEAS,2} \cdot V}{C_3} \cdot e^{-\beta} - \frac{n_{MEAS,1} \cdot V}{C_3} \cdot e^{-\beta} \cdot u_2^2 / u_1^2}{(\vartheta_i - \vartheta_u)_2 - (\vartheta_i - \vartheta_u)_1 \cdot u_2^2 / u_1^2} \quad (9)$$

$$C_2 = \frac{\frac{n_{MEAS,1} \cdot V}{C_3} \cdot e^{-\beta} - C_1 (\vartheta_i - \vartheta_u)_1}{u_1^2} \quad (10)$$

A number of implicit assumptions have been made above.

For the treatment of data from each house:

To begin, outside the house it is assumed that the wind conditions at a reference height near the house is a representative value for determining the wind pressures acting at it.

The leakage paths of the envelope of the house is assumed to be evenly distributed over the total envelope. The possible error introduced with this assumption may be large but the effect is difficult to predict.

The pressure distribution is assumed to be even all over the envelope which definitely is not the case in reality. The implications of such an assumption are difficult to predict too.

The exponent of the leakage function is set to a constant value for all pressure differences. Some authors have claimed that this is not at all the case (2), (5). Their opinion is that the exponent is close to 1,0 (laminar case) at low and close to 0,5 (turbulent case) at higher pressure differences across the envelope. I do not completely agree with that. It rather seems to be so that high leakage rates are caused by big leaks. The dimensions of these are big enough to create greater turbulent flow or flow with so high velocities that in- and outlet effects become considerable. This effect is demonstrated in figure 4 where a leaky house under pressurization test is modelled. The leaks 1 - 9 represent a variety of possible leaks with different sizes. It is obvious that the duct width has an overwhelming influence on the leakage rate. Once a leak of big dimension is introduced three things happen:

- o The total leakage rate increases strongly.
- o The exponent β of the total flow curve is altered.
- o The value of β - in the total flow curve - does not vary much in different pressure difference regimes.

DESCRIPTION OF FLOW PATHS:

FLOW PATH NUMBER	1	2	3	4	5
LENGTH IN FLOW DIRECTION (m)	0,25	0,225	0,20	0,175	0,15
WIDTH (m)	0,000075	0,0001	0,00025	0,0005	0,00075
LENGTH (m)	70	60	50	40	30
ROUGHNESS (m)	0,0000075	0,00001	0,000025	0,00005	0,000075
FLOW PATH NUMBER	6	7	8	9	
LENGTH IN FLOW DIRECTION (m)	0,125	0,10	0,075	0,05	
WIDTH (m)	0,001	0,0075	0,005	0,01	
LENGTH (m)	20	5	2	1	
ROUGHNESS (m)	0,0001	0,00075	0,0005	0,001	

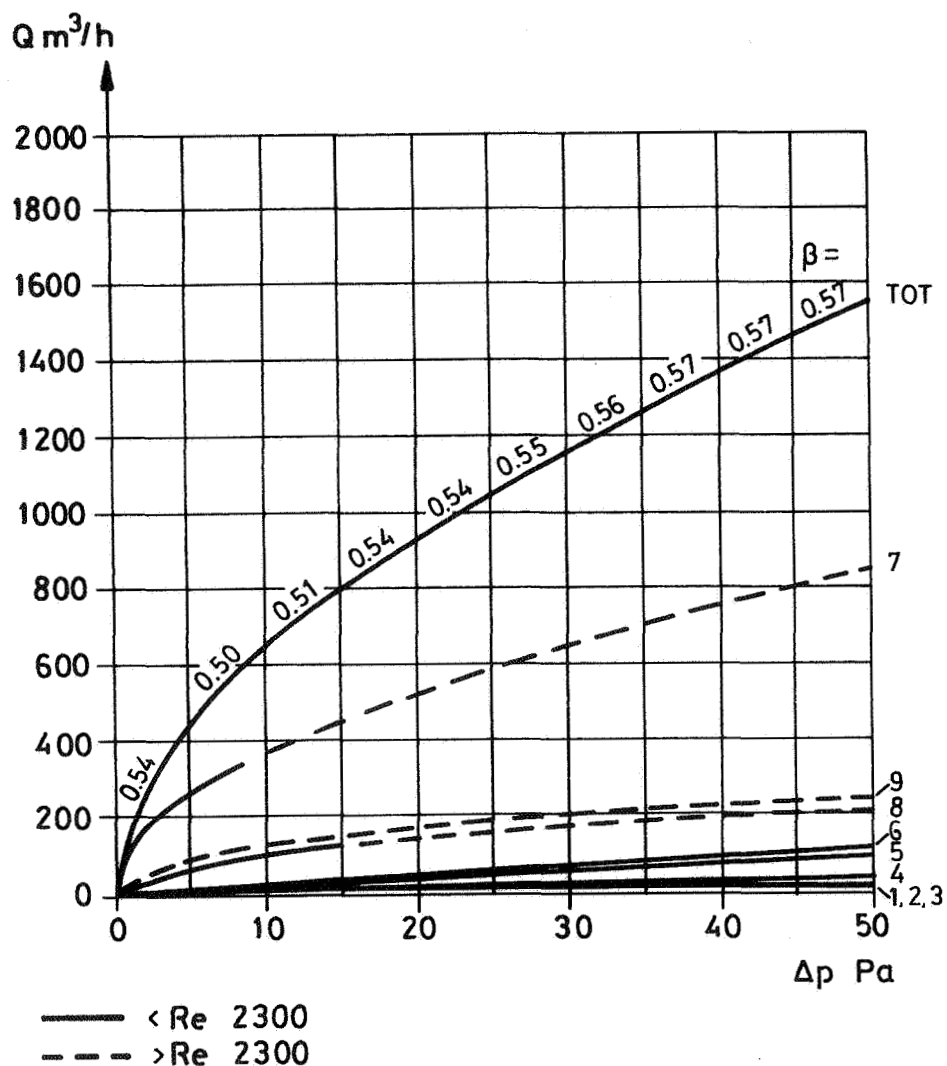


Figure 4.

For the treatment of data from all the houses:

Mean values of C_1 and C_2 from different houses are calculated. To be relevant the resulting formula may not be used for other houses and house sites than the "averaged" ones. This means that it must be one and the same type of houses and the sites may not differ to much from each other.

3 TESTING OF THE HEURISTIC MODEL

The model was tested on 19 $1\frac{1}{2}$ -storey single-family houses. With few exceptions they were built in groups of houses in suburban areas in or

around the city of Gothenburg. The measurements were carried out by the division of Structural Design at Chalmers Institute of Technology (CTH) in Gothenburg (6). The exterior and the lay-out of the houses are shown in figure 5.

The wind velocities were measured at the top of a 10 m high mast placed at an, as far as possible, open place on the windward side of the houses. The pressurization tests were performed according to Swedish practice (4). However, the leakage rate was reported at both 25 Pa and 50 Pa. This made it possible to calculate a flow exponent, β . The tracer gas test were carried out on one summer and one winter occasion. The ventilation rates chosen for this study were the values obtained when devices for ventilation etc were closed. Only the envelope of the house was involved as a leaking component.

The coefficients C_1 , C_2 and C_3 were calculated for each house. The coefficient C_3 - being a leakage coefficient - is individual for each house. The means of C_1 and C_2 from the 19 houses were calculated and this results in the formula:

$$n_{\text{CALC}} = \frac{n_{50}}{50^\beta} (\overline{C_1} (\vartheta_i - \vartheta_u) + \overline{C_2} u^2)^\beta \quad (11)$$

Two cases were studied. The first one implies the use of the wind velocities at the 10 m-level above ground as they are reported. In the second case the wind velocities at 10 m were reduced with 50% and these lower wind-velocities were used.

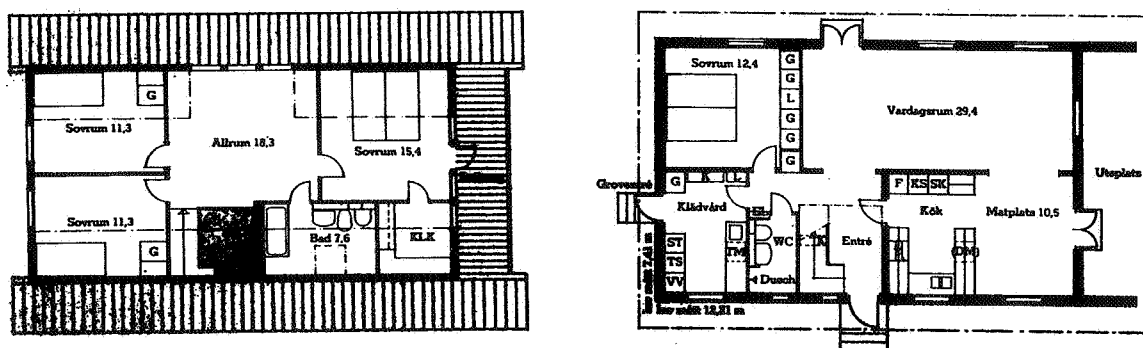
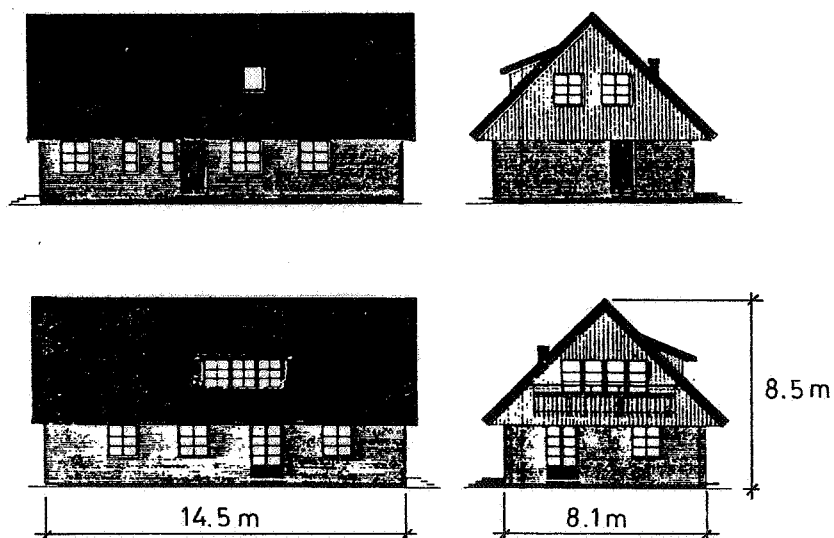


Figure 5. Exterior and lay-out of the houses.

Case 1. No wind reduction

This case resulted in the following expression.

$$n_{\text{CALC}} = \frac{n_{50}}{50^\beta} (0,026 (\vartheta_i - \vartheta_u) + 0,010 u^2)^\beta \quad (12)$$

Plots of the expression for different wind velocities, temperature differences and exponent β -values are shown in figure 6. In this figure n_{50} is chosen to 3 ac/h. n_{CALC} for other n_{50} -values are easily calculated as n_{50} is a single factor in the expression.

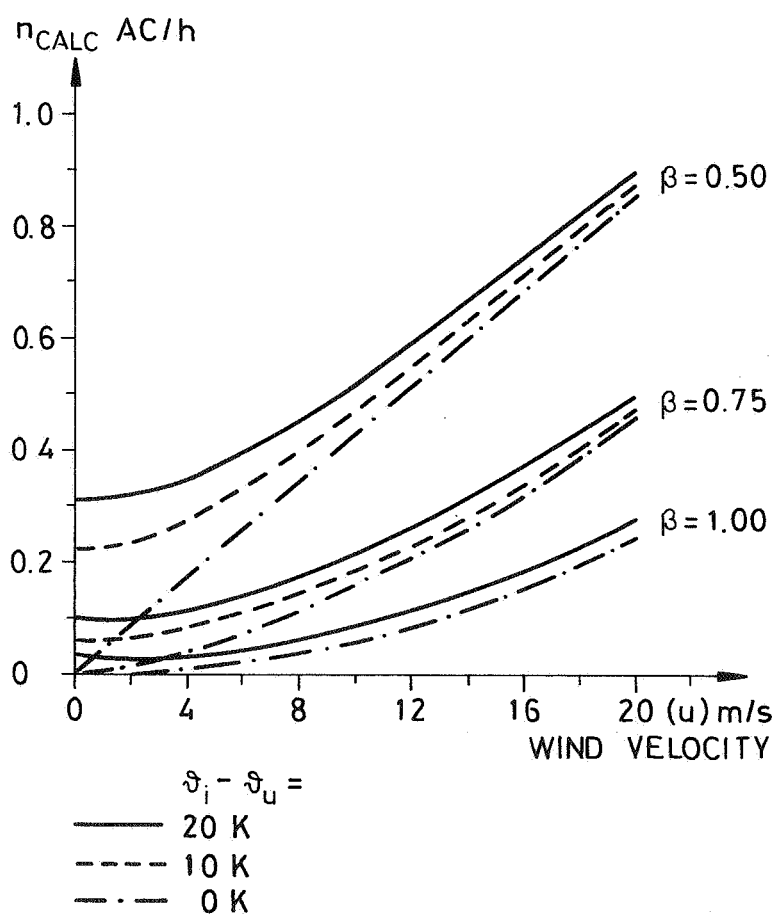


Figure 6. n_{CALC} as a function of wind velocity, temperature difference and exponent β · $n_{50} = 3$ ac/h. No wind reduction.

Case 2. Wind velocities at 10 m reduced with 50%

The resulting expression in this case was:

$$n_{\text{CALC}} = \frac{n_{50}}{50^\beta} (0,026 (\vartheta_i - \vartheta_u) + 0,038 u^2)^\beta \quad (13)$$

Corresponding plots are given in figure 7.

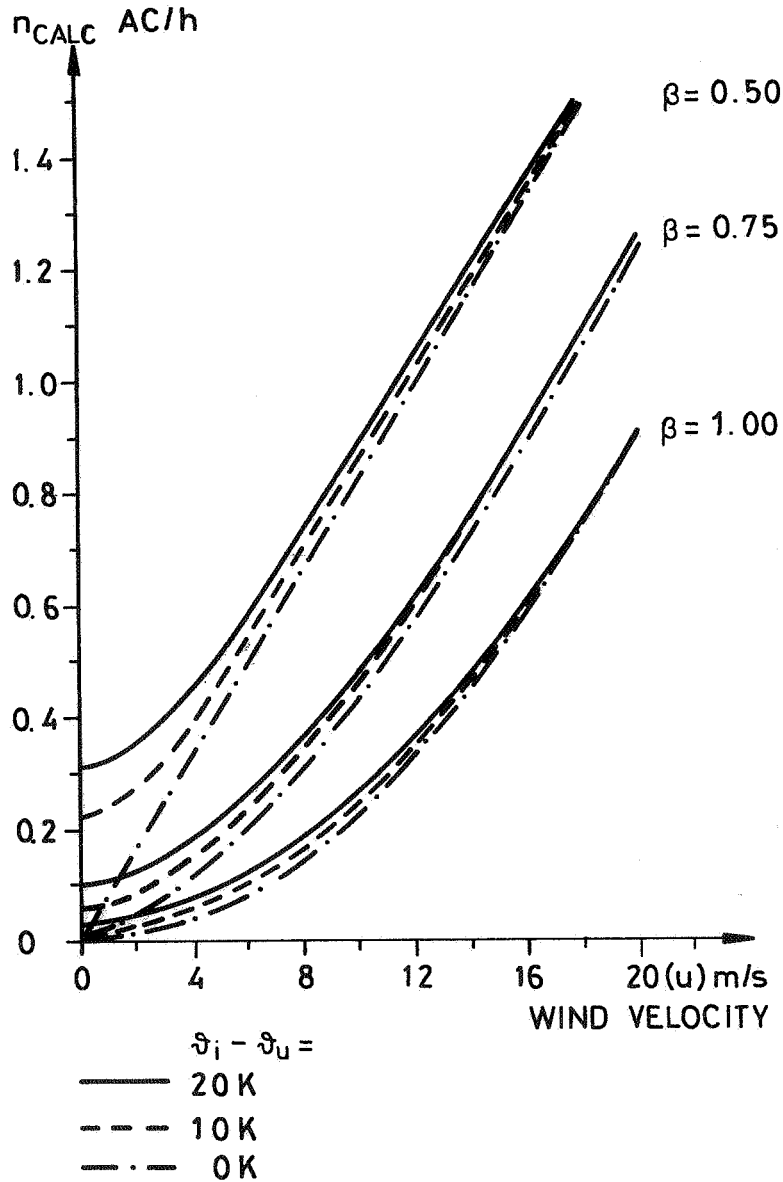


Figure 7. n_{CALC} as a function of wind velocity, temperature difference and exponent β . $n_{50} = 3$ ac/h. Wind velocities at 10 m reduced with 50%.

The calculated ventilation rates, n_{CALC} , were compared with the measured ones, n_{MEAS} . The result can be seen in figure 8.

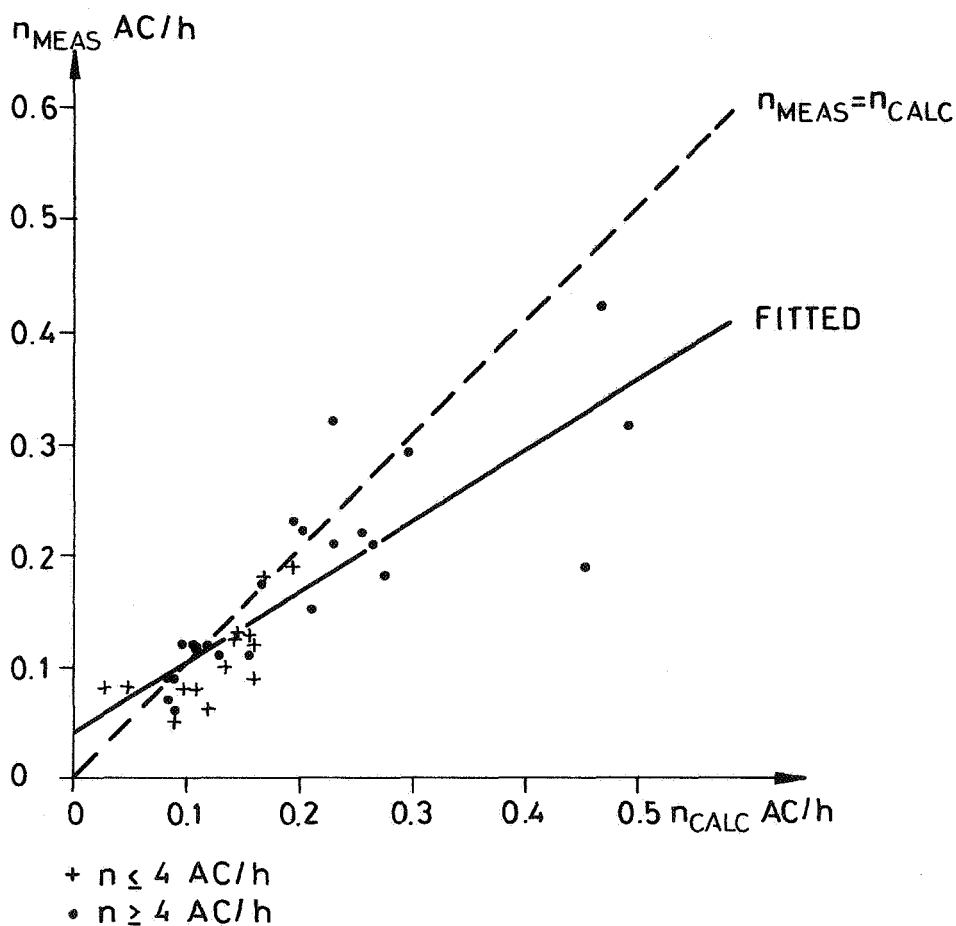


Figure 8. Calculated ventilation rates, n_{CALC} , versus measured ones, n_{MEAS} .

With the technique of linear regression the following analytical expression was obtained:

$$n_{MEAS} = 0,039 + 0,636 \cdot n_{CALC} \quad (14)$$

4 INTERPRETATION OF THE RESULTS

With equation (1) the intention was to "force" the measured values into a model which corresponds to the mechanisms of air infiltration we are familiar with rather than to use traditional regression analysis.

The factor $C_3(m^3/h)/Pa^\beta$ is simply a figure describing the tightness of the house. The value of C_3 is based on n_{50} and the exponent β and differs consequently from house to house.

The factor C_1 (Pa/K) is multiplied with the temperature difference to produce a pressure difference caused by stack effect. The magnitude of the factor is affected by the height up to the neutral zone. The value of 0,026 Pa/K is quite reasonable.

The C_2 -values however, seem to be rather small - 0,010 Pa/(m/s)² in the case with no wind reduction and 0,038 Pa/(m/s)² in the case with 50% wind reduction.

Since Δp caused by wind acting on a building can be written as:

$$\Delta p = \Delta \mu \frac{\rho \cdot u^2}{2} \quad (15)$$

where $\Delta \mu$ is the difference in shape coefficients between out and inside, ρ is the density of the air (kg/m³) and u the wind velocity (m/s). Consider the infiltration case on a cube-shaped building with wind acting perpendicular to one of the sides (the pressure side) then $\overline{C_2}$ could be written as

$$\overline{C_2} = \frac{\overline{\Delta \mu_p} \cdot \rho}{2} \cong 0,6 \overline{\Delta \mu} \quad (16)$$

Where $\overline{\Delta \mu_p}$ denotes the average difference in shape coefficients across the wall.

From this the values 0,010 resp 0,038 Pa/(m/s)² should correspond to

$$\overline{\Delta \mu_p} = \frac{0,010}{0,6} = 0,017 \quad (\text{no wind reduction})$$

$$\overline{\Delta \mu_p} = \frac{0,038}{0,6} = 0,063 \quad (50\% \text{ wind reduction})$$

Since the last given value corresponds to a place with reduced wind velocity it has no meaning to compare this calculated $\overline{\Delta \mu_p}$ value with something else. This is of course due to the fact that μ should transform wind velocity in the free stream into wind pressures.

A further interpretation might be made by taking into account the fact that a rectangular building has one or two windwardfacing sides and the others are leewardfacing. If the total area on the pressure side is de-

noted A_p and the total area of the suction sides is denoted A_s it can be proved with a simple flow-balance equation that

$$\overline{\Delta\mu_p} = \frac{(\overline{\mu_p} - \overline{\mu_s}) \left(\frac{A_p}{A_s}\right)^\beta}{1 + \left(\frac{A_p}{A_s}\right)^\beta} \quad (17)$$

If $\overline{\Delta\mu_p} = 0,017$, $\beta = 0,7$ and A_p/A_s is set to $1/4$ then $\overline{\mu_p} - \overline{\mu_s} = 0,06$.

The influence of the surroundings of the building and the density of the built area may be considerable. These matters are very well demonstrated in works by the people at Sheffield University (6), (7), (8). Figure 9 is taken from (7). It shows shape coefficients for windward and leeward faces of a cube-formed building where y/H is the height relative the total building height and the density being the ratio between built up and total ground area.

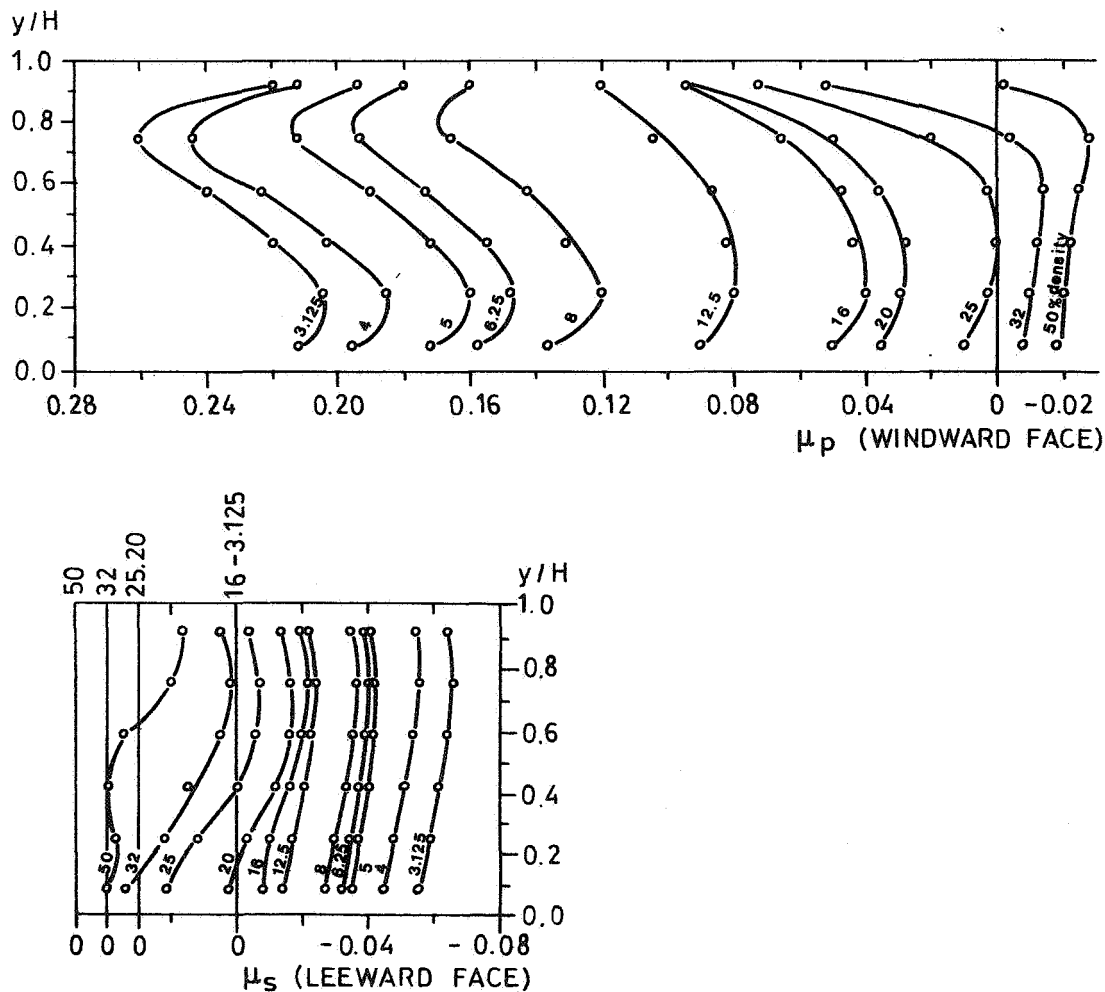


Figure 9. Distribution of mean shape coefficient on the element centre line at all densities. Source: (7).

According to these results it is obvious that a high density can reduce the values of the shape coefficients considerably. The densities of the areas where the 19 houses in this study are situated are not known but normal Swedish areas with one-family houses may have a density of say 15%. If this is the case for the houses studied the values of $\overline{\Delta u_p} - \overline{\Delta u_s}$ as calculated above seem quite reasonable.

5 SUMMARY

Much hope has been fixed upon possibilities of correlating results of pressurization tests with infiltration tests, thus making it possible to predict the ventilation rate of a building with the result of the pressurization test as a basis. This paper describes the application of an a priori designed calculation model based upon the well-established relationship $Q = \alpha \cdot \Delta p^\beta$ in which α and β are determined from pressurization test. Two factors operating at the temperature difference between inside and outside and the square of the wind velocity respectively determined from tracer gas tests at different seasons of the same house settles the p term. The model has been applied to 19 1½-storey single family houses. The calculated factors seem to have reasonable values. However, the density of a house group seem to have very great influence on the magnitude of the shape coefficients. This may explain why calculated mean shape factors seem to be rather low. It would have been very interesting to make similar calculations on other houses in other surroundings.

6 ACKNOWLEDGEMENTS

The paper has been prepared within a research project sponsored by the Swedish Council for Building Research. Miss Lena Thorell typed the manuscript and mrs Lilian Johansson performed the drawing of the figures and the lay out of the paper. They both carried out their work in an excellent way which I very much appreciate.

REFERENCES

1. Kronvall J. Testing of houses for air leakage using a pressure method. ASHRAE transactions 1978 No. 2473.
2. Grimsrud D T et al. Infiltration - pressurization correlations: Detailed measurements on a California house. Lawrence Berkely lab. Dept of enery. Report LBL - 7824. Presented at The ASHRAE-symposium on air infiltration in Philadelphia, PA, USA in Jan 1979.
3. Blomsterberg A et al. A model correlating air tightness and air infiltration in houses. Paper at the ASHRAE/DOE conference on "Thermal performance of the exterior envelopes of buildings" 3 - 5 December 1979 in Florida.
4. Kronvall J. Air tightness - measurements and measurement methods. Swedish Council for Building Research. Report D8:1980, Stockholm 1980.
5. Nylund P O. Infiltration and ventilation. Swedish Council for Building Research. Report D22:1980, Stockholm 1980.
6. Soliman B F. The effect of building grouping on wind induced natural ventilation. Dept of Building Science. University of Sheffield. Report BS 14, Sheffield 1973.
7. Soliman B F. Effect of building group geometry on wind pressure and properties of flow. Dept of Building Science. University of Sheffield. Report BS 29, Sheffield 1976.
8. Lee B E et al. Predicting natural ventilation forces upon low-rise buildings. ASHRAE Journal Febr. 1980. p 35 - 39.

PAPER 15

**THE RELATIONSHIP BETWEEN
TRACER GAS AND PRESSURIZATION
TECHNIQUES IN DWELLINGS**

P. R. WARREN AND B. C. WEBB

**DOE
BRE
Watford
UK**

THE RELATIONSHIP BETWEEN TRACER GAS AND PRESSURISATION TECHNIQUES IN DWELLINGS

by P R Warren and B C Webb

1 INTRODUCTION

Two main methods are currently in use for measuring the infiltration performance of dwellings, tracer gas techniques for determining infiltration rate and pressurisation techniques for measuring the leakage characteristics of the envelope. The infiltration rate is of most interest since it enables the related heat loss to be calculated, and, since the majority of dwellings are naturally ventilated, it also enables possible levels of internal airborne contaminants to be determined. Pressurisation techniques are limited to providing data on the magnitude and the distribution of airflow paths through the building envelope. However pressurisation techniques possess certain advantages; the necessary equipment is relatively cheap, robust and easily operated and the time required on site is short. In contrast, tracer gas measurements require considerable expertise, expensive equipment and are time-consuming, if the full range of variables which affect infiltration are to be included.

The usefulness of pressurisation techniques could be considerably enhanced if a method of linking the results achieved with their use to infiltration rates could be identified and established. The purpose of this paper is to propose such a method, based upon a simple theoretical model of infiltration, and to discuss its validity using whole house pressurisation

A 113/5/1

PD 118/80

and infiltration measurements made as part of field survey of infiltration rates in British dwellings.

2 FIELD MEASUREMENTS

2.1 Pressurisation measurements

Table 1 includes brief details of fifteen houses in which whole house pressurisation measurements were made as part of a larger survey of infiltration and natural ventilation in dwellings. These are labelled A to P for purposes of easy reference. In addition published data on two other dwellings have been taken from references (1) and (2). These dwellings are labelled R and S respectively.

Pressurisation measurements of the air leakage through the envelope of each house was made using the equipment developed and described by Skinner(3). Measurements were made for both positive and negative applied pressure difference across the dwelling envelope, over a range of 10 to 60 Pa. A simple power law of the following form was fitted to the results:

$$Q = Q_T \left[\frac{\Delta p}{\Delta p_T} \right]^n \quad (1)$$

Q is the volume flow rate of air at an applied pressure difference Δp . Q_T is the flow rate at a chosen reference pressure Δp_T . This may be arbitrarily chosen, but for present purposes the value 50Pa will be used to conform with current Swedish practice(4). The values of Q_T and n are listed in Table 1. Also listed for comparison with other published results are the corresponding values of (Q_T/V) and (Q_T/A_p) where V and A_p are the volume and permeable area of each dwelling.

The permeable area is defined as the sum of the areas of the exposed walls, the ground floor, provided that this is not solid, and the area of the ceiling between the topmost floor and the roof space. Party walls in semi-detached and terraced houses are assumed to be impermeable. For all of the results given in Table 1 windows, doors and other controllable openings were fully closed. Extract fans were switched off and their openings sealed.

It is interesting to note that values of (Q_T/V) are substantially larger than the average values found in recent Swedish(5) and Canadian(6) surveys which were 3.5 ach and 4.4 ach respectively.

2.2 Tracer gas measurements

Whole house tracer gas measurements were made in all of the listed houses. In houses A to R nitrous oxide was used as the tracer gas and its concentration monitored using an infra-red gas analyser. All internal doors were set open and fans placed in the open doorways in order to mix the tracer gas throughout the house. The ventilation rate measured is the ratio of the flow rate of air entering the house to the volume of the house. This should be typical of the ventilation rate under normal occupied conditions provided that internal doors are either kept open or present little resistance to flow in comparison with the air leakage paths in the external envelope.

On average approximately twenty measurements of whole house ventilation rate were made. Wind speed and direction were monitored throughout each test period using a lightweight anemometer and windvane mounted on a 10 m high hydraulic mast, situated close to, but not in the immediate

flow field of, the house under test. Air temperatures were measured in each room, as well as externally, using calibrated thermocouples. The output from each of the instruments was recorded, via a data logger, on paper tape for subsequent analysis by mainframe computer. The resulting output consisted of the ventilation rate during the test period (usually of the order of thirty minutes), the average wind speed and direction and the average temperatures as well as measures of the variation of each of these quantities over the period.

3 PROBLEMS IN RELATING TRACER GAS AND PRESSURISATION MEASUREMENTS

3.1 Limitations of pressurisation techniques

(i) The magnitude of the pressure differences used in the pressurisation tests is necessarily higher than those normally generated by the wind and stack effect. The extrapolation of the applied pressure - flow rate relationship defined by equation (1) to lower applied pressures than those to which it was fitted currently lacks experimental validation.

(ii) The pressure differences generated across the building envelope by stack and wind effects are not applied uniformly as they are in the pressurisation technique.

(iii) The simple determination of Q_T and the exponent, n , does not define the distribution of Q_T . The same results would be obtained whether Q_T were lumped together on one external wall or whether it were evenly distributed over the whole envelope. Repeated measurements with chosen components sealed up gives additional information on the magnitudes and distribution of the openings, but removes some of the simplicity and ease of use which makes the technique attractive.

3.2 Choice of characteristic quantities

Further to the problems outlined above there is a difficulty in comparing pressurisation results for a given house with the results of the measurements of infiltration because of the number of variables involved.

The results of the pressurisation tests are defined by two parameters, Q_T and n . Any measured value of infiltration rate, R , is a function of wind speed U , wind direction, ϕ , and the difference between internal and external air temperature, ΔT .

Clearly any method which aims to relate Q_T and Q_V , the infiltration flow rate, must also include the other variables if it is to be used as a basis for predicting the infiltration performance of a given dwelling. The following section outlines a simple theoretical model which aims to accomplish this.

4 A SIMPLE THEORETICAL MODEL FOR INFILTRATION

4.1 Assumptions made in setting up the model

The following assumptions are made in setting up the infiltration model:

(i) The building envelope is represented by a rectangular parallelepiped of height, h . This does not preclude the presence of a pitched roof, but is intended to define the volume of interest from the point of view of infiltration. The maximum overall height of the building, for instance to the top of a pitched roof, is H and is used to specify the air speed required by convention for defining the surface pressure coefficients generated by the wind. The appropriate value of wind speed is given by

$$U = U_r \left[\frac{H}{H_r} \right]^\alpha \quad (2)$$

where U_r is the reference site wind speed for the measurements and α depends upon the nature of the local terrain, as described in reference (7). Reference (7) also enables U to be calculated from standard Meteorological Office wind speeds for design purposes.

(ii) The pressure generated by the wind is uniform across each surface. The values for each surface will depend upon the building shape, its orientation to the wind and any surrounding obstacles, including other houses.

(iii) Air leakage through the envelope is assumed to be uniformly distributed across each surface, but the total leakage Q_T may be distributed in any chosen proportions among the surfaces.

(iv) The exponent, n , is assumed to apply to all leakage paths.

(v) Party walls and solid floors are assumed to be impermeable.

(vi) If the underfloor space is ventilated the assumed surface pressure is obtained by determining the area weighted mean of the pressures on exposed vertical walls.

4.2 Infiltration rate functions F_V , F_W and F_B

The derivation of the model is summarised in Appendix 1. Three relationships are obtained. The first concerns the infiltration flow rate Q_V which is given by

$$Q_V = Q_T \left[\frac{\rho_o U^2}{\Delta p_T} \right]^n F_V (Ar, \phi) \quad (3)$$

F_v may be calculated if the following are known:

(i) The surface pressure coefficients as functions of ϕ . The surface pressure coefficient C_{pi} for any surface, i , is defined as

$$C_{pi} = \frac{(P_i - P_o)}{\frac{1}{2} \rho_o U^2} \quad (4)$$

Surface pressure coefficients are most accurately obtained from wind tunnel model studies of the building under consideration. Approximate values are available for simple building shapes, for instance in the British Standard Code dealing with Wind Loads(8).

(ii) The Archimedes number Ar . This relates buoyancy and inertial forces and in this context is defined as

$$Ar = \left\{ \frac{\Delta T \cdot g \cdot h}{T_I U^2} \right\}$$

The Archimedes number combines the two main meteorological variables U and ΔT , as well as the height, h , defined previously.

(iii) The distribution of the leakage among the exposed surfaces.

Thus given either measured or estimated values of the surface pressure coefficients and the distribution of leakage F_v , and hence Q_v , may be obtained for any combination of values of U , ΔT and ϕ .

When the wind acts alone, the resulting infiltration flow rate, Q_w , may be derived from the model:

$$Q_w = Q_T \cdot \left[\frac{\rho_o U^2}{\Delta p_T} \right]^n \cdot F_w(\phi) \quad (5)$$

Similarly when stack effect acts alone, the resulting infiltration rate, Q_B , is given by

$$Q_B = Q_T \left[\frac{\Delta T \cdot \rho_o \cdot gh}{T_I \Delta p_T} \right]^n F_B \quad (6)$$

F_B is a constant for any given building and F_W is a function of wind direction only.

4.3 Typical values of F_V , F_W and F_B

In order to demonstrate the variation of the function F_V , F_W and F_B derived above with building characteristics values have been calculated for three typical housing types;

- (a) Detached
- (b) Semi-detached
- (c) Centre terrace

The dimensions of the houses are shown in Table 2, together with appropriate pressure coefficients for a selection of wind directions obtained from reference (8). All three functions will vary with n . The calculations have therefore been carried out for three values of $n = 0.5$, 0.6 and 0.7 , in order to cover the range found in practice (see Table 1). The leakage, Q_p , was assumed to be distributed uniformly over the whole of the exposed surface of the envelope in each case. The ground floor is assumed to be impermeable, except for the value of $n = 0.6$, where for purposes of comparison calculations were also made with a permeable floor.

The calculated values of F_W and F_B are given in Table 3(a). F_V is shown in Figures 1(a), (b) and (c). The axes have been chosen to give identical

asymptotes for each set of values of F_V . Inspection of the results for F_W and F_B shows a negligible variation of F_B with house arrangement. There is some variation with n ; a reduction of approximately 10% when n is raised from 0.6 to 0.7, and an increase of approximately the same amount when n is reduced from 0.6 to 0.5. There are substantial variations in F_W with wind direction ϕ for each house type.

5 COMPARISON OF FIELD MEASUREMENTS WITH MODEL PREDICTIONS

As a first step to comparing the results of the field measurements with the predicted values from the model only F_W and F_B will be considered. The aim here is to determine how well values of F_W and F_B derived from the field measurements agree with those given in Table 3(a).

In order to do this it is necessary to isolate those results which are dominated by either stack or wind effect. It is very rare to obtain measurements in the field where either effect is completely absent and it is necessary to establish some form of criterion by which to judge each set of results for a given house to determine whether it may fall into either of the categories required. An indication of a method of achieving this is contained in Figures 1(a) to (c). The ordinate in these figures is, in fact, (Q_V/Q_B) and the asymptote as $(F_W/F_B \cdot Ar^n)$ tends to infinity is, $Q_V = Q_W$. A reasonable proposal is to set the limit for stack dominated infiltration as

$$\frac{Q_V}{Q_B} \leq 1.1$$

and for wind dominated infiltration,

$$\frac{Q_v}{Q_w} \approx 1.1$$

On rearrangement these lead to the following approximate criteria based upon the measured climatic variables,

Stack dominated infiltration: $U^{2n}/\Delta T^n \leq 0.3$

Wind dominated infiltration: $U^{2n}/\Delta T^n > 1.5$

On examining each set of results for the houses listed in Table 1 those sets which fulfil these criteria were extracted and used to calculate the following:

For stack dominated infiltration:

$$\left\{ \left(\frac{Q_v}{\Delta T^n} \right) \left(\frac{\Delta p_T}{\rho_o} \right)^n \left(\frac{T_i}{g_h} \right)^n \right\}$$

and, for wind dominated infiltration:

$$\left\{ \left(\frac{Q_v}{U^{2n}} \right) \left(\frac{\Delta p_T}{\rho_o} \right)^n \right\}$$

From equations (5) and (6) it can be seen that when divided by Q_T these quantities should give values of F_B and F_W respectively. In order to compare these measured results with those calculated using the model, the quantities given above for each house have been plotted against Q_T in Figures (3) and (2) for stack effect and wind effect respectively. For comparison the expected spread of the results due to the variation of F_B with n , and of F_W with n and ϕ has been indicated by the shaded regions on each figure. The results for the stack effect comparison

are very encouraging. Of the houses which lie outside the expected band it is suspected that the values of Q_T for K and J include some leakage through the party wall. This will be checked in a future series of measurements.

The results in Figure(2), for wind, are more scattered. This is, however, to be expected because of dependence of F_W on ϕ as well as n . Figure (4) shows the variation of F_W with ϕ for House F which is a centre-terraced house. It is interesting to note that the infiltration rate with the wind perpendicular to the terrace is considerably greater than when the wind is parallel.

Despite the scatter there is a trend for the values of F_W to lie below the region containing the expected range predicted by the theoretical model. However the pressure coefficients used, as given in Table 2, apply to buildings in isolation. All of the houses in which measurements were made had other buildings, as well as other forms of shelter such as trees and fences in their vicinity. Although detailed data on pressure coefficients other than for isolated buildings is sparse there is evidence, from both full scale(9) and model studies(10) of pressure distributions on low rise buildings, that the values for surface pressure coefficients are substantially reduced by the presence of other buildings of a similar height. Lee et al(10) have demonstrated that reductions of 50% in wall and roof pressure coefficients may be expected in housing of moderate density. The values of F_W given in Table (3a) have therefore been recalculated with the surface pressure coefficients arbitrarily reduced to half of their original value. The new range of predicted values of F_W is given in Table (3b) and shown on Figure (5). In place of the

mean of the measured values of F_W the range is indicated by plotting the maximum and minimum value for each house. The agreement is very much better.

It should be noted that the theoretical results are limited to the house types and dimensions set out in Table 2, and not specifically matched to the dimensions of the houses tested. Further, the leakage area has been assumed to be uniformly distributed over the exposed surfaces of the envelope. Further analysis will be undertaken to compare each set of measured results with predicted values specific to each site. A major problem exists however in the lack of data on pressure coefficients for typical housing arrangements.

6 THE PREDICTION OF INFILTRATION RATES

Given the leakage data for a house, together with its dimensions, the mean surface pressure coefficients for the expected range of wind directions and, if possible, the distribution of leakage among the exposed surfaces the infiltration rate may be calculated using F_V for any combination of wind speed, wind direction and temperature difference. The meteorological data can be presented either in statistical form or as a continuous series for a given period of time. Alternatively F_B and F_W may be calculated and the larger of the two predicted ventilation rates taken. Another possibility which lies between these alternatives is to note that the following simple function fits the predicted results shown in Figures (1a), (1b) and (1c) with a reasonable degree of accuracy

$$\frac{F_V}{F_B} \cdot \frac{1}{Ar^n} = \left[1 + \left[\frac{F_W}{F_B} \cdot \frac{1}{Ar^n} \right]^2 \right]^{\frac{1}{2}} \quad (7)$$

On rearrangement this leads to

$$F_V = \left[(F_B \cdot A r^n)^2 + F_W^2 \right]^{\frac{1}{2}} \quad (8)$$

7 CONCLUSIONS

The agreement demonstrated between the theoretical model and the data from measurements in seventeen houses gives confidence that the simple theoretical model may provide a means of estimating house infiltration rates using leakage data obtained from whole house pressurisation measurements. In addition, however, surface pressure coefficients for typical house shapes, arrangements and surroundings are also required but, at present, there is a dearth of data of this type.

ACKNOWLEDGEMENT

The authors wish to thank those of their colleagues who assisted with the programme of measurements, in particular Mrs L Parkins who carried out much of the analysis of the results. The measurement of infiltration rate in houses M, N and P was undertaken by the Building Services Research and Information Association.

The work described has been carried out as part of the research programme of the Building Research Establishment of the Department of the Environment and this paper is published by permission of the Director.

REFERENCES

- 1 Guillaume M, Ptacek J, Warren P R and Webb B C, Measurements of ventilation rates in houses with natural and mechanical ventilation systems. Proceedings of Meeting of CIB Steering Group S 17, Holzkirchen, September 1977
- 2 Dickson D J. Ventilation with open windows. Electricity Council Research Centre Memorandum ECRC/M1329, April 1980
- 3 Skinner N. Natural infiltration routes and their magnitude in houses - Part 2. Proceedings of Conference - Controlled Ventilation. Aston University, September 1975
- 4 Standard Method Description SP 1977:1. National Swedish Authority for Testing Inspection and Metrology
- 5 Kronvall J. Airtightness - measurements and measurement methods. Swedish Council for Building Research Report D8:1980
- 6 Beach R K. Relative tightness of new housing in the Ottawa area. National Research Council of Canada, Division of Building Research, Building Research Note No 149, June 1979
- 7 Principles of natural ventilation. Building Research Establishment Digest No 210, February 1978
- 8 Code of basic data for the design of buildings. Chapter V. Loading Part 2. Wind loads. British Standard CP3 : Chapter V : Part 2 : 1972
- 9 Eaton K J and Mayne J R. The measurement of wind pressures on two-storey houses at Aylesbury. Building Research Establishment Current Paper CP 70/74. July 1974
- 10 Lee B E, Hussain M and Soliman B. A method for the assessment of the wind-induced natural ventilation forces acting on low rise building arrays. Building Services Engineering Research and Technology (CIBS Series A), Vol 1, No 1, 1980

- 11 Blomsterberg A K, Sherman M H and Grimsrud D T. A model correlating air tightness and air infiltration in houses. Lawrence Berkel Laboratory Report, November 1979
- 12 Sherman M H and Grimsrud D T. Infiltration-pressurisation correlation: simplified physical modelling. Presented at ASHRAE Semi-annual Meeting, Denver, Colorado, June 1980
- 13 Cole J T, Zawacki T S, Elkins R H, Zimmer J W and Macriss R A. Application of a generalised model of air infiltration to existing homes. Presented at ASHRAE Semi-annual Meeting, Denver, Colorado, June 1980
- 14 Shaw C Y. Wind and pressures induced pressure differentials and an equivalent pressure difference model for predicting air infiltration on schools. ASHRAE Transactions, Vol 86, Part 1, 1980
- 15 Lindquist T and Bergenstjerna A. Vardering av lufttathet hos fönster (Assessment of airtightness of windows). Chalmers Tekniska Högskola, Göteborg. Department of Building Construction, Report 1979:12
- 16 Warren P R. Natural ventilation routes and their magnitude in houses - Part 1. Proceedings of Conference - Controlled Ventilation, Aston University, September 1975
- 17 Warren P R. Ventilation of spaces with openings on one side only. Proceedings of International Conference on Heat and Mass Transfer in Buildings, Dubrovnik, September 1977. Publ Hemisphere Publishing Corporation, Washington DC
- 18 Mattingley G E, Harrje D T, Heisler G M. The effectiveness of an evergreen windbreak for reducing residential energy consumption. ASHRAE Transactions, Vol 85, Part II, 1979

NOMENCLATURE

A	Area
a	Substitution function ($= (C_{pi} - C_{pI})$)
b	Substitution function ($= 2Ar$)
C_p	Pressure coefficient
F	Infiltration function (suffices B, V and W)
g	Acceleration due to gravity
H	Height (suffix r)
h	Height of ventilated space
m	Number of vertical surfaces
n	Exponent of building leakage characteristic
p	Pressure (suffices i, I, L, U)
T	Absolute temperature
U	Wind speed (suffix r)
Q	Infiltration flow rate (suffices B, V and W)
V	Volume of ventilated space
w	Width of vertical surface
Z	Dimensionless vertical co-ordinate ($= z/h$)
z	Vertical co-ordinate
Ar	Archimedes No ($= \frac{\Delta T \cdot g h}{T_I U^2}$)
α	Exponent for wind velocity profile
ρ	Density of air (suffices o, I)

Prefix:

Δ	Difference between two values of the same quantity
----------	----------------------------------------------------

Suffices:

B,V,W	Relate to stack effect, combined effect and wind effect respectively
i	Number of a vertical surface
L,U	Relate to lower and upper surface respectively
o,I	Relate to inside and outside of the ventilated space
T	Relates to test reference condition for pressurisation tests
r	Relates to reference wind speed and height

TABLE 1 BASIC DETAILS AND LEAKAGE CHARACTERISTICS OF TEST HOUSES

HOUSE DATA				AIR LEAKAGE CHARACTERISTICS AT 50 Pa			
House	Date	Type	Volume m^3	Q_T m^3/h	n	(Q_T/V) ach	(Q_T/A_p) m^3/hm^3
A	1971	2 B	197	2310	0.57	11.7	12.4
B	1957	2 B	254	2210	0.69	9.7	11.7
C	1957	2 B	249	2910	0.55	11.7	16.6
D	1976	2 C	196	3090	0.64	15.8	23.3
E	1976	2 C	196	2810	0.57	14.4	21.2
F	1956	2 D	164	2210	0.67	13.5	22.2
G	1977	2 D	77	1330	0.58	17.3	40.2
H	1947	2 A	195	3530	0.61	18.1	19.3
I	1978	2 D	179	1760	0.58	9.9	13.9
J	1977	2 C	196	4130	0.64	21.8	31.5
K	1960	2 B	261	3780	0.58	14.5	22.5
L	1960	2 B	261	3990	0.58	15.3	23.5
M	1976	2 E	179	3400	0.53	19.0	39.2
N	1977	3 D	220	3240	0.63	14.7	32.6
P	1970	2 C	221	2310	0.58	10.4	17.3
Q*	1977	1 A	229	2640	0.63	11.6	14.9
R**	1977	2 A	260	1710	0.66	6.6	8.7

Notes: House type: 1, 2, 3 - number of storeys.
 A - detached; B - semi-detached; C - end terrace;
 D - centre terrace; E - quad.

* Reference (1). ** Reference (2).

TABLE 2 SURFACE PRESSURE COEFFICIENTS USED WITH THE INFILTRATION MODEL

Surface	Area m ²	House type					
		Detached		Semi-detached		Centre-terraced	
		0°wind	90°wind	0°wind	90°wind	0°wind	90°wind
Wall 1	33.5	+0.70	-0.60	+0.70	-0.50	+0.70	-0.50
2	33.5	-0.60	+0.70	-0.70	+0.70	--	--
3	33.5	-0.25	-0.60	-0.30	-0.50	-0.30	-0.50
4	33.5	-0.60	-0.25	--	--	--	--
Roof	45.0	-0.35	-0.80	-0.35	-0.80	-0.35	-0.80
Floor	45.0	-0.25	-0.25	-0.10	-0.10	+0.20	-0.50

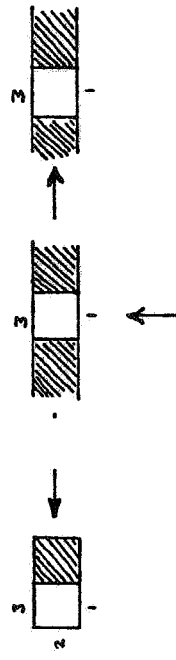
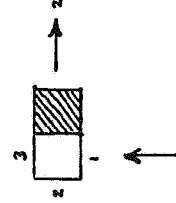
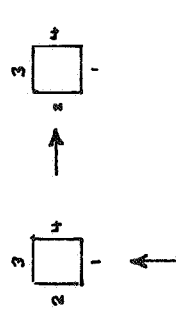


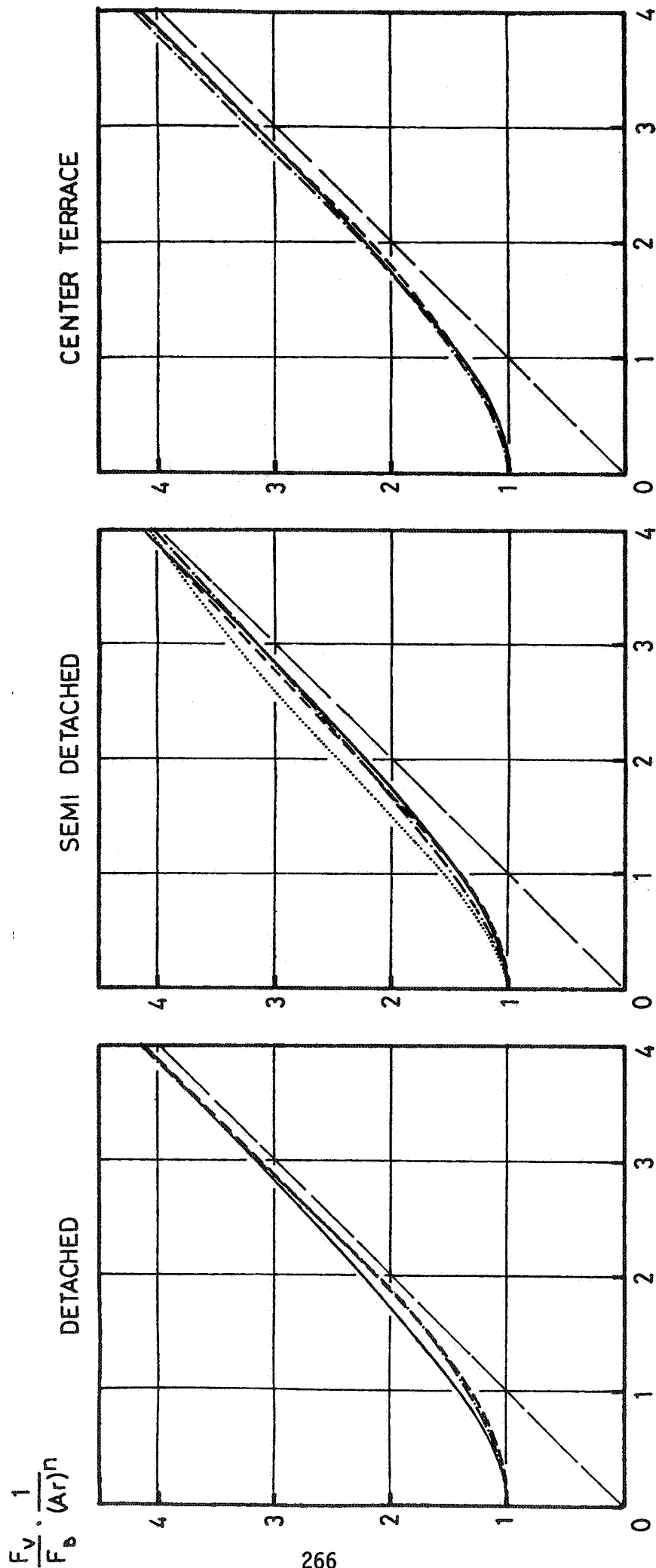
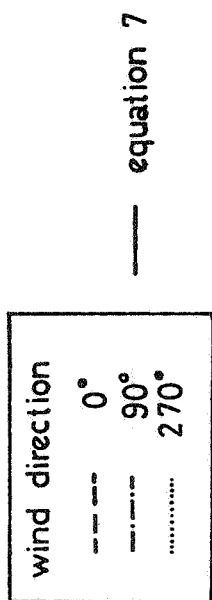
TABLE 3(a) VALUES OF F_B AND F_W CALCULATED USING THE PRESSURE COEFFICIENTS LISTED IN TABLE 2

House type	n	F_B		F_W (0° wind)		F_W (90° wind)		F_W (270° wind)	
		(i)	(ii)	(i)	(ii)	(i)	(ii)	(i)	(ii)
Detached	0.5	0.26	--	0.17	--	0.20	--	--	--
	0.6	0.23	0.26	0.15	0.13	0.18	0.16	--	--
	0.7	0.20	--	0.13	--	0.16	--	--	--
Semi-detached	0.5	0.26	--	0.16	--	0.18	--	0.12	--
	0.6	0.23	0.27	0.15	0.15	0.16	0.18	0.10	0.10
	0.7	0.20	--	0.14	--	0.15	--	0.08	--
Centre-terraced	0.5	0.26	--	0.20	--	0.13	--	--	--
	0.6	0.23	0.27	0.18	0.18	0.10	0.08	--	--
	0.7	0.20	--	0.16	--	0.08	--	--	--

TABLE 3(b) VALUES OF F_B AND F_W CALCULATED USING MODIFIED PRESSURE COEFFICIENTS

House type	n	F_B		F_W (0° wind)		F_W (90° wind)		F_W (270° wind)	
		(i)	(ii)	(i)	(ii)	(i)	(ii)	(i)	(ii)
Detached	0.5	0.26	--	0.12	--	0.14	--	--	--
	0.6	0.23	0.26	0.10	0.08	0.12	0.11	--	--
	0.7	0.20	--	0.08	--	0.10	--	--	--
Semi-detached	0.5	0.26	--	0.12	--	0.13	--	0.09	--
	0.6	0.23	0.27	0.10	0.10	0.11	0.12	0.06	0.07
	0.7	0.20	--	0.08	--	0.09	--	0.05	--
Centre-terraced	0.5	0.26	--	0.14	--	0.09	--	--	--
	0.6	0.23	0.27	0.12	0.12	0.07	0.05	--	--
	0.7	0.20	--	0.10	--	0.05	--	--	--

* (i) - impermeable ground floor ; (ii) - permeable ground floor



$$\frac{F_W}{F_B} \cdot \frac{1}{(Ar)^n}$$

Figure 1 Variation of $(F_V/F_B Ar^n)$ with $(F_W/F_B Ar^n)$ and wind direction, ϕ , for three house types, ($n = 0.6$).

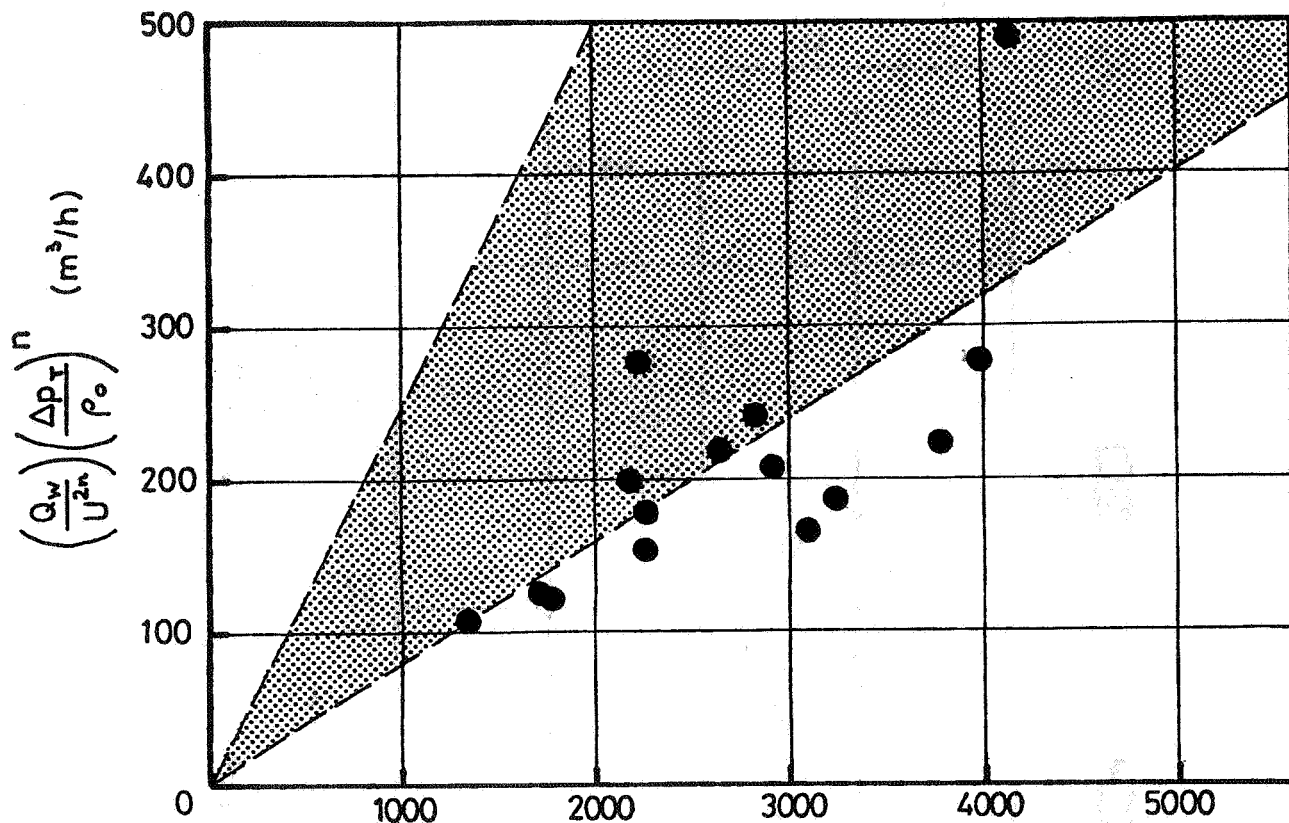


Figure 2 Determination of F_W - wind effect only

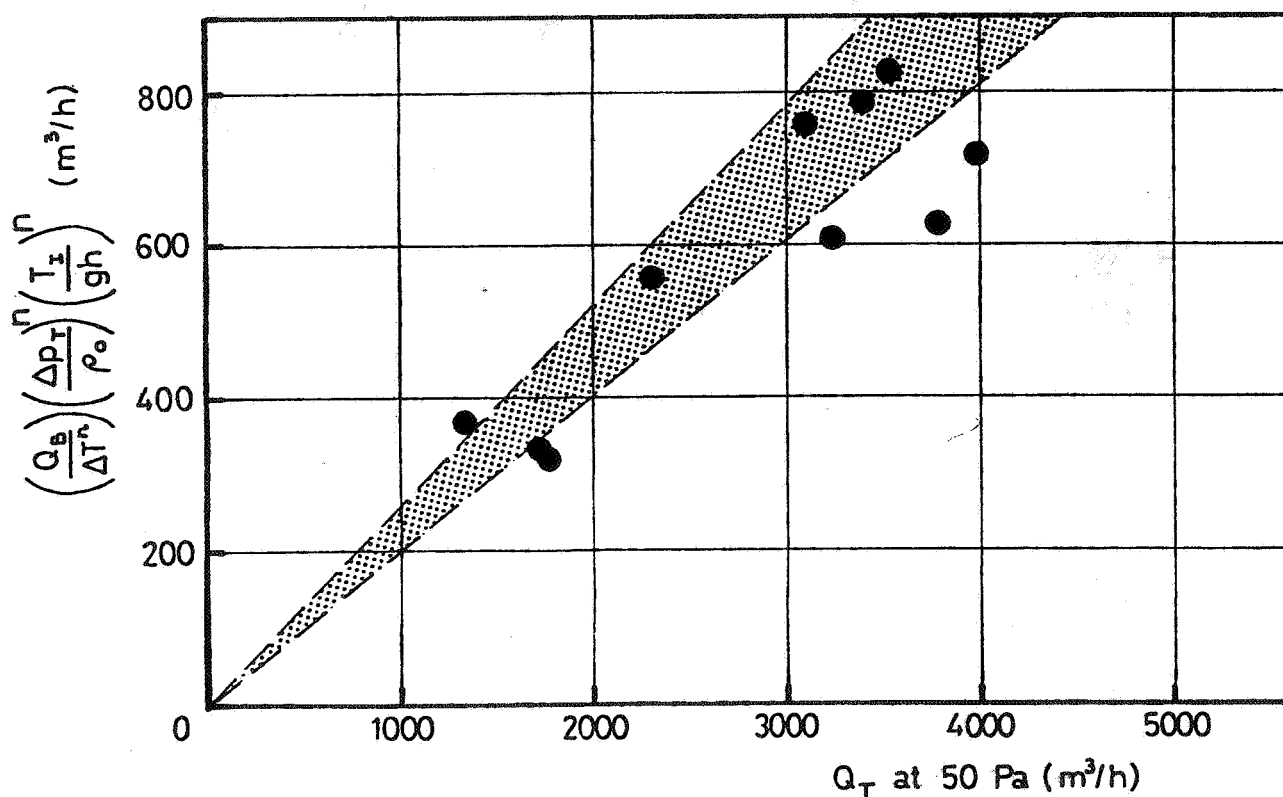


Figure 3 Determination of F_B - stack effect only

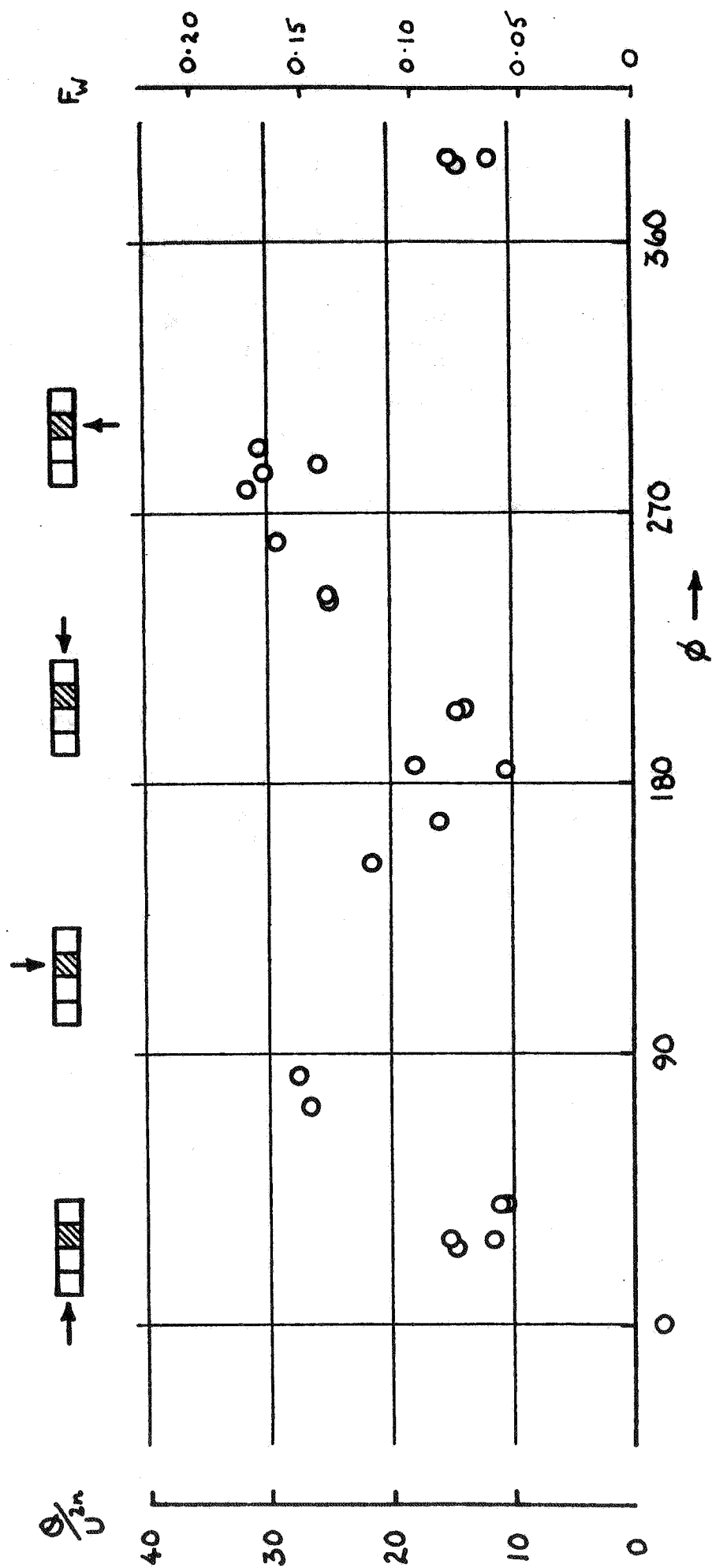


Figure 4 Variation of (Q/U^{2n}) and the infiltration function F_u with wind direction (ϕ) for House F.

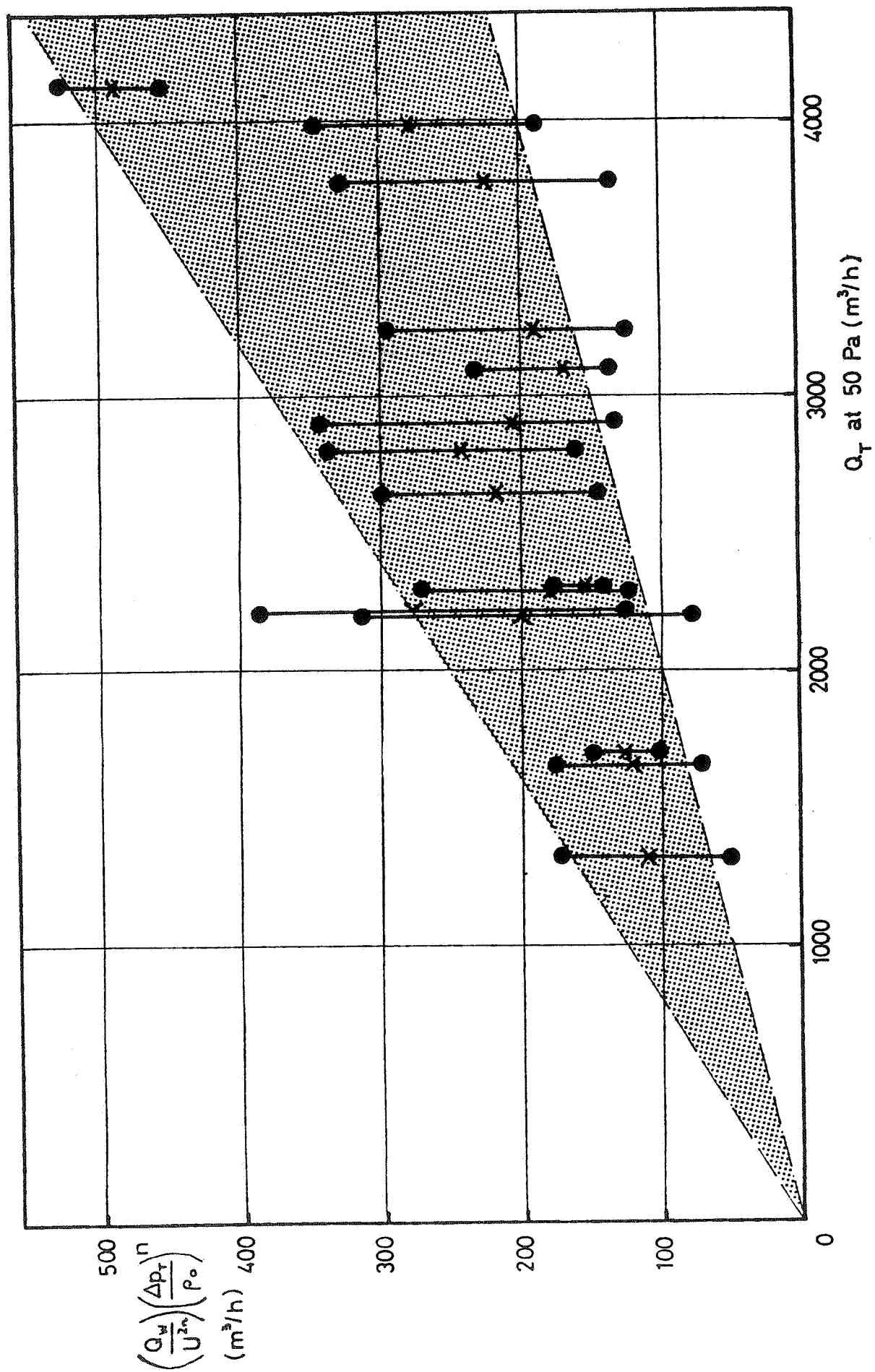


Figure 5 Comparison of the variation of F_u with predicted variation

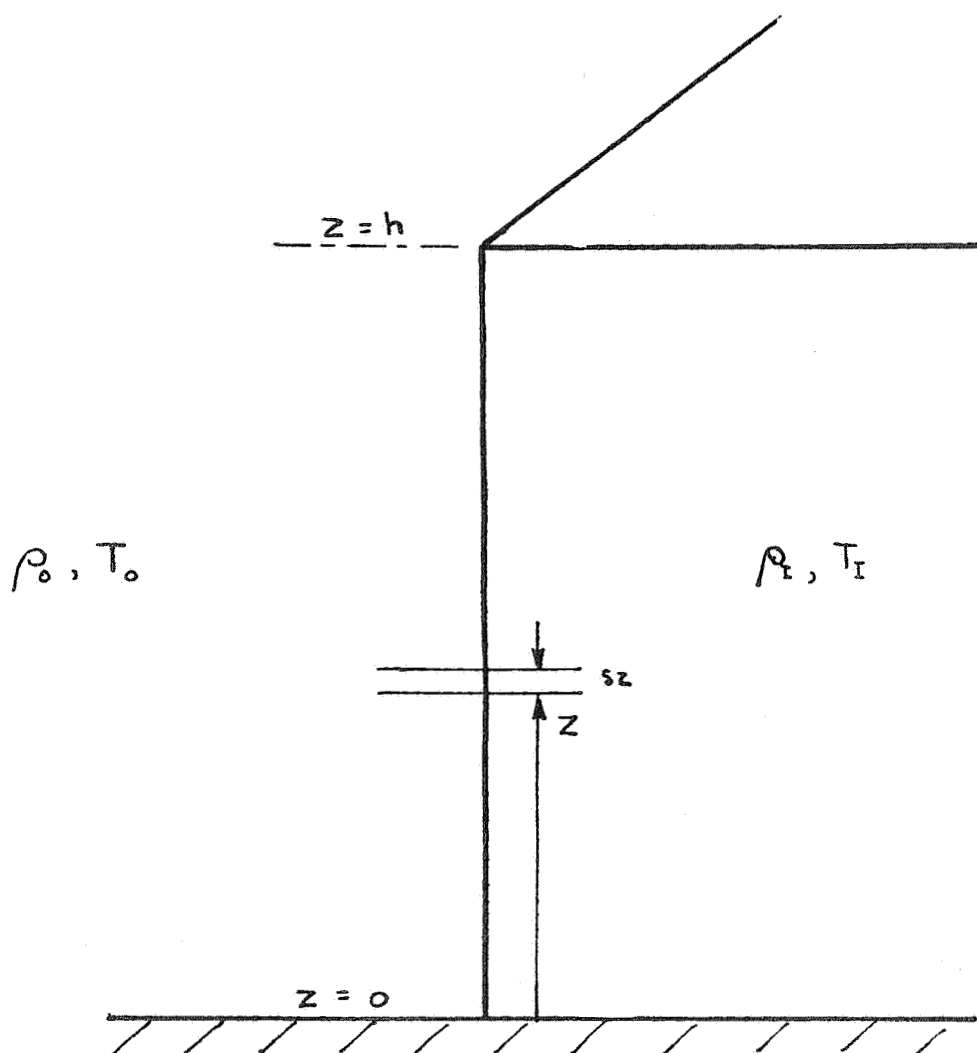


Figure 6 Schematic diagram for flow through vertical surfaces

APPENDIX 1

THE INFILTRATION MODEL

Introduction

The purpose of the model is to provide a method for relating infiltration rate at any given combination of wind speed, direction and difference between internal and external air temperatures to the leakage characteristics of a house, derived from pressurisation tests. The model assumes that the house can be represented as a single 'cell' and ignores any internal subdivisions of the space into rooms. A number of other single cell models have been developed, in particular by Blomsterberg et al(11), Sherman and Grimsrud(12), Cole et al(13), Shaw(14) and Lindquist(15). The present model differs from these in the set of assumptions made. For the present case these have been set out in Section 4 of the main text. In particular, unlike most of the other single cell models, no a priori assumptions concerning internal pressure or the position of neutral layers are made. The characterisation of the combined effect of stack and wind by the use of the dimensionless parameter, Ar , the Archimedes number, follows from its earlier use to illustrate the combined effect of stack and wind on heat losses in a naturally ventilated house(16) and in the analysis of data from field measurements of ventilation of spaces with openings on one side only(17). It is similar to the parameters, M , used by Mattingley et al(18) in the analysis of infiltration measurements, and the parameter, σ , used in a theoretical model by Sherman et al(12).

Derivation of the model equations

The flows through vertical and horizontal surfaces are considered separately:

(i) Vertical surfaces

Referring to the diagram shown in Figure (6), the pressure difference across the i^{th} wall, at a height z from the base of the dwelling, Δp_i , is given by the following equation,

$$\Delta p_i = \left(C_{pi} \cdot \frac{1}{2} \rho_o U^2 + p_o - \rho_o g z \right) - \left(p_I - \rho_I g z \right) \quad A(1)$$

p_I is the static pressure, at $z = 0$, within the house. p_o is the reference static pressure at $z = 0$ in the free wind. For convenience p_I may be expressed as a pressure coefficient,

$$p_I = C_{pI} \cdot \frac{1}{2} \rho_o U^2 + p_o,$$

whence,

$$\Delta p_i = \frac{1}{2} \rho_o U^2 (a_i - b \cdot Z) \quad A(2)$$

Where,

$$a_i = C_{pi} - C_{pI}; \quad b = \frac{(\rho_o - \rho_I) g h}{\frac{1}{2} \rho_o U^2} = 2Ar$$

and $Z = \frac{z}{h}$.

Following from assumptions (iii) and (iv) in Section 4 of the main text, the volume flow rate δQ_i through a section of vertical surface δz is given by

$$\delta Q_i = \frac{Q_{Ti} \cdot w_i}{A_i} \left\{ \frac{|\Delta p_i|}{\Delta p_T} \right\}^n \cdot \text{sign} (\Delta p_i) \cdot \delta z \quad A(3)$$

It is necessary to specify the modulus of Δp_i since this may take either positive or negative values and because $n < 1$. The term $\text{sign}(\Delta p_i)$ is positive for flow into the building and negative for flow out. A_i is the area of the i^{th} vertical surface; Q_{Ti} is the total flow through the i^{th} surface at an applied pressure difference, Δp_T ; w_i is the width of the i^{th} surface. Substituting for Δp_i from equation A(2) into equation A(3) gives, on rearrangement,

$$\delta Q_i = K_i \cdot (|a_i - b \cdot Z|)^n \cdot \text{sign}(a_i - bZ) \cdot \delta Z \quad A(4)$$

On integrating over $Z = 0$ to $Z = 1$, this yields an expression for the net flow through the i^{th} wall;

$$Q_i = \frac{K_i}{b(n+1)} \left[(|a_i|)^{n+1} - (|a_i - b|)^{n+1} \right] \quad A(5)$$

where

$$K_i = Q_{Ti} \left[\frac{\frac{1}{2} \rho_o U^2}{\Delta p_T} \right]^n$$

(ii) Horizontal surfaces

There are two horizontal surfaces, at $Z = 0$, and at $Z = 1$, specified in the following equations by the suffices $()_L$ and $()_U$ respectively.

The total flow through each is readily derived from equation A(4):

$$Q_L = K_L \cdot (|a_L|)^n \cdot \text{sign}(a_L) \quad A(6a)$$

$$Q_U = K_U \cdot (|a_U - b|)^n \cdot \text{sign}(a_U - b) \quad A(6b)$$

(iii) Determination of C_{pI}

Ignoring small density changes, the principle of continuity requires that,

$$Q_L + Q_U + \sum_{i=0}^m Q_i = 0 \quad A(7)$$

where m is the number of vertical surfaces.

Equation A(7) contains only one unknown when the original quantities are resubstituted. This is the dimensionless internal pressure coefficient C_{pI} . Equation A(7) may be solved by simple numerical procedures for C_{pI} , providing that the following are given:

- (a) The leakage characteristics, Q_T and n .
- (b) The value of Q_{TL}/Q_T , Q_{TU}/Q_T etc.
- (c) The values of C_{pL} , C_{pU} , and C_{pi} (for $i = 1$ to m).
- (d) The Archimedes number, Ar .

(iv) The determination of the infiltration flow rate

Let Q_V be the infiltration flow rate. Once C_{pI} is known, Q_V is given by

$$2Q_V = \left\{ \frac{1}{b(n+1)} \sum_{i=1}^m \left\{ (|a_i|)^{n+1} \cdot \text{sign}(a_i) - (|a_i - b|)^{n+1} \cdot \text{sign}(a_i - b) \right\} \cdot K_i \right. \\ \left. + K_L \cdot (|a_L|)^n + K_U \cdot (|a_U - b|)^n \right\} \quad A(8)$$

For any given house, items (a) and (b) above are fixed, and the pressure coefficients are determined by the wind direction, ϕ , only. Q_V may therefore be written in the form,

$$Q_V = Q_T \cdot \left[\frac{\rho_o U^2}{\Delta p_T} \right] F_V(Ar, \phi) \quad A(9)$$

The Archimedes number may be expressed in terms of the temperature difference, ΔT , between internal and external air:

$$Ar = \left[\frac{\Delta T \cdot g \cdot h}{T_I \cdot U^2} \right] \quad A(10)$$

where T_I is the absolute temperature of the air within the house.

(v) Wind acting alone

Q_W , the infiltration flow rate when the internal and external temperatures are equal, may be obtained using the preceding derivation, and setting $\Delta p = 0$. This leads to the equivalent of equation A(9) where,

$$Q_W = Q_T \cdot \left[\frac{\rho_o U^2}{p_T} \right]^n \cdot F_W(\phi) \quad A(11)$$

F_W is given by;

$$F_W = \frac{1}{2^{n+1}} \left\{ \sum_{i=1}^m \left[\frac{Q_{Ti}}{Q_T} \right] \cdot |a_i|^n + \left[\frac{Q_{TL}}{Q_T} \right] \cdot |a_L|^n + \left[\frac{Q_{TU}}{Q_T} \right] \cdot |a_U|^n \right\}$$

(vi) Stack effect acting alone

Q_B the infiltration flow rate when the wind speed is zero may be obtained in a similar way by setting $U = 0$ in equation A(1) and preceding as before, but without putting the unknown quantity, p_I , into pressure coefficient form.

$$Q_B = Q_T \cdot \left[\frac{\Delta T \rho_o \cdot gh}{T_I \cdot \Delta p_T} \right]^n \cdot F_B$$

A(12)

PAPER 16

**MEASUREMENT OF INFILTRATION
USING FAN PRESSURIZATION AND
WEATHER DATA**

**M. H. SHERMAN AND
D. T. GRIMSRUD**

**Lawrence Berkeley Laboratory
University of California
USA**

Measurement of Infiltration
Using Fan Pressurization and Weather Data

M.H. Sherman, D.T. Grimsrud

Energy and Environment Division
Lawrence Berkeley Laboratory
University of California
Berkeley, Ca. 94720

ABSTRACT

In the past expensive instrumentation, usually involving tracer gases, has been required to measure air infiltration; in this paper a technique using fan pressurization results and weather data to calculate infiltration is presented. The geometry, leakage distribution, and terrain and shielding classes are combined into two reduced parameters which allow direct comparison of wind-induced and temperature-induced infiltration. Using these two parameters and the total leakage area of the structure (which is found from fan pressurization) the infiltration can be calculated for any weather condition. Experimental results from fifteen different sites is presented for comparison with theoretical predictions.

INTRODUCTION

Understanding the process of air infiltration is critical to any residential conservation program inasmuch as infiltration is a primary source of energy loss in residences. Yet we are far more capable of calculating conduction losses than losses due to infiltration. The two processes are quite analogous: conduction is the flow of heat due to a temperature difference and infiltration is the flow of air due to a pressure difference. Additionally, to calculate the energy load from air infiltration, the air flow must be combined with the temperature

The work described in this report was funded by the Office of Buildings and Community Systems, Assistant Secretary for Conservation and Solar Applications of the U.S. Department of Energy under contract No. W-7405-Eng-48.

difference between inside and outside. Conduction is more easily calculated than infiltration because the heat transfer is proportional to the temperature difference and does not depend strongly on any other driving force. Infiltration, on the other hand, depends on the interior-exterior pressure difference but is not simply proportional to it. Furthermore, the driving pressures are caused by uncorrelated physical effects (wind speed and indoor-outdoor temperature difference). Although conduction losses can be characterized by means of one parameter, the thermal resistance; infiltration, until now, has had no equivalent quantity.

It is because of these problems that infiltration has been a difficult quantity to model. Previous attempts at modeling infiltration have used statistical fitting¹⁻³ or have involved measurements or calculations that are too difficult to make on a large scale.⁴ This paper introduces a model that sacrifices some accuracy for versatility and simplicity. Rather than predicting accurately the weather induced infiltration of a particular structure, the model is designed to calculate the infiltration of a general structure. Furthermore, the model predicts the impact of retrofits or other changes in the building envelope on the basis of performance changes effected in a few measurable parameters.

The parameters used in the model are:

1) The leakage area(s) of the structure.

The leakage area is the parameter that describes the tightness of the structure (obtained by pressurization). Most retrofits will affect the leakage area or the distribution of leakage area around the building envelope (leakage distribution).

2) The height of the structure.

The height and other geometric quantities are usually known or can be measured directly.

3) The inside-outside temperature difference.

The temperature difference gives the magnitude of the stack effect. It is also necessary for calculating the energy load due to infiltration.

4) The wind speed.

The wind speed is required to calculate the wind-induced infiltration for comparison with the stack effect.

5) The terrain class of the structure.

The terrain class of the structure refers to the density of other buildings and obstructions which influence the dependence of wind speed on (measurement) height near the structure. Knowing the terrain class of the structure allows the use of off-site weather data for the calculation of wind-induced pressures.

6) The Shielding

The local shielding determines how much of the wind pressure gets through to the structure.

The wind speed used by the model can be calculated from a wind speed measured on any weather tower in the area. Using standard wind formulas (See Table 1) the wind speed in any terrain class and at any height can be converted to the wind speed at the site. Thus, on-site weather collection is not necessary in our model. We must emphasize, however, that the measured wind data must be for the "same wind", i.e. there can be no mountain ranges or other major terrain obstructions between the site and the wind tower.

AIR LEAKAGE

Air leakage is the simple process of air passing through openings or cracks in the structure. These openings range in size from those of undampered vents (about 0.2m) to tiny cracks around windows (about 0.2mm).

As we know from hydrodynamics, the character of the air flow through a leakage opening changes as the pressure across the opening changes. At very low pressures, the flow is dominated by viscous forces; at high pressures, by inertial forces. Therefore, at low pressures we expect the flow to be proportional to the applied pressure and at high pressures we expect the flow to be proportional to the square-root of the applied pressure. At intermediate pressures the behavior will be a mixture of these effects.

The pressure range in which the flow behavior changes depends on the geometry of the individual crack. While good data⁵ exist to describe the functional form of the leakage for an individual crack, the leakage characteristic of the entire structure is much harder to model. The flow vs. pressure curve of the structure will be the summation of all of the curves for each individual crack. Since it is impossible to know the geometry of each crack, calculating the flow vs. pressure curve of a real structure cannot be done from first principles.

Field measurements⁶⁻⁹ have shown that the behavior of the actual leakage curve more closely resembles that expected for turbulent flow than for viscous flow in the pressure region typical of the pressures that drive infiltration. These findings indicate that the transition pressure (where the flow changes from viscous to turbulent) is below the experimental range. Therefore, in our model, we assume flow to be proportional to the square-root of the applied pressure.

$$Q = A \sqrt{\frac{2}{\rho} \Delta P} \quad (1)$$

where

- Q is air flow [m^3/s],
- A is the effective leakage area [m^2],
- ρ is the density of air [$1.2 \text{ kg}/\text{m}^3$] and
- ΔP is the applied pressure [Pa].

It is the effective leakage area that characterizes the air leakage. In subsequent discussion we will refer to this parameter as the leakage area.

In an actual structure there are many leakage sites, each having a leakage area. In this model we combine the leakage sites into three areas: A_o is the total leakage area of the structure (the sum of the leakage areas of the floor, walls and ceiling), A_f is the leakage area of the floor, and A_c is the leakage area of the ceiling.

As will be shown in the Appendix, it is necessary to differentiate the floor and ceiling leakages from the total leakage area because the stack and wind pressures influence these locations differently.

Leakage Measurement

Air leakage is usually measured by fan pressurization.⁴ This technique uses a large-capacity fan to push air either into or out of the structure. Flow continuity requires that all the air that flows through the fan must flow out through the building shell. The graph relating pressure drop across the envelope and the resulting flow is called the leakage curve of the building.

In general, leakage curves obtained by this method will not show a square-root dependence on the pressure drop across the envelope. Our model assumes that there is such a dependency, however, and so we extrapolate the leakage curve (if necessary) down into the pressure range of natural weather effects (0-10 Pa). We then fit the leakage curve to a square-root in that region. The fitting procedure gives us the total leakage area of the structure.

Example: Assume that through fan pressurization tests the following flow vs. pressure data have been measured:

ΔP [Pa]	10	20	30	40	50
Q (m ³ /hr]	800	1220	1560	1850	2110

A two-parameter fit of these data to a power law function of the form,

$$Q = C \Delta P^n \quad (2)$$

gives us a flow coefficient of 202 and a pressure exponent of 0.6. Thus the data are described by this equation:

$$Q = 202 \Delta P^{(0.6)}$$

We use this equation to find the flow at our reference pressure. We have chosen 4 Pa as our reference pressure because it is the representative pressure for square-root flow in the 0-10 Pa range.

$$Q(4 \text{ Pa}) = 464 \frac{\text{m}^3}{\text{hr}}$$

Using this 4 Pa flow in Eq. 1, the leakage area is

$$A_o = 500 \text{ cm}^2$$

One can estimate the floor and ceiling leakage areas by measurement, by inspection, or by assumption. Direct measurement of the leakage curve for the floor and ceiling is the most accurate method; however, it is difficult and time-consuming. Direct measurement requires isolating the floor and ceiling from the rest of the structure and conducting a separate fan pressurization test. Accordingly, unless very detailed results are desired, direct measurement is usually not warranted.

Unlike walls, floor and ceiling surfaces have few penetrations. Once the penetrations are located and their physical dimensions measured, their leakage areas (usually smaller than the physical area of the opening) can easily be calculated by estimating the discharge coefficient from the geometry of the leaks. Various standard references contain tables or formulae for discharge coefficients. In cases where a floor or ceiling is made of materials that cannot leak (e.g., a slab floor), its leakage area may be assumed to be zero.

Finally, it is possible to assume a value for leakage not accounted for by measurement or calculation. For example, this can be done by assuming that the amount of leakage per unit shell area is the same for all surfaces (i.e. uniform leakage distribution).

INFILTRATION MODEL

In the Appendix we derive a general theory of infiltration. The model is a physical one which makes use of various empirical facts to reduce the complexity. All assumptions made in the derivation are specified in the Appendix.

In this model, we assume that the structure is a single well-mixed zone; we use typical shielding values for a simple rectangular structure and we neglect terms that depend on the sign of the temperature difference. Most importantly, we split the problem into two distinct parts: the wind-regime, where the dynamic wind pressure dominates the infiltration; and the stack-regime, where the temperature difference dominates the infiltration. Infiltration in the two regimes is expressed as follows:

$$Q_{\text{wind}} = f_w A_o v \quad (3.1)$$

$$Q_{\text{stack}} = f_s A_o \sqrt{gH \frac{\Delta T}{T}} \quad (3.2)$$

where

- Q_{wind} is the infiltration in the wind-regime [m^3/s],
- Q_{stack} is the infiltration in the stack-regime [m^3/s],
- v is the wind speed at ceiling height [m/s],
- ΔT is the inside-outside temperature difference [$^{\circ}\text{K}$],

- g is the acceleration of gravity [9.8 m/s²],
H is the height of the ceiling above grade [m] and
T is the inside temperature [K].

Derivations for f_w and f_s are presented in the Appendix, but their definitions are

$$f_w = C' (1 - R)^{1/3} \quad (4.1)$$

$$f_s = \frac{1}{3} (1 + R/2) \left[1 - \frac{X^2}{(2 - R)^2} \right]^{3/2} \quad (4.2)$$

C' is a generalized shielding coefficient; typical values are listed in Table 2 for a variety of local shielding conditions.

R is the fraction of the effective leakage area that is horizontal (i.e. the sum of the floor and ceiling leakage divided by the total leakage). X is the fractional difference between the floor and ceiling leakage (i.e. the difference in leakage area between the ceiling and the floor divided by the total leakage area):

$$R = \frac{A_c + A_f}{A_o} \quad (5.1)$$

$$X = \frac{A_c - A_f}{A_o} \quad (5.2)$$

The wind speed used in the equations above is the effective wind speed at ceiling height — that is, the wind speed that would exist at the height of the ceiling (above grade) if the building and its immediate surroundings were not there. This wind speed can be calculated from any measurement of the same wind using the following formula:

$$v = v' f_T \quad (6.1)$$

$$f_T = \left[\frac{\alpha \left(\frac{H}{10} \right)^\gamma}{\alpha' \left(\frac{H'}{10} \right)^\gamma} \right] \quad (6.2)$$

where

- v' is the measured wind speed (e.g. from a weather tower)
 f_T is the terrain factor,
 H is the height of the ceiling [m],
 H' is the height of the wind measurement [m],
 α, γ are empirical constants given in Table 1.

The unprimed quantities refer to the structure site and the primed quantities refer to the wind-measurement site.

The expressions for the stack-induced and wind-induced infiltration follow:

$$Q_{\text{stack}} = f_s^* A_o \sqrt{\Delta T} \quad (7.1)$$

$$Q_{\text{wind}} = f_w^* A_o v' \quad (7.2)$$

where

- A_o is the total leakage area [m²],
 f_w^* is the reduced wind parameter,
 f_{s*} is the reduced stack parameter [m/s/K^{1/2}],
 ΔT is the inside-outside temperature difference [K] and
 v' is the measured wind speed [m/s].

For the definitions of the reduced parameters, see the "Table of Defining Relations" and the "Symbol Table" at the end of the text.

The primary advantage (other than simplicity) of displaying the equations in this form is that it demonstrates the fact that we have separated the weather-independent parts (A_o, f_s^*, f_w^*) from the weather variables ($\Delta T, v'$). Thus the weather-independent parts can be calculated once for a particular structural configuration and combined with weather conditions to predict the infiltration.

Another advantage of this form of the equations is that it demonstrates that the infiltration is proportional to the total leakage area. Hence a fractional change in leakage area corresponds to the same fractional change in infiltration. While it is true that the reduced parameters depend on the relative distribution of the leakage among the floor, walls and ceiling, a small change in the total leakage should not affect them significantly.

Superposition Law for Infiltration

We now have expressions that allow us to calculate the stack-induced infiltration and wind-induced infiltration; the only problem that remains is that of combining them. In general, the interaction of such independent phenomena will be quite complicated but in the spirit of our simplified approach, we look only at the way in which each of them affects the differential pressure. Both the stack effect and wind effect influence the pressure distribution; we assume that their superposition can be treated by simply adding their pressure effects. Since we have assumed a square root dependence of flow on pressure, the stack-induced and wind-induced infiltration add in quadrature.

$$Q = \sqrt{Q_{\text{stack}}^2 + Q_{\text{wind}}^2} \quad (8)$$

where

Q is the combined infiltration [m^3/s].

In a previous work¹³ the authors demonstrated that whenever the wind effect or stack effect dominates, the first order term vanishes, making this type of combinatorial rule possible. Accurate prediction of the infiltration in the intermediate region requires detailed knowledge of both the weather and the structural parameters. On the average, however, the above formula will be correct; we will, therefore, use it for all cases, with the understanding that it is suspect whenever the stack and wind infiltrations are approximately equal.

This way of combining infiltrations can be generalized for any air flow that affects the internal pressure. For example, if there were an exhaust vent in operation, to calculate the total infiltration we would still add the independent air flows in quadrature.

$$Q = \sqrt{Q_{\text{stack}}^2 + Q_{\text{wind}}^2 + Q_{\text{vent}}^2} \quad (9)$$

where

Q_{vent} is the flow through the exhaust vent [m^3/s].

This superpositional rule does not apply to processes that do not affect the internal pressure, such as the case for a balanced air-to-air heat exchanger that uses both an intake and exhaust fan to push air in and out. There is, indeed, infiltration from this apparatus but because the flows are balanced there is no change in the pressure distribution; therefore, the infiltration caused by the balanced heat exchanger adds simply to the total of the rest of the infiltration.

We can generalize the combination to include balanced and unbalanced flows:

$$Q = \sum Q_b + \sqrt{\sum Q_u^2} \quad (10)$$

where

Q_b are the balanced flows [m^3/s] and

Q_u are the unbalanced flows [m^3/s].

In most cases all of the vents in a structure will be exhaust vents and, therefore, their flows can be treated as unbalanced. If, however, there are intake vents as well, that part of the exhaust flow which is balanced by intake flow is balanced flow and the remainder is unbalanced flow.

RESULTS

Fifteen different sites were extracted from the literature to represent a large spread in climate, house construction and measured infiltration rates.¹⁰⁻¹² In all cases, leakage data obtained by fan pressurization were available, permitting us to calculate the effective leakage area. (Note that the effective leakage area varies by a factor of 16 from tightest to loosest.) The fraction of leakage in the floor and ceiling, and the terrain parameters, were estimated from the qualitative description of each site. Table 3 contains summaries of the data extracted for each site.

For most of the sites, the data consist of several short-term infiltration measurements made on a single day. Most infiltration measurements were made using a tracer decay technique⁴ averaging infiltration over a one hour period with 5%-10% accuracy. For each measured infiltration point, a predicted infiltration was calculated from the weather variables and house parameters. Figures 1 and 2 contain the plots of predicted vs measured infiltration. Figure 3 displays the deviation of the predicted infiltration (by the percentage difference from the measurement) vs. the leakage area (cm²) for that site.

DISCUSSION

The separation of the weather-independent from the weather-dependant parts of the model allows the construction of a single graph that can be used to predict the infiltration from the weather data (See Fig. 4) First, the reduced stack and wind parameters are calculated from the geometry, leakage distribution, and terrain and shielding classes. Then these parameters are combined with the weather variables (temperature difference and measured wind speed) to find a point on the graph. This point corresponds to a particular ratio of infiltration to total leakage area as can be read from the curved lines of fig. 4. Finally, the ratio is multiplied by the total leakage area to find the infiltration. Since only the weather variables change over time, this method can be used repeatedly on a single site with a minimum of calculation.

Considering the simplicity of the model and the fact that there are no adjustable parameters*, the agreement is good. However, there are a few sites that do not show particularly good agreement; some overpredict and some underpredict. In order to explain these discrepancies, we examined other factors that may affect the infiltration.

Apparently, the biggest single factor affecting the accuracy of our model is the assumption that directional effects are unimportant. Directional effects could become important if the leakage of the walls varies from wall to wall, or if the shielding varies from face to face — either of which is possible.

* We use adjustable to imply that there is no physical meaning associated with that parameter (e.g. regression coefficients). Contrast this with physical parameters that must be estimated (e.g. R).

Aside from directional dependence, non-uniformity of wall leakage area will cause a relative decrease in the actual wind-induced infiltration. For example, if one wall of a structure is much leakier than the rest, it will act like a wind trap; when the wind blows on that wall the internal pressure will rise to mitigate the air flow through that face. Thus the wind-driven infiltration ought to be lower for non-uniform leakage than for uniform leakage. It is generally true that any directional effects will lower the infiltration — on the average.

Most likely, shielding will be the least uniform when it is the greatest, suggesting that directional effects should be more pronounced in more highly shielded situations. If we look at all of the Shielding Class 5 structures (2,8,13) we see a definite pattern of overprediction (19%,43%,19% respectively). While in no way conclusive this may indicate that directional effects are significant for these structures.

Our model has assumed that the floor and ceiling are unaffected by the wind. This assumption is violated whenever a leak through the floor or ceiling leads directly into the wind stream. The most probable instance of this condition is a vent, chimney or flue. If the wind is blowing over the top of a flue the infiltration will be greatly increased over what it would be otherwise. However, this effect is very directional dependent due to the turbulence caused by the wind interacting with the roof structure. The effect will be largest when the flue has a large leakage area; thus we expect to see a large effect in structures that have undampered fireplace chimneys. Two of the test structures had undampered chimneys (10,14) and they showed significant underprediction (-16%,-22% respectively).

While the accuracy of the model is sufficient for a wide variety of applications, the shortcomings described above suggest ways in which accuracy can be improved. Not only can we include new parameters to account for local shielding, but we can extend the model to account for stack flows through vents and flues and for active systems (e.g. furnace fans), all of which may interact with natural ventilation.

Retrofit Evaluation

In addition to predicting the absolute infiltration, the model is useful for predicting the change in infiltration as a result of retrofits. While some retrofits may affect the local shielding, most retrofits that affect infiltration will do so by changing the effective leakage area. Changes in the leakage area affect the three leakage

quantities: total leakage area, horizontal fraction, and ceiling/floor difference (A_0 , R, and X). For small changes in the total leakage area, the changes in R and X can be ignored and the fractional change in infiltration will be equal to the fractional change in leakage area. If the retrofits affect any of the walls, floor, or ceiling more than another, all three parameters must be used to recalculate the reduced parameters and then the infiltration.

CONCLUSION

We have introduced the concept of leakage area as the characteristic quantity associated with infiltration, just as conductivity is the characteristic quantity associated with conduction. Using this concept, we have devised a model for predicting the infiltration based on a few easily determined physical parameters. Houses of widely different construction types and located in various climatic conditions can be measured and compared by means of this model, inasmuch as all of the parameters used (i.e. leakage areas, terrain classes etc.) have physical reality outside of our model and are, therefore, independently measurable.

In future studies, we will explore long-term average infiltration data from a number of dissimilar sites to test the overall scale of the model. In addition, we will measure infiltration before and after retrofit, comparing the predicted infiltration reduction based on our model with the actual infiltration reduction based on tracer gas measurements.

APPENDIX

Derivation of basic model

In this appendix the basic physical model of infiltration will be derived. The derivation presented in this appendix has been explained in much greater detail in a previous work.¹³ Accordingly, we shall present the model used in the text without presenting the useful, though unnecessary, tangents.

First, we separate the driving forces (differential surface pressures) from the response of the structure to the driving forces (air leakage). Second, we combine the surface pressures with the leakage function (and geometry) to calculate infiltration. In the following sections, we will combine these two operations into a complete description of weather-driven infiltration.

LEAKAGE MODEL

Air leakage is the natural flow of air through cracks, holes, etc. across the building envelope. There are two physically well-defined types of air flow: viscous and turbulent. In the viscous regime, the flow is proportional to the applied pressure; in turbulent flow, the flow is proportional to the square-root of the applied pressure. The type of flow is determined by the applied pressure and the geometry of the openings.

Recent evidence⁶ indicates that even at low pressures the flow through a structure is dominated by turbulent flow. That is, viscous forces do not appear to dominate the air leakage at typical weather-induced pressures. This statement is expressed by the equation,

$$Q_j = A_j \sqrt{\frac{2}{\rho} \Delta P_j} \quad (A1)$$

where

- | | |
|--------------|---------------------------------------------------------------------------|
| Q_j | is the flow through the j th leakage site [m^3/s], |
| A_j | is called the effective leakage area of the j th site [m^2], |
| ΔP_j | is the pressure drop across the j th site [Pa]. |

This expression relates the pressure drop across a particular leakage site to the flow rate through it. The parameter that describes the leakage is the effective leakage area.

Although every leakage site can be given an effective leakage area, in any real situation it will be practically impossible to measure all of the sites in the envelope individually. We therefore restrict our attention to only three different (lumped) leakage areas: the floor, the walls and the ceiling.

SURFACE PRESSURES

Now that we have a way of relating pressure drops across the envelope to air flow through the envelope, we must be able to calculate the differential surface pressures across the envelope caused by the weather.

Differential pressures on a structure are caused by the stack effect and the wind effect. The stack effect is the height-varying, hydrostatic, indoor-outdoor pressure difference caused by a difference in densities of the two bodies of air, which, in turn, is caused by the difference in temperature of the two bodies of air. The wind effect is an exterior pressure shift caused by a stream of air impinging upon a stationary object.

In our previous work we found that the stack effect and wind effect can be treated independently. Accordingly, we separate the problem into two regimes: the stack-regime (where the wind effect is ignored); and the wind-regime (where the stack effect is ignored).

Stack Effect

The stack pressure is caused by the existence of bodies of air at different temperatures having different densities. From hydrostatic equilibrium we know that the change in pressure with respect to height is proportional to the density.

$$\frac{dP}{dh} = - \rho g \quad (A2)$$

where

- P is the static pressure [Pa],
h is the height [m],
p is the density of the air [kg/m³] and
g is the acceleration of gravity [9.8 m/s²].

In the case of a structure, the inside and outside bodies of air will usually be of different temperatures; therefore, there will be a differential surface pressure that changes with height:

$$\frac{d\Delta P}{dh} = - p g (1 - \frac{p'}{p}) \quad (A3)$$

where

- ΔP is the differential surface pressure [Pa],
p is the density of outside air [1.2 kg/m³],
p' is the density of inside air [kg/m³],.

Using the ideal gas law, we can replace the density difference factor with a temperature difference factor:

$$\frac{d\Delta P}{dh} = - p g \frac{\Delta T}{T} \quad (A4)$$

where

- ΔT is the inside-outside temperature difference [K] and
T is the inside temperature [295K].

We can now integrate this expression to find the actual pressure difference:

$$\Delta P = \Delta P_o - p g h \frac{\Delta T}{T} \quad (A5)$$

where

- ΔP_o is the internal pressure shift [Pa].

The internal pressure shift is fixed by the requirement that for every cubic meter of air that enters, a cubic meter must leave the structure. We can rewrite this expression by making these definitions:

$$P_s = \rho g H \frac{\Delta T}{T} \quad (A6.1)$$

$$\Delta P_o = P_s \left(\frac{1}{2} + \mu \right) \quad (A6.2)$$

where

- P_s is the stack pressure [Pa],
 H is the height of the structure [m] and
 μ is the normalized neutral level.

The neutral level is the height at which the inside and outside static pressures are equal; μ is equal to the height of the neutral divided by the height of the structure minus one half. Equivalently, μ is the difference between the height of the neutral level and the mid-point of the structure divided by the height of the structure.

Solving for the total pressure difference across the envelope,

$$\Delta P = P_s \left(\mu + \frac{1}{2} - \frac{h}{H} \right) \quad (A7)$$

This expression gives us the differential pressure across the envelope, at every point on it. In order to calculate the air flow through the envelope we must integrate the differential pressures with the air leakage over the entire envelope, making sure to keep track of the infiltration and exfiltration separately.

We are assuming that the floor and ceiling are each at a single height and that their leakage can be considered uniform, thus eliminating the need for integration to calculate the flow through these surfaces. Rewriting the expressions by using the definition that floor is at $h=0$ and, therefore, the ceiling is at $h=H$, we get:

$$Q_{\text{ceiling}}^- = A_c \sqrt{\frac{2}{\rho} P_s \left(\frac{1}{2} - \mu \right)} \quad (A8.1)$$

$$Q_{\text{floor}}^+ = A_f \sqrt{\frac{2}{\rho} P_s \left(\frac{1}{2} + \mu \right)} \quad (A8.2)$$

$$Q_{\text{ceiling}}^+ = Q_{\text{floor}}^- = 0 \quad (\text{A8.3})$$

where

A_c is the effective leakage area of the ceiling [m^2] and

A_f is the effective leakage area of the floor [m^2].

The superscripts \pm imply infiltration/exfiltration respectively

In stack-dominated flow there is no infiltration through the ceiling nor is there any exfiltration through the floor because of the sign of the pressure difference across them.

We can find the infiltration through the walls by integrating from the floor to the neutral level and the exfiltration by integrating from the neutral level to the ceiling. The results are:

$$Q_{\text{walls}}^+ = A_w \sqrt{\frac{2}{p} P_s \left(\frac{1}{2} + \mu \right)} \left[\frac{2}{3} \left(\frac{1}{2} + \mu \right) \right] \quad (\text{A9.1})$$

$$Q_{\text{walls}}^- = A_w \sqrt{\frac{2}{p} P_s \left(\frac{1}{2} - \mu \right)} \left[\frac{2}{3} \left(\frac{1}{2} - \mu \right) \right] \quad (\text{A9.2})$$

where

A_w is the effective leakage area of the walls [m^2].

If we now make the useful definitions,

$$v_s = \sqrt{\frac{2}{p} P_s} \quad (\text{A10.1})$$

$$A_o = A_w + A_c + A_f \quad (\text{A10.2})$$

$$R = \frac{A_c + A_f}{A_o} \quad (\text{A10.3})$$

$$X = \frac{A_c - A_f}{A_o} \quad (\text{A10.4})$$

where

- v_s is the equivalent stack velocity [m/s],
 A_o is the total (effective) leakage area[m²],
 R is the fraction of leakage in the floor and ceiling and
 X is the effective leakage distribution parameter.

We can rewrite the expressions for the total stack infiltration and exfiltration:

$$Q_{stack}^+ = A_o v_s \left[\frac{R - X}{2} \sqrt{\frac{1}{2} + \mu} + \frac{2}{3} (1 - R) \left(\frac{1}{2} + \mu \right)^{3/2} \right] \quad (A11.1)$$

$$Q_{stack}^- = A_o v_s \left[\frac{R + X}{2} \sqrt{\frac{1}{2} - \mu} + \frac{2}{3} (1 - R) \left(\frac{one}{two} - \mu \right)^{3/2} \right] \quad (A11.2)$$

So far μ has been an undetermined parameter; but, by equating the two expressions above we can find an expression for μ . However, this expression is non-linear and cannot be solved in closed form for μ ; therefore, we must solve this equation using approximation methods:

$$\mu = \frac{X}{1 + X^2} \frac{1}{2 - R} \quad (A12)$$

This expression has been verified numerically to vary by no more than a few percent from the exact value.

Any errors in the value of the neutral level will be reflected in the lack of equality between the infiltration and exfiltration. Therefore, the best estimate of the actual infiltration will be the average of these two quantities. As before, the equations are non-linear and approximation techniques must be employed to find the stack infiltration:

$$Q_{stack} = \frac{A_o v_s}{3} (1 + R/2) \left[1 - \frac{X^2}{(2 - R)^2} \right]^{3/2} \quad (A13)$$

Again, this expression is accurate to within a couple of percent. In order to simplify the appearance of this expression, we make the following definitions:

$$f_s = \frac{1}{3} (1 + R/2) \left[1 - \frac{x^2}{(2 - R)^2} \right]^{3/2} \quad (\text{A14.1})$$

$$f_s^* = f_s \sqrt{\frac{gH}{T}} \quad (\text{A14.2})$$

where

f_s is the stack parameter and

f_s^* is the reduced stack parameter $[\text{m/s/K}^{1/2}]$.

Using these definitions yields expressions for the stack-regime infiltration:

$$\begin{aligned} Q_{\text{stack}} &= f_s A_o v_s \\ &= f_s^* A_o \sqrt{\Delta T} \end{aligned} \quad (\text{A15})$$

As a final simplification we may define the reduced stack velocity.

$$v_s^* = f_s v_s = f_s^* \sqrt{\Delta T} \quad (\text{A16})$$

where

v_s^* is the reduced stack velocity $[\text{m/s}]$.

The final simplified expression for the stack-induced infiltration is,

$$Q_{\text{stack}} = A_o v_s^* \quad (\text{A17})$$

In the derivation above we used the leakage distribution parameter, X , to find the height of the neutral level. In some circumstances, the height of the neutral level is measured independently. In this case it is possible to derive an effective leakage distribution parameter (X) from the height of the neutral level.

$$X = \frac{4}{3} \mu \left[1 - R + \frac{1 + R/2}{1 + \sqrt{1 - 4\mu^2}} \right] \quad (\text{A18})$$

where

X is the effective leakage distribution parameter and

μ is the measured neutral level shift.

This relationship between X and μ is exact.

Wind Effect

The dynamic pressure caused by wind striking a fixed object called the stagnation pressure is given by,

$$P_{st} = \frac{1}{2} \rho v^2 \quad (A19)$$

where

P_{st} is the stagnation pressure and

v is the wind speed.

We define the wind speed, v, to be the wind speed at the ceiling height of the structure, as if the structure and immediate surroundings were not there. Thus, in our definition of wind speed, we are excluding any effects of local environment. However, because of the nature of wind dynamics, the wind speed measured at one height in one type of terrain will not be the same as the wind speed measured at another height or in another type of terrain.

To account for this variability, we use a standard formula¹⁴ to calculate the wind speed at any height and terrain class from the wind speed at any other height and terrain class:

$$v = v_o \alpha \left(\frac{H}{10} \right)^\gamma \quad (A20)$$

where

v is the actual wind speed

v_o is the wind speed at standard conditions

α, γ are constants that depend on terrain class

To calculate the wind speed at one site from measured data at another site, we first use the above formula to calculate the standard wind speed for the measurement site; then the standard wind speed is used to calculate the wind speed at the desired site. Standard conditions are defined to be a height of 10 m and a terrain of class II. The following formulae are useful in the calculation of the actual wind speed:

$$v = v_o \alpha \left[\frac{H}{10} \right]^\gamma \quad (\text{A21.1})$$

$$v' = v_o \alpha' \left[\frac{H'}{10} \right]^{\gamma'} \quad (\text{A21.2})$$

$$v = v' \left[\frac{\alpha \left[\frac{H}{10} \right]^\gamma}{\alpha' \left[\frac{H'}{10} \right]^{\gamma'}} \right] \quad (\text{A21.3})$$

In these expressions, the primed quantities are from a wind measurement site. Values for the two terrain class dependent parameters are shown in Table 1.

From the above expression we can define a terrain factor, f_T , that converts measured wind speed into effective wind speed:

$$f_T = \left[\frac{\alpha \left[\frac{H}{10} \right]^\gamma}{\alpha' \left[\frac{H'}{10} \right]^{\gamma'}} \right] \quad (\text{A22})$$

We must take into account the effect of local environment on the wind pressures felt by the structure. We do this by introducing shielding coefficients* that convert the stagnation pressure into the actual pressure felt by the exterior of the structure.

Full-scale studies¹⁵ have shown that the pressure distribution on flat faces can be adequately described by using the average pressure on the face. Accordingly, there is one shielding coefficient for every

* The term shielding coefficient is equivalent to the more standard term of exterior pressure coefficient; the only difference lies in the interpretation. We use the term shielding coefficient to mean the ratio of the average exterior wind pressure to the stagnation pressure at the ceiling height.

face of the structure:

$$\Delta P_j^e = C_j \frac{1}{2} \rho v^2 = C_j P_{st} \quad (A23)$$

where

ΔP_j^e is the exterior pressure rise due to the wind and

C_j is the shielding coefficient for the j th face.

The shielding coefficients are functionally dependent on the angle between the incident wind and the orientation of the structure. Since we will eventually average the shielding coefficients over angle, we have suppressed their explicit dependence on angle.

Similar to the stack effect, the wind effect causes an internal pressure shift. As long as the shielding coefficients themselves are not functions of wind speed, the internal pressure shift will be proportional to the stagnation pressure:

$$\Delta P_o = C^o \frac{1}{2} \rho v^2 \quad (A24)$$

where

ΔP_d is the internal pressure shift [Pa] and

C^o is called the internal shielding coefficient.

From these two equations we can calculate the pressure drop across any of the faces:

$$\Delta P_j = (C_j - C^o) \frac{1}{2} \rho v^2 \quad (A25)$$

To find the infiltration and exfiltration, we must combine this expression with our leakage function:

$$Q_{wind}^+ = \sum_+ A_j \sqrt{\frac{2}{\rho} (C_j - C^o) P_{st}} \quad (A26.1)$$

$$Q_{wind}^- = \sum_- A_j \sqrt{\frac{2}{\rho} (C^o - C_j) P_{st}} \quad (A26.2)$$

The $+$ ($-$) under the summation sign indicates that the exterior shielding coefficient is larger (smaller) than the interior shielding coefficient.

In most cases the ceiling and floor of a structure are well shielded (i.e. there is usually an attic, basement or slab that protects these horizontal surfaces from direct wind effects). Accordingly, we assume that their shielding coefficients are negligible. Substituting the definition of the stagnation pressure and averaging over angle yields,

$$Q_{wind}^+ = A_w v < \sqrt{C_j - C^0} >_+ \quad (A27.1)$$

$$Q_{wind}^- = A_w v < \sqrt{C^0 - C_j} >_- \quad (A27.2)$$

where

$< \dots >_+$ indicates an average for $C_j > C^0$ and

$< \dots >_-$ indicates an average for $C_j < C^0$.

The internal shielding coefficient like the neutral level is fixed by the requirement that the exfiltration must equal the infiltration.

Once the internal shielding coefficient has been determined the wind effect infiltration can be calculated from the average of the two wind flows. We obtain:

$$Q_{wind} = \frac{A_o}{2} v (1 - R) < \sqrt{|C_j - C^0|} > \quad (A28)$$

We must now evaluate the shielding coefficients to finish the calculation of the wind effect. In most cases, the shielding coefficients of a structure will not be known; therefore, we propose to use wind tunnel data for a typically shaped structure within a turbulent boundary layer. Such a study was done at Colorado State University by Akins, et. al.¹⁶ They considered a structure that had no local obstructions (i.e. there were no obstacles within several structure heights). For this case we find the following values:

$$C^0 = -.21 \quad (A29.1)$$

$$< \sqrt{|C_j - C^0|} > = 0.68 \quad (A29.2)$$

In the preceding analysis we completely neglected the effect of the floor and ceiling leakage. Even though we have assumed that the shielding coefficients for the floor and the ceiling are negligible, the shift

of the internal pressure due to the internal pressure coefficient will cause either infiltration or exfiltration in both the floor and the ceiling. This effect can be treated empirically by changing the dependence of the wind effect on R:

$$Q_{\text{wind}} = \frac{A_o}{2} v (1 - R)^{2/3} < \sqrt{|C_j - C^o|} > \quad (\text{A30})$$

The wind tunnel measurements have given us an effective shielding coefficient for the case in which there is no local shielding around the structure; however, in most real cases there will be significant obstruction of the air flow in the immediate vicinity of the structure. Therefore, we will generalize the shielding coefficient to allow for different classes of local shielding. The wind-regime infiltration equation can be rewritten to express this:

$$Q_{\text{wind}} = A_o v C' (1 - R)^{2/3} \quad (\text{A31})$$

where

C' is the generalized shielding coefficient (cf. Table 2).

We can simplify the appearance of this expression much as we did for the stack expressions by defining some new parameters:

$$f_w = C' (1 - R)^{1/3} \quad (\text{A32.1})$$

$$f_w^* = f_w f_T \quad (\text{A32.2})$$

where

f_w is the wind parameter and

f_w^* is the reduced wind parameter.

This leads to more concise expressions for the wind effect infiltration:

$$\begin{aligned} Q_{\text{wind}} &= f_w A_o v \\ &= f_w^* A_o v' \end{aligned} \quad (\text{A33})$$

where

v is the local wind speed [m/s] and

v' is the wind speed measured on a weather tower [m/s].

We define the reduced wind speed as the product of the wind parameter and the effective wind speed:

$$v^* = f_w v = f_w^* v' \quad (A34)$$

where

v^* is the reduced wind speed [m/s].

This leads to a simple expression for the wind effect infiltration:

$$Q_{\text{wind}} = A_o v^* \quad (A35)$$

REFERENCES

1. D.R. Bahnfleth, D.T. Moseley, and W.S. Harris, "Measurement of Infiltration in Two Residences," ASHRAE Trans., 63, p. 439-452, (1957).
2. J.B. Dick, and D.A. Thomas, "Ventilation Research in Occupied Houses," J. Inst. Heat. Vent. Eng., 19, p. 306-332, (1951).
3. N. Malik, "Field Studies of Dependence of Air Infiltration on Outside Temperature and Wind," Energy and Buildings, 1, p. 281-292, (1978).
4. D.T. Grimsrud, M.H. Sherman, R.C. Diamond, P.E. Condon, and A.H. Rosenfeld, "Infiltration-Pressurization Correlations: Detailed Measurements on a California House," ASHRAE Trans., 85, Part 1 p. 851-865, (1979). Lawrence Berkeley Laboratory Report LBL-7824 (1978)
5. D.W. Etheridge, "Crack Flow Equations and Scale Effect," Building & Environment, 12, p. 181-189, (1977).
6. M.H. Sherman, D.T. Grimsrud, and R.C. Sonderegger, "Low Pressure Leakage Function of a Building," Proc. ASHRAE-DOE Conference on the Thermal Performance of the Exterior Envelopes of Buildings, Orlando, Florida, December 1979. Lawrence Berkeley Laboratory Report LBL-9162 (1979)
7. A.K. Blomsterberg, and D.T. Harrje, "Approaches to Evaluation of Air Infiltration Energy Losses in Buildings," ASHRAE Trans., 85, Part 1 p. 797-815, (1979).
8. D.T. Grimsrud, M.H. Sherman, R.C. Diamond, and R.C. Sonderegger, "Air Leakage, Surface Pressures and Infiltration Rates in Houses," Proc. of the Second International CIB Symposium, Copenhagen, Denmark, May 1979, Lawrence Berkeley Laboratory Report LBL-8828 (1979)
9. D.T. Harrje, A.K. Blomsterberg, and A. Persily, "Reduction of Air Infiltration due to Window and Door Retrofits in an Older Home," Princeton University/Center for Environmental Studies Report No. 85, (1979).

10. D.T. Grimsrud, M.H. Sherman, A.K. Blomsterberg, and A.H. Rosenfeld, "Infiltration and Air Leakage Comparisons: Conventional and Energy Efficient Housing Designs," Presented at the International Conference on Energy Use Management, Los Angeles, October 1979. Lawrence Berkeley Laboratory Report LBL-9157 (1979)
11. Johns-Manville Research and Development Center, "Demonstration of Energy Conservation through Reduction of Air Infiltration in Electrically Heated Houses," RP 1351-1, (1979).
12. G.T. Tamura, "The Calculation of House Infiltration Rates," ASHRAE Trans, 85, Part 1 p. 58-71, (1979).
13. M.H. Sherman, D.T. Grimsrud, "Infiltration-Pressurization Correlations: Simplified Physical Modeling," ASHRAE Trans. 86 Part II (1980), Lawrence Berkeley Laboratory Report LBL-10163 (1980)
14. European Convention for Constructional Steelwork, "Recommendations for the Calculation of Wind Effects on Buildings and Structures", Technical General Secretariat, Brussels, Belgium September 1978.
15. S. Kim, K.C. Mehta, "Full Scale Measurements on a Flat Roof Area," Proceedings of the Fifth Int. Conf. Wind Engineering, Boulder, Colorado, July 1979.
16. R.E. Akins, J.A. Peterka, and J.E. Cermak, "Average Pressure Coefficients for Rectangular Buildings," Proceedings of the Fifth Int. Conf. Wind Engineering, Boulder, Colorado, July 1979.

ACKNOWLEDGMENT

The authors would like to thank all the members of the Academy for their support and guidance in the preparation of this report.

TABLE 1: Terrain Parameters for Standard Terrain Classes			
Class	γ	α	Description
I	0.10	1.30	Ocean or other body of water with at least 5km of unrestricted expanse
II	0.15	1.00	Flat terrain with some isolated obstacles (e.g. buildings or trees well separated from each other)
III	0.20	0.85	Rural areas with low buildings, trees, etc.
IV	0.25	0.67	Urban, industrial or forest areas
V	0.35	0.47	Center of large city (e.g. Manhattan)

Table 2: Generalized Shielding Coefficient vs. Local shielding		
Shielding Class	C'	Description
I	0.24	No obstructions or local shielding whatsoever
II	0.30	Light local shielding with few obstructions
III	0.25	Moderate local shielding, some obstructions within two house heights
IV	0.19	Heavy shielding, obstructions around most of perimeter
V	0.11	Very heavy shielding, large obstruction surrounding perimeter within two house heights

TABLE 3.1 : Test Results for Test Site #1

Site ID: IVANHOE
 Reference No. 10
 House Volume¹: 480
 No. of Stories: 2
 Leakage Area²: 100
 Terrain factor: .85
 Shielding Class: 3

 Reduced wind parameter: .19
 Reduced stack parameter³: .16

Predicted and Measured Infiltration ⁴				
Stack	Wind	Total Predicted	Measured	Difference
27	27	38	58	-34%
27	55	61	58	5%
27	41	49	48	2%

TABLE 3.2 : Test Results for Test Site #2

Site ID: Nogal
 Reference No. 10
 House Volume¹: 290
 No. of Stories: 1
 Leakage Area²: 960
 Terrain factor: .70
 Shielding Class: 5

 Reduced wind parameter: .08
 Reduced stack parameter³: .10

Predicted and Measured Infiltration ⁴				
Stack	Wind	Total Predicted	Measured	Difference
60	47	76	64	19%

1) m³

2) cm²

3) m/s/K^{1/2}

4) m³/hr

TABLE 3.3 : Test Results for Test Site #3

Site ID: Telemark
 Reference No: 10
 House Volume¹: 480
 No. of Stories: 2
 Leakage Area²: 140
 Terrain factor: .85
 Shielding Class: 2

Reduced wind parameter: .22
 Reduced stack parameter³: .12

Predicted and Measured Infiltration ⁴				
Stack	Wind	Total Predicted	Measured	Difference
31	53	61	63	-3%
30	42	52	48	8%
30	32	44	38	16%

TABLE 3.4 : Test Results for Test Site #4

Site ID: Torey Pines
 Reference No: 11
 House Volume¹: 233
 No. of Stories: 3
 Leakage Area²: 200
 Terrain factor: .90
 Shielding Class: 4

Reduced wind parameter: .16
 Reduced stack parameter³: .14

Predicted and Measured Infiltration ⁴				
Stack	Wind	Total Predicted	Measured	Difference
43	81	92	82	12%
44	69	82	72	14%
44	81	92	98	-6%
44	92	102	98	4%
45	92	103	89	16%

1) m³

2) cm²

3) m/s/K^{1/2}

4) m³/hr

TABLE 3.5 : Test Results for Test Site #5

Site ID: R-10
 Reference No. 11
 House Volume¹: 233
 No. of Stories: 1
 Leakage Area²: 330
 Terrain factor: .85
 Shielding Class: 3

 Reduced wind parameter: .15
 Reduced stack parameter³: .09

Predicted and Measured Infiltration ⁴				
Stack	Wind	Total Predicted	Measured	Difference
50	80	94	105	-10%

TABLE 3.6 : Test Results for Test Site #6

Site ID: T1
 Reference No. 12
 House Volume¹: 337
 No. of Stories: 1
 Leakage Area²: 330
 Terrain factor: .77
 Shielding Class: 3

 Reduced wind parameter: .14
 Reduced stack parameter³: .10

Predicted and Measured Infiltration ⁴				
Stack	Wind	Total Predicted	Measured	Difference
64	23	68	74	-8%
12	45	46	54	-15%
51	67	84	78	8%

1) m³

2) cm²

3) m/s/K^{1/2}

4) m³/hr

TABLE 3.7 : Test Results for Test Site #7

Site ID: T2
 Reference No. 12
 House Volume¹: 433
 No. of Stories: 1
 Leakage Area²: 680
 Terrain factor: .77
 Shielding Class: 3

Reduced wind parameter: .17
 Reduced stack parameter³: .11

Predicted and Measured Infiltration ⁴				
Stack	Wind	Total Predicted	Measured	Difference
115	112	161	169	-5%
28	29	40	48	-17%
154	196	249	199	25%

TABLE 3.8 : Test Results for Test Site #8

Site ID: HAVEN
 Reference No. 10
 House Volume¹: 230
 No. of Stories: 1
 Leakage Area²: 770
 Terrain factor: .71
 Shielding Class: 5

Reduced wind parameter: .07
 Reduced stack parameter³: .10

Predicted and Measured Infiltration ⁴				
Stack	Wind	Total Predicted	Measured	Difference
55	39	67	49	37%
92	58	109	71	54%
88	78	117	85	38%

1) m³

2) cm²

3) m/s/K^{1/2}

4) m³/hr

TABLE 3.9 : Test Results for Test Site #9

Site ID: PURDUE
 Reference No. 10
 House Volume¹: 240
 No. of Stories: 1
 Leakage Area²: 855
 Terrain factor: .62
 Shielding Class: 4

 Reduced wind parameter: .11
 Reduced stack parameter³: .11

Predicted and Measured Infiltration ⁴				
Stack	Wind	Total Predicted	Measured	Difference
102	67	122	120	2%
102	67	122	125	-2%
102	136	170	154	10%
107	170	200	166	20%

TABLE 3.10: Test Results for Test Site #10

Site ID: NEILSON
 Reference No. 10
 House Volume¹: 250
 No. of Stories: 1
 Leakage Area²: 1275
 Terrain factor: .62
 Shielding Class: 3

 Reduced wind parameter: .15
 Reduced stack parameter³: .12

Predicted and Measured Infiltration ⁴				
Stack	Wind	Total Predicted	Measured	Difference
123	138	185	175	6%
135	138	193	160	21%
110	69	130	185	-30%
123	69	141	340	-59%

1) m³

2) cm²

3) m/s/K^{1/2}

4) m³/hr

TABLE 3.11: Test Results for Test Site #11

Site ID: VALENCIA 1
 Reference No: 10
 House Volume¹: 270
 No. of Stories: 1
 Leakage Area²: 560
 Terrain factor: .81
 Shielding Class: 3

Reduced wind parameter: .18
 Reduced stack parameter³: .12

Predicted and Measured Infiltration ⁴				
Stack	Wind	Total Predicted	Measured	Difference
59	76	96	84	-5%
64	80	102	89	15%

TABLE 3.12: Test Results for Test Site #12

Site ID: VALENCIA 2
 Reference No: 10
 House Volume¹: 270
 No. of Stories: 1
 Leakage Area²: 630
 Terrain factor: .81
 Shielding Class: 4

Reduced wind parameter: .14
 Reduced stack parameter³: .12

Predicted and Measured Infiltration ⁴				
Stack	Wind	Total Predicted	Measured	Difference
82	143	165	173	14%
61	67	90	78	15%

1) m³

2) cm²

3) m/s/K^{1/2}

4) m³/hr

TABLE 3.13: Test Results for Test Site #13

Site ID: FELS
Reference No. 9
House Volume¹: 470
No. of Stories: 2
Leakage Area²: 1480
Terrain factor: .84
Shielding Class: 5

Reduced wind parameter: .08
Reduced stack parameter³: .13

Predicted and Measured Infiltration ⁴				
Stack	Wind	Total Predicted	Measured	Difference
277	170	325	355	-8%
183	426	464	320	45%

TABLE 3.14: Test Results for Test Site #14

Site ID: SAN CARLOS
Reference No. 10
House Volume¹: 145
No. of Stories: 1
Leakage Area²: 845
Terrain factor: .81
Shielding Class: 4

Reduced wind parameter: .15
Reduced stack parameter³: .11

Predicted and Measured Infiltration ⁴				
Stack	Wind	Total Predicted	Measured	Difference
0	76	76	149	-49%
47	49	68	116	-41%
47	89	101	90	12%
0	93	93	107	-13%

1) m³

2) cm²

3) m/s/K^{1/2}

4) m³/hr

TABLE 3.15: Test Results for Test Site #15

Site ID: SOUTHAMPTON
Reference No: 10
House Volume¹: 1000
No. of Stories: 3
Leakage Area²: 1640
Terrain factor: .90
Shielding Class: 3

Reduced wind parameter: .20
Reduced stack parameter³: .16

Predicted and Measured Infiltration ⁴				
Stack	Wind	Total Predicted	Measured	Difference
94	124	156	250	38%
188	124	255	310	-18%
94	124	156	190	-18%

SYMBOL TABLE	
A	is the effective leakage area [m ²]
A _o	is the total leakage area ($\sum_w A_w + A_f + A_c$)
c	is the subscript indicating the ceiling
C	is a (wind pressure) shielding coefficient
C ^o	is the internal (wind) pressure coefficient
C'	is the generalized shielding coefficient
f _s	is the stack-effect factor
f _s [*]	is the reduced-stack effect factor [m/s/ $\sqrt{\theta K}$]
f _T	is the terrain factor
f _w	is the wind-effect factor
f _w [*]	is the reduced wind-effect factor
g	is the acceleration of gravity [9.8 m/sec ²]
h	is a height variable [m]

1) m³

2) cm²

3) m/s/K^{1/2}

4) m³/hr

SYMBOL TABLE

H	is the height of the ceiling above grade [m]
H'	is the height of the wind measurement
j	is an index to denote each face of the structure
L	is a semi-empirical constant leakage coefficient
n	is a semi-empirical constant leakage exponent
P_{st}	is the stagnation pressure ($\frac{1}{2}\rho v^2$) [Pa]
P_s	is the stack pressure ($\rho g H \frac{\Delta T}{T}$)
ΔP	is an applied pressure difference.
ΔP_j^w	is the exterior pressure rise due to the wind
ΔP_o	is the internal pressure change
Q	is air flow [m ³ /sec]
$Q(\Delta T, v)$	is the instantaneous infiltration
Q_{stack}	is the infiltration in the stack regime
Q_{wind}	is the infiltration in the wind regime
R	fraction of leakage area combined in floor and ceiling
T	is the inside temperature [°K]
ΔT	is the inside-outside temperature difference
v	is the wind speed at ceiling height [m/sec]
v^*	is the reduced wind speed
v_o	is the wind speed at standard (terrain) conditions
v_s	critical wind speed
v_s^*	reduced critical wind speed
v'	is the measured wind speed
α	is a constant that depends on terrain class (see tables above)
β	is a normalized height
γ	is a constant dependent on terrain class (see tables above)
μ	is the fraction shift in the neutral level from the mid-point
ρ	is the density of air [1.2 kg/m ³]
\pm	indicates depressurization/pressurization or infiltration/exfiltration, respectively

Table of Defining Relations

$$R = \frac{A_c + A_f}{A_o}$$

$$X = \frac{A_c - A_f}{A_o}$$

$$f_w = C' (1 - R)^{1/3}$$

$$f_s = \frac{1}{3} (1 + R/2) \left(1 - \frac{X^2}{(2 - R)^2}\right)^{3/2}$$

$$v = v' f_T$$

$$f_T = \left[\frac{\alpha \left(\frac{H}{10} \right)^Y}{\alpha' \left(\frac{H'}{10} \right)^{Y'}} \right]$$

$$v^* = f_w v = v' f_w^*$$

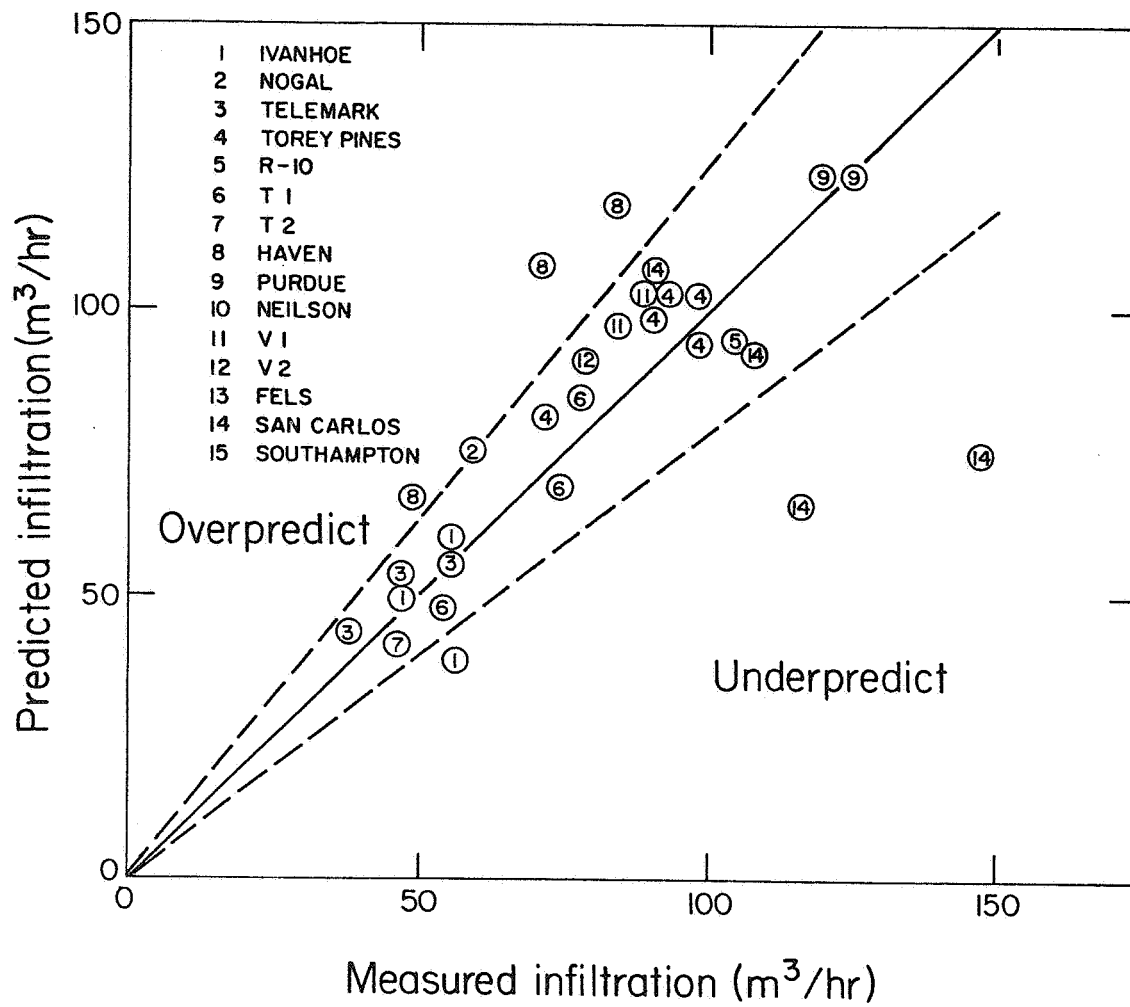
$$f_w^* = f_w f_T$$

$$v_s^* = f_s^* \sqrt{\Delta T}$$

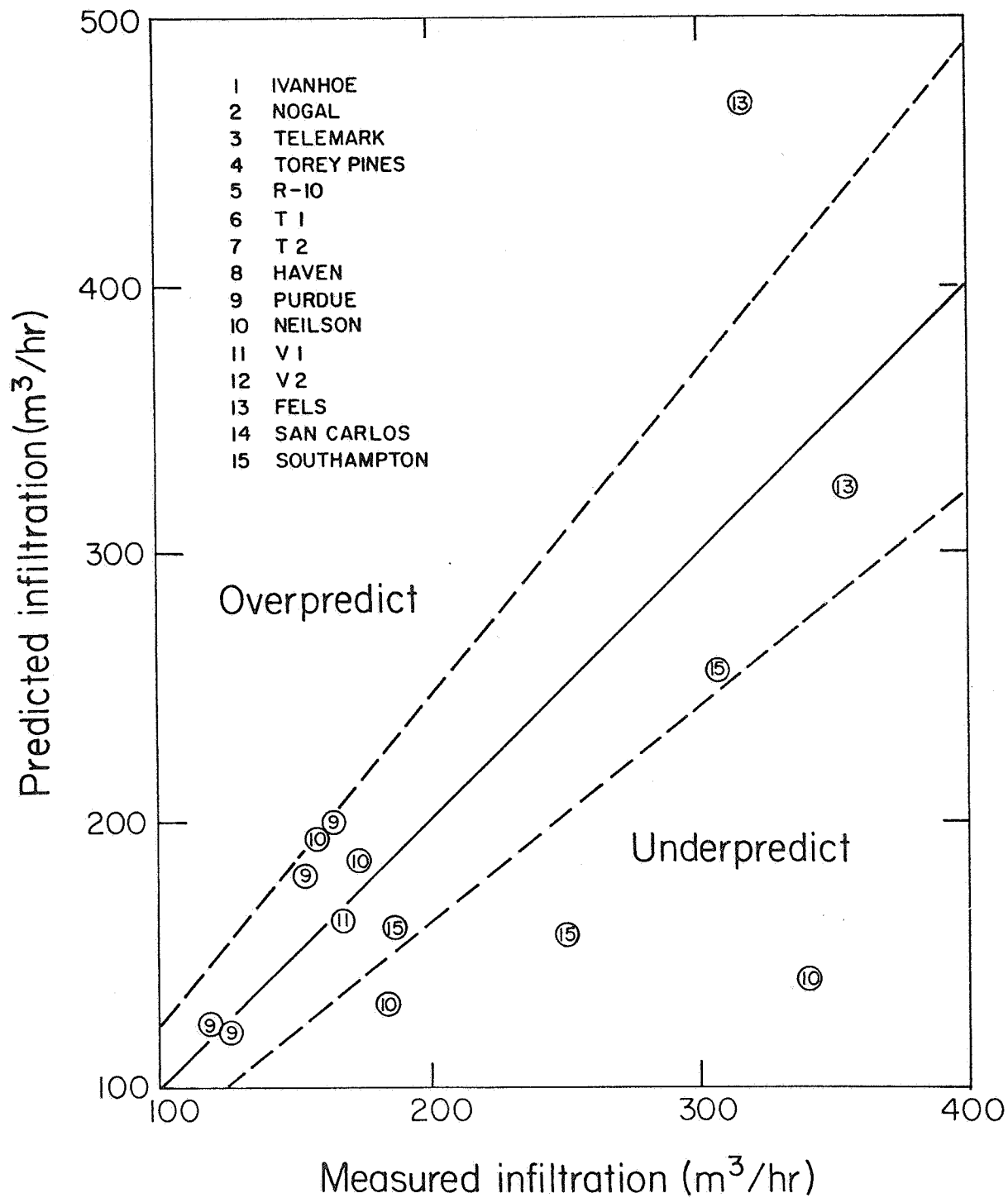
$$f_s^* = f_s \sqrt{\frac{gH}{T}}$$

Figure Captions

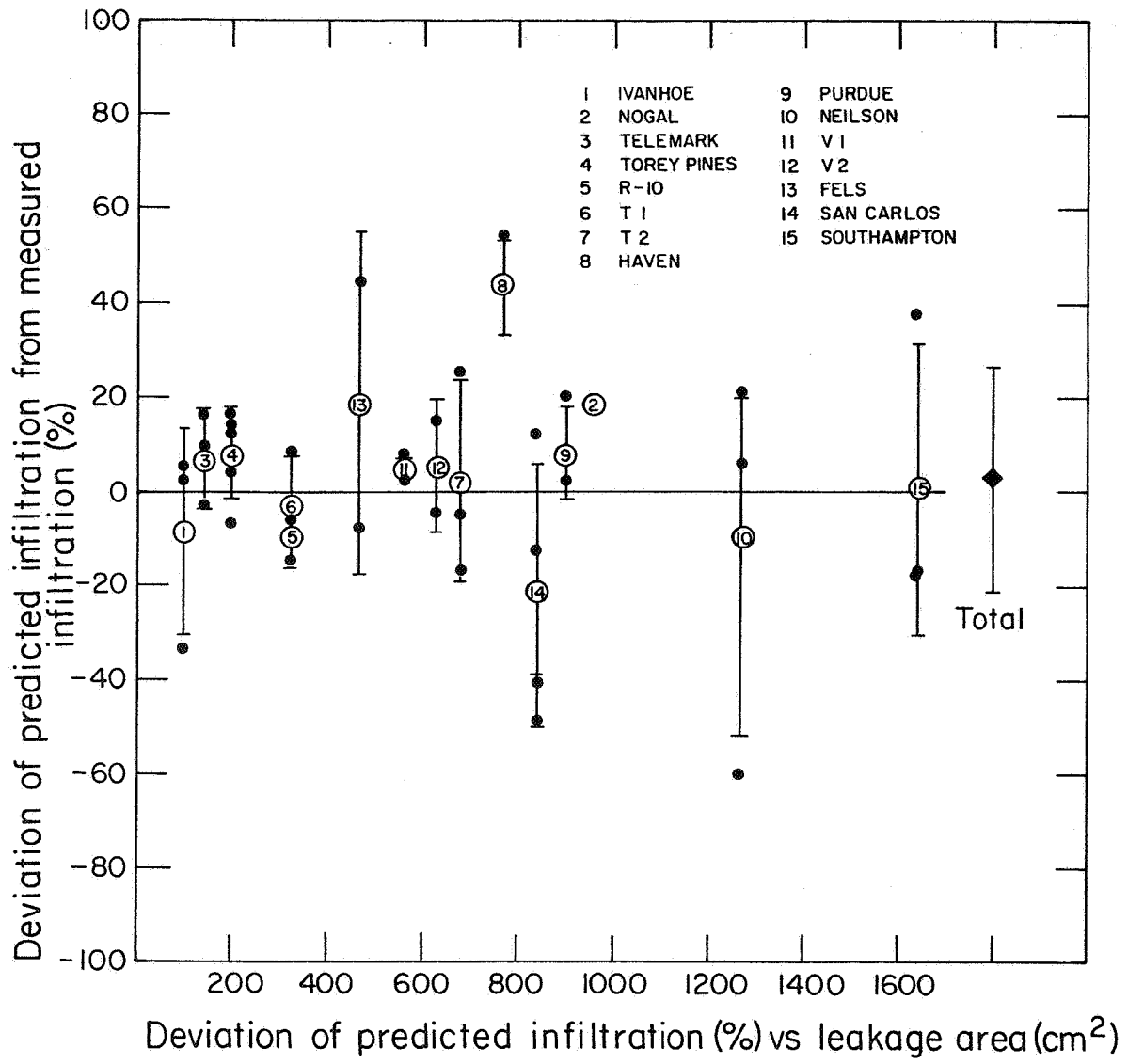
- 1) The correlation of infiltration measured using a tracer gas technique and using the model presented in this paper. Dashed lines represent raw measurement error limits. Only data under $150\text{m}^3/\text{hr}$ is shown.
- 2) The correlation of infiltration measured using a tracer gas technique and using the model presented in this paper. Dashed lines represent raw measurement error limits. Only data over $100\text{m}^3/\text{hr}$ is shown.
- 3) The percentage disagreement between tracer measurements and predictive technique vs leakage area for each site. Solid points are individual measurements; open points with error bars represent site average. Composite for all sites is shown at right.
- 4) A graphical method for calculating infiltration from weather data. f_s^* and f_w^* are pre-calculated. Combine them with ΔT and v' to find the ratio of infiltration to total leakage area.



XBL 805-907

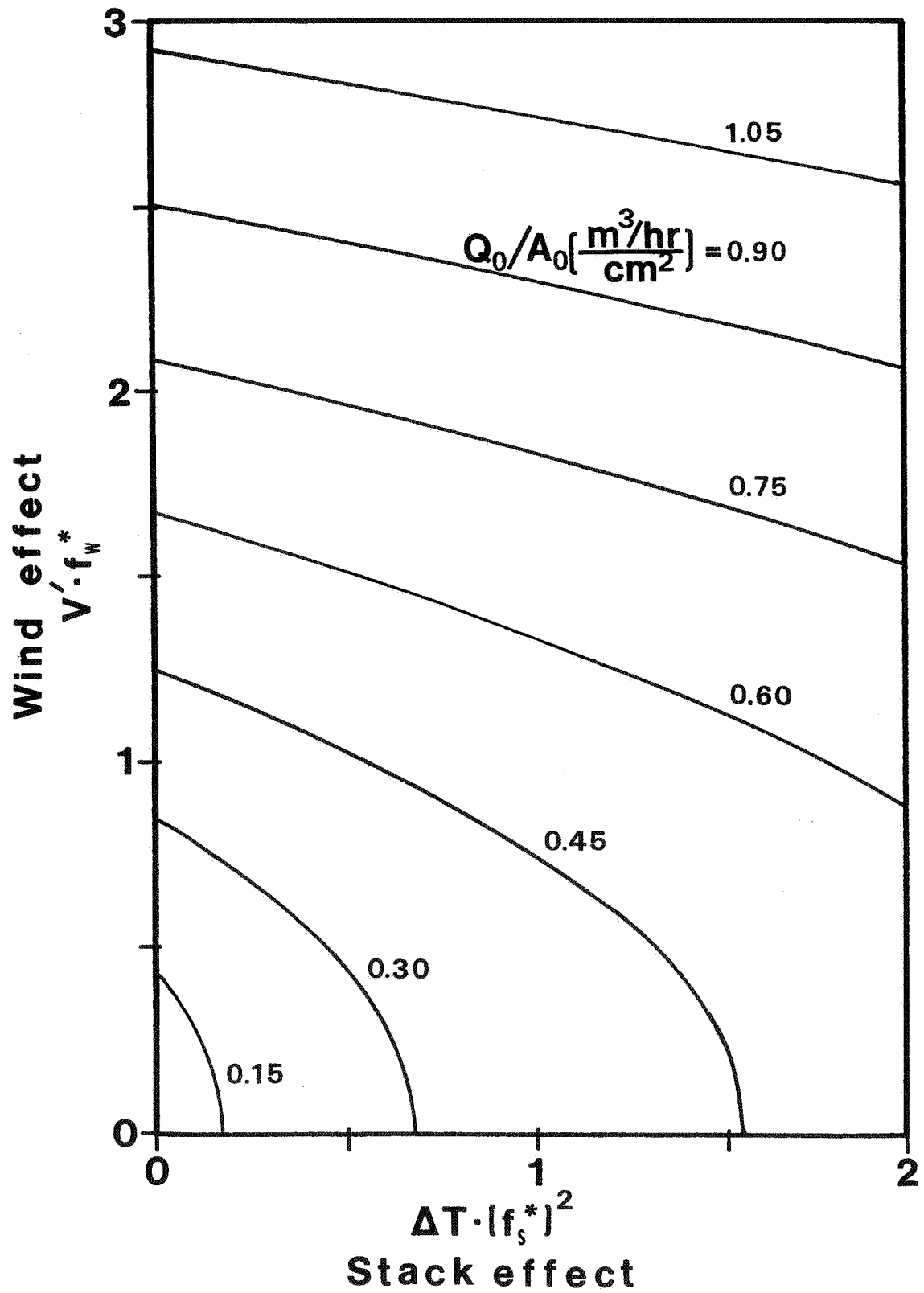


XBL 805-908



XBL 805 - 909

Predicted infiltration per unit leakage area



PAPER 17

**THE MEASUREMENT OF RAPIDLY
FLUCTUATING AIR FLOWS**

P. ROBERTSON AND J. P. COCKROFT

**BSRU
University of Glasgow
Scotland**

INTRODUCTION

For research into wind induced natural ventilation effects we required an anemometer capable of measuring the rapidly fluctuating flows through a window opening. As we wished to correlate these velocities with ventilation rates we were interested in the component of velocity normal to the opening and an indication as to whether the flow was inward or outward. To detect the rapidly fluctuating flows we required good frequency response up to at least 20 Hz. A small computer was to be used to log all the data and perform much of the processing.

In order that we could satisfy the above requirements our choice of instrumentation was between the pulsed wire anemometer (Bradbury and Castro, 1971) and the B.R.E. shielded hot wire anemometer (Cook and Redfearn, 1976). Unshielded hot wire anemometers do not have the ability to sense direction or give the required velocity component and a vibrating low velocity anemometer which does have these abilities is limited to velocities below 0.3 m/s. In order to maintain compatibility with our existing stock of instruments we decided to adopt the shielded hot wire technique.

BRE SHIELDED PROBE

Shown in Fig.1 is the BRE shielded hot wire probe which was developed from an original design by McGill University. The shield was of plastic with wire supports. It was mounted on a standard DISA dual parallel sensor hot wire probe, such that the air flowing through the hole in the shield would pass round one sensor and then the other. The downstream sensor wire would thus be in the thermal wake of the other. The sensors were driven by two DISA K-series linearised constant temperature anemometers, and because of the thermal wake, the anemometer associated with the downstream wire would give the lower output. The output signals from the two anemometers were signed, compared and gated to the readout or recording device by an analogue switching circuit. The response of the system to varying the angle of incidence of the airstream to the probe was fairly close to the ideal cosine curve which would give the true velocity component. However, at certain angles of incidence the system gave output signals of opposite direction to that which was occurring. This was termed "ghosting" and was caused by the downstream sensor being out of the thermal wake of the upstream sensor and/or being subject to a higher velocity.

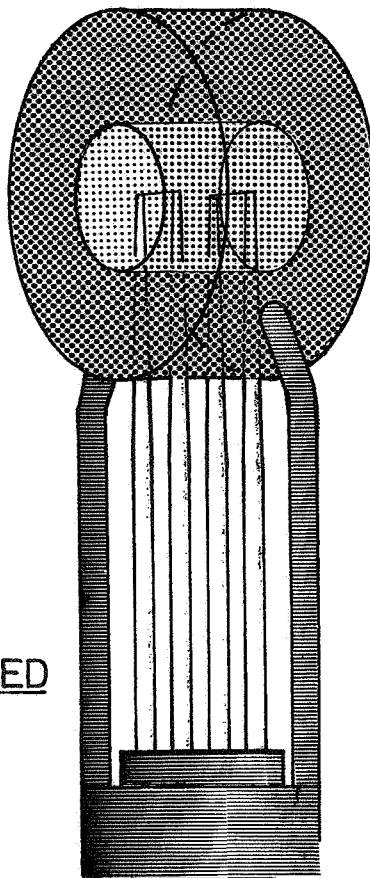


FIGURE 1. BRE SHIELDED
HOT WIRE
PROBE

BSRU SHIELDED PROBE

In order to alleviate the problems of ghosting and to improve upon the cosine response to the BRE probe, the effects of modifying the probe were studied. Various shapes of shield were tested and it was confirmed that the shape used by BRE was close to the optimum in terms of cosine response. A thicker shield was found to give more stable zero readings with the flow at 90° to the probe, but unfortunately this persisted over a considerable band above and below 90° . Reducing the outer diameter had the effect of decreasing the directional sensitivity until one approached a tube shape with almost a square wave response. The resultant probe is shown in Fig.2, the outer diameter having been increased from 5mm to 6.5mm and the diameter of the hole decreased from 2.0mm to 1.8mm. The final shield thickness was 1.3mm.

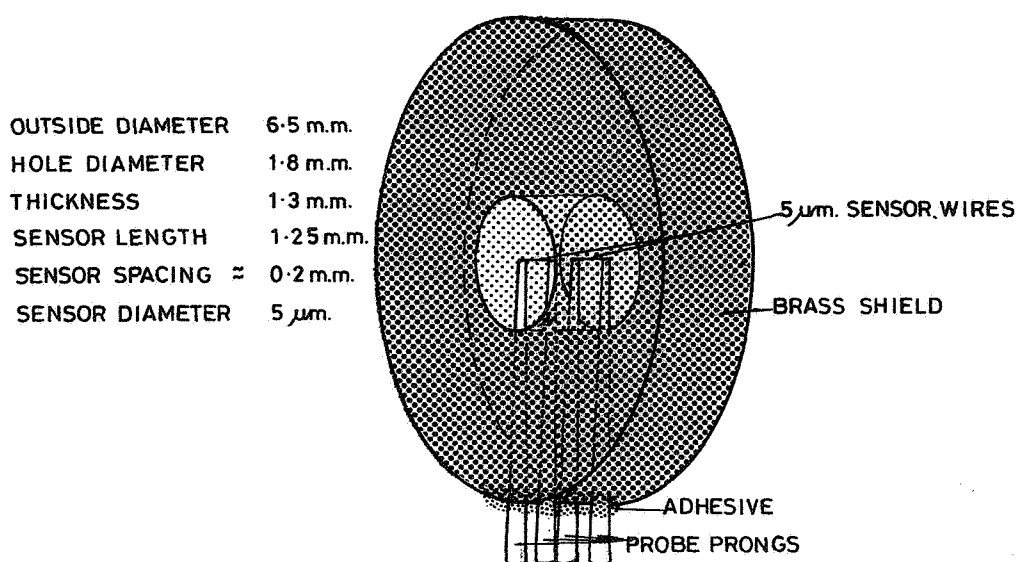


FIGURE 2. BSRU SHIELDED HOT WIRE PROBE

Decreasing the hole diameter was also beneficial in helping to remove the "ghosts" or spurious direction signals at certain angles of incidence. The ghosts were finally removed however by modifying the hot wire probe itself to bring the sensor wires closer together. The wire spacing on the standard dual parallel sensor probe is 0.4mm and this was reduced to about 0.2mm, at which point the probe prongs almost touch. The length of the sensor wires was left at the standard 1.25mm. To achieve this modification the wires were broken, the prongs adjusted and then new 5 micron wires spot welded to the prong tips - a rather delicate and challenging task.

BSRU SHIELDED PROBE (continued)

The shield, made of brass, was then fixed to the probe prongs using an adhesive which was soluble to allow removal yet sufficiently flexible not to distort the prongs. Most solvent based adhesives contracted and broke the wires as they dried. The shield was electrically insulated from the prongs by a layer of adhesive.

The sensors were driven by two DISA K-series, temperature compensated anemometers, the temperature being sensed by a pair of single sensors adjacent to the shielded probe. Temperature compensation was necessary to avoid errors caused by fluctuations between cold outside air and warm room air around the probe. As the signals were to be processed digitally, linearised output was not required and hence linearisers were not fitted to the anemometers.

The signal processing was as shown in Fig.3. The signals from the two anemometers were fed to the analogue inputs of an Altair microcomputer, where individual calibration was applied to each and comparison made to detect the higher and hence the upstream signal. This velocity was then output. For very rapid sampling the raw data could be stored in RAM and analysed subsequently. In this way 8 channels could be scanned at frequencies up to about 50 Hz.

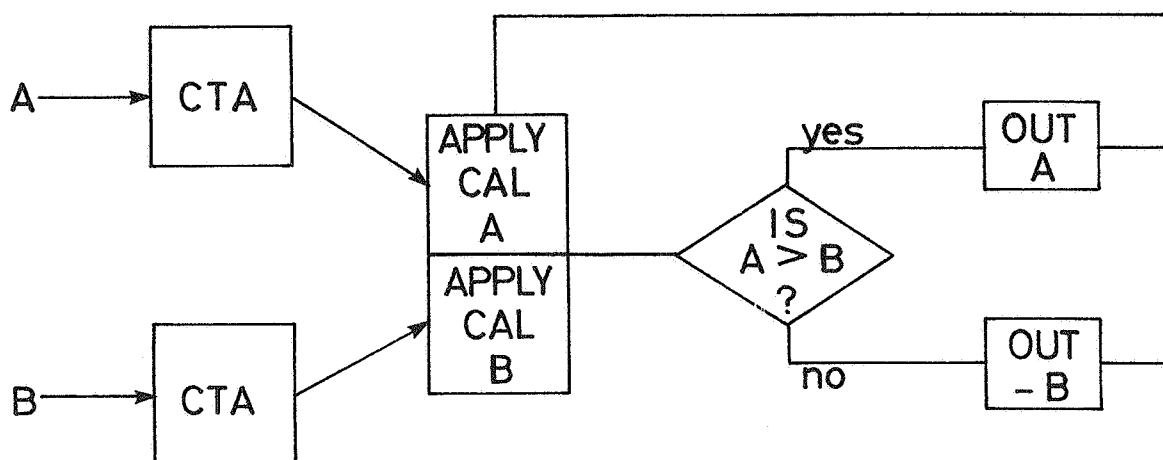


FIGURE 3. B.S.R.U. PROCESS

BSRU SHIELDED PROBE (continued)

The results of performance tests are shown in Fig.4 where the velocity indicated is plotted against the angle of the probe to the airstream. The response of the probe to rotation about the axis of the probe stem (yaw response) is seen to be close to the ideal cosine curve to give the component of velocity normal to the probe. The response to rotation about the axis of the sensor wires (pitch response) is not quite so good at small angles of inclination to the flow. This could be attributed to the fact that the sensor wire is itself insensitive to rotation about its own axis but sensitive to rotation about the axis of the probe stem.

The system is accurate down to 0.2 m/s. We have not tested the frequency response of the shielded probe but by calculation it should be good up to 100 Hz at 5 m/s (Cook and Redfearn, 1976).

A simple application is shown in Fig. 5. This represents the velocity, normal to the direction of travel, induced by a walking subject passing within 100 mm of the probe at a speed of 1.0 m/s. It may be seen that there is an initial outward gust rapidly followed by an inward flow. Clearly a normal hot wire anemometer would never have been capable of resolving the direction and would have indicated two positive peaks.

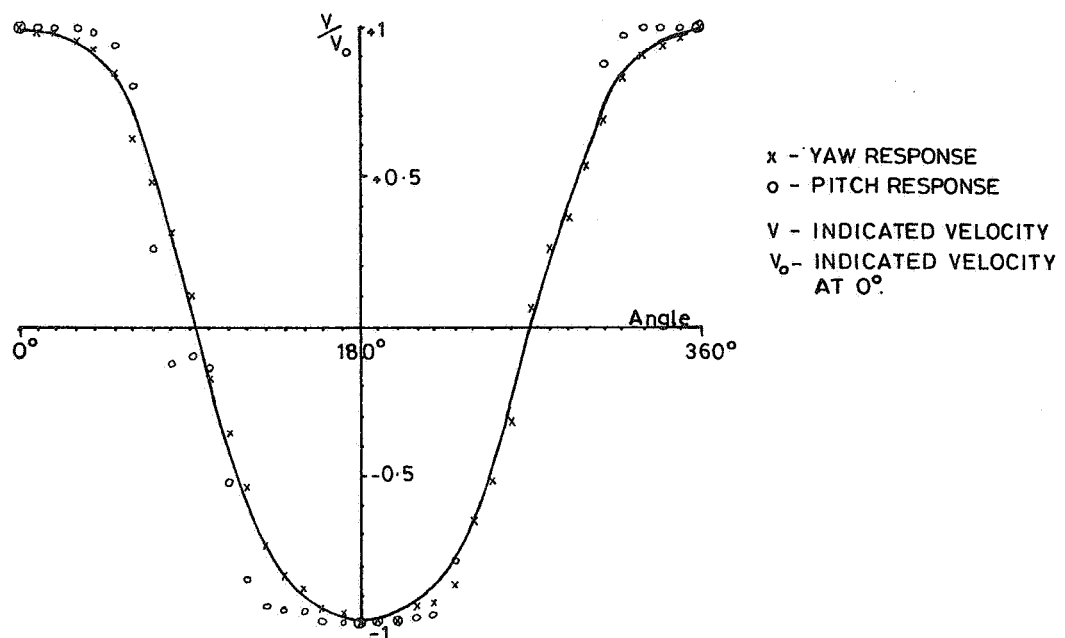


FIGURE 4. RESPONSE TO VARYING ANGLES OF IMPINGEMENT OF AIR FLOW

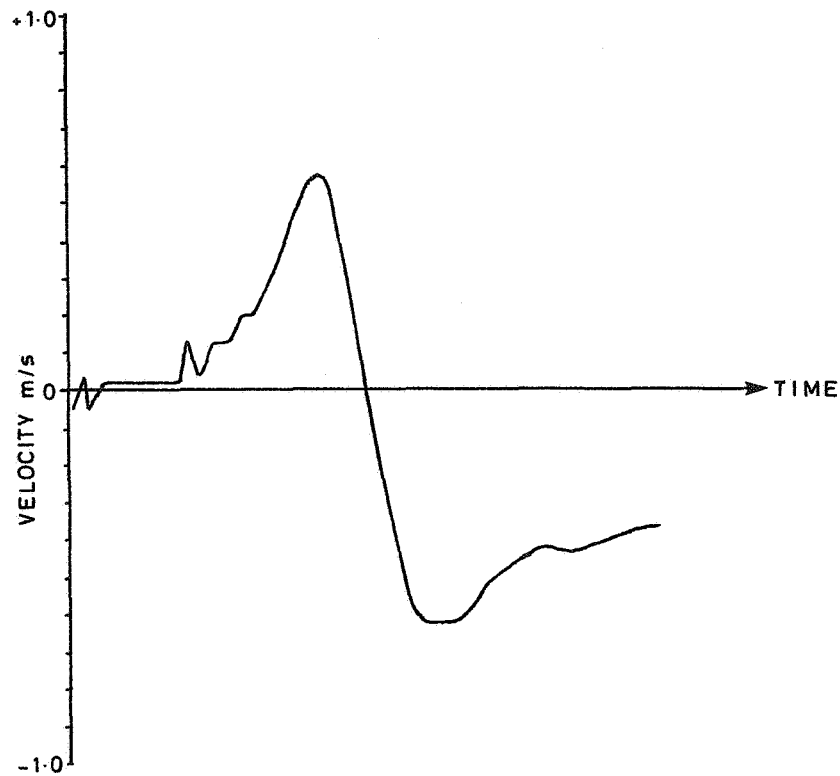


FIGURE 5 APPLICATION OF SHIELDED PROBE -
the velocity normal to the direction of
movement as a subject walks past at
1.0 m/s.

REFERENCES

- Bradbury, L.J.S. and Castro, I.P. (1971) A Pulsed Wire Technique for Velocity Measurements in Highly Turbulent Flows. *Journal of Fluid Mechanics*, 49, 657 - 691.
- Cook, N.J. and Redfearn, D. (1976) Calibration and Use of a Hot Wire Probe for Highly Turbulent and Reversing Flows. *Journal of Industrial Aerodynamics*, 1, 221 - 231. Also BRE current paper CP 18/76.

PAPER 18

**DEVELOPMENT OF A DYNAMIC
PRESSURE ANEMOMETER FOR
MEASURING THE AXIAL VELOCITY
COMPONENT**

J. C. PHAFF

**IMG-TNO
Delft
Netherlands**

DEVELOPMENT OF A DYNAMIC PRESSURE ANEMOMETER FOR MEASURING THE AXIAL VELOCITY COMPONENT

SUMMARY

The dynamic pressure anemometer described here belongs to the group of so-called pressure-tube anemometers (pitot-static tube) and is intended for measurement of one velocity component in a three-dimensional flow field at air velocities of 0,1 up to 10 m/s. The usable flow direction area is unlimited ($0 \dots 360^\circ$) in three dimensions. The maximum error in the indication of the velocity component is less than 5% (if the actual velocity is put at 100%).

At low air velocities ($\ll 1$ m/s) the zero drift of the differential pressure transducer used is the determining factor for the error in the reading which may be considerable.

INTRODUCTION

During a study of the air velocities in and volume flows through an opened window there was a need for simultaneous measurement of the air velocity and the flow direction.

In Figure 1, the situation is given where air with a velocity, v , flows through an open window. In this case it is important to know if the air movement is directed inward or outward. To be able to make an estimate of the volume flow through the window plane it is necessary that the velocity component perpendicular to the window plane be determined.

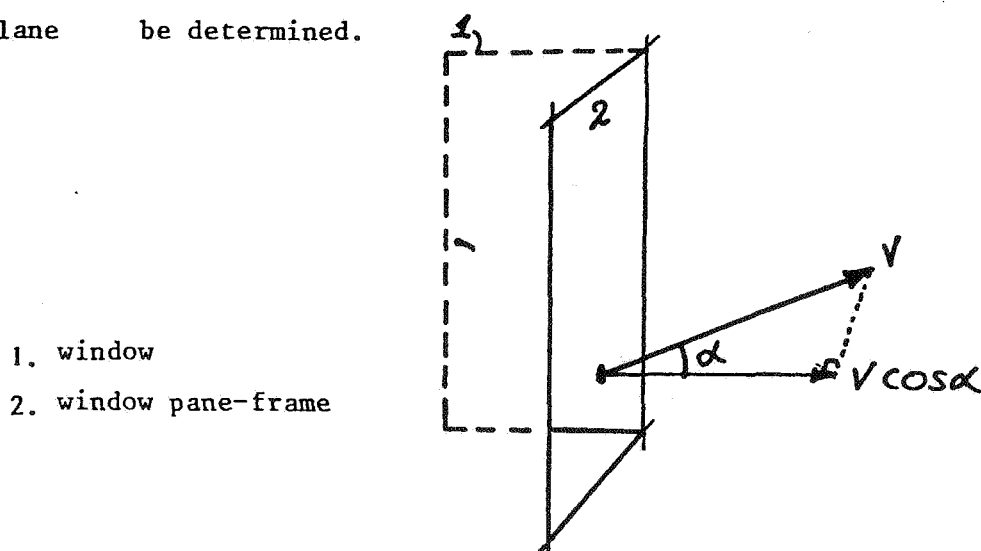


Figure 1 : Air velocity in an opened window.

Determination of the flow direction by means of smoke, as was done sometimes in the past, must be rejected here because this method does not work for fluctuating flows and is not directly suitable for automatic processing of the data.

A configuration like a pitot tube was built to which air would flow from both sides.

After some experimenting with the results of wind pressure measurements around rectangular buildings it seemed not impossible to find a form where the pressure signal might be convertible to the velocity component from one certain direction, as given in formula (1):

$$v \cos \alpha = C \cdot \text{sign}(\Delta p) \sqrt{|\Delta p|} \quad (1)$$

In figure 2, the velocity vector v , and $v \cos \alpha$ are sketched in a system of coordinates.

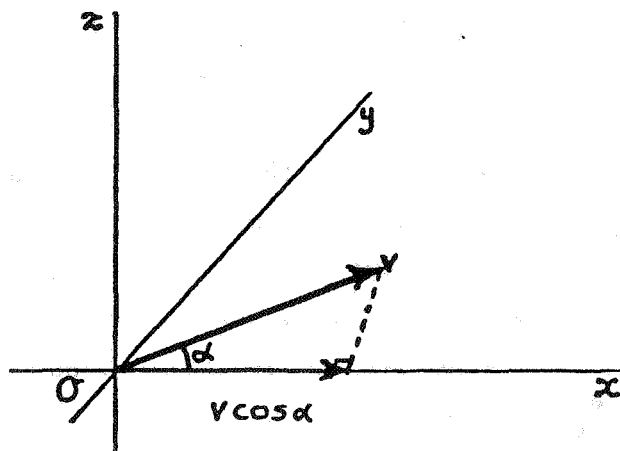


Figure 2 : v and $v \cos \alpha$ given for an angle of incidence, α . The anemometer is situated in O for measuring the x component of v .

INVESTIGATION

After measurements on some prototypes, an investigation into the disc forms with the desired direction characteristic was started. This direction characteristic is

$$\Delta p = K \cdot \frac{1}{2} \rho (v \cdot \cos \alpha)^2 \quad \text{-----} \quad (2)$$

Formula (2) has been derived from formula (1) by defining Δp explicitly. The factor K is the dimensionless proportion between the pressure difference measured and the dynamic pressure.

In this investigation the following parameters were varied:

- . form (section) of the disc
- . diameter of the disc
- . form of the pressure measuring openings in the disc
- . diameter of the pressure measuring openings.

Measurements were also made on discs of porous material. The direction characteristics were taken in two wind tunnels:

at 2 - 12 m/s with a degree of turbulence of about 3%;

at 0,1 - 2 m/s with a degree of turbulence of about 30%.

RESULTS

It appeared that the form of the disc had much influence on the form of the direction characteristics. With a beveled disc form (Figure 3) the best results were obtained (Figure 5).

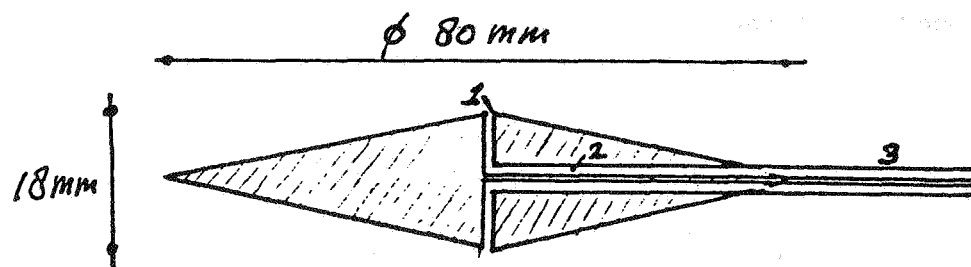


Figure 3 : Section of the velocity pressure disc.

1. Pressure measuring opening (\emptyset 1 mm).
2. Bore to connection pipe.
3. Connection pipe.

The diameter of this disc is 80 mm, but can be made smaller (e.g. 20 mm) without affecting the properties. For comparison, in Figures 4 and 5, direction characteristics of a disc with rectangular section and the disc

of Figure 3 are given.

The direction characteristics appeared practically independent of the velocity. Possibly, the degree of turbulence of the air has some influence on this characteristic.

So, it appeared that the direction characteristics better agreed with formula (1) at a higher degree of turbulence (30%) than one of 3%.

Vertical : proportion between the pressure measured and the velocity

$\uparrow K$ pressure of the flow (K):

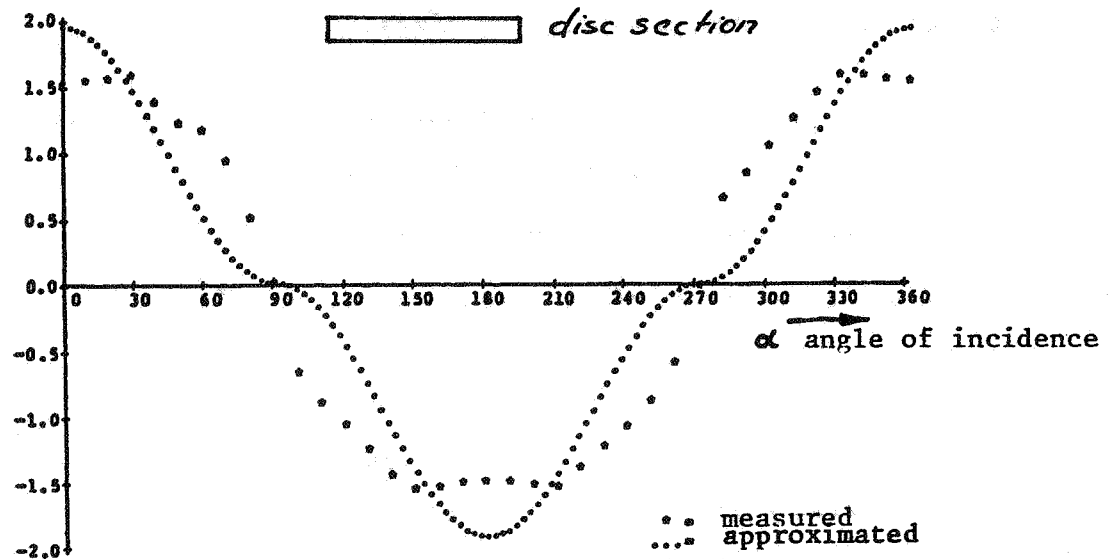


Figure 4 : Direction characteristic of a rectangular disc as a function of the angle of incidence (α); degree of turbulence = about 3%.

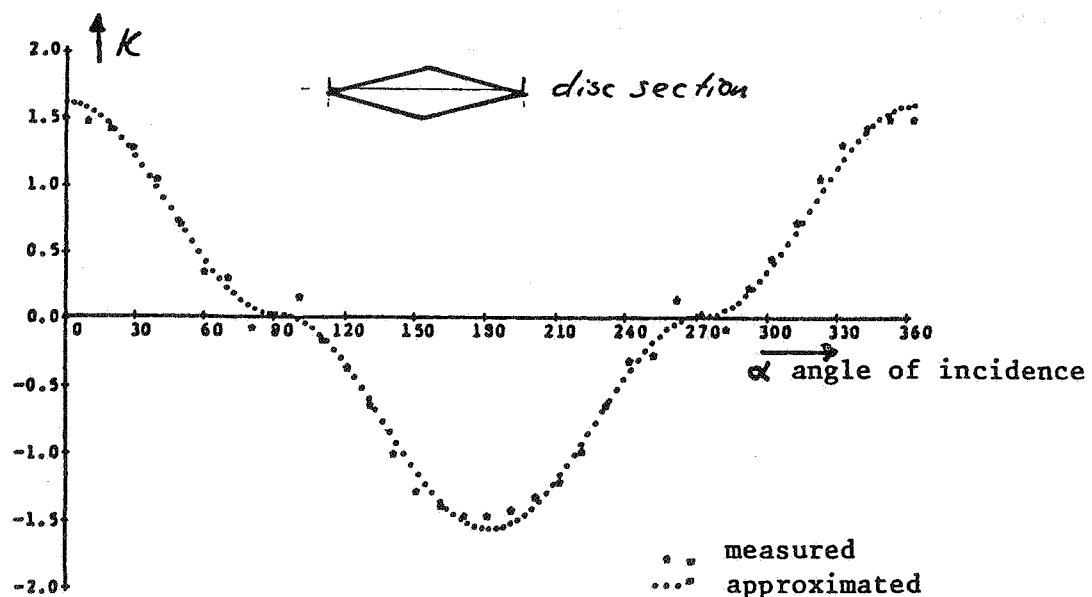


Figure 5 : Direction characteristic of the beveled disc (Figure 3) as a function of the angle of incidence (α); degree of turbulence = about 3%.

In the direction area around 90° and 270° the direction characteristic oscillates through zero. Consequently, the sign of the velocity component which according to formula (1) is calculated from the measuring signal does not agree with the actual velocity component; in other words, while the air enters through a window (nearly parallel to the window plane) the anemometer here indicates that air is flowing outside. It is supposed that this undesirable phenomenon can be prevented by flattening the disc somewhat more near the pressure measuring openings.

With three of these anemometers placed perpendicularly on each other it must be possible to determine the three velocity components and, consequently, the flow velocity in force and in direction.

A condition for this is that the anemometers do not influence each other which will be attained by mounting them at some distance from each other. The flow in this area around the three anemometers must be homogeneous and the dimensions of the eddies must be considerably larger than the distance between the anemometers.

The response time for the discs examined is about 0.1s, so that fluctuations in the air velocity to about 10 Hz can be measured.

APPLICATION

In the above-mentioned investigation into air flows in an open window it was measured with a measuring arrangement as sketched in Figure 6.

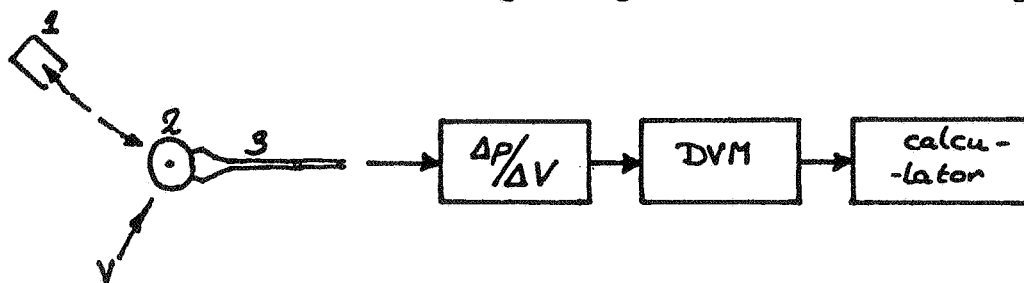


Figure 6: Measuring arrangement.

1. Cap for screening the velocity pressure, measuring disc during determination of the offset voltage.
2. dynamic pressure measuring disc.
3. connecting tubes.

The influence of temperature differences between the connecting tubes of the disc to the differential pressure transducer is minimized by placing these connections horizontally. The offset of the pressure transducer is determined by pushing regularly (every 5 minutes) a cap over the disc, owing to which the air velocity around the disc becomes zero temporarily. The offset voltage determined in this way is subtracted from the measuring values with the calculator before the air velocity component is calculated with it.

For perpendicular flow, the following pressures may be expected, see Table 1.

Table 1 : Relationship between air velocity v , and pressure signal, Δp , for $\alpha = 0^\circ$.

$v \text{ (m/s)}$	$\Delta p \text{ (Pa)}$
0,01	0,0001
0,05	0,0025
0,10	0,01
0,5	0,25
1,0	1,0
10	100,0

In view of the small pressure differences at low velocities it is important to minimize the zero drift of the arrangement and also to determine regularly the offset voltage. For the differential pressure transducer, the zero drift can be about 0.0002 Pa/s. The error in the indication of the air velocity is determined then by the time passed between the measurement and the determination of the offset voltage. In Figure 7, the error in indication is plotted in m/s for some values of the zero error as a function of the velocity. In form of a formula this relationship is:

$$\delta = \text{sign.}(v^2 \cdot C - \Delta) \cdot \sqrt{|v^2 \cdot C - \Delta|} - v, \text{ for } \alpha = 0^\circ \quad (3)$$

where δ = error in indication ;

Δ = zero error of the differential pressure transducer

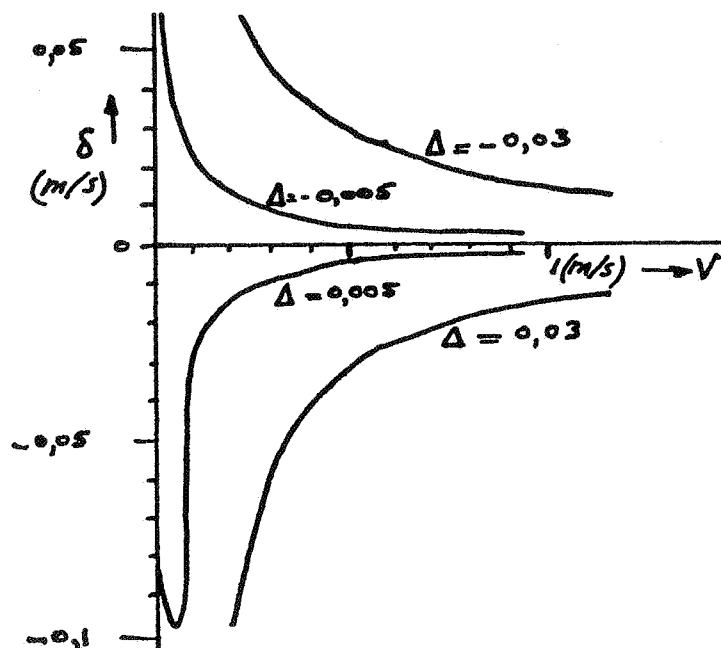


Figure 7 : Reading error of a dynamic pressure anemometer due to a zero error in the differential pressure transducer of ± 0.005 Pa and ± 0.030 Pa.

CONCLUSION

With the dynamic pressure discs described here it is possible to measure air velocity components at air velocities of about 0,1 m/s and more at frequencies lower than 10 Hz.

Information about the flow direction is obtained from the polarity of the pressure signal.

If the offset voltage is determined regularly the measuring errors, e.g. for 0,1 m/s and more can remain within $\pm 0,02$ m/s.

A disadvantage of this measuring method, and of all dynamic pressure anemometers in general is that high demands are made upon the differential pressure transducer because of the quadratic relationship between the pressure signal and the air velocity.

LIST OF SYMBOLS

C = a constant (dependent on temperature)

$$C \approx 1 \text{ at } 20^\circ \text{C. } C = \sqrt{\frac{2}{K \cdot \rho}} \quad [\text{kg}^{-\frac{1}{2}} \cdot \text{m}^{\frac{1}{2}}]$$

K = pressure factor

[-]

p = air pressure difference

[Pa]

v = air velocity

[m/s]

V = electric tension

[V]

α = angle of incidence

[°]

δ = error in indication

[m/s]

Δ = zero error

[Pa]

ρ = specific mass of air

[kg.m⁻³]

PAPER 19

**EVALUATION OF THE INDOOR AIR
QUALITY AS A CRITERION FOR
MINIMUM VENTILATION RATES**

G. HUBER AND H. U. WANNER

**Federal Institute of Technology
Zurich
Switzerland**

INDOOR AIR QUALITY AS A CRITERION
FOR MINIMUM VENTILATION RATE

G. Huber and H.U. Wanner

Federal Institute of Technology
Department of Hygiene and Ergonomics
CH - 8092 Zurich

1. Introduction

Although people spend 70% of their time either at home or in public buildings such as schools, offices, transportation vehicles and terminals, and restaurants, they are more critical towards ambient or outdoor than indoor air pollution. For the following reasons, however, a thorough investigation of indoor air pollutants is necessary:

- Because of the reduced natural and mechanical ventilation in order to save energy for space heating, a general deterioration in air quality is to be reckoned with. This leads us to the question of minimum air ventilation rate necessary to achieve the desired air quality and to avoid the possible impairment of health and performance.
- The second point is the use of modern building materials, furniture equipments and consumer products which can emit noxious substances in air. The resulting effects on health, specially the long-term effects, are not yet known. The chief interest lies here in adopting strong regulations for the permission of materials and products, increasing the checks and thereby reducing the health risk to a minimum.

This paper reviews the pollutants occurring in indoor air. It is based on the papers presented at the international symposium on indoor climate (8), report of the WHO working group on health aspects related to indoor air quality (11), technical meetings on energy conservation (6, 7), and specific investigations on occurrence and effects of indoor air pollutants.

2. Sources and nature of pollutants

Important air pollutants are listed in Table 1. Although we shall not deal here with the pollutants in outdoor air, it should be kept in mind that the pollutants in outdoor air can influence the pollutants in indoor air considerably. Indoor air pollution is caused largely by human activities and behaviour. The type and rate of ventilation should be planned accordingly.

Man himself impairs the indoor air quality by continuous emission of heat, humidity, carbon dioxide, particles and perspiration. Rise in temperature, relative humidity and concentrations of different pollutants depend on the space occupancy and activities of individuals therein. The most common parameters to evaluate the human impact on indoor air quality are carbon dioxide (CO_2) and odour.

Various kinds of pollutants are caused by human activities. In residential buildings they consist primarily of dust caused by normal working and odours from cooking and smoking. Vapours from cleaning agents and solvents, set free while doing normal household chores, are also worth mentioning.

Table 1: Air contaminants

Important sources of air contaminants in residential buildings are listed. Indoor air quality is determined by odours, components of smoke, carbon dioxide and emissions from materials.

Source	Pollutant
<hr/>	
<u>Outdoor air</u>	
Space heating	Sulphur dioxide
Motor vehicles	Oxides of nitrogen
Industry	Carbon monoxide
	Oxidants
	Hydrocarbons
	Particulate matter
	Lead
<u>Indoor air</u>	
Man	Odours
	Carbon dioxide
	Water vapour
	Particles
Tobacco smoke	Carbon monoxide
	Aldehydes
	Particles
Consumer products	Odours
Sprays	Solvents
Cleaning agents	Organic Compounds
Combustion of gas for heating and cooking	Oxides of nitrogen
	Carbon monoxide
	Particles
Materials	Aldehydes
Particle boards *	Asbestos
Building materials	Radon
Paints	Solvents
	Organic materials

* = Chipboards

The use of gas or oil for heating and cooking purposes gives rise to oxides of nitrogen and carbon monoxide due to insufficient combustion. This can lead to acute and chronic damage to health depending upon the concentration and duration of exposure. In this connection combustion of dust should be mentioned. This is what happens in case of warm air heaters and electric storage heaters where heating and burning of dust particles take place. The studies have shown that even in normal operating conditions different reaction products like carbon monoxide, carbon dioxide, oxides of nitrogen, and ammonia are formed. But even in case of heavy dust load the resulting concentrations were not dangerous to health (10).

Smoking of cigarettes, cigars, and pipes constitutes an important source of pollution which directly affects the indoor air quality. Depending upon the intensity of smoking, as well as size and ventilation of room, the concentrations of contaminants can reach the levels which not only cause annoyance but can even damage the health of sensitive persons like patients with heart and circulatory ailments, asthmatics, and children. Studies have shown that concentrations of carbon monoxide, aldehydes, and particulates should be carefully watched in the rooms where smoking is permitted. In case of insufficient ventilation, carbon monoxide levels can exceed the long term standard of 9 ppm (4).

Still less is known about the possible pollution due to building materials, furniture fixtures, floor coverings, paints and coatings. Pollution caused by these sources is independent of behaviour and activities of inhabitants. Take for example Particle boards or chipboards which are used in furniture as well as in interior decoration. Aldehyde containing products are used in manufacture of these particle boards which may have

residual aldehyde that could continuously contaminate the indoor air and cause irritation of eyes and respiratory organs (3).

The question is still open if other organic solvents besides formaldehyde are also emitted. In any case, close examination of building materials with respect to solvent residues is recommended in future.

Another undesirable component in building materials is radon. In case of reduced ventilation, radon containing bricks could cause increased radioactivity in indoor air (11).

Asbestos is a further example of material hazardous to health. Asbestos is used in various building and insulating materials which can pollute the indoor air beyond permissible levels (11).

3. Studies done at the Institute of Hygiene and Work Physiology:

At the Institute of Hygiene and Work Physiology of Swiss Federal Institute of Technology in Zurich, we have two ongoing projects dealing with problems of indoor air quality. In one of them we study the air pollution caused by men; in another we concentrate on pollution caused by materials. The aim of both projects is to prepare recommendations for minimum ventilation rates based on the effects of various parameters on air quality.

Besides measuring physical parameters like temperature, relative humidity, carbon dioxide content of exhaled air and formaldehyde from building materials, we are interested in the contribution of odours to the air quality.

Schematic disposition of both the projects on "minimum ventilation rates" is shown in Figure 1.

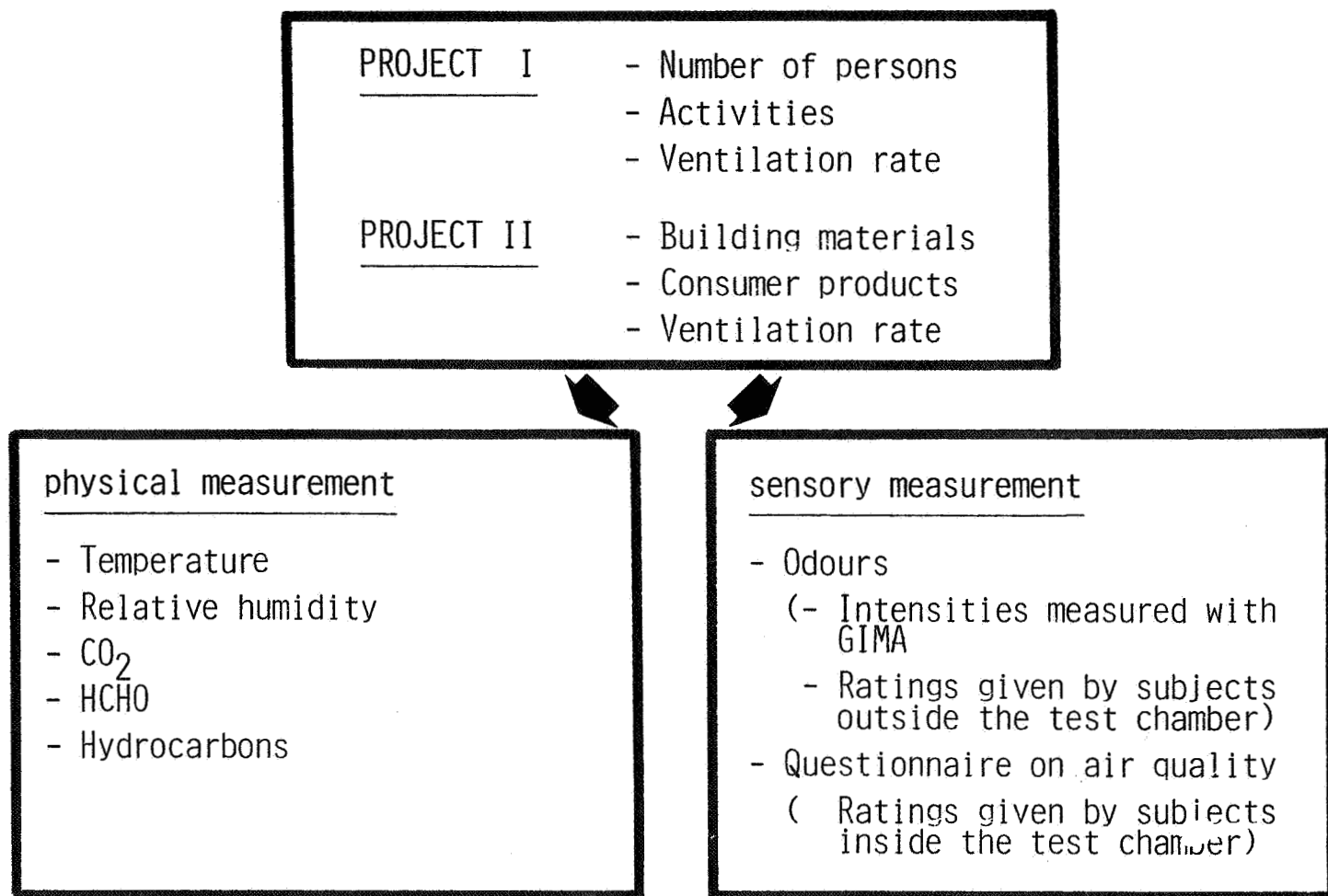


Figure 1:

Schematic presentation of both the projects on "minimum ventilation rates". The central block represents the room under investigation with its known parameters. Variables in Project I are human beings and their activities. Variables in Project II

are building materials and consumer products. Ventilation rate is an additional variable in both the projects. The evaluation of air quality is achieved by physical (temperature, relative humidity, CO_2 , HCHO, Hydrocarbons) and sensory (odour intensity measuring instrument GIMA) measurements and by questioning the subjects in the test chamber.

Methods of odour investigation:

For several years our institute has been dealing with problems of odour annoyance. Initially we employed a pure physico chemical method of gas chromatography, but with limited success. So now we have switched over to sensory techniques taking help of the human nose as a detector. We are now in a position to evaluate the odour perception of subjects in a test panel formed by four or six persons of an average odour sensitivity. We have developed our own instruments for these odour investigations. For sensory evaluation of odours, there are two alternatives:

For determining an odour threshold, the odourous air is diluted with odour-free fresh air till the odour can just be perceived. That concentration is termed as odour threshold. The ratio of odour-free to odourous air is expressed as dilution number.

For determining odour intensity, the stream of undiluted odourous air is presented to the subjects. The intensity of odour perceived can either be expressed on verbal scale (e.g. no odour/ very faint odour/ faint odour/ distinct odour/ strong odour/ very strong odour) or directly in comparison to standardized odours (e.g. pyridine, hydrogen sulfide).

Strong odours as emitted by waste incinerator units and by sewage treatment plants can very well be investigated by either of these two methods (5). Weak odours like those emitted

from human bodies can only be judged with the help of odour intensity, because the odour concentrations are so near the threshold values that further dilution is practically impossible.

For investigating the air quality in connection with minimum ventilation rates, an odour testing apparatus called GIMA was developed: The air to be evaluated is sucked out by a fan from the test chamber and forwarded to the sniffing points via a valve-controlled piping system. All the parts which come in a direct contact with the sampled air are made of glass or Teflon. The sniffing points are so designed that two subjects can simultaneously participate in the experiment. The valves can be adjusted to achieve an air stream of 0.5 m/s at the sniffing points.

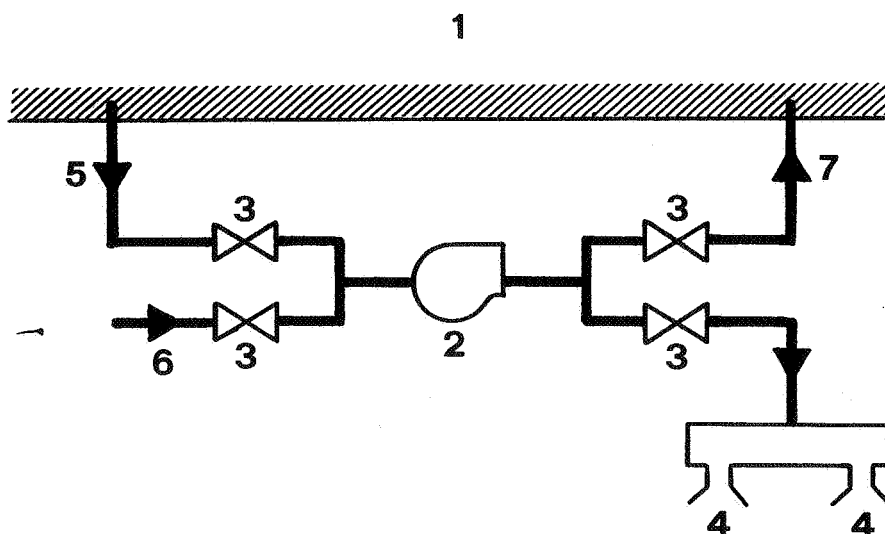


Figure 2: Odour testing apparatus

- | | |
|------------------------------|---------------------------|
| 1. Test chamber | 5. Sample air |
| 2. Fan | 6. Standard air |
| 3. Steplessly variable valve | 7. Backflow of sample air |
| 4. Sniffing points | |

4. Conclusions:

All the contaminants which impair the indoor air quality should be eliminated at their source so far as possible. Control measures to reduce emissions are necessary especially in the case of outdoor air pollution. For indoor air, contaminants arising out of materials should be avoided. To this end strict permit regulations and increased checkings are necessary. Since the elimination of pollution due to smoking requires a long ventilation time, smoking - at least in public buildings - should be restricted to a few rooms only.

Pollution caused by human presence and activities could be taken care of by regulating the supply of fresh air, i.e. ventilation.

Present recommendations about fresh air requirements of rooms or enclosed places are based on practical experience. Scientific study of the problem of building ventilation was started as far back as the 18th century (9). But until today no leading compound could be found for evaluating the air quality. This can be done only for certain work places with high concentrations of specific contaminants.

It is therefore urgently necessary to objectify the problem of indoor air quality and to work out recommendations for minimum air requirements or to replenish the existing guidelines as is the case with USA and Sweden.

The important problem here is whether the necessary fresh air can be secured by natural ventilation - even when the windows are closed. For this, knowledge of the air ventilation rate of the room is necessary. Calculations show that in case of traditional construction style and average occupancy and use of

residential buildings, the demand of fresh air is only partly met by air exchanges through joints and cracks. If the air exchanges are not guaranteed through natural ventilation, additional window ventilation or mechanical ventilation systems should be provided according to the needs.

5. Summary:

Recently all industrial nations are making efforts to conserve energy by optimising building insulation. In this connection the hygienically relevant question arises as to how far the indoor air quality is modified by such measures. Investigations are under progress to evaluate the air quality as a function of occupancy, activities, and ventilation rate. The decisive criteria are temperature, relative humidity, carbon dioxide, odours and contaminants from consumer products and building materials.

Based on occupancy and proposed use of the room, guidelines for a minimum ventilation rate should be drawn.

Literature

- (1) Adamson B.: New Swedish Building Regulations in Order to Conserve Energy. Lund Institute of Technology, Department of Building Science. Report BKL 1977.
- (2) ASHRAE: Standards for Natural and Mechanical Ventilation, 62-73. American Society of Heating, Refrigerating and Air-Conditioning Engineers, Inc. (1973).
- (3) Deimel M.: Erfahrungen über Formaldehyd-Raumluftkonzentrationen in Schulneubauten. In "Organische Verunreinigungen in der Umwelt", S. 416-427; K. Aurand et al. (Herausgeber), Erich Schmidt Verlag, Berlin, 1977.

- (4) Fischer T., Weber-Tschopp A. und Grandjean E.: Ausmass und Wirkung der Luftverunreinigung durch Tabakrauch unter experimentellen Bedingungen und in Gaststätten. Schweiz. Blätter für Heizung und Lüftung 45, 3-8 (1978).
- (5) Hangartner M.: Erfassen und Beurteilen von Geruchsemissionen. Wasser, Energie, Luft 72, 163-166 (1980)
- (6) Hollowell C.D., Berk J.V., Lin Ch. and Turiel I.: Indoor Air Quality in Energy-Efficient Buildings. Second International CIB Symposium on Energy Conservation in the Built Environment, Copenhagen, 1979.
- (7) Hollowell C.D., Berk J.V. and Traynor G.W.: Impact of Reduced Infiltration and Ventilation on Indoor Air Quality in Residential Buildings. ASHRAE Symposium on Air Infiltration, Philadelphia, 1979.
- (8) Indoor Climate, Effects on human comfort, performance and health. Edited by P.O. Fanger and O. Valbjørn. Danish Building Research Institute, Copenhagen 1979.
- (9) Klauss A.K., Tull R.H., Roots L.M., Pfafflin J.R.: History of the Changing Concepts in Ventilation Requirements. ASHRAE Journal 6, 51-55 (1970)
- (10) Satish J. und Wanner H.U.: Emissionen bei der Versengung von Raumlufstaub. Zbl. Bakt. Hyg. I. Abt. Orig. B. 160, 499-508 (1975).
- (11) World Health Organisation, Regional Office for Europe. Report on Working Group on Health Aspects Related to Indoor Air Quality. Symposium in Bilthoven 1979.

DISCUSSION

DISCUSSION

SESSION 1

(Points arising from Max Sherman's presentation (Paper 1))

David Harrje:

Over the years the mixing problem referred to by Max Sherman (Paper 1) has proved not to be a problem after all. By using the mechanical circulation systems of large office buildings, we have been able to mix 5 million cubic feet of air ($4.6 \times 10^5 \times 10^5 \text{m}^3$) in 15 minutes.

Rodney Gale:

In our work we have obtained satisfactory mixing in naturally ventilated houses by using small mixing fans and by injecting gas in areas of rapid air movement, for example near radiators.

Richard Grot:

Would Max Sherman clarify his definition of effective volume and state how it is related to the physical volume ?

Max Sherman:

When using the decay method, you are measuring over an effective volume. This is often smaller than the physical volume and arises when part of the space does not communicate well with the remainder. Reasons for this include "dead" spaces, such as cupboards and closets, or stratification which may isolate large volumes of air near ceilings.

To determine the air change rate the volumetric air infiltration rate is divided by the true physical volume of the structure. The resultant air change rate could be in error by up to 20%.

Sometimes the effective volume turns out to be greater than the physical volume. This happens when attached spaces, such as attics etc., communicate with the living space.

Peter Warren:

Can you be sure that your "dead" spaces really exist? We have conducted ventilation measurements in single houses with internal doors and internal ventilators open and have found that the difference in ventilation rate between rooms was small. This rather implied that there are no "dead" spaces.

Max Sherman:

We have found that in leaky structures or when additional mixing is added, for example using circulating fans, there were few "dead" spaces; however, when the internal mixing is small and the infiltration is low there can be "dead" spaces. Furthermore, the room-to-room infiltration can vary significantly.

David Harrje:

In experiments that we have performed we found that the air change rate between a room and closet was approximately 5 ac/hr. In general the interior communication was better than that with the outside.

Richard Grot:

The continuity equation given by:

$$C_t = C_0 e^{-\int_{t_0}^t A(\tau) d\tau} + \int_{t_0}^t Q(t, \tau) f(\tau) d\tau$$

Term 1

Term 2

where $Q(t, \tau) = \text{response function} = e^{-\int_{t_0}^t A(s) ds}$

C_0 = tracer gas concentration at time t_0 .

C_t = tracer gas concentration at time t .

A = air infiltration rate

τ = mixing period

s = source term/unit volume

has an exact classical solution. In the constant flow technique, referred to by Max, the assumption is made that Term 2 of the equation drops out. This is not true. This assumption is only valid if the infiltration rate is constant.

Max Sherman:

When we speak of infiltration we are talking about a quantity that is averaged over a particular volume. Since the minimum time for a signal to propagate in that volume is the mixing time, it would be nonsense to talk about a time-averaged infiltration with a time scale shorter than the mixing time. Therefore it is not only desirable but necessary, to use averaged infiltration values of this length; the assumption of constant infiltration over a 30 minute period is a consequence of this.

David Harrje:

Would Max Sherman give a more detailed description of this long-term constant flow technique using injection and sampling bags. In particular, what are the time schedules involved for leaving the equipment in the building and how does the technique take into account such factors as window opening behaviour and climatic variations ?

Max Sherman:

Two bags, one empty and one filled with a known quantity of SF_6 are brought into the building. A two-channel pump is used to gradually inflate the initially empty bag with air from the building and to gradually evacuate the bag of SF_6 . At the end of the test period, usually 1 month, the apparatus is brought back to the laboratory for analysis. The total amount of tracer gas discharged and the SF_6 concentration in the initially empty bag is measured. The results are used to calculate the average inverse infiltration. Because the air infiltration over the period is not constant, a correction factor (as described in the paper) must be applied to convert the results to average infiltration.

Peter Jackman:

Would anyone like to comment on the comparison of different tracer gas techniques ?

Rodney Gale:

We have monitored air infiltration in each room of the British Gas test house using tracer gas decay and have compared the results with those using the constant concentration method. We believe that there was some over-estimation with the decay method but the differences were not greater than 10%. There was not much difference in results between different tracer gases.

Peter Jackman:

Has anyone experienced adsorption or absorption problems ?

Rodney Gale:

SF₆ gets absorbed by bedding and curtains. N₂O also gets absorbed by these materials but not to the same extent as SF₆.

David Etheridge:

One of the advantages of the constant concentration techniques is that this problem has only an initial effect.

Peter Hartmann:

We have performed a number of N₂O experiments in a closed box in which different building materials were placed. There was no evidence of absorption. We have not performed these experiments with soft furnishings.

Richard Grot:

We have performed absorption experiments on building materials but not soft furnishings. Our results confirm the findings of Peter Hartmann.

Max Sherman:

Our experiments show that SF₆ is absorbed to a negligible extent on plastic furnishings. Adsorption can be important if plastic lines are used in the injection or sampling of the tracer gas.

Peter Jackman:

Are there any points on the general safety aspects of tracer gases ?

Max Sherman:

We have abandoned the use of N₂O as we are not permitted to use concentrations of greater than 25 ppm in occupied areas.

Peter Warren:

What regulations govern the use of nitrous oxide as a tracer gas in the USA ?

Max Sherman:

The National Institute for Occupational Safety and Health recommended standard is 50 ppm; our laboratory safety staff then required us to conform to a 25 ppm maximum. While I personally feel that this restriction is too stringent, there have been some definitive studies showing long-term health effects at the level of several hundred parts-per-million.

The full reference of this NIOSH standard is

"Occupational exposure to waste anesthetic gases and vapours"

US Department of Health Education and Welfare

Public Health Service Center for Disease Control

National Institute for Occupational Safety and Health

DHEW (NIOSH) Publication No. 77-140

March 1977

David Harrje:

SF₆ tends to have a very high margin of safety as we only need concentrations less than one ten thousandth of the maximum permitted concentration. This means that we can use it in automated systems with complete safety because, even in the event of a total discharge of the gas cylinder, the SF₆ concentration will still be in the safe range.

Richard Grot:

Regarding public reaction to the use of SF₆, we have found that, provided we explain to occupants what we are doing, there is generally no hostile reaction to its use.

(Points arising from David Etheridge's presentation (Paper 2))

Johnny Kronvall:

Would David Etheridge define his meaning of leakage area ?

David Etheridge:

The leakage area is determined by pressure testing at pressures well above those induced by the weather. Use of the crackflow equation described in the paper gives an "effective area" of openings which is independent of the applied

pressure. Thus the leakage area may be determined simply from the flow rate and pressure difference. This is not so for power law equations as the area becomes a function of the pressure difference. In addition to being dimensionally correct, I think that our crackflow equation can be applied as easily as power law equations.

Peter Warren:

The power law equation of the form $Q = k (\Delta P)^{1/N}$ is a reasonable approximation if you do not know the precise geometry of the cracks. Although it must be regarded as an approximation it is just as acceptable as the use of the power law velocity profile equation.

David Harrje:

The power law exponent allows you to do very practical things. For example, we can use it to readily compare the effective leakage areas of many buildings.

Max Sherman:

We use the power law as an empirical description of crack flow. While it may not have a physically justifiable form, it has been repeatedly shown to describe measured data very well. The alternative is to measure the exact geometry of each crack and apply the appropriate crack equations - this is impractical as a field technique.

SESSION 2

(Points arising from Robert Dumont's presentation (Paper 3))

Max Sherman:

How often do you calibrate the gas chromatograph ?

Peter Jackman:

Also, how do you perform the SF₆ calibration ?

Robert Dumont:

The gas chromatograph is calibrated at three-monthly intervals. There is no significant change between periods. The calibration process involves injecting into the chromatograph a known quantity of 100% SF₆ using a hypodermic syringe.

David Etheridge:

Would you please give more details of the fan you used.

Robert Dumont:

This is an aircraft surplus axial flow fan. It runs off 24 volts DC but may be modified to run from the mains.

David Harrje:

You are measuring ventilation rates of 0.2 air changes per hour. How far does this go to meeting internal ventilation needs ?

Robert Dumont:

We have tested houses constructed from 1910 onwards. The air change rates for the older houses have been found to be much the same as those for the newer dwellings. Many of the pollutants are also still the same. The measured ventilation rates seem to be satisfactory.

(Points arising from Peter Hartmann's presentation (Paper 4))

David Harrje:

The indication from your results is that all the rooms perform in the same way. What type of interconnections between rooms do you have ?

Peter Hartmann:

Room interconnection was via part-open doors.

John Shaw:

In your chamber experiments, have you checked your equipment for flows below 1 air change per hour ? We are having problems at air change rates below 0.4/hr and I think that this is due to the mixing fan creating local pressure differences.

Richard Grot:

We have experienced similar problems with small chambers - we were getting insufficient mixing. With larger chambers we had no problem.

Peter Hartmann:

We have not had any problems measuring ventilation rates with this equipment, but did not go below an air change of 0.8/hr.

(Points arising from Richard Grot's presentation (Paper 5))

Max Sherman:

How many zones can the system deal with ?

Richard Grot:

The system is able to cope with up to 10 sampling points and 5 injection points.

John Shaw:

What kind of tubing did you use for your sample tubes ? We have tried copper tubing in an attempt to eliminate the adsorption problems associated with nylon tubes but have experienced poor results due to leaking.

Richard Grot:

We have been using nylon tubes without serious problems for sampling. These are of $\frac{5}{8}$ " bore for the long fetches to the sampling pumps and of $\frac{1}{8}$ " bore for the sample lines.

Max Sherman:

What type of tracer gas decay do you get; are the curves smooth enough to be sampled at such widely spaced intervals ?

David Harrje:

The decay curves in these buildings are smooth, therefore it is possible to take samples from each part sequentially rather than monitoring just one zone continuously. The flexibility of the computer allows us to look at any zone at any times.

Rodney Gale:

Is the flow through the sample tube continuous ?

Richard Grot:

Yes, but in order to get a good sample the flow has to be quite high.

SESSION 3

(Points arising from Willem de Gids's presentation (Paper 6))

Peter Warren:

What exponent, n , do you use for your building components ?

Willem de Gids:

For the total shell we use values between $1/1.6$ to $1/1.7$

For individual components the exponent ranges from between $1/1.2$ and $1/1.8$

John Shaw:

How do you measure the leakages through various components ?

Willem de Gids:

We pressurize each room in turn and tape off all outside cracks. If there is leakage to adjacent rooms, these cracks are also sealed.

Peter Collet:

You have quoted leakage rates through building components at a pressure of 1 Pascal. Bearing in mind that the pressure tests must be conducted at much higher pressures than this, so that the results are not influenced by the effects of weather, is it reasonable to quote the leakages at such a low pressure ?

Willem de Gids:

These tests were usually conducted at 50 Pascals. The results were then scaled down and expressed at a pressure difference of 1 Pascal. By doing this the leakage is expressed directly in SI units.

Max Sherman:

By calculating the leakage in the manner Willem has proposed, he is implicitly assuming that the flow is proportional to the pressure. Therefore, the leakage number he quotes is calculated by dividing the measured flow at 50 Pascals by 50. If the leakage is not linear, this number will have no relation to the actual flow at 1 Pascal.

Willem de Gids:

The flow rate (qv) is proportional to the pressure difference (Δp) to a certain power ($1/n$).

In formulae:

$$q_v = C (\Delta p)^{1/n} \quad \text{in which} \quad C = \text{air leakage coefficient}$$

This coefficient is in fact a flow rate by 1 Pa pressure difference. It is achieved by extrapolating the measured values, which normally goes to about 5 Pa. I agree, nevertheless, that there is no relation with the actual flow at 1 Pa.

(Points arising from Per Olof Nylund's presentation (Paper 7))

Willem de Gids:

What pressure difference did you use in these tests ?

Per Olof Nylund:

For the reciprocity tests, pressures of between 20 to 25 Pascals were used. This is about normal for this type of work. For pressure testing in general we use 50 to 100 Pascals. A pressure of 1 Pascal is too small.

(Points arising from John Shaw's presentation (Paper 8))

David Harrje:

You mentioned part-opened loading doors as a source of air infiltration. Do you find that drop-ceilings are a problem ?

John Shaw:

Yes, these are also an important source of air infiltration.

SESSION 4

(Points arising from Johnny Kronvall's presentation (Paper 9))

Willem de Gids:

How do you deal with openings to the roof, when pressure differences have only been measured across the facades of the building ? Also, what allowances do you make for wind direction ?

Johnny Kronvall:

The effects of roof openings and wind direction have not been considered in this example.

David Harrje:

In your early work you had a reasonable correlation between similar houses. Do you have good correlations for a wider range of houses ?

Johnny Kronvall:

We require more work on other houses before we can say.

(Points arising from Peter Warren's presentation (Paper 10))

Rodney Gale:

The distribution in leaks can be important. Does your method take this into account ?

Peter Warren:

These results are based on the assumption that leaks are uniformly distributed. For our purpose this seems to be a reasonable assumption. The model allows for variation of leakage between surfaces.

David Harrje:

In some instances we have found a non-uniform distribution of leaks. Windows and doors may account for only 25% of the total openings. Cracks in ceilings can be an important source of leaks.

Rodney Gale:

There is no difficulty in determining the component of air infiltration through ceilings. All this is required is the use of a different tracer gas in the loft to the rest of the building.

(Points arising from Max Sherman's presentation (Paper 11))

Martin Liddament:

If the measured exponent of the power law function is significantly different from the value of 0.5 used in this approach, then large errors in computed flow may result when the pressure difference deviates from 4 Pascals.

Max Sherman:

The fractional error will be at most equal to the ratio of the average pressure over 4 Pascals raised to the difference between the actual exponent and one-half. For example, if the mean surface pressure were 5 Pa and the exponent were .65, then the maximum amount of error would be:

$$\left(\frac{5}{4}\right)^{(.65 - .5)} - 1 = 3\%$$

Martin Liddament:

For more severe pressure differences, say those corresponding to high stack pressures or high wind speeds, the error will be much greater. For example, an exponent of 0.7 and a pressure difference of 10 Pascals would yield a maximum error of 20%.

Max Sherman:

There are two types of error that we talk about - the average error of the mean or the maximum error in a sample. In my example, I have selected values to represent the mean conditions to get an estimate of the mean error. In your example you have selected values to represent the worst case and, hence, get a maximum error. Either method of presenting this data is acceptable provided that it is clear which method we are talking about.

Rodney Gale:

An easy way to determine the various values of component leakage would be to carry out tracer gas tests using more than one tracer gas. Thus, for example, the leakage across the ceiling may be determined by injecting carbon dioxide in the roof space and sulphur hexafluoride in the remainder of the building.

SESSION 5

(Points arising from Peter Robertson's presentation (Paper 12))

David Etheridge:

How does the computer logic cope with the gap in pitch response ? Also, have you thought of using laser doppler shift ?

Peter Robertson:

The cosine response is a function of the sensor itself. All the computer does is to receive the information from the sensor. Laser doppler equipment is too bulky for our work.

Hans Phaff:

Is the output voltage of the instrument linear with respect to velocity ?

Peter Robertson:

No. A calibration equation is programmed into the computer to give a direct readout.

Peter Collet:

Have you thought of using a tri-axial probe ?

Peter Robertson:

This gives more information than we require and increases the complexity of the computing. All three readings would have to be computed.

Johnny Kronvall:

Does the velocity measurement go as low as you require ?

Peter Robertson:

Yes. The instrument measures velocity down to 0.2 m.s^{-1} .

Peter Collet:

Can you measure direction and wind speed at low velocities simultaneously ?

Peter Robertson:

Below 0.2 m.s.^{-1} measurement of direction becomes unreliable because the frequency response is too low.

(Points arising from Hans Phaff's presentation (Paper 12))

David Etheridge:

Do you have any evidence for the flow patterns through the window you illustrated ?
Is this a full-scale window ?

Hans Phaff:

The flow pattern is only an opinion. It is a full-scale window but a small window.

Peter Collet:

Did you use a Validyne differential pressure transducer ?

Hans Phaff:

Yes.

(Points arising from Gabriel Huber's presentation (Paper 13))

David Etheridge:

How do you choose and prepare human subjects ?

Gabriel Huber:

The subjects inside the test chamber ("producing odours") are selected by chance without special criteria. For each test the following parameters are considered:

- time of last bath before the beginning of the test,
- time of last meal before the beginning of the test,
- clothing during the test.

Acclimatisation can be a problem. However, we take what precautions we can to prevent the acclimatisation to odours upsetting results.

Further Discussions

At the completion of the formal sessions there followed a general discussion on the use of units. This discussion was introduced by Rob Dumont who sought views on the units to be used to express ventilation and air infiltration rates. Should one use SI units or express air infiltration in terms of the number of air changes per hour ?

David Harrje said that the ASHRAE guide specifies fresh air requirements for people in units of litres/sec. On the other hand the use of air changes/hour gives a good indication of the adequacy of the ventilation rate, provided building size and accuracy are adequately described.

More important, however, was air quality. As homes become tighter, will the ventilation rate be adequate during certain times of the year ? It would be useful to have year-on measurements of ventilation rates so that the seasonal variation of these rates could be observed.

Peter Jackman stated that there was no real answer to the problem of units. The units used relate very much to the problem being solved.

The effects of season and the ageing of a building on air infiltration rates was also discussed. Peter Warren cited results for an unoccupied, timber-framed house in which there was a 30% difference in leakage between summer and winter. This difference was attributable entirely to changes in background leakage.

THE AIR INFILTRATION CENTRE was inaugurated through the International Energy Agency and is funded by eight of the member countries:

Canada, Denmark, Italy, Netherlands, Sweden, Switzerland, United Kingdom and United States of America.

The primary role of the Air Infiltration Centre is the technical support of active research in air infiltration in buildings. Its main aim is to bring the prediction of air infiltration rates and the associated energy implications up to a level comparable with that developed for other energy transfer processes in buildings.

Air Infiltration Centre Old Bracknell Lane, Bracknell, Tel: 0344 53123
Berkshire, Great Britain, RG12 4AHTelex: 848288 (BSRIAC G)

Operating agent for International Energy Agency, The Oscar Faber Partnership, Upper Marlborough Road, St. Albans, Herts, Great Britain.

Printed by HNB (Litho) Ltd., The Square, Bagshot, Surrey

